Panspermia – The Survival of Micro-Organisms During Hypervelocity Impact Events

A Thesis Submitted for the Degree of Doctor of Philosophy

By

Luna Pasini

July 2017

Centre for Astrophysics and Planetary Science

School of Physical Sciences

University of Kent at Canterbury

ABSTRACT

The possible spread of life between planetary bodies has significant implications for any future discoveries of life elsewhere in the solar system, and for the origin of life on Earth itself. Litho-Panspermia proposes that life can survive the shock pressures associated with giant impacts which are sufficiently energetic to eject life into space. As well as this initial ejection, life must also survive the impact onto another planetary surface.

The research presented shows that the micro-organisms *Nannochloropsis oculata* phytoplankton and tardigrade *Hypsibius dujardini* can be considered as viable candidates for panspermia. Using a Two-Stage Light Gas Gun, shot programmes were undertaken to impact frozen organisms at different velocities to simulate oceanic impacts from space. It is demonstrated that the organisms can survive a range of impact velocities, although survival rates decrease significantly at higher velocities.

These results are explained in the context of a general model for survival after extreme shock, showing a two-regime survival with increasing shock pressure which closely follows the pattern observed in previous work on the survival of microbial life and spores exposed to extreme shock loading, where there is reasonable survival at low shock pressures, but a more severe lethality above a critical threshold pressure (a few GPa). Hydrocode modelling is then used to explore a variety of impact scenarios, and the results are compared with the experimental data during a thorough analysis of potential panspermia scenarios across the universe.

These results are relevant to the panspermia hypothesis, showing that extreme shocks experienced during the transfer across space are not necessarily sterilising, and that life, could survive impacts onto other planetary bodies, thus giving a foothold to life on another world.

ACKNOWLEDGEMENTS

Firstly, I would like to thank Charlotte for being there for me, through thick and thin, through the laughter and the tears, for all these years.

I would also like to thank a great number of people for their support, both moral, and educational, over the duration of my Ph.D.

My mum and sister, for their constant nagging of "start writing your thesis!" as well as their moral support.

My brother, whose adventures around the world inspire me to enjoy life.

My nan, who put a roof over my head while writing this thesis.

My supervisor Mark Price for endless support, understanding, help, advice, and wisdom throughout my Ph.D.

All my office & lab buddies, that entertained me with gossip, chatted with me when I needed a break, listened to me moan, and supported me through some big life changes: Agata, Nisha, Lindsey, Dave, Penny, Chrysa, Sally, Rebecca, Tim, & Ricky.

The Science & Technology Funding Council for funding 'most' of my Ph.D.

Mike Cole for firing the gun, training me in its operation, and some real good dead pan jokes.

Mark Burchell for help and advice throughout my Ph.D.

If I have forgotten anyone, it was not intentional, and you also have my thanks, as well as my apologies.

CONTENTS

LIST OF FIGURES

LIST OF TABLES

CHAPTER 1
INTRODUCTION

"This is insane, Crichton."
"Four years on and you're finally gettin' that?"

Scorpius & John Crichton, *Farscape*

Aliens! The idea of life existing outside the Earth is a concept that has captivated the imaginations of people across the globe for centuries. Before the heliocentric revolution revised the understanding of Earth's position in the universe (i.e. it is not the centre of the universe, and is nothing special), ideas about beings not-of-the-Earth was largely philosophical or mythological (Crowe, M. 1999; Wiker, B. 2002). Cosmic pluralism, or 'the plurality of worlds' became a lot more popular during the scientific age of enlightenment, and many prominent scientists and astronomers (like Giordano Bruno and William Herschel) supported the idea of other worlds, and possibly life on these worlds throughout the 16th to 19th centuries. In the late 19th century the notion of life on Mars became a hot topic as Percival Lowell made a telescopic observation of 'canals' on the Martian surface. Although these observations were later explained as optical illusions (Evans, J. et al. 1903), Lowell still went on to write the book 'Mars and its Canals' in 1906. However, the apparent discovery itself 10 years earlier caught the imagination of H.G. Wells and he went on to write the novel 'War of the Worlds', and the concept of menacing alien life exploded into the minds of the general population in 1897 with its release. For the next fifty years

Martians and creatures from outer space would be a popular genre for novelists.

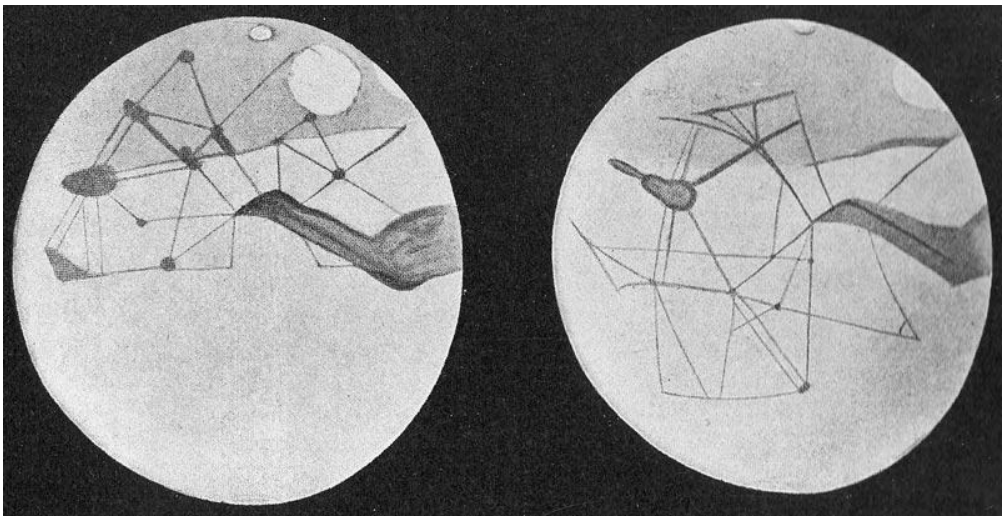

Figure 1.1: Percival Lowell's depiction of the Canals of Mars. *Image courtesy: bbvaopenmind.com*

After the Second World War, in 1947, the 'Roswell Incident' (Nickell, J. and McGaha, J. 2012) ignited public minds again with the idea of aliens, and people's fascination with the concept has grown enormously in the following 70 years; films, books, and serious science.

In 1961 Frank Drake produced the famous Drake Equation that attempts to estimate the number of intelligent species in the universe (see Burchell, M. 2006 for a recent review), and together with SETI (the Search for Extra-Terrestrial Intelligence) serious scientific work in the hunt for radio signals produced by other worldly intelligences began, and continues to this day (Sullivan, W. and Baross, J. 2007). Although the 'wow' signal (detected on August 15, 1977, by Ohio State University's Big Ear radio telescope in the United States) raised hopes of an extra-terrestrial intelligence, this was

ultimately never repeated and although the ‘wow’ signal is the best candidate to date, this search is still yet to produce positive results.

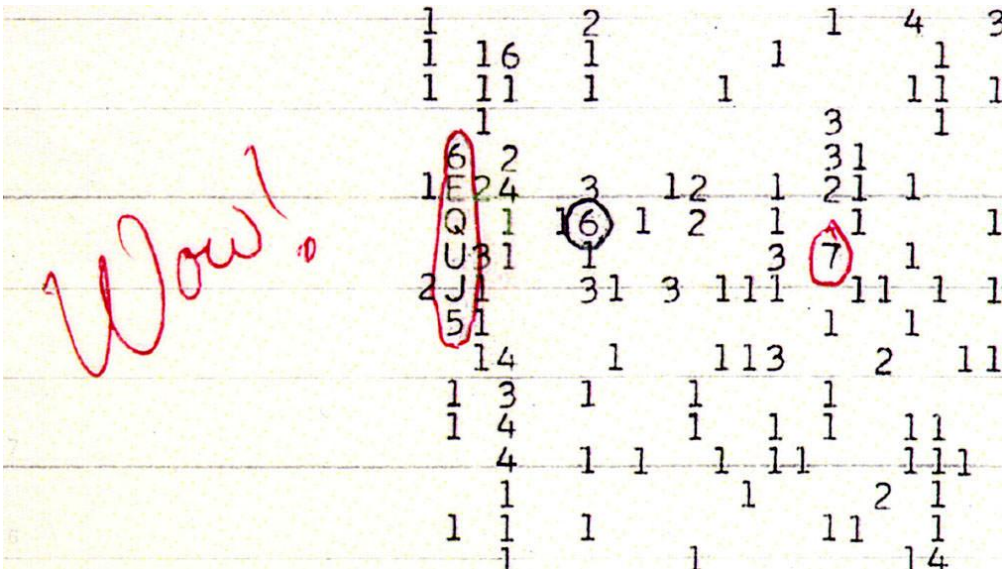

Figure 1.2: The ‘wow’ signal. *Image courtesy: universetoday.com*

The scientific search for life elsewhere in the universe is not restricted to only intelligent life. A large part of the biomass of the Earth is made up of single-celled microbial life, with an estimated ~5×10^{30} cells, and 550 billion tons of carbon (Whitman, W. et al. 1998), this equates to almost 50% of the total global biomass (Groombridge, B. and Jenkins, M. D. 2000), and so this seems a logical place to start when looking for life elsewhere. However, any search for life must also be a search for the places where life (as we currently understand it) could exist, and thus the genesis and evolution of life on the Earth needs to be considered to allow such a search to be productive.

There have been many theories on the origin and evolution of life on the Earth throughout human history, right back to the dawn of civilisation itself in ancient Sumer, and the Anunnaki Gods that created mankind of their

blood, and in their image, as described in the 5000 year old epic poem 'The Epic of Gilgamesh', telling the exploits of the king of Uruk from the third dynasty of Ur and his friend Enkidu (Jacobsen, T. 1949). However, whilst the creation myths of many religions the world over held sway for millennia, the advent of the scientific age caused many to question this divine origin.

Figure 1.3: King Gilgamesh (right) with one of the two lions he wrestled to submission, and his friend and companion Enkidu (left) the part human Wildman. Image courtesy: *beforeitsnews.com*

In the 19th century Darwin proposed the theory of evolution of the species, and took God 'out of the equation'. Then, in the early 20th century, Arrhenius proposed a theory for the transfer of life between worlds via radiation pressure which would later become known as radiopanspermia (Arrhenius, S. 1903). However, the general term panspermia (literally 'seeds everywhere') has come to encompass the various versions of the theory. The theory suggests that life can be transferred between planetary bodies via some mechanism, such as meteors, asteroids, or other naturally occurring interplanetary bodies.

There are three main variations to the panspermia hypothesis. Radiopanspermia, as proposed by Arrhenius, suggests that microbial life can form and exist in space, and that the radiation pressure from the sun can propel them into the gravity wells of planets. The second version of the theory is known as directed panspermia, and suggests that life is transferred between worlds in the universe artificially by extra-terrestrial intelligences (e.g. Crick, F. and Orgel, L. 1973). The third variation, and considered the most likely to occur, is lithopanspermia. This version suggests that rocks and/or ice are used as the transfer mechanism. The rocks and/or ice are ejected into space via meteorite, or cometary, impacts into a planetary surface, and then fall on other worlds as impactors themselves thus carrying and seeding life in the process (Melosh, H. 1988).

Panspermia as an idea has been examined by many different disciplines of science, and seems set to continue to be a focus of research for much time to come. In 1996 the controversial Martian meteorite ALH84001 (found in Antarctica in 1984), was announced as the first proof of extra-terrestrial life. Analysis of the rock discovered tiny carbonite nano-structures within the rock which the researchers took for micro-fossils (McKay, D. et al. 1996). However, this was later determined to be of a non-biological origin (Sears, D. and Kral, T. 1998, Buseck, P. et al. 2001). There have now also

been some experiments testing various microbial life-forms for survival against the type of shock induced pressures witnessed during a large scale impact event. For example, some experiments have shown that bacteria (Burchell, M. et al. 2001, 2004), and yeast (Price, M. et al. 2013), can survive pressures of ~30 GPa; well in the range of such life-seeding impacts.

More recent discoveries in the surface topography and chemical composition of early Mars have led researchers to suggest that Mars may have been more conducive to the creation of life than the early Earth; presenting evidence for an abundance of molybdenum as well as desert-like expanses, as opposed to the Earth which was flooded during the same period of time (Benner, S. and Kim, H. 2015). This lead to the speculation that life could have first originated on Mars, and then through a panspermia-style impact was transported to the Earth. These recent finding have kept the theory of lithopanspermia at the forefront of research in many scientific disciplines.

There are three main phases to the lithopanspermia theory:

1. ejection from, and escaping the gravity well of, the host planet,

2. transfer through interplanetary space to the destination planet,

3. arrival to the destination planet via an impact.

These three phases each contain hazards to life, and any organisms that may be capable of a lithopanspermia-style journey must be able to survive the constraints placed upon them by each of these phases. Hypervelocity impact experiments, and hydrocode simulations, have now been performed to test the limits of various different species in regard to the lithopanspermia hypothesis. These experiments and simulations, along with their results are reported here in this thesis, as well as discussions, and speculations, about the

types, and likelihood, of possible panspermia-style transfers that could occur naturally in the universe.

The structure of this thesis is as follows. Chapter 2 introduces the varied discipline of astrobiology. This is defined as the search for, and exploration of, the origin, evolution, and distribution, of life throughout the known universe. Then there is a discussion of the history and evolution of life on Earth, and the Earth itself, and then the definition of life as we know it, and the requirements of life are considered. Finally, the potential habitats for life within the Solar System, and within other star systems in the Milky Way Galaxy are discussed.

Chapter 3 describes the theory of panspermia in detail, and presents recent results concerning the validity of the theory. The various dangers faced by organisms involved in such a panspermia-style transfer at each phase of the journey are then discussed, along with recent evidence of viable organisms capable of surviving such dangers. Finally, possible interplanetary Solar System routes for potential journeys are discussed in terms of the average, and most optimum, transfers for material between planets based on current knowledge of planetary impact ejecta, and its movement around the Solar System.

Chapter 4 introduces the equipment and facilities used in this research. The light gas gun, as well as the optical and scanning electron microscopes used are briefly described. The selection of the two different species for experimentation is then explained in detail, before the description of pressure calculations for impact experiments. Finally, a brief overview of hydrocode modelling is presented in relation to its use within this research.

Chapters 5 and 6 present the experimental research programmes for the two species chosen. Chapter 5 reports the results of the experimentation with the phytoplankton species *Nannochloropsis oculata*, and Chapter 6

reports the results of the experimentation with the tardigrade species *Hypsibius dujardini*. Both chapters give detailed accounts of the methodology undertaken to conduct the programmes, as well as the results from the hypervelocity shot programmes, and the complementary results of the hydrocode modelling of the shot programmes. The phytoplankton were loaded into projectiles and fired directly into water targets simulating a large oceanic impact event. However, the tardigrades were frozen into the target and this target was then impacted with a nylon projectile, simulating an impact that could lift material into space. The survival results for each programme are then presented. Hydrocode modelling for both programmes allowed these results to be quantified in terms of survival against the various impact shock pressures for different conditions. Finally, the implications of these results are discussed in the context of panspermia.

Chapter 7 presents the description, and results, for a variety of different hydrocode models, that were created to simulate different panspermia-style impact conditions, and therefore analyse different species survival parameters, in different impact scenarios.

Chapter 8 brings together the experimental research of Chapters 5, and 6, with the hydrocode simulations of Chapter 7. A description for a best case scenario is presented, followed by different panspermia-style scenarios. An analysis of different micro-organisms that could potentially survive each of the conditions is then presented for the Solar System, and then beyond it. Numerical errors within the hydrocode at extreme velocities are then discussed, before a re-evaluation of the analysis is undertaken. Finally, an equation for the panspermia journey is presented as a tool for future research, with some speculative discussion as to what it could imply for life on Earth or elsewhere in the universe.

Chapter 9 presents the overall conclusions to all of the results and discussions from the previous chapters.

To summarise: this thesis investigates the theory of panspermia, and some of the organisms that might be able to successfully achieve it. Experimental shot programmes using a light gas gun to impact targets at hypervelocities were undertaken. Analysis was performed to determine survival rates of organisms from these programmes. Hydrocode modelling was used to create simulations of different panspermia-style impact conditions. An analysis of these simulations against the survival rates of different organisms was performed to determine the different impact scenarios these organisms could potentially survive. And finally, an equation to determine the possible number of panspermia-style life transfers between planets is presented as a tool for future use in potentially determining where to look for life that could confirm the panspermia hypothesis.

The work presented here confirms the ability of two different organisms to survive the extreme pressure regimes that occur in a panspermia-style journey, as well as showing possible scenarios different organisms could potentially survive. However, this does not prove that panspermia does happen, or has happened in the past, on Earth, or any other world.

CHAPTER 2

LIFE, AS WE KNOW IT

"However life started, once established, it persisted for over 3.5 billion years and evolved from microbial slime to the sophistication of human civilization."

David C. Catling

2.1 Introduction

This chapter introduces the varied discipline of astrobiology, which is defined as the search for, and exploration of, the origin, evolution, and distribution of life throughout the known universe. While there are many aspects to this field of study, the concept of panspermia is of central interest in this work. However, in order to investigate how life could travel between worlds, an understanding of what life is, and where it came from, must be established. While there may be many unknowns surrounding the origins of life, what we do know is that, life does exist on the Earth, the Earth exists as part of the Solar System, and the Solar System is at least 4.6 billion years old, so this, it would seem, is a good place to start.

The chapter begins by describing the formation of the Solar System and the Earth, and then goes into a brief history of the Earth. Next, an attempt is made to define life, as we know it, before a discussion on the current theories of how life on the Earth may have originated. A brief discussion of the history of life on Earth is then presented. Next, the requirements for life

as we know it are looked at, before a discussion on the possible habitats life could survive within the Solar System, and beyond. Finally, concluding remarks are passed.

2.2 Birth of the Solar System

The Solar System formed approximately 4.6 billion years ago (Bouvier, A. and Wadhwa, M. 2010), from the remnants of first generation stars (made primarily of primordial hydrogen and helium) that had previously 'died' via the violent process known as a supernova, creating more heavy elements in the process. Some of the gas and dust from these first generation supernovae coalesced over time, causing local increases in density within this giant molecular cloud (this may have been due to shockwaves from nearby supernovae). At a critical point the gravity at this localised dense region was enough to cause part of the cloud to collapse under gravity. This gravitational collapse brought gas and dust together increasing the density, and thus increasing the speed of the collapse due to gravity. As this dense pocket of material further collapsed it began to rotate due to the conservation of angular momentum. This effect, combined with the magnetic fields within the spinning cloud, caused it to flatten into a disc-like shape, with a protostar at its core (Montmerle, T. et al. 2006). The protostellar phase of the early sun took about 1 million years, during which the thermal gas pressure within the protostar grew, this halted the total collapse of the cloud, and increased the protostar's temperature. The protostar then went through a ~30 million year journey of continued collapse (due to gravity) and expansion (due to internal thermal pressures) before reaching hydrostatic equilibrium and taking its place on the main sequence (see Figs. 2.1 and 2.2) of stars (Yi, S. et al. 2001). It is thus known as second generation star.

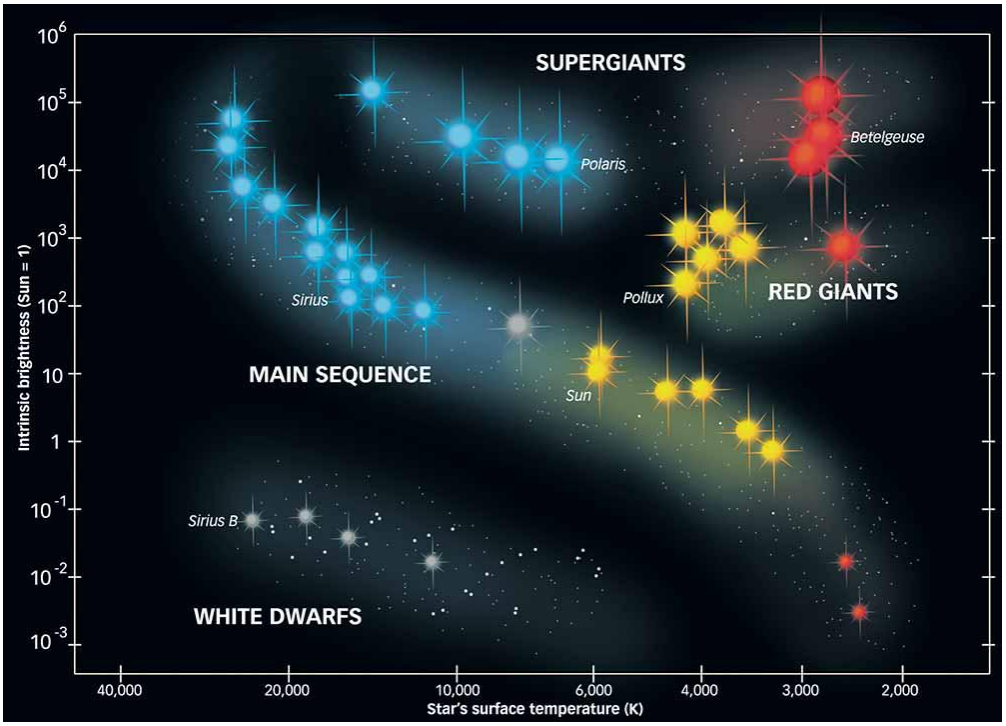

Figure 2.1: Hertzsprung-Russell diagram showing the different classifications of stars. *Image courtesy: graphicnet.co.uk*

As the spinning disc was pulling material into the centre forming the protostar, the conservation of momentum was also forcing other material out into the flattened disc orbiting around the protostar. As this material collided with each other it began to form small clumps of dust. As the temperature in the protostar increased it eventually reached a critical point at which hydrogen fusion reactions began and the star 'turned on'. The radiation pressure blew away all the remaining small dust grains and debris from the disc leaving only the larger grains and clumps, and these would then go on to form the planets of the Solar System (Lin, D. 2008). As the clumps interacted with each other they began to accrete together and grow larger.

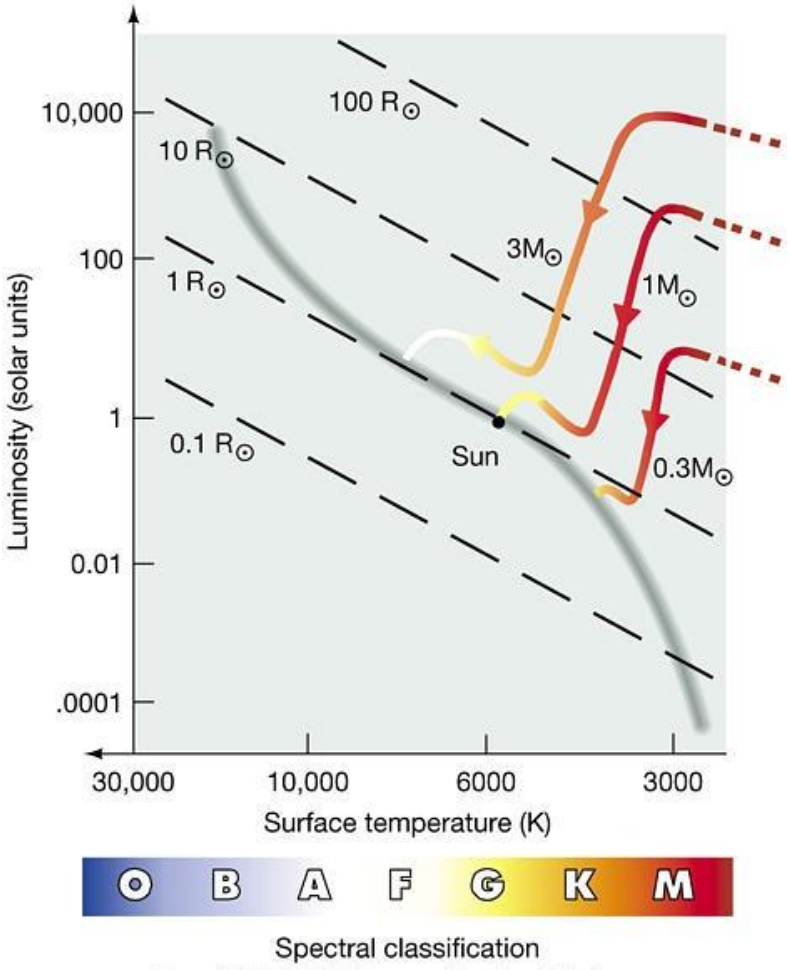

Figure 2.2: Showing the sun's ~30 million year journey from protostar to main sequence star. *Image courtesy: uoregon.edu*

When the average diameter of the growing bodies in the solar disc was around 10 km there would have been approximately 1 trillion of these 'planetesimals'. Over time, these continued to accrete and grow until just a few large planetesimals began to dominate. These then went on to sweep up all the remaining material in and around their orbital paths until most of the material was accreted into the planets seen today. However, the planets were not yet settled in their orbits. The four gas planets were at this stage much closer (~5.5 – 17 AU) and on near circular orbits (Crida, A. 2009).

Gravitational interactions and mean-motion resonances caused planets to migrate around the Solar System over several hundred million years (Hansen, K. 2005). These disruptions caused most of the mass of the outer disc to be removed (Tsiganis, K. et al. 2005), and many small planetsimals were thrown into the inner Solar System creating a sudden influx of impacts on the terrestrial planets – the Late Heavy Bombardment (Gomes, R. et al. 2005), as evidenced from cratering records on these planets. This massive bombardment is thought to be responsible for delivering most of the volatile materials, and possibly organic compounds to the Earth (Chyba, C. et al. 1990). This formation model is known as the Nice model (Desch, S. 2007), and it explains many of the features of the Solar System that are otherwise unexplained.

2.3 Earth – A History

About 20 – 100 million years after the Solar System had coalesced (around 4.5 billion years ago), a Mars sized object called Theia impacted the early Earth. The debris of this collision would accrete into the Moon that now orbits the Earth; this is known as the ;giant impact hypothesis; (Canup, R. and Asphaug, E. 2001).

After the initial formation of the Earth there was a ~20 million year period of condensation, where differentiation of materials began to take place within the Earth. Radioactive decay of unstable isotopes caused the planetary interior to melt, allowing heavy elements like iron to sink, forming the solid (inner) and liquid (outer) iron nickel core, whilst lighter elements such as silicates rose closer to the surface. The outer silicate layers formed the crust, or lithosphere; a thin layer of rocky material (only 7 - 70 km thick) that covers the much larger mantle (2900 km – and 84% of the Earth's total volume) below (Sorokhtin, O. et al. 2011).

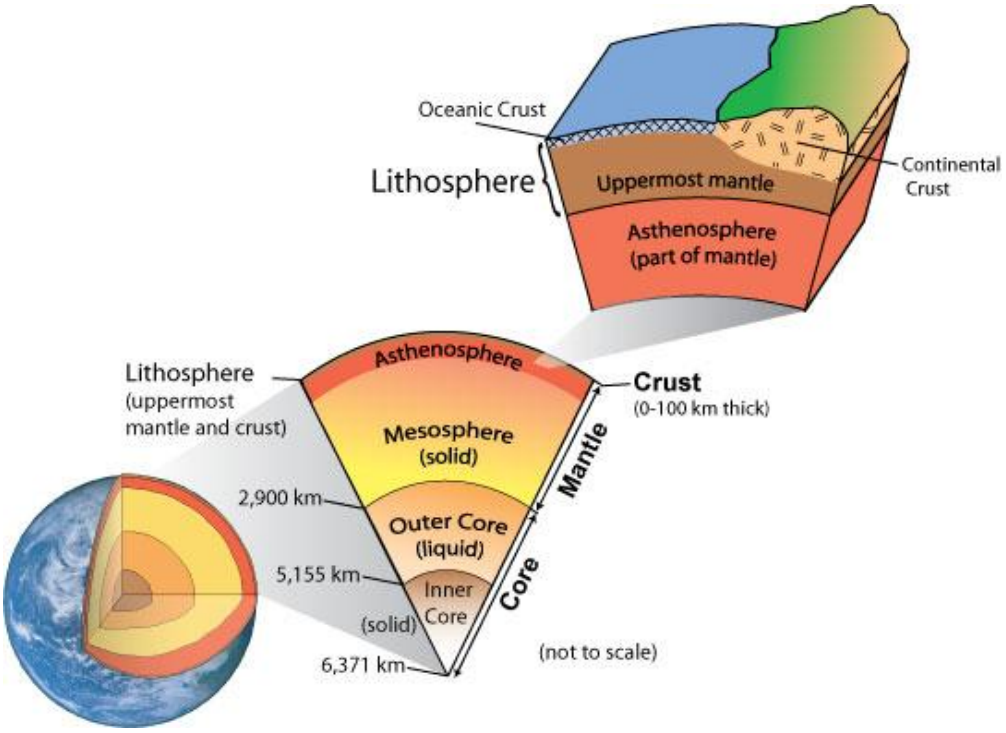

Figure 2.3: Structure of the Earth, showing the inner and outer core, the mantle, and crust. *Image courtesy: p5cdn4static.sharpschool.com*

The crust is broken up into 'plates' which dynamically move around the surface over time via a process known as plate tectonics. The movement of these plates has caused the landmasses on the surface to coalesce into supercontinents, then separate, then recoalesce again in a cycle of supercontinent formation that takes around 300 – 600 million years to complete. After the delivery of the volatile materials during the Late Heavy Bombardment, the Earth was largely flooded (Benner, S. and Hyo-Joong, K. 2015), then, as the crustal plates moved around, the first supercontinent Vaalbara was formed around ~3.5 billion years ago (Zhao, G. et al. 2004). Over the next 3 billion years the supercontinent cycle produced several more supercontinents; Ur (~3 billion years ago), Kenorland (~2.7 to 2.1 billion years ago), Columbia, aka Nuna (~1.8 to 1.5 billion years ago), Rodinia (~1.25 billion to 750 million years ago), Pannotia (~600 million years ago),

and the last supercontinent Pangaea (~300 million years ago). The break-up of Pangaea, which began ~200 – 180 million years ago, produced the fragments that would come to form the continents as they are seen today (Zhao, G. et al. 2002), after going through several intermediate stages, such as Laurasia and Gondwanaland (Fig. 2.4).

Figure 2.4: The last supercontinent Pangaea formed ~300 million years ago, and began breaking up ~200-180 million years ago. **Top:** showing the outlines of today's continents. **Bottom:** showing the two largest continental forms after the break-up of Pangaea. *Image courtesy: top: xearththeory.com, bottom: hosho.ees.hokudai.ac.jp*

2.4 What is Life?

The definition of what exactly life is, is not an easy one, nor a rigid one. Throughout history great thinkers have tried to fathom what life is and what constitutes it. Democritus (460 BC) reasoned that the characteristic of life is having a soul. He reasoned that fiery atoms make a soul, in the same way atoms and the void make up all things, but elaborates that fire is the key component as there is a connection between life and heat, and fire moves, as living beings do. Empedocles (430 BC) believed the universe was made of four fundamental eternal elements, earth, air, fire, and water, and that all forms of life were created from the unique mixtures of these four elements (Parry, R. 2010). Aristotle (322 BC) attempted a thorough definition of life in a huge treatise composed of three books called 'On the Soul' (Aristotle, c.350 BC.; Shiffman, M. 2011). Aristotle put forward the theory of Hylomorphism, in which he regards all material in the universe as having both matter and form, and the form of a living thing is its soul. There is the vegetative soul of plants, which causes growth and decay, and allows them to feed, but does not cause motion or sensation. There is the animal soul which allows animals to move and feel. Then, there is the rational soul, which is the source of reasoning and consciousness which, he believed, is only to be found in mankind. Each higher soul has all the attributes of the lower souls. He believed that matter can exist without form (i.e. inanimate objects), but form cannot exist without matter, and thus, the soul cannot exist without the body (Marietta, D. 1998).

However, there are always exceptions to the rule. Mountains, crystals and even islands can grow, yet they are known to be inanimate. Fire moves and grows as if alive, as Democritus noted, and it also consumes and metabolises combustible fuels and oxygen into waste products (carbon dioxide and soot), yet, again, it is not considered as alive. A borderline case is the example of a virus, which has all the hallmarks of life, but is still not

considered a life-form. The currently accepted definition for life in mainstream science is that organisms maintain homeostasis, are composed of cells, undergo metabolism, can grow, adapt to their environment, respond to stimuli, and reproduce; with the two key elements being, the ability to reproduce the species, and to use a form of energy to drive the chemical reactions that allow adaption, response, growth, and reproduction.

In the early 17th century Rene Descartes brought back the ancient Greek ideas of the materialism of life and revised it for the beckoning scientific age, suggesting that life was an assemblage of parts that came together and functioned as a machine, and later advances in cell biology in the 19th century further strengthened this view (Thagard, P. 2012).

2.5 Life, an Origin

There are certain basic requirements for life as we know it to form. Complex organic molecules such as amino acids, and proteins, are necessary for life to form, and there have been a variety of different mechanisms hypothesised for how they are synthesised. The famous Miller/Urey experiment (Miller, S. 1953) used four gases to simulate a primitive atmosphere (methane, hydrogen, ammonia, and water vapour), as it was believed at the time that the primitive atmosphere of Earth was a reducing one (Fig. 2.5). A continuous electric current was passed through the atmosphere to simulate lightning, which was common on the early Earth. After several weeks they analysed the simulated ocean and found that between 10% and 15% of the carbon in the system had become integrated into organic compounds. 2% of this had been used to form glycine (an amino acid used in the production of proteins). However, the yield was very small; just a few milligrams. Later Juan Oro was able to produce glycine, alanine, and adenine, via reactions between ammonia and hydrogen cyanide (Oro, J.

1961). Adenine synthesis was an important discovery, as this is one of the four nucleotide bases for RNA, and DNA, and further work showed that the other bases could also be synthesised in these reactions. However, these experiments relied on the primitive reducing atmosphere, but the current consensus is that reductive molecules did not dominate the atmosphere of the early Earth, but that it was dominated instead by CO_2, N_2 and water vapour (e.g. Horneck, G. 1995). Other problems with these models are that the energy input (i.e. the electric current) was far too high, as the early Earth would have had common, but not continuous, lightning storms. Also, the ammonia and methane used in the experiments would not have remained stable in the atmosphere of the early Earth, due to photodissociation by solar ultraviolet radiation (Jakosky, B. 1998).

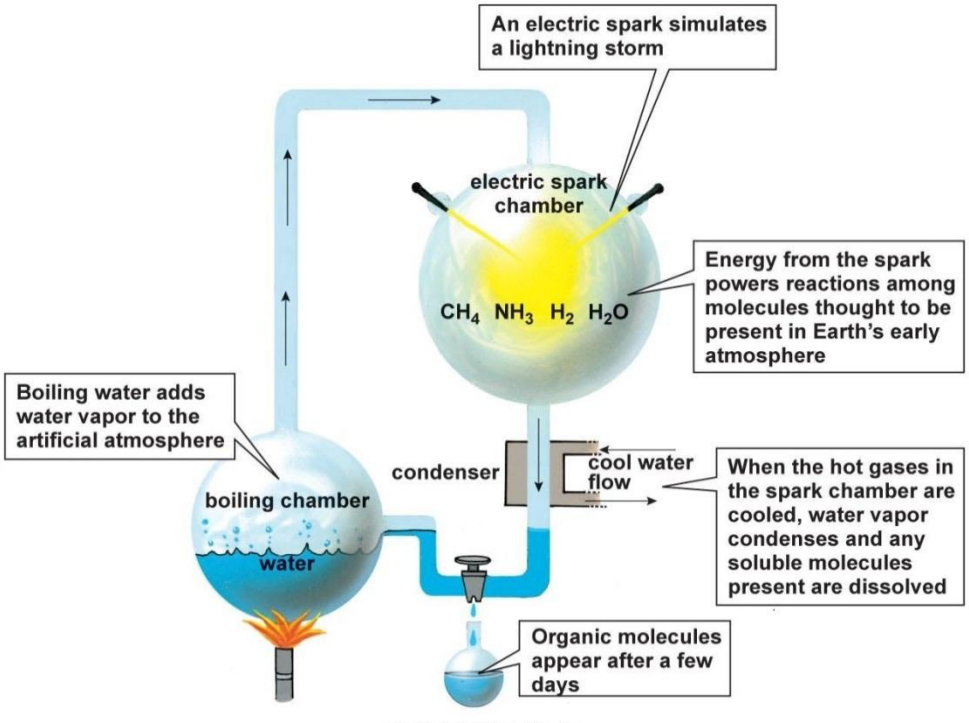

Figure 2.5: Diagram of the Miller/Urey experiment. *Image courtesy: Pearson Education, Inc.*

Other suggestions have since been put forward to explain how complex organic material was present on the early Earth, and these are related to impacts from space. Comets and meteorites could impact the Earth delivering organic molecules that were already formed on the impactors themselves. Meteorites have been found on the Earth that contain amino acids (i.e. see Sephton, M. and Gilmour, I 2000), for example, analysis of the Murchison meteorite has discovered more than 70 amino acids, many of which are not found on the Earth (Cronin, J. et al. 1995). However, this does not answer how they were formed in the first place. One possible method for this is shock synthesis, where the energy of a violent impact into basic materials is the catalyst for their production. Martins, Z. et. al. (2013) performed hypervelocity impact experiments that demonstrate comets impacting into rocky surfaces, or meteorites impacting into icy surfaces, can produce several α-amino acids, including racemic mixtures of alanine and norvaline, and the non-protein amino acids α-aminoisobutyric acid and isovaline. Their results provide a realistic production pathway for the components of proteins in the Solar System, expanding the locations where life may originate.

The current consensus for a non-impact driven pathway from chemistry to biology on the early Earth is hydrothermal vents on the oceans' floor powering the process. It has been shown that the conditions present at these vents can produce organic molecules, and the earliest known life-forms on Earth were hyperthermophilic, and did not use light as an energy source (Holm, N. and Anderson, E. 1995). However, while the earliest known life-forms survive in a hot submarine environment, some doubt has been cast as to whether they originally formed there. This is due to the so called 'Water Paradox'. Benner, S. (2014) describes this paradox as follows:

> *The Water Paradox: Water is commonly viewed as essential for life, and theories of water are well known to support this as a requirement.*

> *So are biopolymers, like RNA, DNA, and proteins. However, these biopolymers are corroded by water. For example, the hydrolytic deamination of DNA and RNA nucleobases is rapid and irreversible, as is the base-catalyzed cleavage of RNA in water. This allows us to construct a paradox: RNA requires water to function, but RNA cannot emerge in water, and does not persist in water without repair. Any solution to the "origins problem" must manage the paradox forced by pairing this theory and this observation; life seems to need a substance (water) that is inherently toxic to polymers (e.g. RNA) necessary for life.* – S. Benner (Paradoxes in the Origin of Life, 2014).

While many terrestrial origin theories for life run into this problem, the impact driven shock synthesis for organic molecules does not.

The transition element molybdenum is of essential importance for almost all biological systems, as it is required by enzymes catalyzing diverse key reactions in the global carbon, sulphur and nitrogen metabolism (Mendel, R. and Bittner, F. 2006), thus for the formation of RNA 'the first Darwinian molecule', molybdenum (as well as boron) appears to be crucial. Benner, S. and Hyo-Joong, K. (2015) propose early Mars as a viable location for the formation of life, as the early Earth was largely flooded, yet large desert-like expanses on the early Martian surface could allow processes that form RNA under prebiotic conditions, effectively negating the 'Water Paradox'. As well as this, the molybdenum content of the early Earth would have been diluted into the expanses of water on the Earth, preventing RNA formation to occur at a quick enough rate to overcome the corrosive destruction water causes to RNA. However, recent Martian meteorite evidence (Stephenson, J. et al. 2013) points to molybdenum and boron on Mars in high enough concentrations for RNA to form and stabilise. This coupled with the desert expanses would indicate early Mars could have been a possible origin for life as we know it; but if this was the case, how did it get to the Earth? One such

mechanism is known as panspermia, and this is discussed in detail in the next chapter.

There are many hypothetical pathways from a prebiotic landscape to a state of life; these are depicted in Figure 2.6 below.

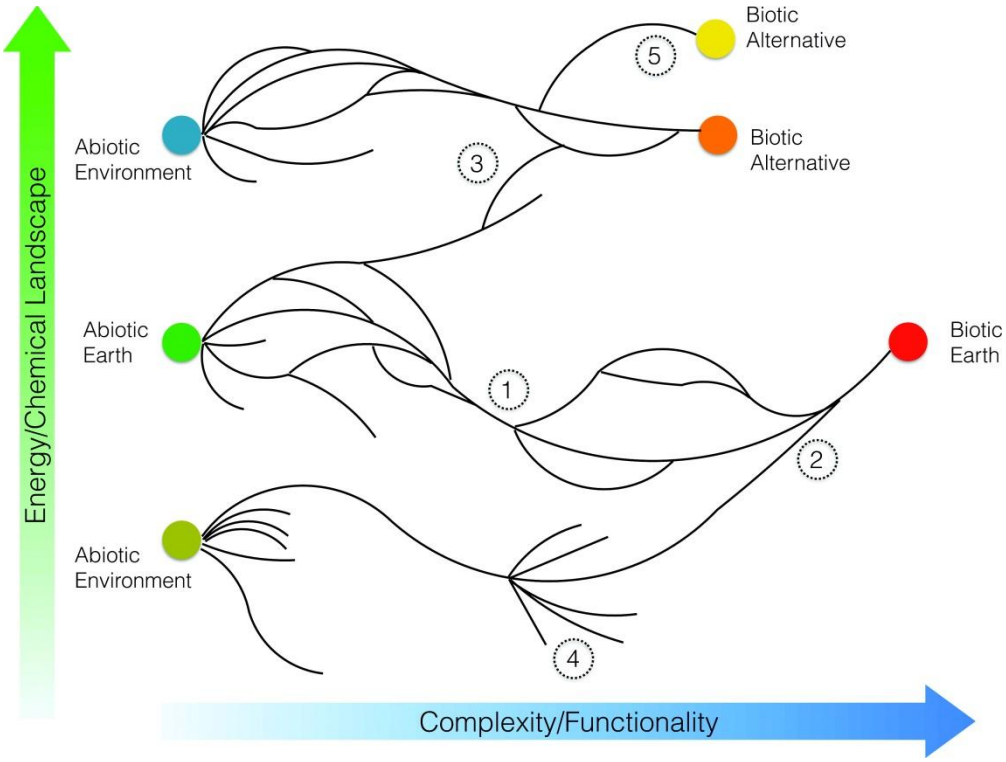

Figure 2.6: Hypothetical pathways to life. **1:** A bottleneck through which all pathways to a terrestrial origin-of-life must pass. **2:** An alternate (non-terrestrial) prebiotic environment that still leads to a terrestrial origin-of-life, or at least an origin-of-life that matches the terrestrial one. **3:** A terrestrial prebiotic environment that leads to an alternative (non-terrestrial) biotic system but of lower complexity than terrestrial life. **4:** a pathway that exhibits rapid diversification of prebiotic systems, but only one leads to a terrestrial origin-of-life. 5: a non-terrestrial pathway splits at advanced complexity and leads to a separate origin-of-life event in the same prebiotic environment from which it started. (Caleb, S. et al. 2015).

Once the precursors to life, such as RNA are formed, there are still other processes that must be accomplished for the prebiotic molecules to become fully-fledged life-forms. The production of membranes around them to allow an environment that differs from their surroundings (i.e. forming a cell), as well as a mechanism to pass the genetic information to a next generation and thus reproduce, must be accomplished. However, this alone does not necessarily constitute a life-form in and of itself.

Take a virus for example; these contain RNA and genes within a housing, and they replicate those genes to new generations, and evolve via natural selection, but they are not alive. The reason for this is that they do not metabolise, and must use a host cell's energy to power their replication, leaving them just short of the definition of life (Koonin, E. and Starokadomskyy, P. 2016). Viruses are considered as being 'on the edge of life' and the self-assembly within host cells, may support the hypothesis that life could have started out as self-assembling organic molecules (Koonin, E. et al. 2006).

2.6 Life on the Earth

The Earth's history can be divided into four aeons; the Hadean, the Archean, the Proterozoic, and the Phanerozoic. The earliest confirmed evidence for life is just after the beginning of the Archean aeon, about 3.8 billion years ago (Nutman, A. et al. 1997; Ohtomo, Y. et al. 2014). Sometime between this time and 3.5 billion years ago is when the 'last universal common ancestor', or LUCA, to all life now on the Earth is believed to have existed. No direct fossil evidence for the composition of LUCA exists, but it can be studied by the comparison of the genome of its descendants, i.e. all life on today's Earth.

In 2016 a study by Weiss, M. et al. identified 355 genes that LUCA would have had; some are universal genes, like those that are involved with reading genetic code, but others point to particular characteristics LUCA would have had. One characteristic of nearly all cells is the ability to pump ions across a membrane in order to generate an electrochemical gradient, which is then used to make adenosine triphosphate molecules which transfer chemical energy within cells for metabolism. The study by Weiss, M. et al. (2016) suggests LUCA could not generate the gradient needed to form adenosine triphosphate molecules, but rather it harnessed an already existing gradient to form adenosine triphosphate. After LUCA the tree of life split into the branches of bacteria and archaea (Fig. 2.7).

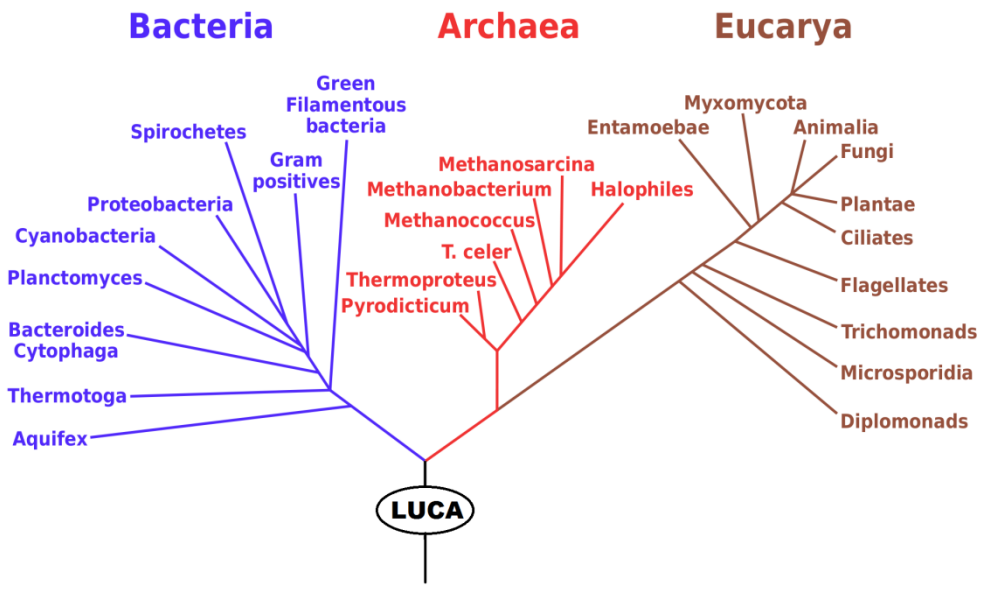

Figure 2.7: Tree of life diagram, showing the path from LUCA for all life on Earth. *Image courtesy: Wikipedia – originally in NASA article (no longer available)*

The fact that LUCA exists at all is problematic for the origins of life on Earth. If the Earth was capable of a genesis-of-life event, why did it only happen once? Or, if it did happen multiple times, where are the other trees of life, why did only one tree survive, and if there were others, where are the fossils showing these?

There are potentially answers to these questions, although to date no conclusive proof has been offered for any of them. Perhaps life did only form once, even though conditions were right for it. Perhaps other trees of life did form, but were short lived, and evidence for them is sparse, and has not been found. Perhaps after the formation of life a giant impact occurred that completely sterilised the Earth wiping away all traces of life, but some life-forms were thrown into space, and survived a fall back to the Earth sometime later, re-seeding the Earth with life from only one tree. This is a kind of 'Noah's ark' scenario and is explored in Chapter 8, Section 8.6.

Another possibility is that the Earth was not suitable for life to form, but it was suitable for it to survive, and life came from somewhere else (e.g. Mars) via a panspermia-style impact event in the distant past. This is an idea once thought impossible, but recent findings have shown several simple species are capable of surviving this type of journey, such as bacteria (Burchell, M. et al. 2001, 2004) and yeast (Price, M. et al. 2013).

It was at around 2.5 billion years ago that the Archean aeon gave way to the Proterozoic aeon. This boundary is loosely set when the 'Great Oxygenation Event' occurred, an event that led to an oxygen-rich atmosphere on the Earth, when photosynthesising cyanobacteria began producing O_2 for the first time. During this aeon around ~2.1 billion years ago the first eukaryotic cells (cells with a nucleus) began to appear, and formed the symbiotic relationship with the former prokaryotic organisms known as

mitochondria, which produce most of the adenosine triphosphate for eukaryotic cells (Margulis, L. and Sagan, D. 1986).

The supercontinent Pannotia broke up ~600 million years ago at the end of the Proterozoic aeon. The distribution of land masses across the globe allowed many separated niche environments (such as coastlines in different climates and latitudes) where life could evolve distinctly. At the same time an accumulation of atmospheric oxygen, allowed the formation of an ozone layer around the Earth. This afforded protection to surface life from solar ultraviolet radiation (Beraldi-Campesi, H. 2013), and allowed life to begin diverging at an increased rate, leading to the 'Cambrian Explosion', around ~570 million years ago, as the Phanerozoic aeon began. It was during this event that most major animal phyla appeared, as indicated by the fossil record (Maloof, A. et al. 2010).

With the advent of skeletal animals, life continued to evolve, and change, and go extinct (when some species could not adapt to changes in environment, or other factors, leading to their demise). From this point until today there have been a number of distinct extinction level events that have caused massive losses to the species that were present on the Earth at the time of the event.

These extinction events quite often left environmental niches open for the remaining life to fill with newly evolving species (McElwain, J. and Punyasena, S. 2007). Amongst these many events, the 'Big Five' stand out due to the sheer number of species that went extinct during these events (Alroy, J. 2008). These 'Big Five' are listed in Table 2.1:

Table 2.1: *The 'Big Five' extinction events of the Phanerozoic aeon.*

Name of Event	***Date (Mya)***	***Species Lost***	***Probable Cause***
Ordovician–Silurian Extinction Event:	~440	~86% of all species were lost, including graptolites	Global cooling and sea level drop possibly due to gamma-ray burst (Melott, A. et al. 2004)
Late Devonian Extinction Event:	~375	~75% of all species were lost, including all trilobites	Viluy Traps volcanic events (Ricci, J. et al. 2013)
The Great Dying: (Permian Period)	~251	~96% of all species were lost, including tabulate corals, and most extant trees and synapsids	Wilkes Land Antarctic Impactor (von Frese, R. et al. 2009), which caused the Siberian Traps (Campbell, I. et al. 1992)
Triassic–Jurassic Extinction Event:	~200	~80% of all species were lost, including all of the conodonts	Central Atlantic Magmatic Province volcanic eruptions (Blackburn, T. et al. 2013)
The K-T Event: (Cretaceous Period)	~66	~76% of all species including all ammonites, mosasaurs, ichthyosaurs, plesiosaurs, pterosaurs, and non-avian dinosaurs	Chicxulub impact event (e.g. Alvarez, L, et al. 1980, & Randell, L. 2015), or Deccan Traps volcanism event (e.g. Courtillot, V. 1990)

2.7 Requirements for Life

The previous definition for life as we know it, stated earlier, makes it clear there are certain things that life requires in order to live and reproduce. Energy is required, be it direct via light or chemicals, (i.e. primary producers, using photosynthesis, or chemosynthesis to create their energy), or be it secondary, via the ingestion of other life-forms. Nutrients and minerals are required that can be used in the organism for building structures, or for chemical reactions, powered by the energy they get via the mechanisms stated above. A safe way to release waste products is also required, as waste products can be toxic to the organisms that produce them. To solve this many ecospheres have symbiotic relationships, the obvious example being animals and plants. The carbon dioxide excreted by animals is ingested by plants, which excrete oxygen, and this oxygen is then ingested by animals, and so on and so forth. Additionally external things are required as well; correct temperature environment, correct pressures, non-toxic (to the organism in question) surroundings, and limited, or no threat of predation, such that would make survival unsustainable.

There are some basic elements that are vital to the continued survival of all species on Earth. These elements are known as the ‘biogenic elements’ and consist of elements such as hydrogen, carbon, nitrogen, oxygen, phosphorus, and sulphur. While different species can require vastly different conditions for survival, growth, and reproduction, these six elements are needed by them all. Other useful elements used by many species are, calcium, chlorine, potassium, sodium, magnesium, and iron. The Earth’s lithosphere contains many of these elements, the most abundant being oxygen, silicon, iron, sodium, calcium, aluminium, and potassium. So, life has not used the most abundant elements in its formation, but rather those that allow some chemical advantage in its make-up or function. It follows then, that life as we know it, could have been formed on any planet or moon

that contains these elements regardless of abundance. However, this presupposes that life did form on the Earth. If it formed elsewhere, where the main biogenic elements were the most abundant, then this could be the reason for their use, rather than other elements; for example calcium is used for vertebrate skeletons, but silicon is more abundant and just as capable (Trimble, V. 1997), so is it that life formed elsewhere, where calcium was more abundant, or is it that life formed on the Earth, but calcium was favoured over silicon for chemically advantageous reasons?

One of the most important chemicals that all life (as we know it) depends on is water, and this is the most abundant chemical in the biomass of the Earth. Water is a polar molecule (i.e. has a net charge across the molecule, known as a dipole moment), and can thus dissolve other polar molecules (such as salts, ammonia, sulphur dioxide, ethanol, and hydrogen sulfide). However, non-polar molecules (such as methane, ethylene, benzene, carbon dioxide, and lipids) do not dissolve into solution in polar liquids such as water, the general rule being 'like dissolves like'. This is why cell membranes are constructed of phospholipids, as they remain stable while immersed in, and surrounded by, water. Water is also vital to life as we know as it, as it is used as the main transport mechanism. In many vertebrate species for example, it is used to transport many components of blood around their systems, as well as carrying waste products away, and can also be used as a cooling mechanism via vasodilatation and vasoconstriction. If life was to form on a world with an abundance of a non-polar liquid such as methane (Saturn's moon Titan has large expanses of liquid methane on the surface, Hanley, J. et al. 2016), its chemistry would be vastly different from life as we know it. As water is such an important molecule for life as we know it, the search for life elsewhere is usually the search for water elsewhere, this is generally known as the 'follow the water' method of searching. But, for life as we know it, water must be in a stable liquid state, and this requires the

correct pressure and temperature ranges being present. Such places where these conditions are met, and liquid water can exist in a stable form, are known as ‘habitable zones’.

2.8 Habitable Zones

The habitable zone around a star is defined as the range of orbital distances around a star, where a planet would have the correct temperature for water to exist in a stable liquid state at the surface (Fig. 2.8), given sufficient atmospheric pressure (Huggett, R. 1995). The habitable zone around a star may be extended slightly if a planet has an atmosphere that can create a greenhouse effect allowing water to stay liquid at an orbital position slightly beyond the range for solar heating alone. Alternatively, such greenhouse effects could also shorten the habitable zone, for example a planet at the inner (hot) edge of a zone that experiences extreme greenhouse warming (similar to Venus) may become too hot to sustain liquid water at the surface. As a star progresses through its life and changes, the hard limits of the habitable zone can change, but there may be orbits that remain in the habitable zone for long enough periods for life to form and evolve, and these are known as ‘continuously habitable zones’ (Hart, M. 1978). The Earth clearly lies in such a continuously habitable zone, as life is known to have existed here for at least 3.8 billion years. Mars may have also been within the habitable zone in the distant past (when its core temperature was much higher than it is today), but today lies just outside it. This is yet another reason why Mars should be included in any origins-of-life discussions.

There are also other places within the Solar System that could potentially be conducive to life that lie outside of the habitable zone, and these are known as ‘habitable niches’. These can be areas where the local environment allows conditions to exist such that some life could survive

there. Such niches where once thought to be very limited or even non-existent, but with the discovery of organisms that can survive in extreme environments, and the possibility of liquid oceans in the outer Solar System (Nimmo, F. and Pappalardo, R. 2016), these niche environments now seem to be abundant throughout the Solar System and beyond.

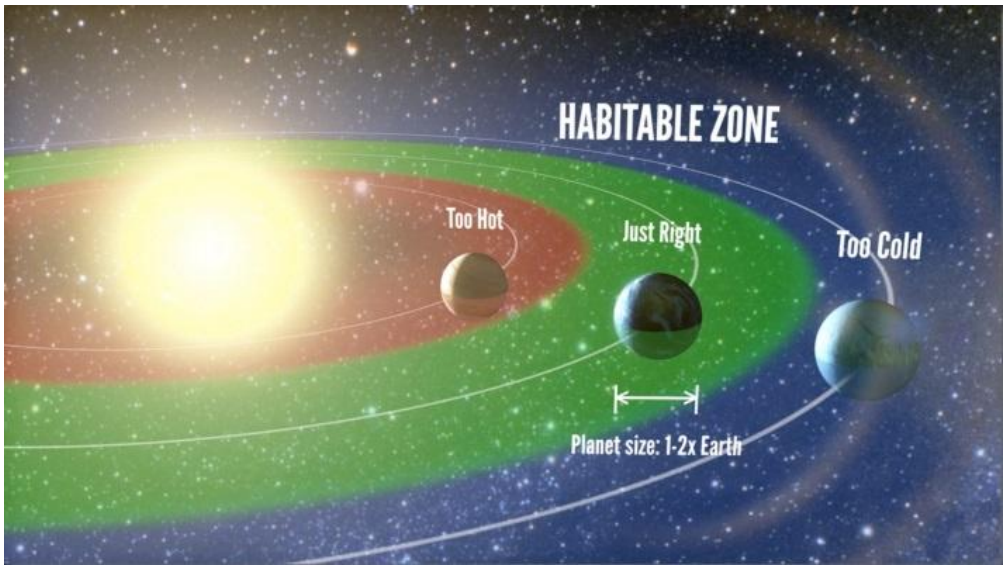

Figure 2.8: Diagram of habitable zone that corresponds to the range of orbital distances where water can exist in liquid form. *Image courtesy: keckobservatory.org*

2.8.1 Extremophiles

Extremophiles are organisms that can thrive in environments that have extreme conditions that would be detrimental to most life-forms (Rampelotto, P. 2010). Almost all niches in the Earth's environment that were once thought to be sterile have shown some forms of extremophile life that exist in them. Many environments that are extremely acidic, hot, cold, pressurised, dark, and radiation drenched, have proved to be home to some

very hardy organisms. The existence of extremophiles has broadened the habitats on Earth that life can exist in, and this has thus widened the habitats elsewhere in the universe that life may be able to exist. Some examples of extremo-tolerant organisms are as follows:

Acidophile: an organism with optimal growth in pH levels ≤3 (Quaiser, A et al. 2003).

Alkaliphile: an organism with optimal growth in pH levels ≥9 (Horikoshi, K. 1999).

Anaerobe: an organism that does not require oxygen. A facultative anaerobe can tolerate both anaerobic and aerobic environments, but an obligate anaerobe will die in an environment with even trace levels of oxygen (Schöttler, U. 1979).

Cryptoendolith: an organism that can live in microscopic spaces inside rocks, such as pores between aggregate grains (Wierzchos, J. et al. 2011).

Halophile: an organism that requires at least a 0.2 Molarity concentration of salt for optimal growth (Ollivier, B. et al. 1994).

Hyperthermophile: an organism that can survive and prosper a temperatures >80^{o}C (Stetter, K. 2006).

Hypolith: an organism that can survive beneath rocks in cold deserts (Cockell, C. and Stokes, M. 2004).

Lithoautotroph: an organism that derives its carbon solely from carbon dioxide and exergonic inorganic oxidation (Ramos, J. 2003).

Metallotolerant: an organism capable of tolerating high levels of dissolved heavy metals in solution (Romaniuk, K. et al. 2017).

Oligotroph: an organism that can survive and prosper in a nutritionally limited environment (Sioli, H. (1975).

Osmophile: an organism that can survive and prosper in an environment with high sugar concentrations (Beuchat, L. (1981).

Piezophile/Barophile: an organism that can survive and prosper in high pressure environments (Sharma, A. et al. 2002).

Psychrophile/Cryophile: an organism that can survive and prosper at temperatures <–15^{o}C (Neufeld, J. et al. 2013).

Radioresistant: an organism that is resistant to high levels of ionising radiation (Sghaier, H. et al. 2008).

Thermophile: an organism that can survive and prosper in temperatures between 45^{o}C – 122^{o}C (Madigan, M. and Martino, J. 2006).

Xerophile: an organism that can survive and prosper in extremely dry, desiccating environments, such as deserts (Hocking, A. and Pitt, J. 1981).

Polyextremophile: an organism that falls into more than one of the above catagories, e.g. a thermoacidophile, an organism which is a combination of the thermophile and acidophile categories; these prefer temperatures of 70-80^{o}C and a pH around 2-3 (Zaparty, M. and Siebers, B. 2011).

With so many types of life that are capable of surviving such extremes in environmental conditions, the range of potential habitats outside of the Earth is far more diverse than was previously thought. Other terrestrial planets, the moons of the gas planets, asteroids, comets, and Kuiper belt objects, even extrasolar planets may all have environmental niches that life could exploit to survive.

2.8.2 Solar System Habitable Niches

Mars is the obvious place to look for life beyond the Earth, as it was once more suitable to the conditions that life requires to form and prosper. However, to date, no direct evidence for life has yet been found, although indirect signs are often highlighted in the news; such as atmospheric methane on Mars being a possible biogenic signature for life (e.g. Meyer, M. and Vasavada, A. 2015), and the famous Martian meteorite ALH84001 (see Chapter 3, Section 3.2) that NASA announced may contain possible extra-terrestrial microfossils.

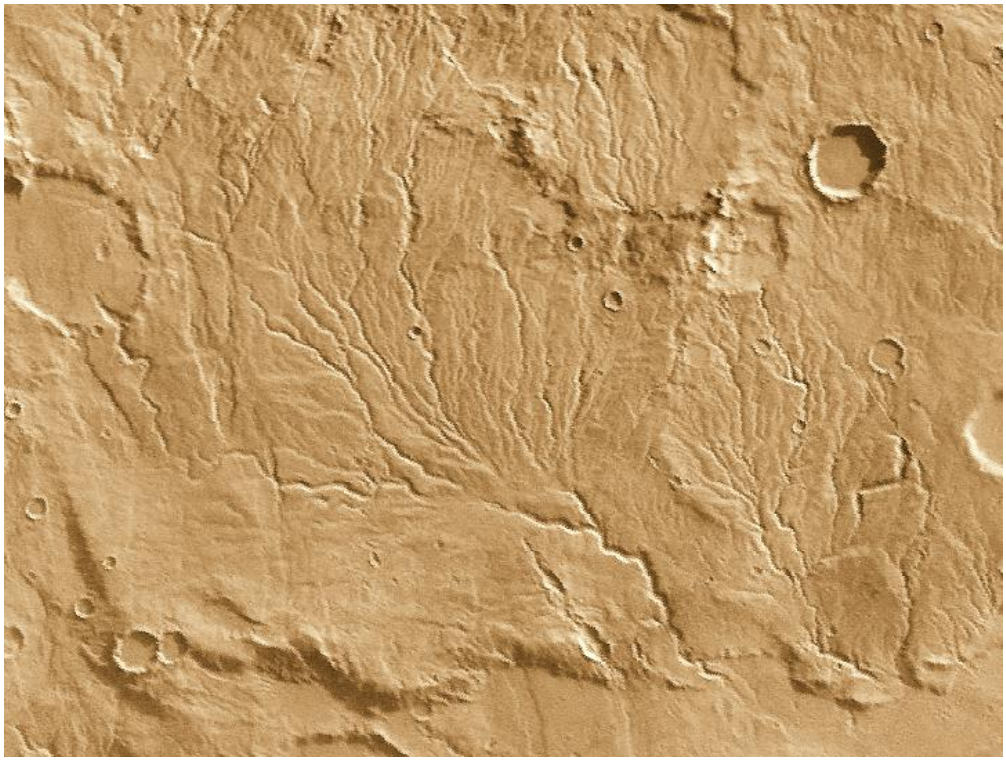

Figure 2.9: Image of the Martian surface taken by Mars Global Surveyor, showing valley networks similar to those on the Earth that are formed by running water. *Image courtesy: Nasa*

The discovery of gullies and possible drainage channels suggest evidence for short lived liquid water on, or beneath, the surface of Mars (e.g. Hargitai, H. et al. 2017). Although exactly how this occurs is not yet understood, it is hypothesised that frozen ice beneath the surface is subject to heating, and may burst through to the surface, and run freely before evaporating into water vapour. Valley networks similar to those on the Earth have also been seen across the Martian surface implying that water may have flowed freely in the past (Fig. 2.9). However, today almost all of Mars' water appears to be frozen as ice, with a small amount present in the atmosphere as water vapour. The atmospheric pressure is too low (~600 Pa) for a standing body of water to exist on the surface.

Another possible location within the Solar System that may be survivable by extremophile life-forms is comets. Comets are made up of three main parts, the tail, the coma, and the nucleus. If life does exist on comets, it is likely to be in the nucleus (Fig. 2.10), the permanently solid part consisting of mostly dust and ice, as well as some organic compounds such as hydrogen cyanide, methane, and formaldehyde, as discovered by the Vega and Giotto spacecraft (Kissel, J. and Krueger, F. 1995).

Comets have highly eccentric orbits that can range from a few years to 10's or even 100's of thousands of years. These eccentric orbits mean that there are extended periods when the comet is away from the sun, so any life on/within the comet would need to be able to survive without the sun as an energy source, or at least be capable of extreme hibernation during the long trips away from the sun. There are also radioisotopes with short half-lives, such as ^{26}Al, that could provide heating to the nucleus that could sustain life buried deep within.

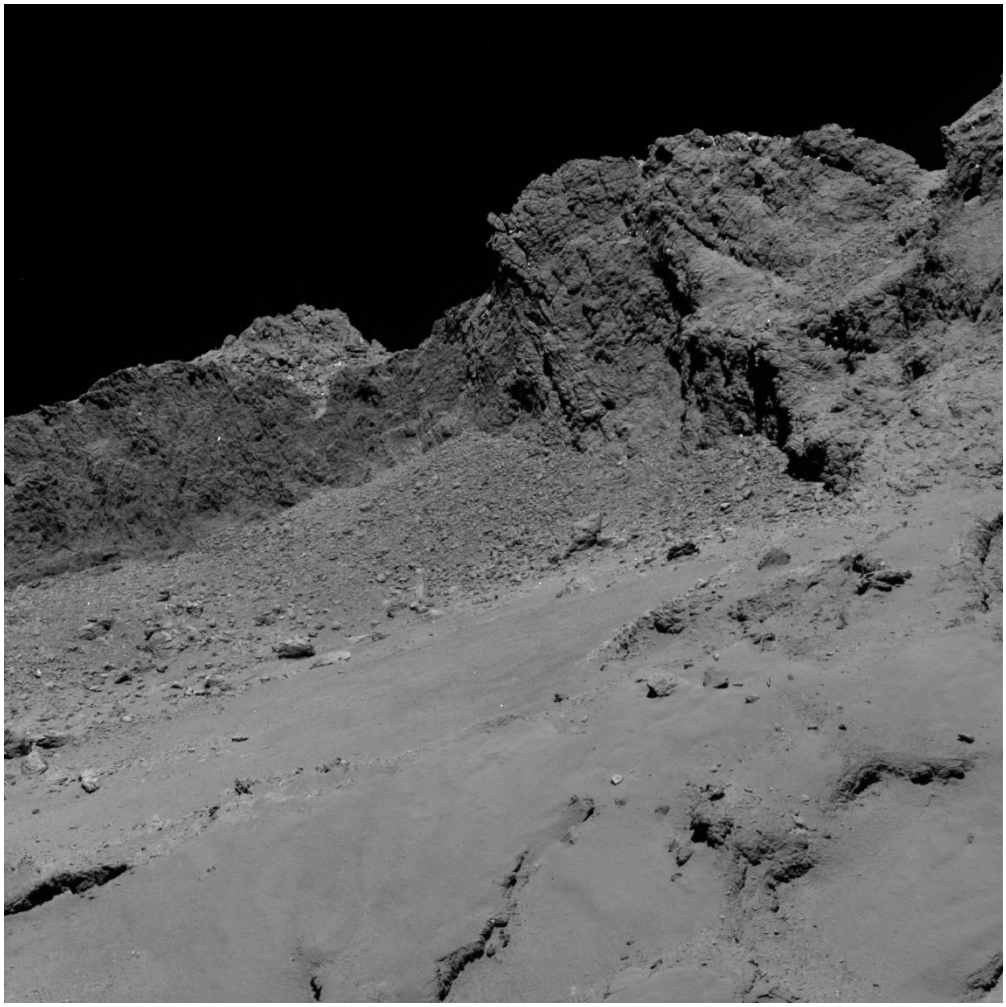

Figure 2.10: Image of the surface of the comet 67P/Churyumov-Gerasimenko from 16 km away taken by the Rosetta spacecraft. *Image courtesy: Esa*

Venus is another place that life may be able to survive. Although Venus today has a crushing surface pressure 92 times greater than the Earth, and an average temperature of 462^{o}C – hot enough to melt lead, there may be life-forms that have evolved to deal with such extremes. Quite often when an environment on Earth has been assumed to be sterilising to life, later discoveries have shown extremophiles happily thriving there. There may be undiscovered polyextremophiles with qualities that incorporate the traits of hyperthermophiles, cryptoendoliths, lithoautotrophs, and barophiles, that

would thrive beneath the surface rocks, or in the cooler upper atmosphere of Venus (Gilli, G. et al. 2017). However, the extreme 'Hell-like' nature of Venus makes it a difficult place to simply explore, let alone carry out sensitive tests for life. Another extreme environment that could house extremophile life is Jupiter's moon Io, a cold landscape of ice volcanoes drenched in radiation. Some form of polyextremophile with Psychrophile and radioresistant qualities may be able to live there. Psychrophile type organisms could also exist on Saturn's cold moon Titan. However, life as we know it needs water, so the 'follow the water' approach would seem to be the most prudent measure when looking for life in the Solar System and beyond.

There is an estimated content of liquid water in the Solar System (outside of the Earth) of ~25-50 times the volume of Earth's 1.3 billion cubic kilometers of water (Frank, E. and Mojzsis, S. 2010), and this would seem an obvious place to look for signs of life (Fig. 2.11).

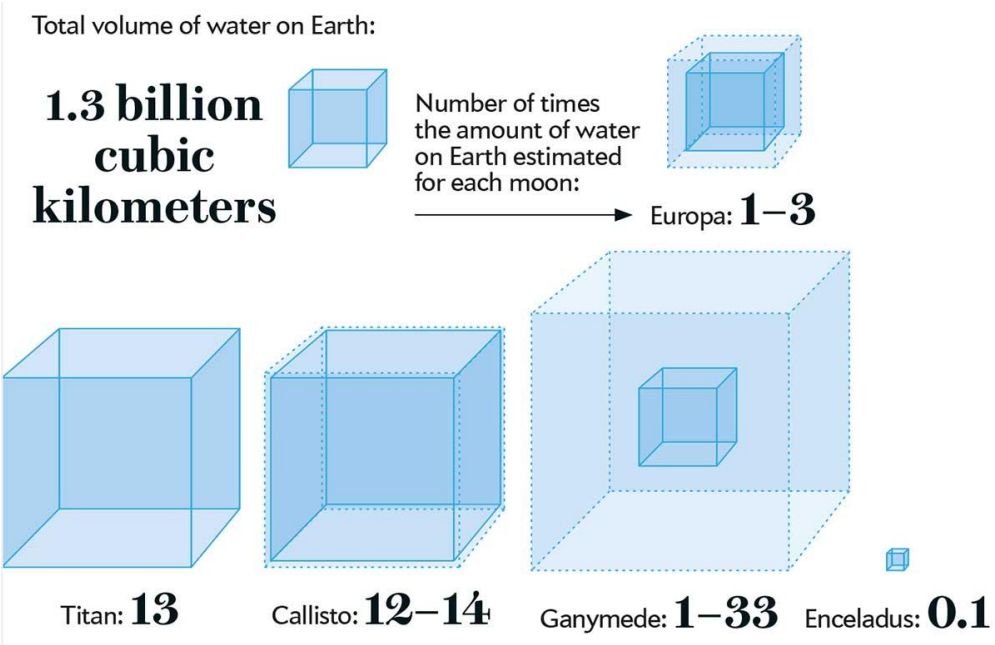

Figure 2.11: Liquid water estimates for some of the moons in the Solar System. *Image courtesy: Amanda Montañez*

The surface of Jupiter's moon Europa shows a dynamic landscape of fractured frozen ice (Fig. 2.12). The tidal stresses imparted onto Europa from Jupiter cause the icy shell to crack, allowing liquid water to rise up and then freeze on the surface. This mechanism neatly explains the lack of impact cratering seen on Europa's surface as well, which indicates it is under constant renewal. The liquid ocean beneath the icy shell is thought to be twice the volume of Earth's entire water content (Fig. 2.11, Chyba, C. and Phillips, C. 2002), making it much deeper, and allowing for a much larger ecosystem – if life is present there.

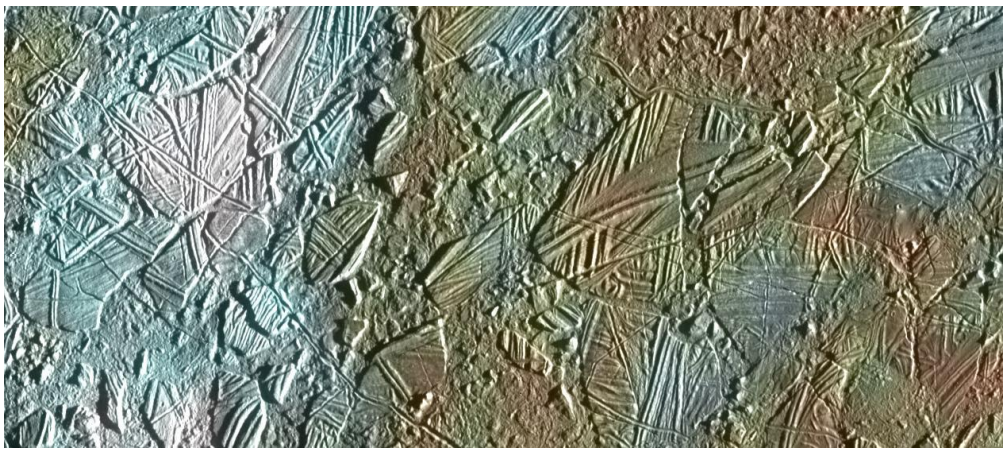

Figure 2.12: Europa's Fractured frozen surface. *Image courtesy: Nasa*

Tidal heating from Jupiter may cause hydrothermal vents at the bottom of the subsurface ocean, and this would be an ideal environment for life, similar to how it is in the oceans of the Earth (Chyba, C. 2000).

Recent observations of icy plumes from the surface of Enceladus, and the thermal anomaly at its south polar region have suggested that this moon too has a subsurface ocean (Roberts, J. and Nimmo, F. 2008). Figure 2.13 shows a diagram of the subsurface ocean mechanism, showing the tidal flexing induced hydrothermal vents that are theorised to keep the subsurface oceans liquid, and the plumes bursting through the icy surface.

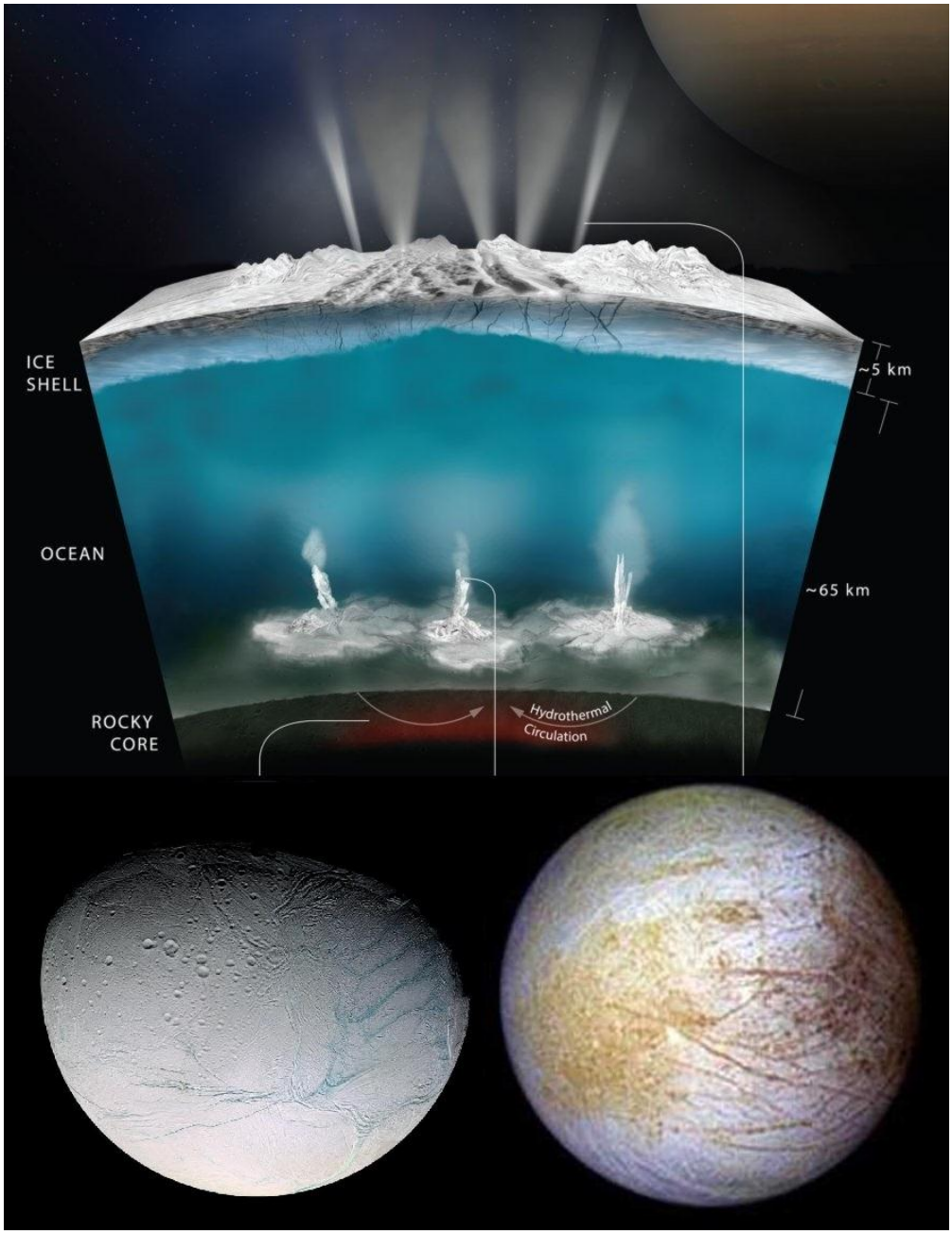

Figure 2.13: Top: Diagram of possible subsurface oceans on moons, and small bodies in the Solar System (such as, **Bottom Right:** Jupiter's fourth largest moon Europa, and **Bottom Left:** Saturn's sixth largest moon Enceladus), hydrothermal vents powered by the gravitational tidal force from the parent planet warm the ocean keeping it liquid. Plumes of water can also melt and break through the surface creating geysers. *Image courtesy: top: dsx.weather.com, bottom left: annesastronomynews.com, bottom right: astronomy.com*

Jupiter's largest moon Ganymede has also recently be theorised to have a saline subsurface ocean. Patterns in the auroral belts, and 'rocking' of the magnetic field suggest the presence of an ocean estimated to be 100 km deep with the surface lying below a crust of ice 150 km thick (Nimmo, F. and Pappalardo, R. 2016). Ceres, the dwarf planet, may also have a subsurface ocean. In 2014 water vapour emissions were detected in several regions, which is unusual for asteroidal bodies, but more common in comets. Ceres also has a large mountain called Ahuna Mons which is believed to be a cyrovolcano which facilitates the movement of high viscosity cryovolcanic magma consisting of water ice softened by its salt content (Ruesch, O et al. 2016).

Juptier's moon Callisto, the dwarf planet Pluto, Neptune's moon Triton, and Saturn's moon Titan, have all recently been theorised to contain subsurface oceans (Fig. 2.14, Nimmo, F. and Pappalardo, R. 2016).

The Late Heavy Bombardment that delivered much of the Earth's volatiles, could also have delivered volatiles, and complex organic materials, to these moons and dwarf planets ~4 billion years ago. They would have been much warmer at this time, and thus would have had much thinner icy shells, or even, possibly, short-term exposed liquid water at the surface.

The implication is that the minerals and biogenic elements necessary for life as we know it may be present in these oceans, making them a place where life could have had a genesis and subsequent evolution. Therefore these subsurface oceans would appear to hold the best chance of finding other (extant) life in the Solar System, and this is where the future of the search for extra-terrestrial life is heading. NASA has announced the 'Europa Clipper' mission to be launched in the 2020's that will perform multiple fly-bys of Europa attempting to determine if Europa is habitable, possessing all three of

the ingredients necessary for life; liquid water, chemical ingredients, and energy sources sufficient to enable biology (see nasa.gov/europa).

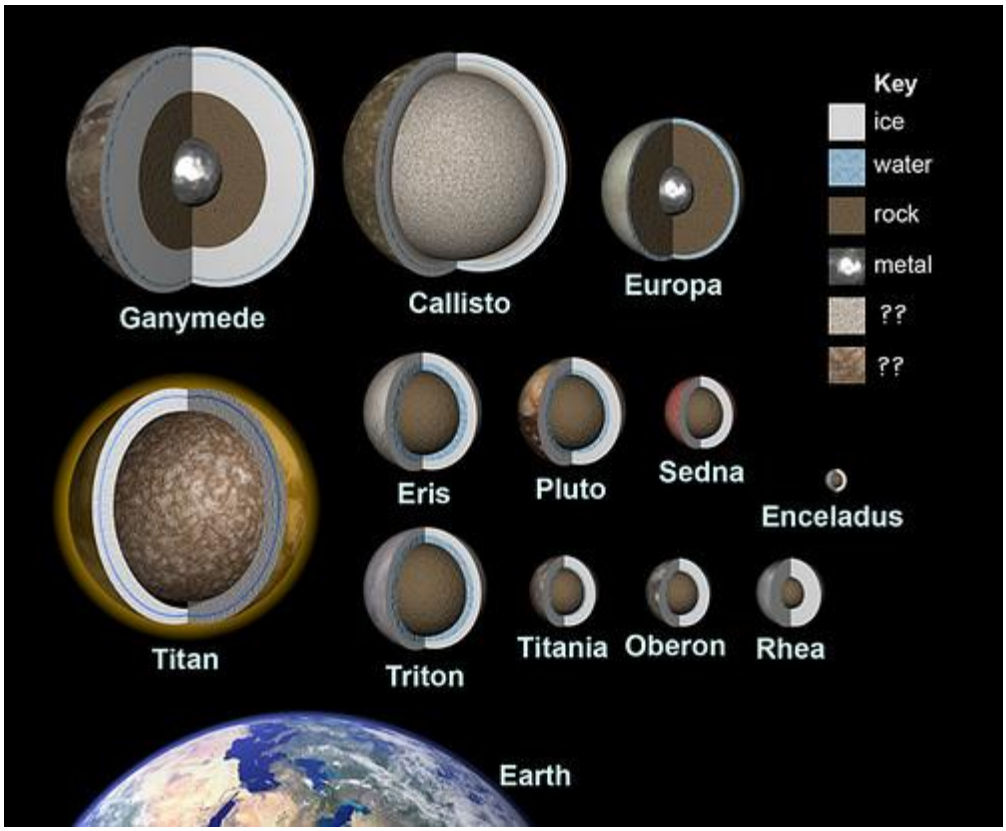

Figure 2.14: Some of the possible bodies where subsurface oceans may exist in the Solar System. *Image courtesy: farm9.staticflickr.com*

2.8.3 Extrasolar Habitable Zones

Potential habitats for life could also be found further afield, around other stars in the galaxy, so-called extrasolar planets, or exoplanets. There have been many exoplanets discovered in recent years that are within the habitable zone of their parent stars, such that liquid water could exist if the

planet was capable (Vogt, S. et al. 2010). This rules out gas planets, and planets with atmospheric pressures too low, but even so, this leaves a potential huge number of planets that could support life. Earth-like planets are the most likely for meeting the criteria for supporting life, these are generally known as Super-Earths as they tend to be larger than the Earth, but this is mainly due to detection bias as even these Super-Earths are just within current detection limits, so it is not that smaller ones do not exist, it is simply that we cannot detect them yet.

In 2010 a Super-Earth that was unlike any previously detected was discovered. The system (Star: 61 Virginis) was the first known example of a G-type sun-like star hosting a Super-Earth mass planet. Other multiple planet systems have been detected orbiting other types of stars with orbital periods less than an Earth year; some of these are, HD 75732 (55 Cnc), HD 69830, GJ 581, HD 40307, and GJ 876 (Vogt, S. et al. 2010).

In 2013 the Kepler Telescope was designed to hunt exoplanets and, since its launch, it has more than doubled the known number of exoplanets. Data from the telescope has led astronomers to suggest that there could be as many as 40 billion Earth-sized planets that are orbiting in the habitable zones of sun-like and red dwarf stars within the Milky Way Galaxy, with 11 billion of these orbiting sun-like stars (Petigura, E. et al. 2013).

Proxima Centauri b, located about 4.2 light-years from Earth in the constellation of Centaurus, is the nearest known exoplanet. It is orbiting in the habitable zone of its star. The habitable niches of solar systems in the Milky Way Galaxy are also of particular interest to the emerging field of ‘habitability of natural satellites’, because planetary-mass moons with habitable niches around planets in the other solar systems may outnumber the planets, just as they do in our Solar System.

So far the Kepler Telescope has discovered more than 1000 confirmed exoplanets, and of these just 12 are less than twice the size of the Earth, and orbit within the habitable zone of their parent stars. Again, this is mainly due to detection bias; with improved detection capabilities the percentage of exoplanets detected that fall into this category may increase. Figure 2.15 shows their relative sizes to the Earth (for more information on the Kepler telescope see nasa.gov/kepler).

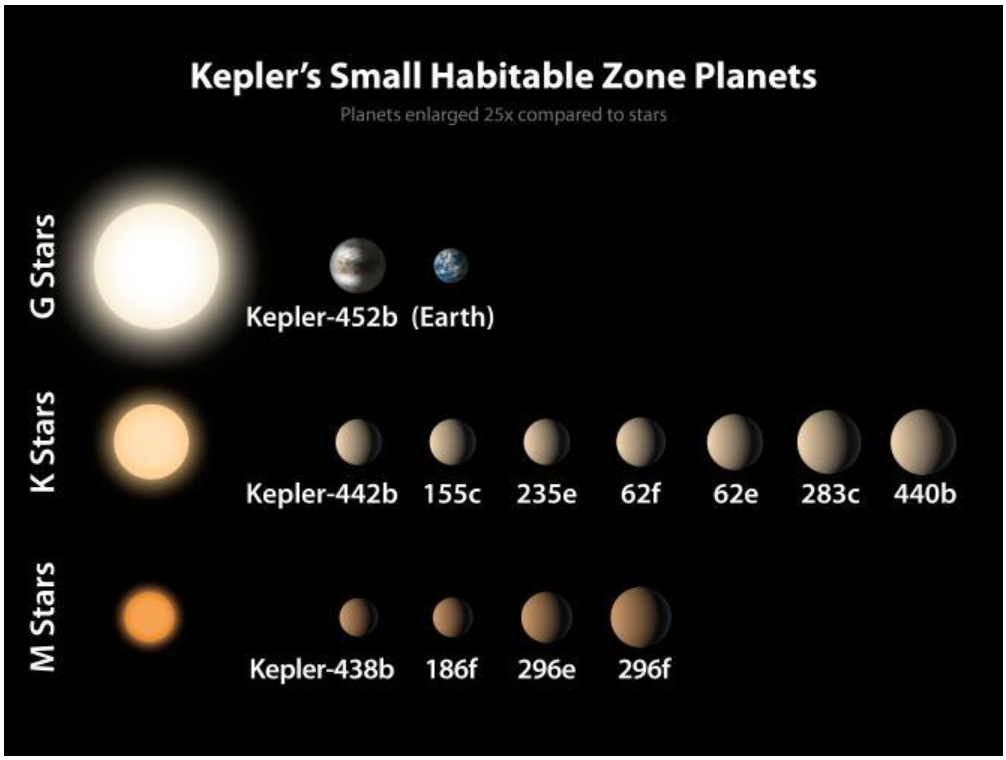

Figure 2.15: The 12 exoplanets Kepler has found that are less than twice the size of the Earth and have orbital periods less than one Earth year. The planets are shown with relative sizes to each other, but are enlarged 25 times compared to the stars for ease of viewing. *Image courtesy: Nasa*

2.9 Conclusion

This chapter looked at the history of the Earth from its formation in the Solar System through to the emergence of complex higher life-forms. A discussion of what constitutes life was then presented, and the possible origins of life were considered. Then, the history of life upon the Earth and the requirements for life were carefully examined. It was concluded that life as we know it depends upon certain biogenic elements and in particular the chemical, water. In light of this, a 'follow the water' style examination of the Solar System was presented to determine what possible habitable niches may exist within the Solar System that life could inhabit and successfully survive. Further to this, extrasolar planets, or exoplanets, were also considered for the habitability of life, and some of the known terrestrial like planets that orbit within the habitable zones of their parent stars were presented. The next chapter will look at the mechanisms for how life might naturally migrate between such habitable planets.

CHAPTER 3
PANSPERMIA –
DESTINATION UNKNOWN

"Is there anybody out there?
Is there anybody out there?
Is there anybody out there?
Ah, is there anybody out there?''

Roger Waters

3.1 Introduction

This chapter describes the hypothesis of panspermia, beginning with a look at the history of the idea, and then some of the variations of the theory. The dangers and constraints of panspermia are then discussed, before a discussion on the possible routes within the Solar System, and the timescales involved, that may be conducive to the idea of panspermia.

3.2 What is Panspermia?

The hypothesis of panspermia – the migration of life-forms through the universe – is a very old theory. Ancient Sumerian creation myths such as the 'Epic of Gilgamesh' speak of great beings the 'Anunnaki' (literally, 'those who from heaven to Earth descended') that came to the Earth from their home 'Nibiru' far in the heavens and created life on the Earth. The

Babylonians tell of similar tales in the 'Enuma Elish' with the great creator Marduk (Sitchen, Z. 1976). The African Dogon tribe have oral traditions that claim they are descendents of 'Sky People' that came from a planet of the star Sirius (Temple, R. 1998). In the traditions of the native American Spomi-tapi-ksi or "Blackfoot'' tribe, the 'Above People', or 'Sky Beings', were the first creations of the Blackfoot god Apistotoke. They believe the celestial bodies are representations of real beings, the Sun, Natosi, the moon goddess, Komorkis, the immortal hero Morning-Star, and all the stars in the sky. The 'Above People' are said to have their own land and their own society above the clouds (Clark, W. 1908). Such myths and legends are cited by those who believe in the 'Ancient Astronaut' theory, suggesting intelligent life visited the Earth in the remote past. If such a theory were true, and life was created this way, it would be a form of 'directed panspermia' (see Section 3.3.2).

As fascinating as these ancient myths are, the first mainstream evidence of the panspermia theory is seen as far back as 500 BC with the Greek Philosopher Anaxagorus who proposed the idea as a possible origin for life on Earth (Roten, C. et al. 1998). The idea was wildly radical for the time and quickly discarded. Although many noteworthy philosophers and scientists through the years have believed in the concept of alien life (see Chapter 1) the idea of panspermia was not revisited seriously until the late 19th century. Scientists such as Helmhotz, Richter, and Lord Kelvin proposed 'Cosmozoa', a theory suggesting life may have arrived on the Earth in the form of seeds from some other world inhabited by life, via meteorite impacts (Jackson, F. and Moore, P. 1962, Crowe, M. 1986). A few years later in 1903, Arrhenius proposed a similar theory, and then in 1908 he renamed the theory as panspermia, meaning 'seeds everywhere' (Arrhenius, S. 1908). In Arrhenius' theory there were no meteorites to deliver life, he instead proposed bacterial spores could exist in space and travel via stellar radiation pressure, falling to planets through gravitational attraction (see Section

3.3.1). However, with the advent of the understanding of cosmic rays and the radiation environment of space, the idea lost favour again, and spontaneous emergence through chemical reaction became the favoured theory for the origin of life on Earth (see Davis, R. 1988).

Over the decades little thought was given to panspermia scientifically (although the 'Roswell incident', and others like it, did bring panspermia as a concept back in many non-scientific works). Sir Fred Hoyle made a suggestion that sudden outbreaks of diseases in localised areas could be due to panspermia (Hoyle, F. and Wickramasinghe, C. 1980). However, these claims have largely been refuted or ignored, as viral pathogens evolve alongside their host organisms. A virus from an extraterrestrial environment would be unlikely to have a make-up that was readily compatible with life on Earth, and would thus be unable to use Earth life as a host organism to infect and replicate.

In 1996 panspermia was thrust back into the fore again as NASA scientists announced an amazing discovery to the world's press; "Extraterrestrial Life!".

These NASA scientists claimed to have found evidence for fossilised life (a type of bacteria) inside a meteorite (McKay, D. et al. 1996), known to have originated on Mars (Mittlefehldt, D. 1994); the now famous Martian meteorite ALH84001 (see Fig. 3.1), found on the Allen Hills ice sheet in Antarctica where it had rested since falling around 13,000 years before being collected in 1984. Carbonate globules discovered inside the meteorite contained small nano-structures that looked much like bacterial micro-organisms (see Fig. 3.1). Although other meteorites have since been found containing similar structures, seemingly strengthening the claims of McKay et al. (Gillet, P. et al. 2000, Gibson, E. et al. 2001), the claims have been refuted by many other scientists (Sears, D. and Kral, T. 1998, Buseck, P. et

al. 2001). To this day it has not been conclusively shown how these features in the meteorite could have been formed. A 2004 press release by NASA (see nasa.gov – news releases 2004) claimed a team lead by D. C. Golden had recreated similar features in a laboratory environment without biological inputs. However, McKay claims that these results were obtained using unrealistically pure raw materials and will not therefore explain many of the features described in the 1996 paper. McKay later stated to USA today (Crenson, Matt 2006-08-06) that any plausible inorganic model "must explain simultaneously all of the properties that we and others have suggested as possible biogenic properties of this meteorite".

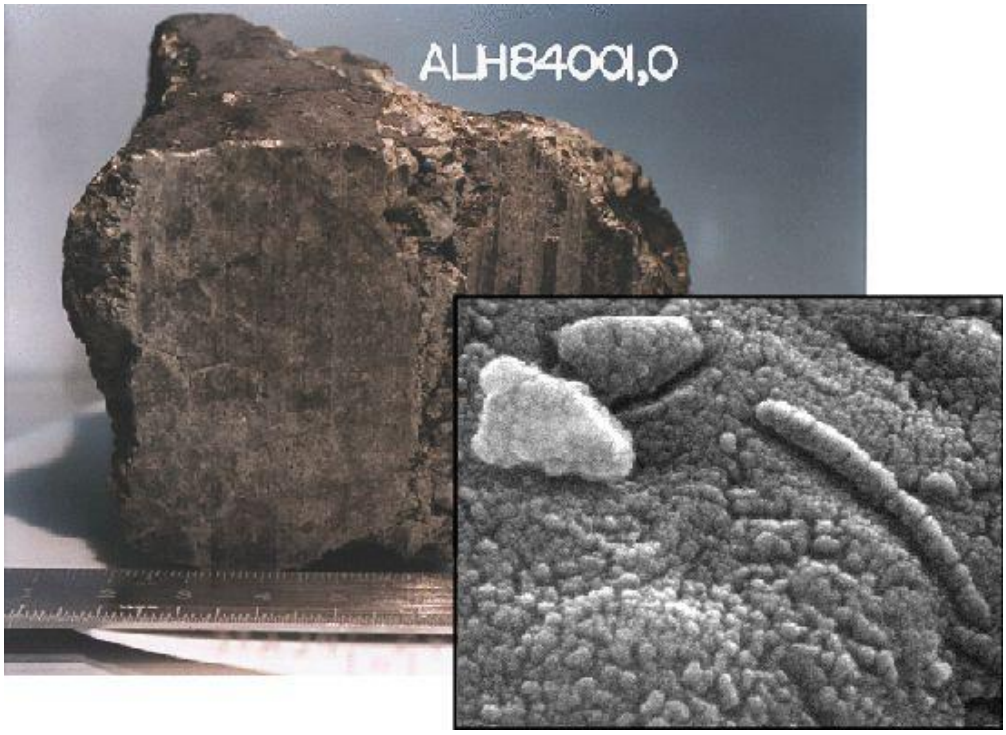

Figure 3.1: The controversial ALH84001 Martian meteorite. Inset: the electron microscope image showing tiny structures similar to microfossils that were thought to be evidence of fossilised life from Mars. *Image Courtesy: aerospaceweb.org*

The structures within ALH84001 are 20-100 nm (in line with the theorised nano-bacteria) which is much smaller than any known cellular life, and the basis for the structures being biogenic in origin is due to morphology alone. However, the scientific consensus is that "morphology alone cannot be used unambiguously as a tool for primitive life detection." Interpretation of morphology is notoriously subjective, and its use alone has led to numerous errors of interpretation (Garcia-Ruiz, J. 1999). Therefore the general consensus in the scientific community currently is that extraterrestrial life is still yet to be discovered.

However, panspermia received another boost when Burchell, M. et al. (2001) showed that bacteria could survive impacts of up to 5.4 km s^{-1}, the pressures of such an impact being ~30 Gpa. This was the first definitive proof that a life-form really could survive the type of impact needed to naturally deliver life to another planet, and beckoned a resurgence in work relating to panspermia. Flyer plate experiments showed that the lichen species *Xanthoria elegans* could survive pressures above a few GPa (Horneck, G. et al. 2001b, 2008), and in 2013, Price, M. et al. showed that yeast spores could survive impacts up to 7.4 km s^{-1}, in a similar pressure range to bacterial spores ~30 GPa.

Recently Benner, S. and Hyo-Joong, K. (2015) presented evidence that the early Martian surface provided a much more appropriate setting for the necessary steps for life to emerge chemically; the main claim being the desert like expanses (as opposed to an Earth flooded at the same time), and the abundance of, molybdenum. This lead to the speculation that life could have first originated on Mars, and then through a panspermia-style impact was transported to the Earth, and as the climates of both planets changed, life thrived upon the Earth, but died out on Mars. If such a claim was ever proven true, the implications would be enormous. These recent findings have kept

the concept of panspermia firmly in the limelight, and many researchers now work on similar themes around the world.

3.3 Variations of Panspermia

The previous section described panspermia as a method for life-forms to migrate throughout the universe. A more detailed description, providing more information on the panspermia hypothesis is presented in this section. While the main idea of panspermia is the migration of life throughout the universe, there are variations to this main theme, and these differing individual theories can be combined together with each other, to allow for the most optimal transport conditions for life.

3.3.1 Radiopanspermia

Radiopanspermia was first proposed by Arrhenius in 1903 (although he did not name it as such at the time). Arrhenius proposed that microbial organisms could naturally exist in space, and that they could be propelled through the interstellar medium via the pressure of stellar radiation. If, while drifting through space, the organisms pass close to a planet, the gravitational pull of that planet would pull them in, and bring them down to the surface of that world. Although the main criticism to this version of the theory is that the organisms have no protection against the harsh radiation environment of space (Secker, J. et al. 1996, Clark, B. et al. 1999), recent studies aboard the International Space Station have shown that in fact several species are capable of surviving prolonged exposure to space with no protection (Rebecci, L. et al. 2009, Rebecci, L. et al. 2011, Vukich, M. et al. 2012, Frosler, J. et al. 2017). The bacterium *Deinococcus geothermalis* as a biofilm has been shown to survive simulated space-like conditions of radiation (Frosler, J. et al. 2017). The Tardigrade Resistance to Space Effects (TARSE) project showed that microgravity and radiation had no effect on survival or

DNA integrity of active tardigrades. During the flight mission, tardigrades molted, and females laid eggs. Several eggs hatched, and the newborns exhibited normal morphology and behaviour (Rebecci, L. et al. 2009). Additionally, the Endeavour mission in 2011 carried out the TARDIKISS (Tardigrades in Space) experiment, with initial results showing that microgravity and cosmic radiation did not significantly affect the survival rate of tardigrades (Rebecci, L. 2011, Vukich, M. 2012). However, Rizzo, A. et al. (2015), showed there was a significant difference in activities of reactive oxygen species (ROS) scavenging enzymes, the total content of glutathione, and the fatty acid composition between tardigrades sent into space and control animals on Earth.

The current Japanese Tanpopo mission hopes to further test life to the extremes of the space environment at the Exposed Facility of the International Space Station (Kawaguchi, Y. et al. 2016).

3.3.2 Directed Panspermia

Directed panspermia is a deliberate seeding of life from one planet to another via artificial means, such as a spacecraft. Crick, F. and Orgel, L. (1973) argue that if humans are now capable of travelling into space and seeding life onto another world by design, then other intelligent life in the universe with space faring capabilities could have seeded the Earth ~4 billion years ago while it was still barren of life. While directed panspermia has the advantage of overcoming the radiation issues associated with radiopanspermia, it does require the assumed presence of intelligent alien life more than 4 billion years ago. However, this variation of panspermia may have already occurred, accidently. In the early years of space exploration there was no stringent precautions in place to avoid unwanted organisms

from existing on, or within, these early spacecraft. Even with modern day precautions, there is always a chance that a rogue organism could find its way into a spacecraft destined for another planet, and with lander missions to Mercury, Venus, the Moon, Mars, Saturn's moon Titan, the asteroids Eros, and Itokawa, and the comets 9P/Temple 1, and more recently, 67P/Churyumov-Gerasimenko, already completed, who knows how many bodies in our Solar System we may have accidently transferred life to. Indeed, 30 months after the end of the Lunar Surveyor III lander completed its mission, the crew of Apollo 12 brought back the camera, and bacteria (*Streptococcus mitis*) were discovered inside the camera housing (Clark, B. et al. 1999). Because of this discovery and similar concerns, NASA implemented the Outer Space Treaty. This ensures the design of any interplanetary mission complies with the Planetary Protection Policy (see planetaryprotection.nasa.gov/overview - for an overview), which aims to prevent the biological contamination of both the target body, and the Earth (in the case of a sample return mission).

3.3.3 Lithopanspermia

Lithopanspermia or 'rocky panspermia' describes the viable propagation of micro-organisms through space on or within rocky bodies such as comets, asteroids, and meteors (Melosh, H. 1988). This involves launching rocky, life-bearing, material into space from a planetary surface, its transfer around the Solar System, and its eventual impact onto a new planet. There are a number of steps involved in the survival and transfer process of an organism to another Solar System body (for example, see De Vera, 2012, and Mileikowsky et al., 2000). It has to survive: (i) the initial impact that launches it into space from its parent body; (ii) the freezing journey through the radiation and vacuum of space; (iii) the impact of delivery onto the new

potential habitat. The delivery onto a new body will likely involve a high speed impact (above 1 km s^{-1}) which would generate a significant shock pressure in the range of 10's of GPa. If ejected rocks could successfully transfer viable micro-organisms across the Solar System, then the micro-organisms would need to be able to survive the shocks involved in both the initial impact that launched the rocks, and the resulting impact that delivers them to the new body. This variation of panspermia, like radiopanspermia, is natural and requires no intelligent life for it to occur. However, unlike radiopanspermia, organisms trapped within porous rocks, or frozen in ice, are afforded some protection against the radiation environment of space by the very materials they are trapped within. Therefore, the main obstacle for life to overcome, to become a successful candidate to survive a lithopanspermia style journey, is the impact into the target body; this is further discussed in the next section. Not long ago it was believed that no organism could possibly survive the extremely high shock pressures of an impact onto a planetary body from space. However, recent studies have shown that several microbial species (in both active and spore states) can be successfully transferred from a projectile to a target in impacts above 1 km s^{-1}, and thus survive shock pressures in the GPa range (Burchell et al., 2001, 2004); and the list of potential organisms that can survive such extremes, is steadily growing (see Section 3.4.4 for more detail). This version of panspermia can also be affected by the same propulsion method as radiopanspermia, namely stellar radiation pressure, as well as gravitational attraction.

With the protection from the radiation environment of space inherent in this version of panspermia, it is considered the most likely case for natural migration through space. As this is the version of panspermia being considered in this research, the next section will provide a more detailed look at the process of a natural interplanetary journey.

3.4 An Interplanetary Journey

Lithopanspermia as a concept has three main stages that any organism on the journey would have to survive (See Fig. 3.2). The first stage of any interplanetary journey is getting off the planet, and into space. The second stage of the journey is travelling through the harsh environment of interplanetary, interstellar, or even intergalactic space. The third stage, upon arrival at the destination planet, is the descent to that planet's surface. These three stages and their implications for any potential panspermia-capable life-forms will be discussed in depth in this section.

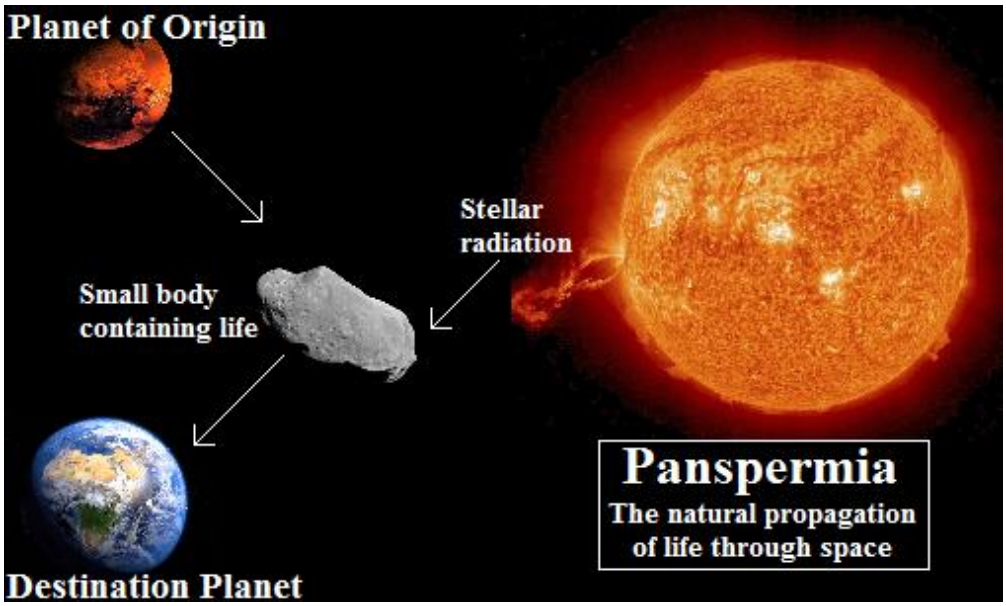

Figure 3.2: The three stages in the interplanetary journey for any potential lithopanspermia-capable life-forms. **Stage one:** ejection from the planet of origin at a velocity higher than the escape velocity. **Stage two:** the journey through space on or within rocks and/or ice. **Stage three:** descent to the planet's surface via hypervelocity impact. *Figure composed by author*

3.4.1 Impact Cratering.

For lithopanspermia, rocks and/or ice must be ejected into space from the planet's surface, this inevitably requires a highly energetic process as the material must be accelerated to a velocity beyond the planet's gravitational escape velocity (for the Earth, this is 11.2 km s^{-1}, whereas for Mars it is 5.08 km s^{-1}). While it is possible for volcanism to eject dust particles (capable of containing life) into space at velocities greater than the escape velocity of the Earth (Wilson, L. and Keil, K. 1997), such particles are very small and would provide little protection against radiation, and would likely burn up during entry into a planetary atmosphere. Realistically, much larger particles would be required for lithopanspermia to be successful, and volcanism cannot lift such particles into space at the necessary velocities. To naturally lift larger particles into space at velocities greater than the escape velocity requires the violent process of a hypervelocity impact. A hypervelocity impact is an impact in which the projectile's velocity is greater than the sound speed of the projectile material. The sound speed is determined as the speed at which a shockwave travels and dissipates through a material (Burchell, M. et al. 1999). In such an impact, when the front of the projectile makes contact with the target and experiences extreme deceleration, the shock information generated does not have time to reach the back of the projectile, before the back has continued to travel some distance further. This causes an extreme compression of the projectile, generating extreme temperatures, often vaporising the material. Impacts such as these are typically over a few km s^{-1}.

When hypervelocity impacts occur onto solid bodies (e.g. a rocky or icy planet), craters are formed. There are two types of craters involved in large scale hypervelocity impacts: simple craters, and complex craters. Simple craters (see Fig. 3.3 for an example) look fairly circular; have a raised

rim, an almost parabolic cross-section, and a rim-to-rim diameter that is approximately five times the rim-to-floor depth (Melosh, H. 1989). However, at a given threshold diameter (determined by the local gravity of the target body) the structure is affected by gravitational collapse of the crater, forming a complex crater (see Fig 3.4 for an example). Melosh, H. (1989) determines the relation to be the inverse of the local force of gravity per unit mass, (i.e. the higher the local gravity, the lower the threshold diameter for collapse). This in turn gives threshold diameters for the Earth of ~2 – 4 km, for Mercury ~7 km, and for the Moon ~ 10 – 20 km.

Figure 3.3: Meteor Crater in Arizona, USA; an example of a simple crater. The crater is 1.2 km wide, approximately 50,000 years old, and was created by an asteroid travelling at 11.9 km s^{-1}, releasing more energy than a 20 megaton thermo-nuclear explosion. *Image courtesy: meteorcrater.com*

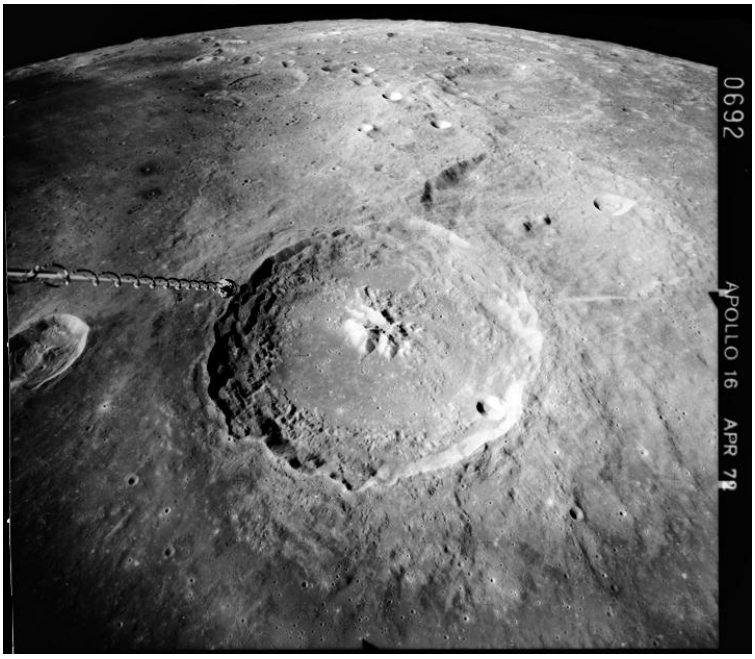

Figure 3.4: An oblique view of the 100 km wide Theophilus Crater on the Moon; an example of a complex crater – note the central peaks. Image taken with the Apollo 16 metric mapping camera. Compared to the other craters on the Moon, this is a relatively young one. *Image courtesy: Nasa*

During complex crater formation, the material compressed beneath the crater can produce a significant upwards force as it rebounds after the initial compression from impact. This force can distort the shape of the final crater producing a central peak (and in some cases, inner rings of peaks, or wall terraces). However, not all materials behave the same way. Bray, V. (2009) notes that, no peak-ring centres are observed on the icy satellites of Jupiter, and instead central pits are witnessed, sometimes with raised rims (see Melosh, H. 2009 for a description).

There are five phases of crater formation before the final crater is formed (see Fig. 3.5). During the compression phase (which occurs immediately after the projectile makes contact with the target body), a

significant fraction of the projectile's kinetic energy is transferred to the target body, and due to the conservation of energy, the projectile reduces in velocity as the target material resists penetration. As the projectile impacts into the target body it pushes material out of its way, compressing and accelerating it. These changes in velocity and morphology are affected by shock waves, originating at the point of contact and propagating into both the projectile and the target body. For most hypervelocity impacts the peak shock pressures tend to be in the GPa range as opposed to most material strengths being in the MPa range (Melosh, H. 1989). When the shock pressure is much higher than the material strength, the material will 'flow' and act as though it has no strength, behaving like a fluid. As the projectile is unloaded from the high pressure state it can melt, or even vaporise.

This phase of the impact process is only considered to last as long as it takes for the initial shock wave (and subsequent rarefaction wave) to cross the projectile. Melosh, H. (1989) determines this to be approximately:

$$T_C = \frac{L}{V_i} \qquad \text{(Eq. 3.1)}$$

where T_c is the time it takes the shock wave to cross the projectile (s), L is the length of the projectile (m), and V_i is the velocity of the projectile (m s^{-1}). To give an example, a hypervelocity impact with a 10 cm meteorite impacting the earth at 20 km s^{-1}, T_c would be ~5 μs. Only in truly giant impacts does this phase exceed one second; at 20 km s^{-1}, an impactor would have to be 20 km or more.

After the compression phase, the excavation phase begins. The shock wave continues to propagate through the target body in an approximately hemispherical wavefront. This wavefront sets into motion the material it passes through. This opens the crater via a subsonic evacuation flow of

material away from the epicentre of the impact event. This is why craters appear fairly circular, and their diameters are much larger than the diameters of the projectiles that caused them. However, as impact velocities reduce below the regime of hypervelocity, the crater cavity grows at a decreasing rate until eventually, when the impact induces pressures that are much less than the material strength of the target body, crater formation is halted altogether, by the strength of the target material and the lithostatic pressure applied by the rocks surrounding the impact site (Melosh, H. 1989).

As the shock wave spreads, it dissipates, and the shock pressures fall. Accordingly, this allows the material strength, and gravity, to become more important to the process, towards the end of this phase (eventually leading to the modification phase). The evacuation phase is much longer than the compression phase. For example, if the material strength is ignored (as is the case when impact pressures are orders of magnitude higher than the material strength of the target), then the time taken for the maximum depth of the crater to be achieved can be approximated to the freefall time an object experiences falling the same distance:

$$T_e = \sqrt{\frac{2D}{g}} \qquad \text{(Eq. 3.2)}$$

where T_e is the time to evacuate the crater (s), D is the maximum crater depth (m), and g is the acceleration due to local gravity (m s^{-2}) (Melosh, H. 1989). To give an example, consider Meteor Crater in Arizona (see Fig. 3.3). At a depth of 170 m and Earth's local gravity being 9.81 m s^{-2}, the excavation phase would have lasted just 5.89 s. The 'transient crater' will then begin to collapse under gravity as it enters the modification phase. In this phase, loose debris can fall down steep inner walls, accumulating at the base of the crater. In larger impacts, elastic rebound provides an upthrust force on the crater.

This can lead to the formation of central peaks, as described in complex craters above. The length of this phase is of a similar order of magnitude to the excavation phase. It can be approximated as the time taken for a piece of material to traverse the slope of the crater:

$$T_m = \sqrt{\frac{D}{g}} \qquad \text{(Eq. 3.3)}$$

where T_m is the time for modification (s), D is the maximum crater depth (m), and g is the local gravity (m s^{-2}) (Melosh, H. 1989). Considering Meteor Crater again, the modification time would be 4.2 s.

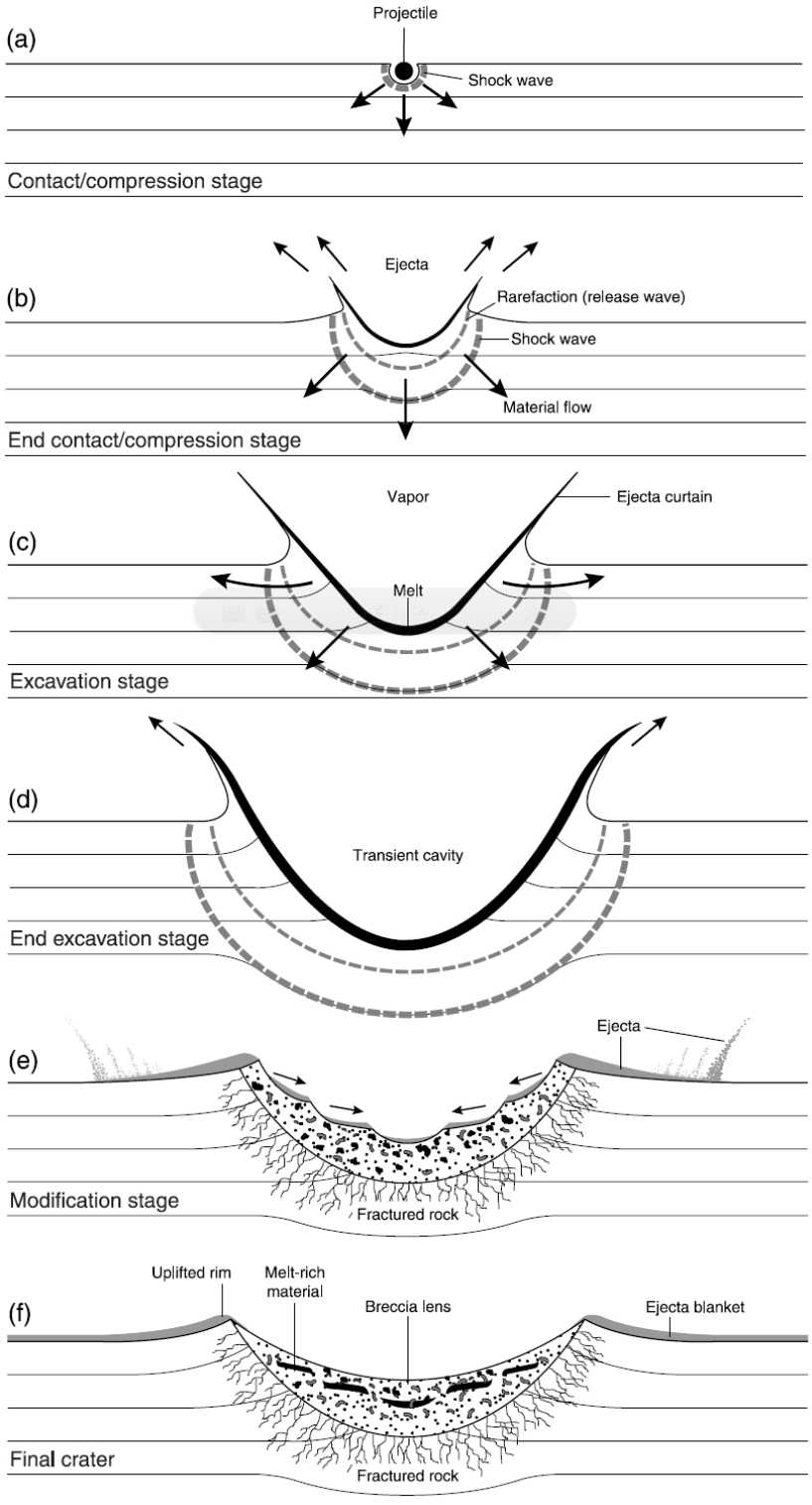

Figure 3.5: The five phases of crater formation (French, B. 1998).

3.4.2 The Ejection of Life

When giant impacts occur, much of the surface materials where the crater is formed are vaporised. Those which are not vaporised are thrown as ejecta, much of which falls back to Earth some distance from the crater, forming an ejecta blanket around the crater. However, some of this ejecta gets thrown into space and escapes the gravity of the Earth. It is this ejecta that has the potential to lift micro-organisms into space for a panspermia style journey.

Organisms that reside underground, or are frozen in subsurface ice, seem the most likely to survive such a process, as they will not be directly affected by the vaporisation of the surface layers above them during impact. Cockell, C. and Barlow, N. (2002) have shown evidence of micro-organisms at the typical depths in the Earth that rocks would be ejected into space should such an impact occur. Horneck, G. et al. (2001b) have tested the survivability of bacteria to the pressures of a large scale impact that could eject them into space via explosive shocks up to 32 GPa. Although the percentage of survival was low (0.01%), this is a positive result showing 1 in every 10,000 organisms could survive such ejection from a planet.

Another important effect that can occur during a hypervelocity impact, which has significance for panspermia (notably, the ejection of life into space stage) is known as ‘spallation’. As the shock wave of an impact radiates outward from the contact point of impact, the pressures can break material away from the body (these are known as spall, see Fig. 3.6), and these can be ejected from the surface with enough force to escape the gravitational field of the Earth, and any life on such spall material would also be carried into space.

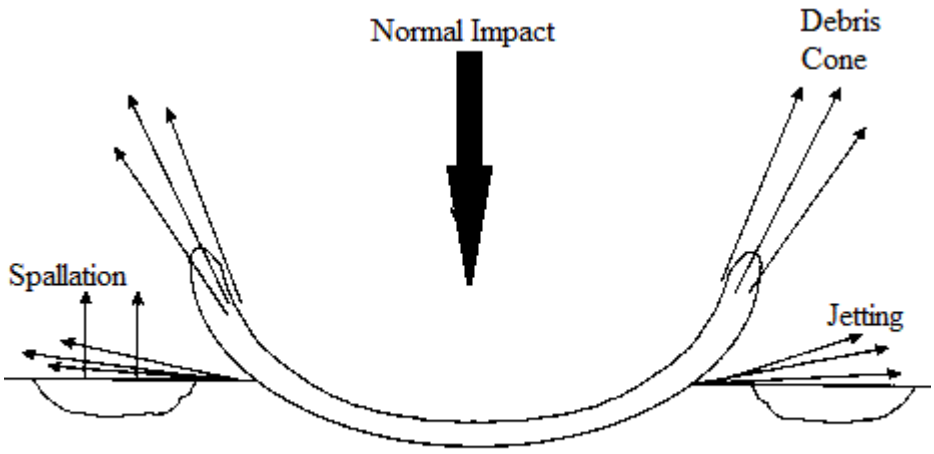

Figure 3.6: Impact cratering showing spallation lift at a distance from the impact epicentre. *Image courtesy: Esa*

While ejecta thrown directly from the impact epicentre can also lift material into space, this material is subjected to much higher pressures. Spallation materials can be ejected into space having only been subject to pressures up to an order of magnitude lower than those of the impact itself (Burchell, M. et al. 2003), thus giving a far greater probability of survival to any life ejected this way. Indeed, it has been shown that viable microbes can be carried on ejecta launched at high speed due to a nearby impact event (Burchell et al., 2003; Fajardo-Cavazos et al., 2009).

3.4.3 A Cosmic Adventure

Once life-forms are successfully launched into space encased within ice and/or rocks they then have to face the long journey through the harsh radiation of interplanetary, interstellar or even intergalactic space. Gladman,

B. (1997) and Eugster, O. (2006) have shown that the measured cosmic ray exposure ages of some meteorites imply this process can take millions of years (for examples, see Table 3.1 for Martian meteorite travel times). During this transfer phase any life-forms would need to survive the exposure to the vacuum of space, the harmful radiation, and the freezing temperature. The more material that surrounds and encases the organisms, the more protection they are provided against the radiation and vacuum.

Although once believed to be completely sterilising (Clark, B. et al. 1999), recent work has shown several species can survive direct exposure to space (see Section 3.3.1 for examples). Additionally, within the last 20 years, it has been shown that a number of prokaryotic species are able to survive simulated, and real, space exposure conditions. Bacteria and Archaea are able to resist high doses (113 kGy) of ionising radiation (Brandt, A. et al. 2017), as well as UV radiation (Xue, Y. and Nicholson, W. 1996, Riesenman, P. and Nicholson, W. 2000, Rainey et al. 2005), vacuum, and extreme high and low temperatures (Horneck, G. et al. 1994, 2001a, Moeller, R. et al. 2007, 2008a, 2008b, 2010, Morozova, D. et al. 2007; Wagner, D. and Morozova, D. 2008). Recently a review by De Vera, J. (2012) has highlighted that some eukaryotic species (lichens - symbiotic associations between a fungus and an alga, or a cyanobacterium) can also survive the damaging environment of space.

While these organisms can survive such extremes in experiments, most natural transfers between planets will be on the order of millions of years, and thus these short exposure experiments cannot predict the effects of exposure for such long periods. However, Valtonen, M. et al., (2009) has shown that protection from radiation within rocks can last into the order of millions of years. In a group of rocks with average radii 2.33–2.67 m, *D. radiodurans*-like bacteria could survive for up to 400–500 million years in interstellar space.

The best possible option for any life-forms would be a combination of good protection from the elements, and a minimal transfer time. The optimal transfer times between planets – Hohmann Transfer Orbital Paths – are discussed in Section 3.5.

3.4.4 Arrival at an Alien World

Once at the destination planet, assuming there are the minimal nutrients and minerals needed to sustain life, some of the transferred organisms must reach the planet's surface (or atmosphere) in a viable state for seeding to occur, and thus lithopanspermia to have been successful; i.e. they must survive the descent to, and impact on to, the planet's surface.

Any object travelling through space towards a planet with an atmosphere, will undergo a change of environment, travelling through a near vacuum to suddenly travelling in an area densely populated with gas molecules (dense relative to the near vacuum of space). When travelling at velocities typical of meteors, asteroids, and comets in the Solar System (~20 km s^{-1}, but can be individually lower, or higher than this), the change in environment is equivalent to an impact. This creates high pressures and temperatures and as the material passes through the atmosphere, the collisions with the gas molecules create additional heating. The atmospheric drag experienced by smaller impactors can actually slow the impactor significantly allowing it to impact the surface with a lot less force. However, larger impactors smash through the atmosphere far more violently, and can often break apart during flight due to the shear stresses. The fragments of the parent impactor continue to fall causing multiple hypervelocity impacts on the surface (Melosh, H. 1989).

As recently as 20 years ago it was widely believed that no living organism could possibly survive such extreme conditions of atmospheric entry, and hypervelocity impact, on the surface of a planet. However, as touched upon in Section 3.2, Burchell, M. et al. (2001), have demonstrated the ability of bacteria to survive hypervelocity impacts of 5.4 km s^{-1} with peak impact pressures of ~30 GPa. Experiments using magnetically accelerated flying plate impacts to generate shock pressures have also demonstrated the ability of micro-organisms and lichens to survive peak shock pressures above a few GPa (Horneck et al., 2001b, 2008; Willis et al., 2006; Stöffler et al., 2007), and the survivability of yeast spores in impacts up to 7.4 km s^{-1} has also been shown (Price et al., 2013). There is thus a growing volume of data demonstrating the survival of organisms in this shock pressure regime (Burchell et al. (2010) gives a review). However, while this applies to smaller organisms (1-10 μm in size), larger (mm sized) more complex objects, such as seeds, are broken apart during impacts of approximately 1 km s^{-1} and pressures of 1 GPa (Jerling et al. 2008, and Leighs et al. 2012).

The atmospheric heating during entry is also not as hazardous to life as it might seem. During the passage through the atmosphere, Vaz, J. (1972), and Sears, D. (1975), suggest the extreme temperatures only extend a few millimetres into the surface of the impactor. The intense heat starts to melt the surface layer, and this forms a glassy surface called a fusion crust which effectively insulates the rest of the impactor. Analysis of the magnetic features of ALH84001 by Weiss, B. (2000), showed that the meteorite's interior had not been subjected to more than 40^{o}C since before the impact that launched it into space from the Martian surface. Wright, I. et al. (2000) also suggested that the presence of delicate structures of organic molecules, such as amino acids, found inside meteorites, confirms that temperatures within the rock do not exceed tolerable levels for life.

3.5 A Solar System Road Map

Having established in the previous section that some forms of life are capable of potentially surviving the three main stages of lithopanspermia, this section looks at some of the possible routes within our Solar System that could provide viable transfers for life (various possible interstellar journeys are discussed in Chapter 8, Section 8.3.2).

Most meteorites are asteroidal, or cometary in nature, and a few are classified as originating on other bodies such as the Moon, or Mars. Of the more than 61,000 meteorites documented on earth, 196 are confirmed to be of Martian origin (Meteorical Bulletin Database). This is direct evidence that transfer from Mars to Earth is not only possible, but occurs with some frequency. It seems reasonable then that this route should be the first to be discussed.

So, just how often do impacts on the Martian surface cause the transfer of material to the Earth? Melosh H, and Tonks, W. (1993) suggest that approximately 20% of all Martian ejecta that makes it into space eventually accretes onto the Earth. The timescale for such transfers is estimated to be in the range of 0.6 – 15 million years (Wetherill, G. 1984). A list of several Martian meteorite groups and their associated ages can be seen in Table 3.1 below.

Table 3.1: *Martian meteorite types and ages (Eugster, O. et al. 2006).*

Martian Meteorite Type	***Age (Millions of years)***
Dhofar 019, olivine-phyric shergottite	19.8 ± 2.3
ALH 84001, orthopyroxenite	15.0 ± 0.8
dunite (Chassigny)	11.1 ± 1.6
Five nakhlites	10.6 ± 1.0
Lherzolites	3.8 – 4.7
six basaltic shergottites	2.4 – 3.0
Five olivine-phyric shergottites	1.2 ± 0.1
EET 79001	0.73 ± 0.15

It is of course possible for surface material to be ejected such that it crosses the Earth's orbital path almost immediately, and if the Earth happens to be at that point in its orbit, then the transfer could, theoretically, be less than a year. Gladman, B. (1997) suggests the probability for this to happen is 10^{-7}, but however small the probability, the possibility remains valid. Such optimal crossings between planets are called Hohmann Transfer Orbits, and are used to calculate when to launch missions to other bodies in the most optimal time.

A Hohmann Transfer Orbit is an elliptical orbit (around the Sun) that crosses the orbit of the origin planet and the destination planet. The time taken to travel the part of the orbit that intersects with the origin planet to the part that intersects with the destination planet is calculated. Once this is calculated a spacecraft can be scheduled for launch such that the destination planet will reach the intersection at the same time as the spacecraft.

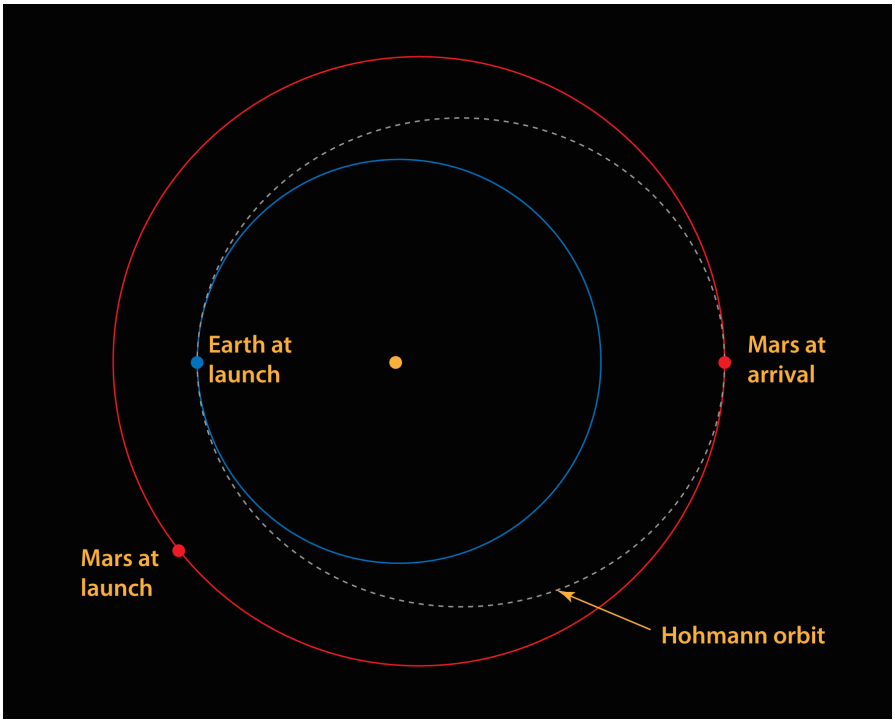

Figure 3.7: Example of Hohmann Transfer Orbit, a hyperbolic escape from the orbit of Earth, into an elliptical orbit around the sun determined by a Hohmann transfer orbit, with a hyperbolic capture into orbit around Mars for a complete interplanetary transfer. *Image courtesy: Brian Koberlein*

A Hohmann transfer orbit is normally calculated from either a planetary orbit or from orbit around a planet; it is the most optimal route between two planets, and is used to reduce as much as possible the time it takes to reach a planet (see Fig. 3.7 and Table 3.2).

The celestial mechanics of the Solar System are such that there will be various windows of opportunity for Hohmann style transfers to different planets every so often, and it is quicker overall to wait for these windows than to launch earlier and take a longer route (in the case of Earth to Mars the window appears roughly every two years).

Table 3.2: *Showing the time it takes to reach various planets in a Hohmann Transfer Orbit, and the change in velocity needed for spacecraft to achieve such an orbit from the Earth's orbit, and Low Earth Orbit (Lo, M. and Ross, S. 1997).*

Destination Planet	***Orbital Radius (A. U.)***	***ΔV from Earth's Orbit (km s^{-1})***	***ΔV from Low Earth Orbit (km s^{-1})***	***Journey Time From Earth (years)***
Mercury	0.39	7.5	5.5	0.3
Venus	0.72	2.5	3.5	0.4
Mars	1.52	2.9	3.6	0.7
Ceres	2.77	N/A	N/A	1.3
Jupiter	5.2	8.8	6.3	2.7
Saturn	9.54	10.	7.3	6.1
Uranus	19.19	11.3	8.0	16.1
Neptune	30.07	11.7	8.2	31.3
Pluto	39.48	11.8	8.4	46
Eris	67.8	N/A	N/A	100
Infinity	∞	12.3	8.8	∞

The best case for any meteorite carrying life is to be thrown from an impact onto a trajectory that matches a Hohmann Transfer Orbit. For an unaided natural Hohmann Transfer the impact would have to eject material from the Earth into an elliptical orbit that matches the path of a Hohmann

Transfer Orbit within the correct window, such that when the material reaches the orbit of the destination planet, the planet is at that point in space, and its gravity well can capture the material, allowing it to fall to the surface. This is the best case scenario if the time the organism is frozen or exposed to space is a limiting factor.

As stated above the probability for a Mars to Earth natural Hohmann Transfer is 10^{-7}. While that appears unlikely given the current Martian impact rate for impacts large enough to lift material into space, that may not have been the case in the past during the Late Heavy Bombardment period 4.1 – 3.8 Billion years ago – right at the cusp of the current estimates for the oldest evidence of life on Earth (see Chapter 2, Section 2.5). During this period, with the increased large scale impact rate (Burt, D. et al. 2008), the probability for such an optimal transfer would be raised also, and in a period lasting some 300 million years it is possible several such occurrences could have happened.

The remaining 80% of all Martian ejecta that makes it to space, is suggested to impact Venus (20%), be expelled from the Solar System due to gravitational perturbations caused by Jupiter (20%), or fall back onto the Martian surface at a later date (40%) (Melosh, H. and Tonks, W. 1993).

The journey from the Earth to Mars also happens, but is a lot less likely due to travelling against the pull of the Sun's gravity. However, 5% of space bound Earth ejecta has been shown to fall on Mars in computational simulations (Melosh, H. and Tonks, W. 1993). 30% of the Earth's space bound ejecta falls on Venus within ~15 million years, 20% is ejected from the Solar System by Jupiter's gravitational perturbations, and the remaining ejecta is re-accreted by the Earth. This means that it is entirely possible that the Earth has seeded life onto Mars or Venus, once, or indeed many times, in the last several billion years.

Any discoveries of life on these planets should therefore be viewed with caution as it may not be a second genesis at all, but merely a migrant "Earthling" and/or its subsequent evolutionary offshoot.

Ejecta from Venus that makes it into space mostly re-accretes back onto the surface of Venus. However, as with the Earth and Mars, about 20% of this ejecta is gravitationally perturbed by Jupiter and is ejected from the Solar System, and some 30% makes it to the Earth's surface, on a timescale of around 12 million years (Melosh, H. and Tonks, W. 1993). However, no Venusian meteorites have yet been determined, mainly because the Venusian surface soil has never been chemically analysed for its composition. Barsukov, V. et al. (1980) made models to attempt a prediction of the surface rocks' composition based on data from the Venera 11 and 12 missions, but these were still unable to give any direct knowledge. The implication here being, there may be Venusian meteorites in the world's collections, but their Venusian origins are simply not known.

Simulations by Worth, R. et al. (2013) showed that materials ejected from the Earth and Mars in large impacts can also make it to the moons of Jupiter and Saturn, albeit much more rarely. Such transfers would have been more likely to occur during the Late Heavy Bombardment and the 2 billion years following it, during which time the icy moons such as Enceladus and Europa, were warmer and likely had little or no icy shell to prevent meteorites from reaching their liquid interiors.

The fact that 20% of all space bound Martian, Venusian, and Earth ejecta are subsequently ejected from the Solar System has implications for interplanetary panspermia, both conceptually with possible seeding from our Solar System to another, and with the possibility of life arriving here from another planetary system elsewhere in the galaxy. This concept will be further discussed in Chapter 8, Section 8.3.2.

3.6 Conclusion

This chapter follows on from the discussion of life and its origins in Chapter 2 and described the concept of panspermia - a hypothesis describing the possible natural migration of life between different celestial bodies in the universe. A number of different variations were presented, and the most plausible one due to environmental protections within rocks and/or ice is lithopanspermia. This was then discussed in further detail as it will be the version that is considered within the context of the research conducted here. The process of impact craters was described in detail before the three main phases of lithopanspermia; ejection from a planet, crossing the gulf of space, and arriving at an alien world. After these phases had been discussed, possible routes through the Solar System with regards to panspermia were described as well as the average timescales involved and the most optimal routes – Hohmann Transfers.

CHAPTER 4

PROCEDURES AND EQUIPMENT

"What you do next will decide whether your crap day becomes everyone's last crap day or just another crap day. Get some guns to the back of their heads."

Negan, *The Walking Dead*

4.1 Introduction

This chapter describes the various pieces of equipment that were used to perform the research presented in the following chapters. The selection of species for testing is discussed, and methods for the preparation of both projectiles and targets are described. Then two methods for calculating impact pressures are explained. Finally, the hydrocode modelling software used is discussed in detail before concluding remarks.

4.2 The Two-Stage Light Gas Gun

Regular powder burning guns are limited in the velocities of the projectiles they fire. This is due to the uneven rate at which the powder burns over small timescales, and this creates a substantial pressure gradient through the column of gas behind the projectile (Stephenson, W. 1961). As the front of the column accelerates faster than the rear, the gas kinetic energy dissipates, resulting in a relatively inefficient transfer of energy to the projectile. This creates an upper limit to velocities achievable in powder burning guns known as the muzzle limit. This upper limit is around ~1.25 km

s^{-1} (Crozier, W. and Hume, W. 1957). However, some high precision rifles claim velocities up to 1.7 km s^{-1}. While impressive, it is no use for experiments testing hypervelocity impacts that require velocities in the 1–9 km s^{-1} range. Such experiments require the use of a Two-Stage Light Gas Gun.

4.2.1 Main Gun Set-up

The Two-Stage Light Gas Gun was designed to overcome the muzzle velocity constraint with standard guns and reach much higher velocities. Instead of firing the projectile and the gas at the same time, a Two-Stage Light Gas Gun separates the projectile and gas into two stages, hence the name (see Fig. 4.1).

Figure 4.1: The Two-Stage Light Gas Gun at the University of Kent's Impact Laboratory. The target chamber in the upper left of the picture.

A schematic diagram of the light gas gun can be seen in Fig. 4.2 and, following that diagram, the firing process occurs from left to right. Once the gun has been set up and the target is in place a large brass pendulum (PE) is lifted and then, upon firing, is released. The pendulum swings and forces a firing pin into a powder shotgun cartridge (C), this ignites the charge (just like a standard gunshot) and forces a nylon piston (P) along the pump tube into the entrance of the breech. The breech is already preloaded with a low molecular weight gas (a light gas such as hydrogen, helium, or nitrogen) which has been pumped in to a certain high pressure (on the order of 10–80 bar, depending on the shot velocity that is required). A small disc called the 'burst disc' (see Fig. 4.3) separates the breech from the launch tube (which is placed under vacuum). As the piston is forced into the breech the gas is pressurised even further, and then when the pressure is too great the burst disc ruptures (the burst disc can be scored if needed so that it ruptures at a lower pressure depending on the velocity required, see Fig. 4.3). A sabot (S) holding the projectile (sometimes the sabot *is* the projectile) is then accelerated down the launch tube due to the expansion of the gas out of the breech into the vacuum of the launch tube.

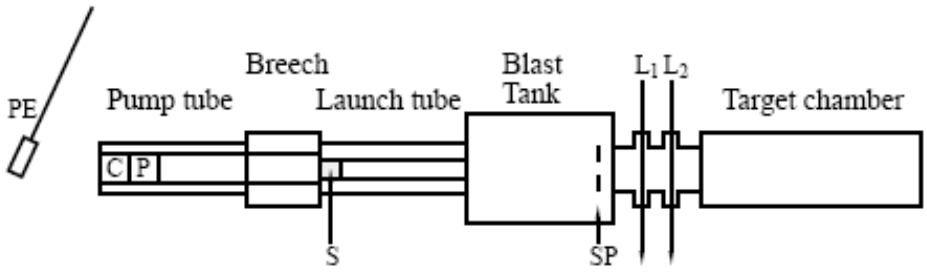

Figure 4.2: Schematic of the Light Gas Gun, the firing process occurs left to right, see main text for detailed description of operation.

Figure 4.3: Burst discs, approximate diameter ~1.25 cm. Left: a scored disc before (top) and after (bottom) firing. Right: a non-scored disc before (top) and after (bottom) firing.

The launch tube is rifled to spin the projectile, allowing it to follow a more accurate path down the gun; this is also useful when the sabot is holding a projectile (see below). If the sabot is the projectile then it will travel through the blast tank passing through two laser curtains (L_1 and L_2) used to measure the velocity, and if successful, impact the target in the target chamber. If the sabot is not the projectile but is simply carrying it through the launch tube then the rifling can be very useful. This is especially true for the type of sabot that is known as a 'split sabot' (see Figs. 4.4 and 4.5).

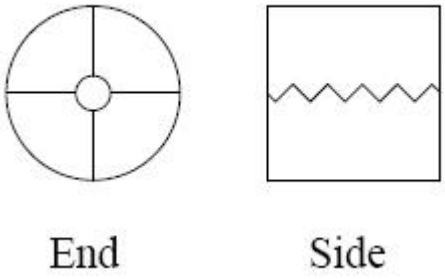

Figure 4.4: Schematic of a four piece split sabot showing end-on and side views. Note, the cavity to hold the projectile penetrates halfway through the length of the sabot.

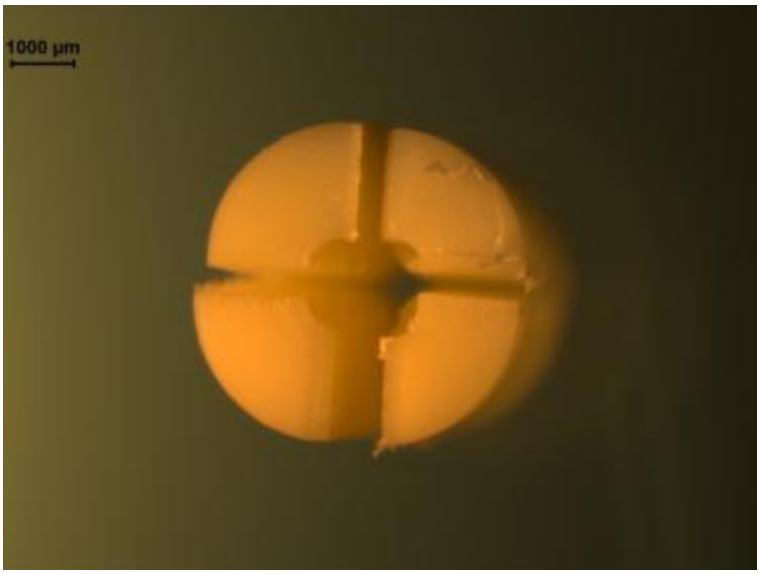

Figure 4.5: Photograph of a nylon four piece split sabot. Note, the cavity to hold the projectile penetrates halfway through the length of the sabot.

The split sabot holding the projectile travels through the rifled launch tube, and upon exiting the launch tube and entering the blast tank, the centripetal force of the spinning sabot causes the four quadrants of the sabot

to travel off-axis at an angle of approximately 6° from the line of travel of the projectile (impacting the stop plate, SP) leaving the projectile to enter the target chamber and impact the target.

The hypervelocities are achieved due to the efficient method of gas expansion used in this two stage set-up. The lower the molecular weight of the gas the higher the expansion velocity of the gas, and thus the faster the projectile is accelerated. This is because of the inverse relation of the molecular weight of the gas to its expansion speed. The molecular kinetic energy of the gas can described as:

$$KE_{AV} = \frac{3}{2}kT \qquad \text{(Eq. 4.1)}$$

where KE_{AV} is the molecular kinetic energy of the gas (J), k is the Boltzmann constant (J K^{-1}), and T is the temperature (K). When free to expand fully (as when expanding into a vacuum) this expansion energy will be almost equivalent to the molecular kinetic energy.

$$\frac{1}{2}mv^2 = \frac{3}{2}kT \qquad \text{(Eq. 4.2)}$$

where m is the mass (kg), and v is the expansion velocity (m s^{-1}). If the temperature is held constant, then the expansion velocity will be inversely proportional to the root of the mean molecular weight of the gas:

$$v \propto \sqrt{m} \qquad \text{(Eq.4.3)}$$

Therefore, the lower the molecular weight of the gas, the faster the expansion velocity, using hydrogen gas it is possible to reach ~9 km s^{-1} (Moritoh, et al. 2001).

Predicting the velocity of any shot is a difficult process as many factors contribute to the overall velocity a projectile will achieve. The amount of gun powder in the charge, the molecular weight of the gas, the initial preloaded pressure of the gas, the thickness and/or scoring of the burst disc, and the size and weight of the projectile itself are all factors affecting the velocity that is achieved. It thus takes a skilled gun operator is be able to set-up the gun such that a velocity can be predicted to with 0.1 km s^{-1} margin of error, fortunately Kent has an experimental officer capable of this. Table 4.1 shows some of the parameters than need to be considered to predict a shot velocity.

Table 4.1: *Showing some of the parameters needed to achieve particular velocity ranges.*

Shot Velocity (km s^{-1})	***Gas Used***	***Variables***
1.1	Nitrogen + SF6	14 bar SF6 raised to 40 bar with the nitrogen and 10 g of gunpowder
1.2 – 2.2	Nitrogen	40–70 bar and 8–10 g of gunpowder
3.3 – 4.3	Helium	45–70 bar and 10 g of gunpowder
4.4 – 5.7	Hydrogen	35–70 bar and 8–10 g of gunpowder

The gun can also be used to perform lower velocity shots by simply using only the preloaded pressurised gas, with no powder charge, and thus no additional pressurisation with the nylon piston. For this method an electric current is used to ‘burn’ the burst disc causing it to rupture and the gas is released; the process then continues as described above.

In order to accurately measure the velocity achieved, the projectile passes through two laser light curtains (L_1 and L_2, Fig. 4.2), its passage interrupts the signals from two photodiodes illuminated by the laser curtains. The timing between the resulting signal spikes, combined with the known separation of the two laser light curtains, allows a calculation of the velocity of the shot to be made that is accurate to within $\pm$ 1%.

4.2.2 The Cold Gun

Another feature of the gun at Kent is its ability to perform 'cold shots' and is colloquially referred to as the 'cold gun'. The 'cold gun' allows a frozen projectile to be mounted into the gun via a special brass holder (previously stored in a freezer). The launch tube is kept in a CO_2 freezer overnight (at -180^{o}C) prior to the shot. The gun is set-up as far as it can be before the cold elements are needed. A set of cooling pipes are in position at the position of the projectile and coolant fluid is pumped round to minimise the heat transfer to the projectile while the final parts of the gun are being set up. Once the gun is ready, the cold shot can be fired. The temperature critical part can be performed in less than 15 minutes, and temperature gauges at the breech confirm the temperature of the projectile at the time of the shot; these are usually around -20^{o}C or so, confirming the projectile remained frozen as it was fired (as this is the temperature of the outside of the breech, which is the surface and warms the fastest – the interior is colder). This was the method used to fire the phytoplankton shots that required the organisms to be frozen into a projectile and fired; more detail on those shots is provided in the relevant methodology in Chapter 5.

4.3 Species Selection

Two species were chosen for the main experimental phase of this exploration of panspermia; one flora, and one fauna. The reasoning here is that the flora (a phytoplankton) could be used as a potential food source for other more complex organisms that may be capable of panspermia. The reasoning for the other species is that no multi-cellular complex organisms have yet been shown to be capable of surviving the type of hypervelocity impacts necessary for panspermia to occur. The tardigrade species chosen here is a complex multi-cellular creature known to be able to survive in extreme environments (Beltran-Pardo, E. et al. 2015), and so it was selected for testing in hypervelocity impact scenarios.

Any life-forms travelling to a new world devoid of life would need to be primary producers and create their own energy (such as photosynthetic or chemosynthetic organisms do), else they would need a companion life-form that is a primary producer. Any transfer of life onto a lifeless world would require a new food chain to be set up, primary producers can do this, but more complex organisms such as the tardigrade cannot. Without a suitable food chain in place, any non primary producing organism would very quickly die out. The tardigrade eats various kinds of algae and therefore, if it was capable of surviving the trip to a new world, it would need a food source, such as phytoplankton. Any impact that lifted tardigrades into space on a panspermia style journey, would invariably also lift algae as well, thus both of these species have been selected for the experimental hypervelocity test programme.

4.3.1 Phytoplankton Species *Nannochloropsis oculata*

Nannochloropsis oculata Phytoplankton is a eukaryotic photosynthesizing autotroph that can survive in both freshwater and marine environments. These micro-organisms inhabit the euphotic zone in the world's oceans (i.e. the sunlit surface layers of the oceans), and most bodies of fresh water. Photosynthesis by phytoplankton accounts for almost half the total photosynthetic energy on Earth, as the net annual photosynthesis by ocean dwelling phytoplankton alone is of a similar magnitude as that achieved by all terrestrial plants (Field et al., 1998; Behrenfeld et al. 2001) and thus phytoplankton are directly responsible for much of the Earth's atmospheric oxygen. They are also primary producers, and create organic compounds from the carbon dioxide that is dissolved in the water, and this process helps sustain the aquatic food web, making phytoplankton the base of several large food chains (Ghosal et al., 2001). For this reason, Phytoplankton was chosen for this study. Similar experimental studies have been conducted with prokaryotic organisms, such as bacteria (Burchell et al., 2004), and this study aims to add data for eukaryotic species into the panspermia debate. Phytoplankton are also excellent candidates for relocating to other environments, as they require only a few basic minerals and light to grow and reproduce, and, as photosynthesizing organisms, they also have the power to transform an atmosphere via oxygenation.

4.3.2 Growth media

The culturing fluid was a mixture of HPLC (High Performance Liquid Chromatography) grade water (1900 ml) and 'Phyto Nutrient - Modified F/2 Medium' (10 ml diluted), purchased from Reefphyto.co.uk (see Fig. 4.6).

The formula is based on the Guillard's F/2 medium (Guillard et at., 1962) and has exactly the same nitrogen, phosphorus, trace element, and vitamin content as the original F/2 medium. This mixture was used to culture the organisms originally, and the same formula was then subsequently used for all samples. The culture starter may have been potentially impure; however this was not checked directly. Later microscope analysis showed very uniform cells lending weight there being single species present but this was by no means definitive.

Figure 4.6: Left: *Nannochloropsis oculata* Starter Culture. **Right:** Guillard's F/2 medium, used as a food source to provide all the trace nutrients and minerals to the water that phytoplankton thrive on.

4.3.3 Preparation of *Nannochloropsis oculata*

The original culture (from which all subsequent cultures were obtained) was purchased from Reefphyto.co.uk (see Fig. 4.6). Plastic bottles were filled with 1900 ml of HPLC grade water and a portion of the phytoplankton starter culture was thoroughly mixed into each one, forming a light green mixture. To this, 10 ml of Guillard's Modified F/2 Medium was added to provide the necessary nutrients to the water for the phytoplankton to grow. A small length of air-hose was placed into the bottles and connected to a small aquarium air-pump, and set to slowly release bubbles of air throughout the water and introduce a small measure of turbulence to allow the water to move and flow, mimicking natural conditions.

Figure 4.7: Example of phytoplankton cultures. **Top:** After one day. **Bottom:** After five days.

The initial culture took nine days to go from almost unseen trace amounts of phytoplankton, to a viscous, opaque, green solution (see Figs. 4.7 and 4.8).

Figure 4.8: Example of phytoplankton culture ready to be halved and diluted to form two new cultures.

This demonstrated that phytoplankton could be cultured easily. This culture was then split and re-cultured, to verify the culturing technique was repeatable. This second culture was split into two, one half was again re-cultured, and the other was frozen to -20^{o}C. The re-cultured half grew in an identical way to the first two cultures. The frozen sample was left in a domestic refrigerator (at -20° C) for one week, and then it was re-cultured again to see if the organism was able to survive the freezing process, as any transfer between planetary bodies would involve the freezing temperatures of space. It also needed to be frozen in order to fire it in the light gas gun. The frozen sample was successfully re-cultured, albeit at a slower rate than before, suggesting that not all of the organisms survived the process and/or that they have been damaged in a way which slows their ability to enter the active growth state. The culture only achieved a dark green colour after ~20 days (c.f. 9 days for the unfrozen culture). This frozen/defrosted culture was then used as the source for all the 'live' shots in the programme, now that it was established there would be some surviving organisms after freezing.

Nannochloropsis oculata is a single celled organism that can survive as a free floating organism (with enough cells eventually the water will begin to turn green), or they can conglomerate with other cells to form sheets or 'fuzzy' growths.

Fig. 4.9 shows the living cells of *Nannochloropsis oculata* under an optical microscope. Fig. 4.10 shows deceased 'dry' cells of *Nannochloropsis oculata* phytoplankton under the Scanning Electron Microscope.

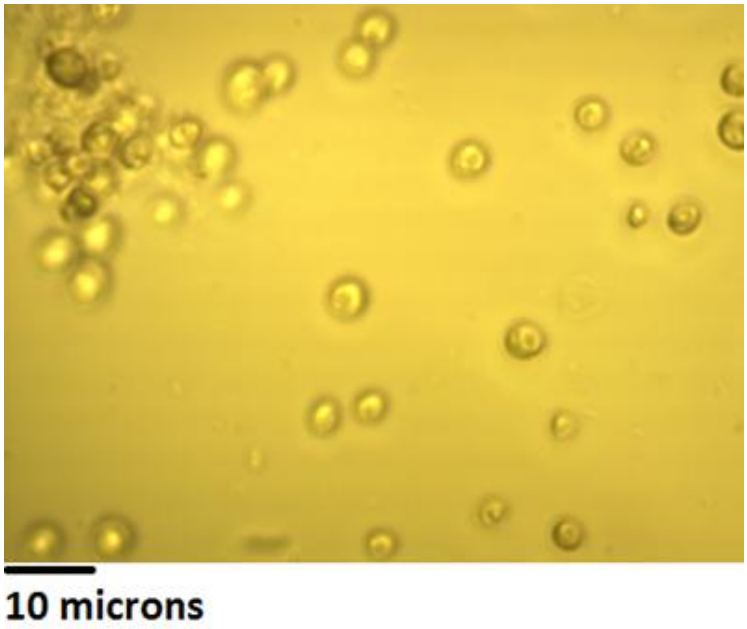

Figure 4.9: Optical microscope image of living, unshocked, phytoplankton.

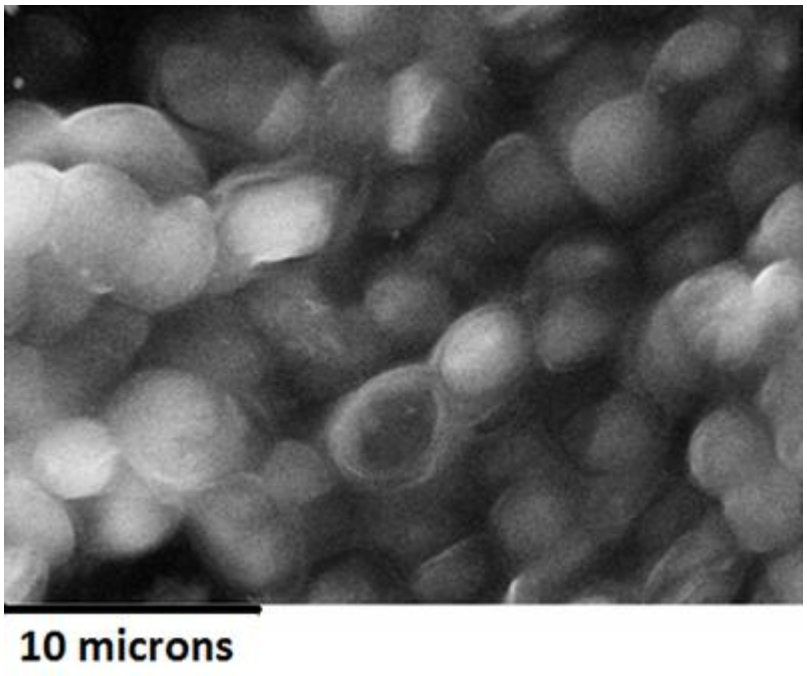

Figure 4.10: Scanning Electron Microscope image of deceased 'dry', unshocked, Phytoplankton. The average cell diameter is approximately 5 microns, and the cells have a spherical morphology.

4.3.4 Tardigrade Species *Hypsibius dujardini*

Whilst many simple single celled organisms have now been shown to survive hypervelocity impacts (and the associated pressures) similar to those encountered during the possible migration of material from one planet to another (see Chapter 3, Sections 3.2 and 3.4.4), complex multi-cellular organisms have either largely not been tested or, those that have been, have not survived the process (Jerling et al. 2008).

Tardigrades (literally ‘slow walkers’), also known as ‘water bears’ or ‘moss piglets’, were first discovered in 1773. Over 1000 different species of tardigrade are now known, and they have been around for over 530 million years (Guidetti, R. and Jonsson, K. 2002).

Hypsibius dujardini (see Fig. 4.11), like most species of tardigrade, are complex organisms composed of approximately 40,000 cells (Seki et al. 1998). They have a lifecycle of approximately 3-4 weeks, and undergo asexual reproduction as they are parthenogenetic (i.e., progeny develop from unfertilized eggs), with females laying eggs that undergo meiosis and then restore a diploid chromosome number by reduplicating chromosomes (rather than by fertilization; Barnes, 1982, Bertolani et al. 2004). Each tardigrade is born with a full complement of cells and the organism grows as the cells grow; they do not undergo any cell division during their lifecycle, the outer skin is molted as a husk, much like how a snake sheds its skin (Barnes, 1982; Kinchin, 1994; Seki et al., 1998).

Tardigrades have also been shown to tolerate exposure to high doses (over 4,500 Gy) of ionizing radiation (May et al., 1964; Jonsson, 2007; Beltran-Pardo, E. et al., 2015). When the ambient humidity decreases they can shut down their metabolism almost entirely and enter a highly dehydrated state known as a ‘tun’. This is an extremely desiccated state, as they release

up to 97% of their body water, and they can survive extreme temperatures (as low as -253°C, or as high as 151°C), as well as exposure to X-rays and the vacuum of space (Seki et al., 1998) while in this state. When exposed to water again they will rehydrate and reanimate. The current record is 120 years from being frozen to reanimation again (*Franceschi, T. 1948).*

Figure 4.11: False colour Scanning Electron Microscope image of a tardigrade *(image courtesy: themagazine.ca)*

These abilities and tolerances make them ideal candidates for a study into the feasibility of panspermia with multi-cellular complex organisms.

The tardigrades used for this study required no culturing as they were purchased from Sciento.co.uk and then transferred directly into the samples that would be used for testing, either as a ‘natural’ un-tampered sample, a frozen control sample, or a frozen sample that would be used for testing in hypervelocity impacts (see Fig. 4.12 for examples).

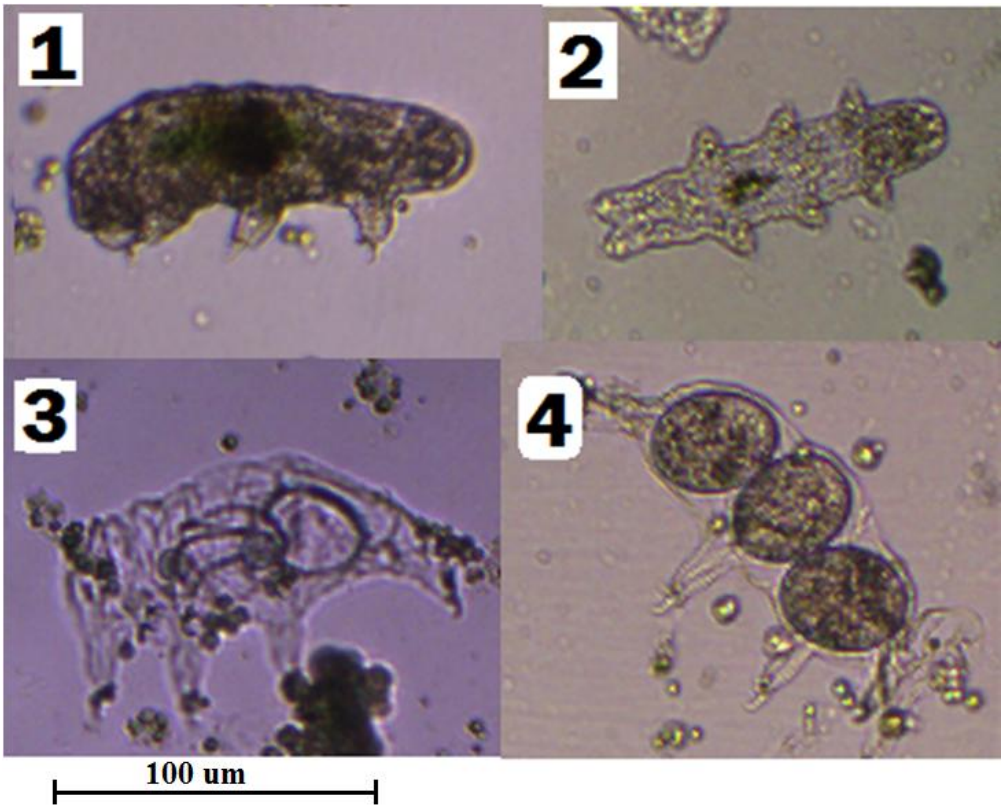

Figure 4.12: Optical images of *Hypsibius dujardini*. **Panel 1:** A living organism. **Panel 2:** A dead organism. **Panel 3:** A discarded cuticle, or ‘husk’. **Panel 4:** An egg laden cuticle

4.4 Target Materials

The target fluid for the phytoplankton shots was a mixture of HPLC (High Performance Liquid Chromatography) grade water (700 ml) and 'Phyto Nutrient - Modified Guillard's F/2 Medium' (3.5 ml diluted). This mixture was split between two glass bottles (previously sterilised at 120^{o}C for three hours in an autoclave), one was sealed as a control, the other was used as the target for the phytoplankton shot, and then used to culture any potential surviving phytoplankton recovered from the target chamber post-impact.

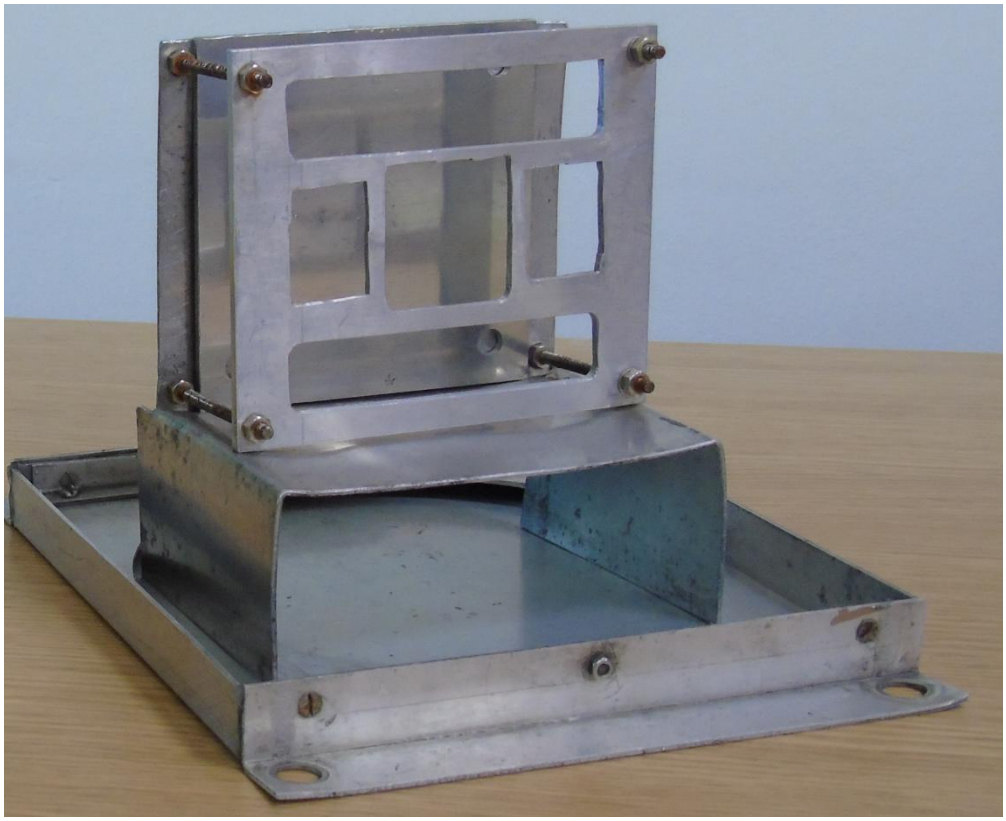

Figure 4.13: The specially made target holder for the phytoplankton (and tardigrade) shots. Water targets were placed such that they would be impacted by the projectile as it passed through the central square hole. A housing (not shown) covers this and then the bottom tray captures the water after impact. Base is 17.5 x 17.5 cm.

The water for the target was placed into two extremely thin (~50 μm) polythene bags. These were then taped into place within a specially made target holder such that the bulk of the water was in line with the central square opening (see Fig. 4.13). Once the target was prepared it was loaded into a special holder and clamped into place within the target chamber of the gun (see Fig 4.14). The methodology section in Chapter 5 (Section 5.2) provides more detailed information about the set-up for these materials prior to firing.

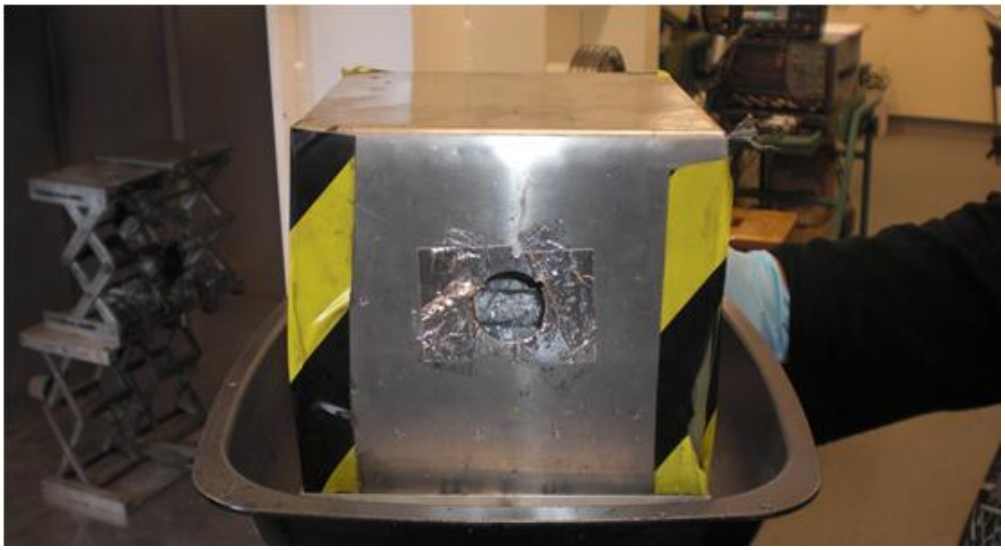

Figure 4.14: The specialised target holder used to house the target materials for the phytoplankton shots. The central hole lines up with the square hole of the inner holder. The additional tray is used to capture any water that may make it through the joints of the holder. Holder base is 17.5 x 17.5 cm, and 17 cm high.

For the tardigrade shots the tardigrades themselves were embedded within ice inside a small plastic container. This was then placed at 90^{o} within the specially made target holder such that the surface of the ice was in-line with the main central square hole, leaving the frozen tardigrades distributed

across the back edge of the target (see Fig. 4.15). This set up mimics an impact into a frozen body of water with tardigrades approximately 1 cm below the surface.

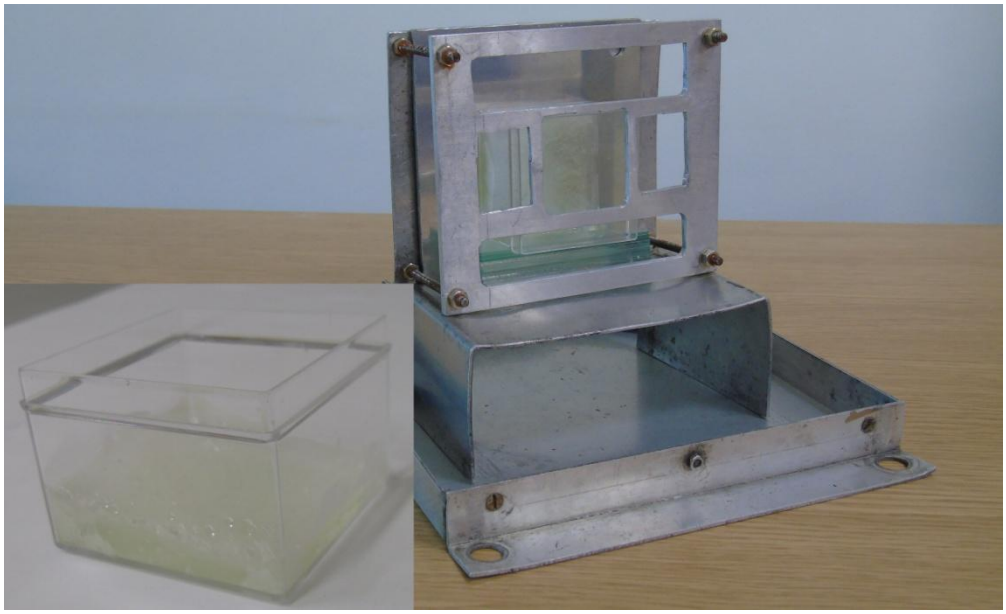

Figure 4.15: Internal target holder as used for the tardigrade shots. **Inset:** Frozen tardigrades embedded in ice **Main Image:** Frozen tardigrades are placed at 90^{o} such that the frozen surface is in line with the target area (central square hole). Base is 17.5 x 17.5 cm.

The internal target holder was then placed inside a plastic bag (see Fig. 4.16) with a hole cut into it in-line with the projectile path (to make recovery of ice and water easier), then the housing was place on top and everything was clamped into place within the main target chamber of the gun. Prior to every shot the target holders were sterilised at 120^{o}C for three hours in an autoclave, and fresh sterile bags and disposable equipment used.

Figure 4.16: Tardigrade internal target holder and outer housing.

4.5 Projectile Materials

For the phytoplankton shots a solid cylindrical nylon sabot was used with a cavity drilled into it (see Fig. 4.17) for each shot. These sabots are similar to the 4-piece split ones described earlier (Section 4.2.1) but one solid piece (with an object (or objects) that fill the cavity) acting as the projectile(s) rather than spinning away in-flight. A section of the sheet-like phytoplankton cells was removed from the main culture bottle and placed into the cavity in the sabot to maximise the number of phytoplankton cells in the projectile. Added to this was a single drop of water (also from the culture, and thus containing some free floating cells as well). This was then placed in a freezer at -20^{o}C 48 hours before the projectile was to be fired. 24 hours before the shot, the frozen projectile was placed into, and held by, a special brass projectile loader (with has a large thermal inertia) so that the

phytoplankton mixture remained frozen during the loading of the projectile into the launch tube of the light gas gun. This was left in the freezer until the latest possible moment before firing to ensure no melt of projectile contents occurred (see Section 4.2.2 on the 'cold gun'). The methodology section in Chapter 5 (Section 5.2) provides more detail on the shots.

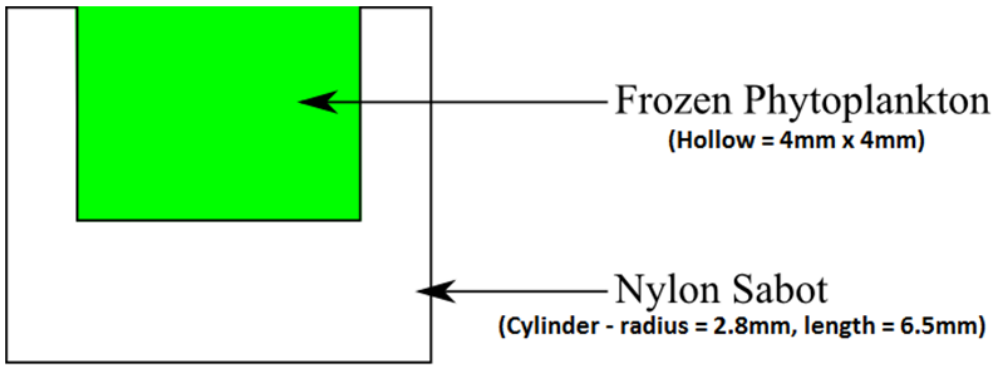

Figure 4.17: Schematic of the projectile used for phytoplankton shots.

For the tardigrade shots, as a frozen tardigrade sample is being fired onto, the projectile can be very simple. A cylindrical nylon sabot was chosen (much like for the phytoplankton shots, but with no cavity) as nylon is a material that has been well studied in hydrocode modelling, so creating computational simulations of the experiments would allow accurate modelling of the pressure conditions experienced during the impact process. Shooting solid nylon cylinders such as these is also extremely reliable, and the impact speed can be accurately controlled.

4.6 Life as a Projectile

The main focus for the Phytoplankton shot programme was to determine whether or not this species could survive a hypervelocity impact event. However, to do this, it was necessary to fire the micro-organisms themselves through the two-stage light gas gun, which, in turn, means they were not subject to the impact event alone. The phytoplankton were also subject to acceleration and jerk during the firing process of the light gas gun. Thus the surviving phytoplankton cells recovered post-shock would have also survived these aspects of a typical panspermia type journey.

The projectile naturally starts from a stationary position within the launch tube of the gun and is then accelerated down this launch tube reaching its final impact speed as it leaves the launch tube and enters the blast tank. Knowing the length of the launch tube (0.7 m) and the maximum impact speed in the phytoplankton shot programme (6.93 km s^{-1}, see Chapter 5), Newton's equations of motion can be used to give an approximate value for the acceleration. Assuming a constant acceleration then:

$$v^2 = \mathrm{u}^2 + 2as \qquad \text{(Eq. 4.4)}$$

where v is the projectile's final velocity (m s^{-1}), u is the initial projectile velocity (m s^{-1}), a is the acceleration (m s^{-2}), and s is the projectile's final position assuming the initial position is zero (m). As the projectile is stationary to begin with, this sets $u = 0$, and thus the equation can be rearranged into:

$$a = \frac{v^2}{2s} \qquad \text{(Eq. 4.5)}$$

This yields an approximate acceleration of 34,300 km s^{-2}. Again, assuming this to be a constant acceleration then the rise time for this acceleration can be found by using:

$$s = ut - \frac{at^2}{2} \quad \text{(Eq. 4.6)}$$

Rearranged for time *t*, and taking *u* = 0, this can be simplified to:

$$t = \sqrt{\frac{2s}{a}} \quad \text{(Eq. 4.7)}$$

This yields a rise time for the acceleration of approximately 0.2 ms. This, in turn, corresponds to a rate-of-change of acceleration (or jerk) of 17×10^{10} m s^{-3}.

Using a rifle to fire bacteria into a plasticene target, Mastrapa et al., (2001) subjected spores of *B. subtilis* and cells of *Deinococcus radiodurans* to jerks and accelerations in order to test their ability to survive in a panspermia style ejection from a planet. They subjected the cells and spores of the micro-organisms to accelerations of 4.5×10^6 m s^{-2}, and jerks of 1.5×10^{11} m s^{-3}.

These values are comparable to the predictions made for the jerk and acceleration that are involved in the impact generated ejection from the surface of a planet the size, and mass, of Mars (Mastrapa et al., 2001). The values obtained for the light gas gun in the highest velocity shot with phytoplankton are of a similar order of magnitude to those found by Mastrapa et al., 2001. Therefore the phytoplankton recovered from the target after being fired through the light gas gun post-impact must be capable of surviving these planetary ejection stresses as well as the impact process itself.

4.7 Optical and Scanning Electron Microscopes

For analysing the phytoplankton and tardigrades while still alive an optical microscope was used. This optical microscope was enclosed within a chamber to protect against contaminations, and is capable of magnifications ranging from 10–1000×. The microscope is part of a Raman spectrometer system, but served well as a method for analysing the phytoplankton. The sample stage could be moved remotely and electronically from outside such that the area of coverage could be accurately measured. This allowed the same size areas in multiple samples to be analysed, reducing any potential errors that may have arisen from any bias in the size of areas used for analysis. A camera was attached to the microscope allowing images (or videos) to be taken at any point during the analysis. Fig. 4.18 shows the set-up of the optical microscope used for all the optical images of phytoplankton and tardigrades provided in this work.

For obtaining detailed images of phytoplankton, a Scanning Electron Microscope was used. This required the phytoplankton to be dried out as the sample stage is placed under vacuum and any liquid would ‘boil off’ at such low pressures. A Hitachi S-3400N was used for the obtaining images of the dried phytoplankton (see Fig. 4.19), this is capable of more than 300,000× magnification. However, increased magnification comes as a trade off with resolution. It is more commonly used at lower magnifications (typically a few thousand times) allowing higher resolution and clarity of image.

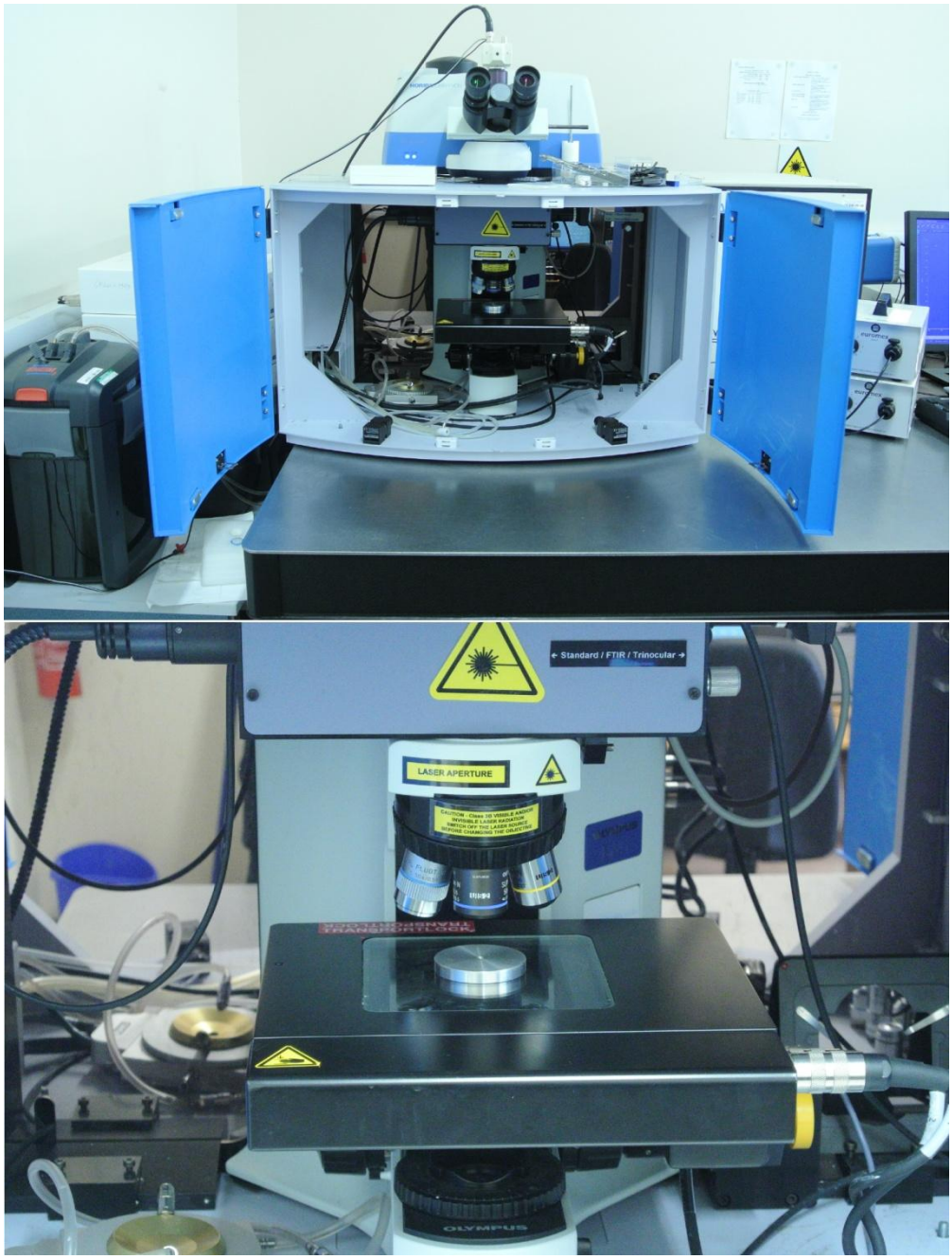

Figure 4.18: The optical microscope set-up used for analysis and image capture of phytoplankton and tardigrades. **Top:** The external casing housing the microscope with doors open. **Bottom:** Close up view inside the casing showing the sample stage and microscope lens.

Figure 4.19: The Hitachi S-3400N Scanning Electron Microscope used for collecting detailed images of phytoplankton.

4.8 Late-Stage Effective Energy Calculation

To complement the results of the experimental shot programmes the approximate peak shock pressures, P (Pa), experienced during the impact of all shots at all velocities (The highest being v = 6930 m s^{-1}) were calculated using the Late-Stage Effective Energy method developed by Mizutani et al., 1990 and used in Burchell et al., 2004. This method was originally proposed as a way to scale laboratory impact data to Solar System scales, using impact physics (Shrine, et al., 2002).

The original formulation of the Late-Stage Effective Energy is described using:

$$LE = \frac{m\nu}{2}\left(C + \frac{s\nu}{2}\right) \quad \text{(Eq. 4.8)}$$

where v is the projectile velocity (m s^{-1}) and m is the projectile mass (kg). C and s are the linear shock wave speed parameters, and these can be derived from the linear shock-particle velocity relation (Melosh, 1989):

$$U = C + su \quad \text{(Eq. 4.9)}$$

where U is the velocity of the shockwave (m s^{-1}), and u is the velocity of the particle (m s^{-1}). Therefore, the peak pressure that is generated during an impact can be calculated using:

$$LE = PV_p \quad \text{(Eq. 4.10)}$$

where P is the generated pressure (Pa) and V_p is the volume of the projectile m^3). By combining Eq. 4.8 and Eq. 4.10 we can generate an equation that can calculate the peak pressures during an impact:

$$P = \frac{m\nu}{2\mathrm{Vp}}\left(C + \frac{s\nu}{2}\right) \quad \text{(Eq. 4.11)}$$

where v is impact speed (m s^{-1}), V_p is the projectile volume (for the phytoplankton shots these were 160.1 × 10^{-9} m^3 at speeds less than 5 km s^{-1}, and 68.73 × 10^{-9} m^3 at higher speeds) and m is the mass (for the phytoplankton shot these were 0.3 × 10^{-3} kg at low speed and 0.1 × 10^{-3} kg at high speed). C and s are the linear shock wave speed parameters. Here C and s for ice and the phytoplankton species *Nannochloropsis oculata* are required, however these are not available. Instead the cells are approximated

as consisting of 100% water, and thus the appropriate values for water are used in the calculations. These calculations will be compared with hydrocode modelling of the same impact events. Currently, the hydrocode used does not have a standard model for ice. It needs a full Equation of State, strength model, etc. This could possibly be developed, but the work would be a major research effort outside of the scope of this thesis. Therefore water is used in place of ice in the hydrocode, and for consistency in all the various simulations and calculations as well, even though C and s values for ice are available in the literature. There are a range of C and s values for water in the literature. Both those of Trunin et al., (2001): C = 1483 m s^{-1} and s = 1.75, and those of Melosh (1989): C = 1480 m s^{-1} and s = 1.60 are used in order to establish a sensitivity to these parameters. Although the Planar Impact Approximation method (see Melosh, 1989) is more widely used, the Late-Stage Effective Energy method allows for the finite extent of millimetre scale projectiles, whilst the Planar Impact Approximation method does not. Price et al., 2012 and Parnell et al. 2010, compared the peak shock pressures obtained from both of these methods for impacts by millimetre sized projectiles of different compositions (shale and stainless steel). They found that the Late-Stage Effective Energy method gave higher values for the peak shock pressure than the Planar Impact Approximation method did (typically 13% higher).

4.9 Hydrocode Modelling

To further complement the experimental shot programmes and the Late-Stage Effective Energy calculations, hydrocode modelling was performed to determine the peak shock pressures experienced during hypervelocity impacts. This section will briefly describe what a hydrocode model is, what it is used for, and the underlying principles in its operation.

Ansys' AUTODYN, is a commercially available hydrocode (Hayhurst & Clegg, 1997) with a wide variety of material modelling capabilities to provide a platform to solve non-linear dynamical problems; it is therefore ideal for use in simulations of hypervelocity impact events. It is used in this work to model the peak shock pressure experienced within the projectile, at the point of impact (see Chapter 5), and across the target medium (see Chapter 6). AUTODYN allows for a more accurate determination of the shock pressure, as well as allowing estimates of the pressure versus time to be made. It has also been used by other researchers to model the shock pressures in impact studies of yeast and bacteria up to 1-2 GPa (e.g. Burchell, M. et al., 2004, Hazell et al., 2010, Price, M. et al., 2013).

As well as modelling the experimental procedures and producing peak shock pressure estimates, AUTODYN is also used to model hypothetical impact scenarios based on real data to determine the possible panspermia style hypervelocity impact events that various micro-organisms may be able to endure and survive (Chapter 7discusses this in more detail).

Hydrocodes are pieces of software written to describe the response of different materials to various external stimuli, by analysing shock wave propagation. As described in Chapter 3, Section 3.4.1 the pressures of shock waves in hypervelocity impacts are over an order of magnitude higher than typical material strengths. Therefore, hydrocodes simulate materials as if they have no shear strength, i.e. hydrodynamically (Johnson, W, and Anderson, C. 1987). The hydrocode works by breaking down a physical system into discrete units of space (cells) and time, then a series of equations are simultaneously solved. The input for these equations are the initial conditions present within each cell. The equations then return to each cell a new condition after a given time-step Δt. Cells can remain unchanged, or have their shape and size altered, or their internal properties altered, or a combination of these outcomes. The properties of each cell are then taken as

the initial conditions for the next iteration of the equations (Pierazzo, E. and Collins, G. 2004). A cell is the smallest unit of the hydrocode, and is internally homogenous; therefore there can be no change 'within' a cell, only 'between' different cells. It follows that cells must therefore be smaller in size than the length of the smallest physical process that influences the system, and the time-step must be smaller than the time taken for the smallest process to occur. This is generally taken as the time needed for any information to cross the length of a cell to ensure no large changes are possible between each iteration of equations. A crude method to relate the time-step to the cell size is:

$$\Delta x = c\Delta t \qquad \text{(Eq. 4.12)}$$

where Δx is the length of the cell (m), c is the propagation velocity of the wave (m s^{-1}), and, Δt is the time-step (s) (Anderson, C. 1987). Hydrocodes use finite differencing methods to relate the theoretical continuous x-values to the discrete cells in the model. Finite difference methods assume the cell size is small enough that for a function of F, $\Delta F/\Delta x$ starts to approximate dF/df. This leads to:

$$\frac{dF}{dx} = \frac{F(x+dx) - F(x)}{\Delta x} \qquad \text{(Eq. 4.13)}$$

$$\frac{dF}{dx} = \frac{F(x) - F(x-dx)}{\Delta x} \qquad \text{(Eq. 4.14)}$$

$$\frac{dF}{dx} = \frac{F(x+dx) - F(x-dx)}{2\Delta x} \qquad \text{(Eq. 4.15)}$$

where equations 4.13, 4.14, and 4.15, are the forward, backward, and central difference approximations respectively (Anderson, C. 1987).

For the model to accurately simulate the true physics of an impact, equations governing the conservation of energy, momentum and mass are required, as well as the equations of state for the materials being used in the model. However, the purely mechanical conservation law equations do not account for chemical, electromagnetic, or heat conduction effects.

The equations for describing the conservation of energy, momentum, and mass are described in equations 4.16, 4.17, and 4.18 respectively:

$$\frac{De}{Dt} = \frac{\Pi_{ij}\dot{\varepsilon}_{ij}}{\rho} - \frac{P}{\rho}\frac{\partial v_i}{\partial x_i} \qquad \text{(Eq. 4.16)}$$

$$\frac{Dv_i}{Dt} = f_i + \frac{1}{\rho}\frac{\partial \sigma_{ij}}{\partial x_j} \qquad \text{(Eq. 4.17)}$$

$$\frac{D\rho}{Dt} = -\rho\frac{\partial v_i}{\partial x_i} \qquad \text{(Eq. 4.18)}$$

where e is the specific internal energy (J), Π_{ij} is the deviatoric component of the stress tensor (N m^2), $\dot{\varepsilon}_{ij}$ is the deviatoric strain, ρ is the material density (kg m^{-3}), P is pressure (Pa), v_i is velocity (m s^{-1}), σ_{ij} is the stress tensor (N m^2), and f_i are the external body forces per unit mass (N kg^{-1}). Summation is implied by repeated indices as in standard tensor notation (Anderson, C. 1987).

The equation of state can account for the changes in density and irreversible thermodynamic processes such as shock heating (Blundell, S. and Blundell, K. 2006). The equation of state is generally expressed in terms of pressure as a function of energy and volume, $P = P(E,V)$. A change in the pressure is then expressed as:

$$dP = \left(\frac{\partial P}{\partial V}\right)_E dV + \left(\frac{\partial P}{\partial E}\right)_V dE \qquad \text{(Eq. 4.19)}$$

The Grunesian Parameter is defined as:

$$\Gamma = V\left(\frac{\partial P}{\partial E}\right)_V \qquad \text{(Eq. 4.20)}$$

Substituting this into Eq. 4.19, then integrating, and using the values (P_H, E_H) from the Hugoniot to eliminate the constants of integration:

$$P = P_H(V) + \frac{\Gamma}{V}\left(E - E_H\right) \qquad \text{(Eq. 4.21)}$$

This gives P as a function of V and E as needed, and is called the Mie-Grunesien equation of state (Rice, M. et al. 1958, McQueen, R. et al. 1970).

The iteration process for these equations will continue until a fixed time limit has been reached, if a failure limit is reached, or if the user manually terminates the simulation, determining that it has completed enough cycles to yield the data that are required (Pierazzo, E. and Collins, G. 2004).

There are two different computational methodologies used in this type of hydrocode: Eulerian, and Lagrangian, and they each have their own advantages and disadvantages. The Langrangian mesh ties points in the material to cell boundaries, and holds the mass within a cell constant so that as external forces deform the cell shape, its volume is altered. This can become a problem if a cell deforms too much. To avoid this, stringent failure limits must be applied to the model, so beyond a certain threshold of failure the cell is discarded, and the simulation continues without the cell (referred to as ‘erosion’). For this work, a Lagrangian mesh is used in all instances, as it was deemed most appropriate for the models that were required.

In a Eulerian system, the mesh is fixed (normally with rectangular cells) and material advects through this mesh. This allows for much more accurate modelling of fluid flow, but is less suitable to modelling impacts where there will be considerable deformation to solid components.

4.10 Conclusion

This chapter described the Two-Stage Light Gas Gun, and its operation for firing projectiles at hypervelocities; both the main set-up and the 'cold gun'. Then, the two species selected for experimental testing with the light gas gun were described, and the rationale behind why they were chosen was explained. A brief explanation of the target and projectile materials was then given, ahead of the more detailed descriptions that follow in the relevant experimental chapters (Chapters 5 and 6). A description of the journey phytoplankton faces as a projectile through the gun was then given, before a brief description of the microscopes used in the analyses of the organisms. Then, the Late-Stage-Effective-Energy calculations used to determine pressures in the phytoplankton shots were discussed. Finally, the hydrocode based simulation software AUTODYN was described.

Further information relating to the experimental shot programmes and the hydrocode modelling performed will be provided in the subsequent chapters (Chapters 5, 6, and 7) dealing with those projects.

CHAPTER 5
SURVIVAL OF THE PHYTOPLANKTON SPECIES NANNOCHLOROPSIS OCULATA

"After death, life reappears in a different form and with different laws. It is inscribed in the laws of the permanence of life on the surface of the earth and everything that has been a plant and an animal will be destroyed and transformed into a gaseous, volatile and mineral substance."

Louis Pasteur

5.1 Introduction

The experimental facilities, computational techniques, procedures, and micro-organisms used for this experimental and computational programme were described in detail in the previous chapter. This chapter will provide more detailed information regarding the two experimental shot programmes that were performed for the phytoplankton species *Nannochloropsis oculata*. The initial testing was a proof-of-concept phase designed to investigate whether or not the idea of phytoplankton surviving during hypervelocity impact events was at all plausible and thus whether the organism would be a viable candidate for further testing. The chapter begins by describing the initial shot programme in detail, with the accompanying results. Then the 'velocity range' shot programme is described and the results presented. The results from the hydrocode modelling and calculations of the experiment are then given, followed by a summary of the all the main results.

Analysis and discussion are then presented before final concluding remarks are passed.

5.2 Experimental Methodology

Two shot programmes were performed for this study. The principle aim of the first shot programme was to ascertain whether phytoplankton could be fired in the light gas gun, and then to determine if any organisms were viable for recovery post-impact. If viable organisms could be recovered, and there were surviving organisms that could be re-cultured, then a second shot programme could be initiated. The second shot programme aimed to show if there was survival of the phytoplankton under various increasing impact velocities and thus increasing peak shock pressures.

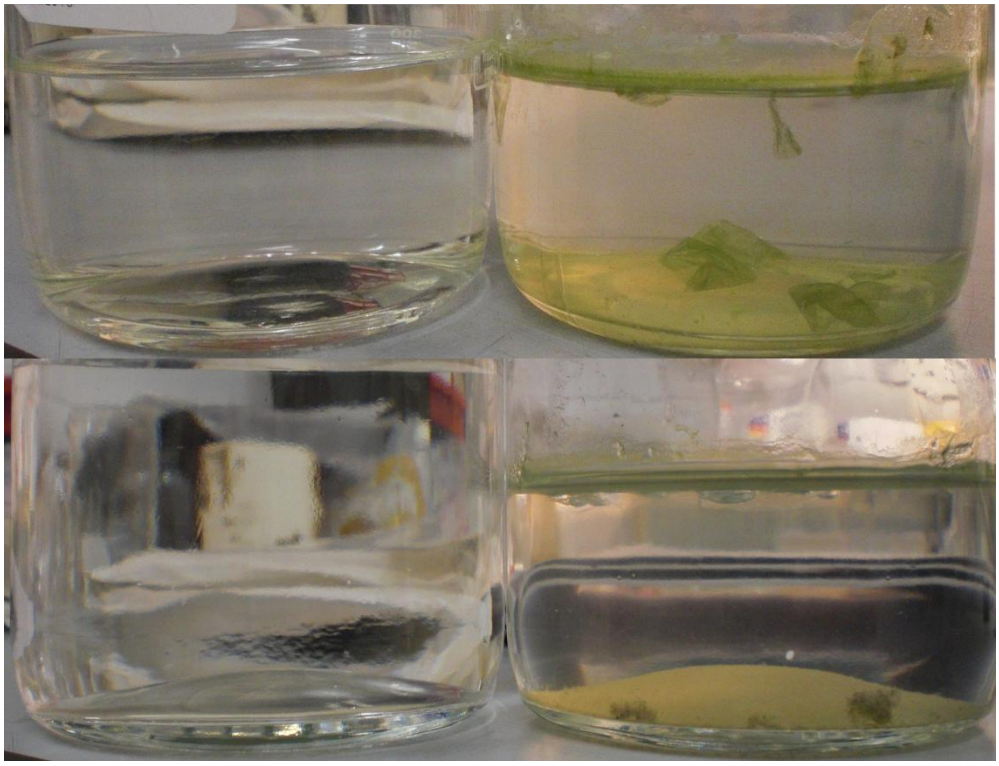

Figure 5.1: Examples of 'empty' control bottles (Left), and phytoplankton laced ones showing growth (Right).

5.3 Shot Programme #1

Two sterile glass bottles were prepared for the test programme, one for the post-shot recovered sample, and the other for the contamination control check. The surfaces and surroundings were first thoroughly sterilised using HPLC grade isopropyl alcohol. 700 ml of HPLC grade water was placed into a sterile container and then 3.5 ml of the Phyto Nutrient – 'Modified F/2 Medium' was added and then stirred with a sterile glass rod until well mixed.

400 ml of this mixture was transferred to one of the sterile glass bottles and sealed as a contamination control check. The remaining 300 ml was placed into two sterilised polythene bags, each 50 microns thick (150 ml in each bag). These bags were then mounted in a specifically designed target holder (Fig. 5.2) which had been autoclaved at 120^{o}C at a pressure of 1 bar for 35 minutes prior to all shots to kill any possible contaminants.

This experimental procedure required the use of the capability of the Light Gas Gun to fire frozen projectiles. Instead of a solid cylindrical nylon projectile, here a sterile hollow nylon cylinder was filled with a mixture of water, and Phyto Nutrient (Fig. 5.3. left image). A small amount of phytoplankton was then added to it such that approximately 10% of the 4 mm deep and 2 mm radius cylindrical cavity in the nylon was filled. (Note: All the shots in Shot Programme #2 filled the cavity to capacity with phytoplankton, with a single drop of fluid added to freeze the contents in place, as described in Chapter 4, Section 4.5). The filled cylinder was then placed in a freezer 48 hours before firing and frozen at approximately -20^{o}C. This served as the projectile (see Fig. 5.3 for dimensions of length and diameter).

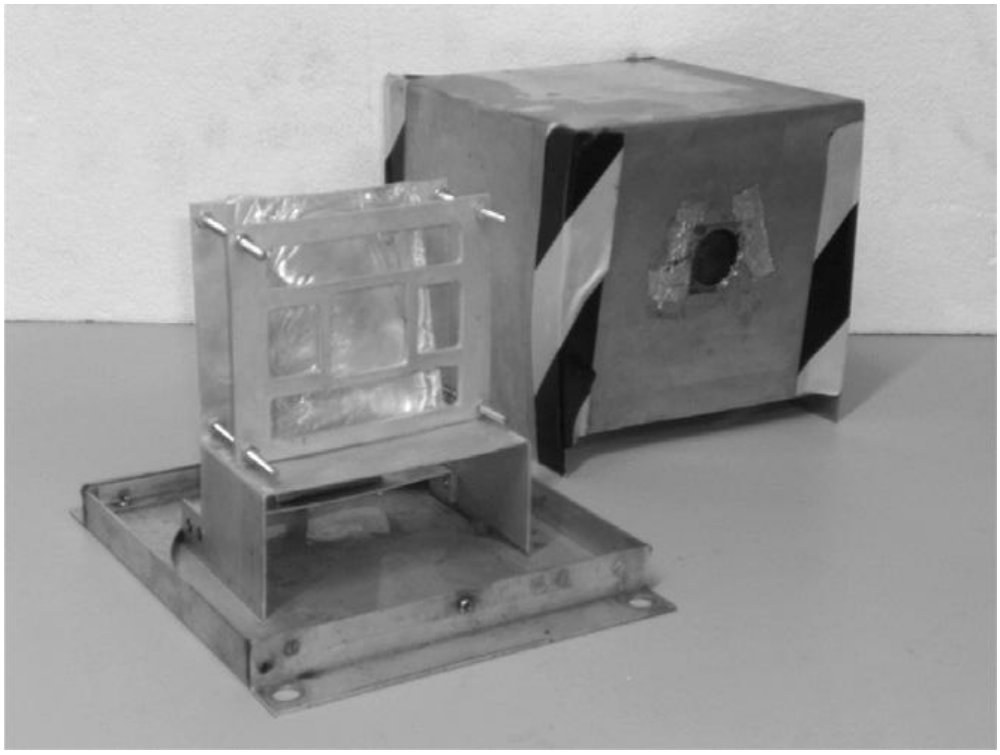

Figure 5.1: Photograph of the target fluid holder (foreground) showing one of the polythene bags held within the support frame. The aluminium box in the background is the covering for the target holder and acts to retain as much of the target fluid as possible during the impact. After the first shot however, it was realised that the tray leaked slightly and an additional larger sterile tray was placed under the whole structure. The box in the background is 17.5 cm wide, 17.5 cm deep, and 17.0 cm high.

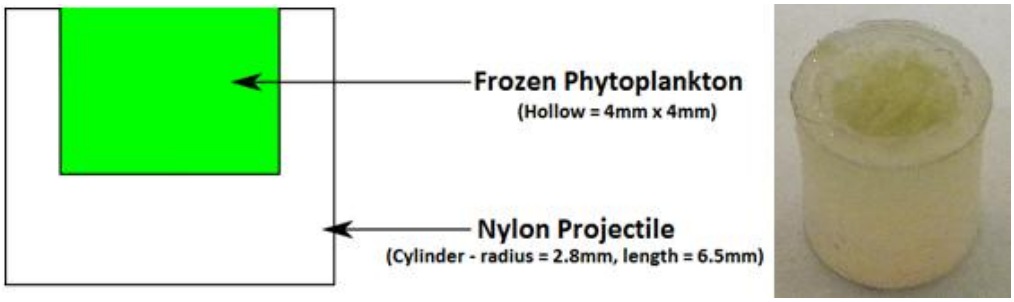

Figure 5.2: Left: Schematic diagram showing a cross sectional area of the projectile structure and dimensions (not to scale). **Right:** Actual filled projectile.

The frozen, filled projectile was then transferred to the reconfigured light gas gun (the 'Cold Gun' see Chapter 4, Section 4.2.2) as quickly as possible to avoid unwanted melting of the projectile. The launch tube of the cold gun was pre-chilled overnight in a CO_2 chest freezer (at a temperature of -180^{o}C). The frozen projectile was held in a special brass projectile loader (with a large thermal inertia) so that the phytoplankton mixture remained frozen during the loading of the projectile into the launch tube. The approximate time interval between loading the projectile and firing the gun was 15 minutes. Post shot temperature readings taken at the central breech verify that the projectile had remained frozen at the moment of firing the shot, as all temperatures measured were below -10^{o}C (this was the case for all shots on both programmes).

In order to accurately measure the speed achieved, the projectile passes through two laser light curtains, (as described in Chapter 4) allowing the speed to be calculated to within $\pm$1%. During each shot, the target chamber of the light gas gun is partially evacuated to avoid any deceleration due to aero-drag forces. The pressure used when firing onto the water targets here was 50 mBar, as the water will start to boil at pressures below this.

After a shot, the target chamber was returned to atmospheric pressure and the target holder removed. The water remaining in the target holder was carefully tipped out via a sterile glass funnel into the remaining sterile glass bottle, and then sealed. Both the contamination control check bottle and the 'live' shot bottle were placed under a constant (24 hours a day) light source (a tungsten filament desk lamp). Contamination control shots were also performed later (during the second shot programme) after several 'live' shots had taken place to check the cleanliness of the gun. For the contamination control shots the target (and holder) were prepared in an identical fashion to the 'live' shots. However, the projectile used was a sterile hollowed-out nylon cylinder filled with HPLC water ice rather than the phytoplankton mix

used for the 'live' shots. The recovered samples were retrieved in an identical fashion to the 'live' shots. This was a necessary step to ensure that the handling procedures used were not cross-contaminating the targets, and that there was no spurious contamination from the light gas gun itself.

5.4 Shot Programme #1: Initial Results

The shot performed (shot ID: G220312#1) for this first programme was done at a velocity of 1.26 km s^{-1} – the lowest speed achievable with the current gun configuration. The recovered target fluid was then left to re-culture for several weeks. The bottle containing the recovered target fluid also contained some debris from the shot (mostly torn and twisted nylon from the remnants of the projectile), this was a white colour and the only visible colour in the initial mixture. After 20 days a noticeable amount of green colouration (a sign of phytoplankton growth) was witnessed on the nylon debris within the bottle. A few days later there was also noticeable green around the water line in the bottle. This was a clear sign that there was phytoplankton surviving, and reproducing, within the bottle. However, the time to produce even noticeable amounts of phytoplankton was much longer here than in the original, and even frozen, samples (which only took ~3 days). Once a noticeable amount of green was witnessed, it continued to grow at the reduced rate, taking a long period (approximately a further 25 days) to double in concentration (compared to only a few days for unshocked samples, see Chapter 4, Section 4.3.3).

The rate of growth may also have been influenced by a lack of air supply, as the glass bottle was sealed to avoid contamination, and thus the air supply was limited for the organism. However, this was not an issue as the growth itself was evidence that there was living organisms present in the

sample – the goal of this initial shot. The contamination control check water bottle remained totally clear throughout the experiment. These initial results led to the conclusion that the witnessed growth was indeed due to the recovered shocked phytoplankton fired in the shot.

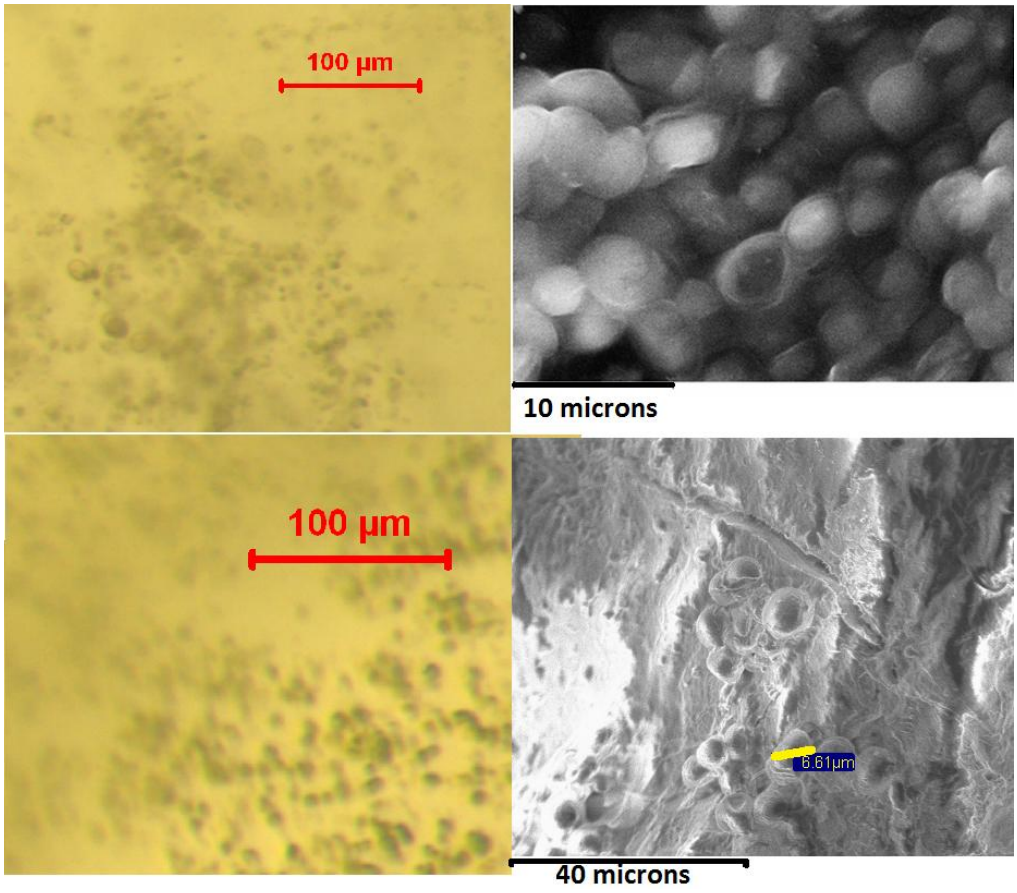

Figure 5.3: Top left: Unshocked live phytoplankton cell photographed under a high power optical microscope. **Top right:** An SEM image of unshocked deceased dried phytoplankton cells. **Bottom left**: Live descendants of shocked phytoplankton cells one year after firing. **Bottom right:** SEM image of dried descendants of shocked phytoplankton cells one year after firing.

A small sample of the shocked phytoplankton in the bottle was taken and examined under optical microscopes and the scanning electron microscope (SEM) to see if there was any noticeable differences between the shocked and unshocked phytoplankton cells, as, to-date, no studies have been performed to look for DNA damage during hypervelocity impacts that could affect the shape or size of the cells. (Fig. 5.4). No detectable differences were found in the morphology of the samples.

5.5 Shot Programme #2: Survival at Increased Velocities

In this work an exact measure of the quantity of organisms present before and after was not obtained. This was partly due to reproducibility issues when loading the projectiles and partly due to loss of target water during the impact, which may have lost an unknown fraction of the phytoplankton delivered to it. Accordingly, what is determined here is whether or not survival occurs, and the time taken for subsequent growth to be witnessed (appearance of the first green patch visible by eye). Price et al., (2013) carried out control experiments firing projectiles loaded with frozen blue ink, and demonstrated that the ink is evenly distributed throughout the target (and the target container). Thus there is confidence that the recovered target fluid and the phytoplankton are well mixed after impact.

A series of shots was undertaken at varying velocities, and thus shock pressures, to identify if the organisms survived (or not) with increasing shock pressures. Then the time until witnessed growth occurred in the post-shocked recovered samples was measured, and used to conjecture possible survival trends. However, for the higher speed shots (>5 km s^{-1}) a smaller internal diameter gun barrel was needed to obtain the higher speeds. This necessitated

the use of smaller nylon projectiles (mass 0.1 g compared to the larger 0.3 g projectiles) with a reduced cavity volume of phytoplankton (see Table 5.1).

Table 5.1: *Details and summary of results for shot programme #2 to establish if survival occurred for Nannochloropsis oculata Phytoplankton. Note, no error estimates are given as only one shot per velocity has been performed.* ***** *Ice control shots. ** Subsequently identified as a non-phytoplankton contaminant. ND = none detected.*

Shot ID	***Recorded Velocity of Shot (km s^{-1})***	***Volume of Phytoplankton mixture (mm^3)***	***Time Elapsed until observable growth (days)***	***Continued Growth of Sample?***
G041012#1	1.25	50.3	4	Yes
G251012#2	2.33	50.3	4	Yes
G101012#2	2.60	50.3	5	Yes
G311012#1	3.28	50.3	9	Yes
G221112#3*	1.32	50.3 (ice only)	62**	Minimal**
G281112#2	3.93	50.3	15	Yes
G110113#3	5.61	14.1	35	Yes
G060213#1	6.07	14.1	42	Yes
G071212#1	6.93	14.1	70	Minimal
G140213#2*	6.28	14.1 (ice only)	ND after 118 days	No

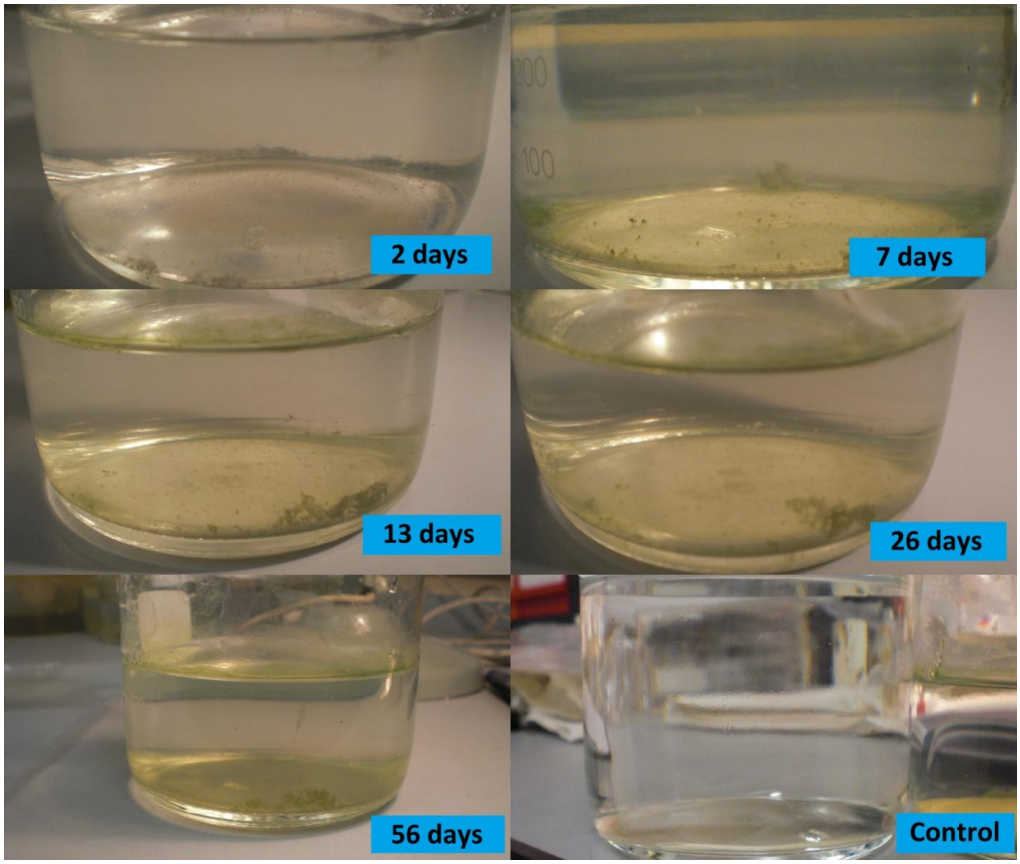

Figure 5.4: Shot G041012#1 (1.25 km s^{-1}) after 2, 7, 13, 26, & 56 days, and contamination control check for comparison (bottom right). Note that growth mainly occurs on the bottom, and around the water line. Growth (first observable green patch) was witnessed after four days, which appears to be the minimum time needed to achieve this observable growth, even with unshocked organisms.

After each shot the recovered water was placed into sterile glass bottles and sealed. In each case a separate bottle of unused target water was also sealed as a contamination control check, as in the first shot program. The bottles were then checked regularly for signs of growth, until there was a barely noticeable green patch in the bottle. This was the point at which growth was positively identified, and the time from recovery noted. Continued checks were made to confirm that the sample was continuing to grow.

Two 'ice-only' samples were also fired as contamination controls to check the cleanliness of the gun and to identify any possible contamination during the handling and transfer of target and projectile throughout the procedure. One was shot G221112#3 (a low speed shot at 1.32 km s^{-1}), the other G140213#2 (a high speed shot at 6.28 km s^{-1}). Each was performed after several 'live' shots had been conducted to allow for maximum possible contamination conditions (i.e. a worst case scenario).

5.6 Modelling and Simulation of Results

As described in Chapter 4 Sections 4.8 and 4.9, two methods were used to determine an estimate of the pressure conditions experienced by the Phytoplankton *Nannochloropsis oculata* during the hypervelocity impact process.

5.6.1 Late Stage Effective Energy Method

Using the Late-Stage Effective Energy method for impact calculations described in Chapter 4, Section 4.8, the impact pressures generated in the projectile, and thus experienced by the phytoplankton, can be calculated. While there are no *C* and *s* values for phytoplankton, like most life-forms they can be approximated as water; then the values of Trunin et al., (2001): $C = 1483$ m s^{-1} and $s = 1.75$, and those of Melosh (1989): $C = 1480$ m s^{-1} and $s = 1.60$ can be used in order to establish a sensitivity to these parameters, as described in Chapter 4. Using these values the Late-Stage Effective Energies were calculated (LE), and the associated pressures (P) were calculated for both sets of *C* and *s* parameters.

Table 5.2: *Showing the Late-Stage Effective Energy (J) and pressure (GPa) experienced by the phytoplankton cells across a range of velocities for both the Trunin and Melosh parameters.*

Shot Velocity (km s^{-1})	***Trunin Parameters***		***Melosh Parameters***	
	LE (J)	***P (GPa)***	***LE (J)***	***P (GPa)***
1.25	0.480	3.00	0.462	2.89
1.26	0.486	3.04	0.469	2.93
1.32	0.520	3.25	0.499	3.12
2.33	1.231	7.69	1.168	7.30
2.60	1.464	9.15	1.388	8.67
3.28	2.145	13.4	2.017	12.6
3.93	2.897	18.1	2.721	17.0
5.61	1.793	26.1	1.670	24.3
6.07	2.061	30.0	1.924	28.0
6.28	2.192	31.9	2.041	29.7
6.93	2.611	38.0	2.433	35.4

Table 5.2 shows there are the range of pressures experienced by the phytoplankton cells, 3.00 – 38.0 GPa (Trunin parameters), and 2.89 - 35.4 GPa (Melosh parameters).

5.6.2 Ansys' AUTODYN Method

As described in Chapter 4, Section 4.9, Ansys' AUTODYN, is a commercially available hydrocode (Hayhurst & Clegg, 1997) and was used to model the peak shock pressure experienced within the projectile. AUTODYN allows for a more accurate determination of the shock pressure, as well as allowing estimates of the pressure versus time to be made.

The experiment was modelled using a lagrangian mesh and the target was modelled as an 80 mm cylinder water target 40 mm thick. However, due to the axial symmetry of the model, this was cut in half giving a target that was a semi-cylinder of water, comprising 160,000 equally sized cells. The projectile was modelled as a 6.5 mm long nylon cylinder 5.8 mm thick, with an internal cavity filled with water, as no model for ice existed (2.9 mm deep and 3.2 mm diameter), comprised of 1900 cells (Fig. 5.6). However, a smaller projectile was used for the four highest speed shots to replicate the actual experiment; this was comprised of 1000 cells and had a height of 4.48 mm, diameter 4.42 mm, with a 3.00 mm diameter by 3.00 mm deep cylindrical cavity. Forty seven software gauges were placed inside the cells within the projectile in order to track the pressure during the impact event. The equation-of-state parameters were taken from the AUTODYN material library and are detailed for nylon in Matuska (1984) and water in Trunin et al. (2001). As before, the phytoplankton was modelled as pure liquid water, as no equation of state parameters could be found in the literature for phytoplankton. Price et al. (2012) demonstrated the relative insensitivity of the calculated peak shock pressures on the exact form of the equation of state, and given other experimental uncertainties, these approximations can be deemed as valid. The peak pressures in the simulations occur just after the projectile penetrates the water target (Fig. 5.6. see Table 5.3 for the results of these simulations). The peak shock pressures for both AUTODYN and those calculated using Eqn. 4.11 are also shown in Table 5.4 for comparison.

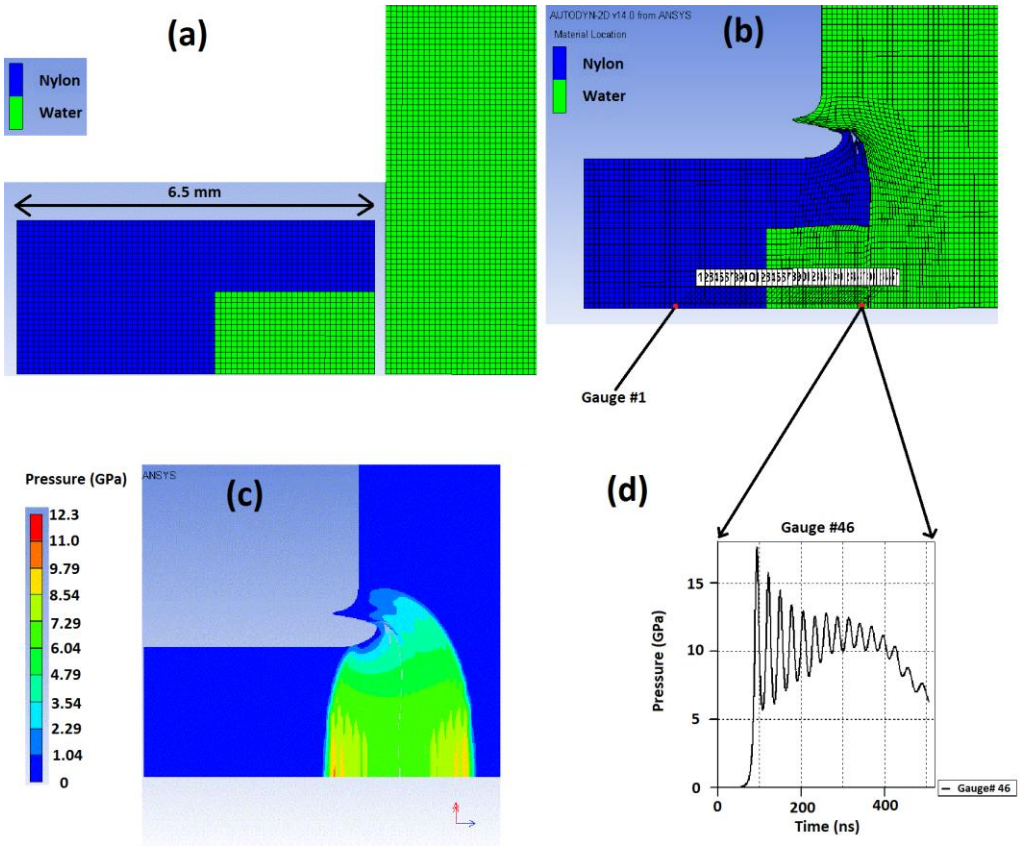

Figure 5.5: Example output from AUTODYN simulations for a 3.93 km s^{-1} impact into water. **(a)** The model shown prior to impact. **(b)** The model shown after impact showing the location of software measurement gauges to monitor the pressure during the impact event and the composition of the projectile. **(c)** Contour map of pressure 507 ns after impact. **(d)** The time evolution of pressure for gauge #46 (the gauge that showed the highest pressure).

It can be seen in Table 5.3 that the peak pressures rise from 2.84 to 58.6 GPa in the experiments presented here, as the impact velocity increases from 1.25 to 6.93 km s^{-1}. For the highest impact velocity (6.93 km s^{-1}) the peak shock pressure is 58.6 GPa which occurred 30 ns after impact. A comparison of both methods of pressure calculation is presented in Table 5.4 in the next section.

Table 5.3: *Showing AUTODYN pressure result for the pressures experienced by the phytoplankton cells over a range of velocities, as well as the time the peak pressure occurred after impact.*

Velocity (km s^{-1})	***P (GPa)***	**Δt *(ns)***
1.26	2.87	1163
1.25	2.84	1166
2.33	6.54	652.6
2.60	7.76	135.6
3.28	12.2	110.5
1.32	3.03	1134
3.93	17.6	94.20
5.61	37.0	111.4
6.07	43.8	78.60
6.28	47.3	65.70
6.93	58.6	30.00

5.7 Summary of Results:

Table 5.1 shows the time interval from impact to observed growth for each shot. The two methods for the calculation of the peak shock pressures described above were then used. Table 5.4 gives the peak shock pressures attained by both these methods for each shot, along with the corresponding time at which the peak pressure was experienced after impact. Both methods of obtaining peak pressures agree at speeds below 5 km s^{-1}, but then start to diverge at higher speeds. The hydrocode results give a noticeably higher peak shock pressure, but this is confined to a small region of the projectile material, whilst the LSEE method gives a value more indicative of the peak pressure to which most of the material is shocked.

All post-impact samples of phytoplankton (descendants of the originally shocked cells) were examined under both an optical microscope (living 'wet' samples) and a scanning electron microscope (SEM) (deceased 'dry' samples, necessary before placing in the vacuum chamber of the SEM). No samples showed any apparent change in morphology from the original unshocked sample (Figs. 5.4 & 5.11) except G221112#3 (v = 1.32 km s^{-1}) which is discussed further below in Section 5.9 and is shown in Fig. 5.12.

Table 5.4 shows the Late-Stage Effective Energy method produces a pressure value similar to the AUTODYN simulations for the larger (used for velocites < 5 km s^{-1}) projectile, although there is a larger discrepancy when the projectile volume is reduced at the higher speeds.

Table 5.4: *Peak pressures, P, from AUTODYN simulations, and Eqn (4.11) as a function of impact velocity. Also shown are the time, Δt, after impact at which the peak pressure is experienced. * Ice control shots.*

Shot ID	***Velocity (km s^{-1})***	***P (AUTODYN) (GPa)***	***P (Eqn. 4.11, C and s from Turnin et al., 2001) (GPa)***	***P (Eqn. 4.11, C and s from Melosh 1989) (GPa)***	***Δt (ns)***
G220312#1	1.26	2.87	3.04	2.93	1163
G041012#1	1.25	2.84	3.00	2.89	1166
G251012#2	2.33	6.54	7.69	7.30	652.6
G101012#2	2.60	7.76	9.15	8.67	135.6
G311012#1	3.28	12.2	13.4	12.6	110.5
G221112#3*	1.32	3.03	3.25	3.12	1134
G281112#2	3.93	17.6	18.1	17.0	94.20
G110113#3	5.61	37.0	26.1	24.3	111.4
G060213#1	6.07	43.8	30.0	28.0	78.60
G140213#2*	6.28	47.3	31.9	29.7	65.70
G071212#1	6.93	58.6	38.0	35.4	30.00

The time until noticeable growth from shot programme #2 are plotted against peak shock pressure in Fig. 5.7. The shock pressures from Eqn. 4.11 (with *C* and *s* values taken from Melosh (1989)) were used, as the LSEE method seems to give a peak shock pressure more typical of the bulk of the phytoplankton. The data shows an exponential increase in time until appreciable growth is observed with increasing shock pressure (see Fig. 5.7).

If a sample of phytoplankton were taken which were frozen in a projectile, but instead of firing in the gun were directly placed in a flask of water, the time for the on-set of growth as used here was observed to be 2.5 - 3 days. There is thus a clear difference between shocked and un-shocked samples.

Since there is a suggestion in the data (see Table 1) that at low shock pressures, the delayed growth time is roughly constant, the lowest shock pressure datum in Fig. 5.7 was excluded and the fit repeated. No significant change in the fit parameters occurred.

As a further test of the data, since we used two separate sizes of projectiles in this work, the data were split into low (<5 km s^{-1}) and high (>5 km s^{-1}) data-sets. These are shown fitted separately in Fig. 5.8. The exponential delay time appears to increase as shock pressure increases, but the number of data points at high speed is low. However, at present, no analysis has been performed to determine why this delay in obvious growth occurs, this may possibly be due to the kinetic recovery time of the organism, or the surviving fraction, or more likely a combination of both; it is hoped that this will be the subject of a future work by the author.

5.8 Analysis and Discussion

Significant data now exist that demonstrates the survival of organisms in shock event experiments at the GPa scale. For example, Burchell et al. (2004), shows that there is a logarithmic decrease in survival with increasing shock pressure in the GPa regime. The logarithmic trend was also observed by Stoffler et al (2007), and this group has gone on to publish several studies showing this same trend (e.g. Horneck et al., 2008; Meyer et al., 2011). While these works focus on survival fraction of the organisms, the new work presented here focuses on whether survival actually occurs or not. However, as all shots showed survival, the time until the first appearance of a green patch was then used to conjecture on possible trends of survival. The time recorded here is likely due to a combination of decreased survival rates at higher shock pressures, combined with damage to the survivors, delaying the on-set of growth. However, the exact nature of the relation between these two effects is not yet known and, accordingly, the author is currently working towards attaining a more precise quantification of survival for the organism. However, the data presented here do show an exponential increase in the time taken for noticeable growth with increasing shock pressure, and thus an exponential decay of time until noticeable growth by surviving organisms (see Figs. 5.7 & 5.8).

This follows the same trend proposed by Burchell (2007) and Burchell et al., 2010, (see Fig. 5.9). However, there is likely to be some proportionality factor that needs to be added, as well as the recovery time of the organism at each shock pressure, for a quantitative analysis of the actual surviving fraction to be undertaken. It is further noted that the model proposed by Burchell (2007) and Burchell et al., (2010) shows an increase in lethality as shock pressures rise, which is compatible with the increased

growth delay time at the higher impact speeds (and higher shock pressures) suggested in Fig. 5.8.

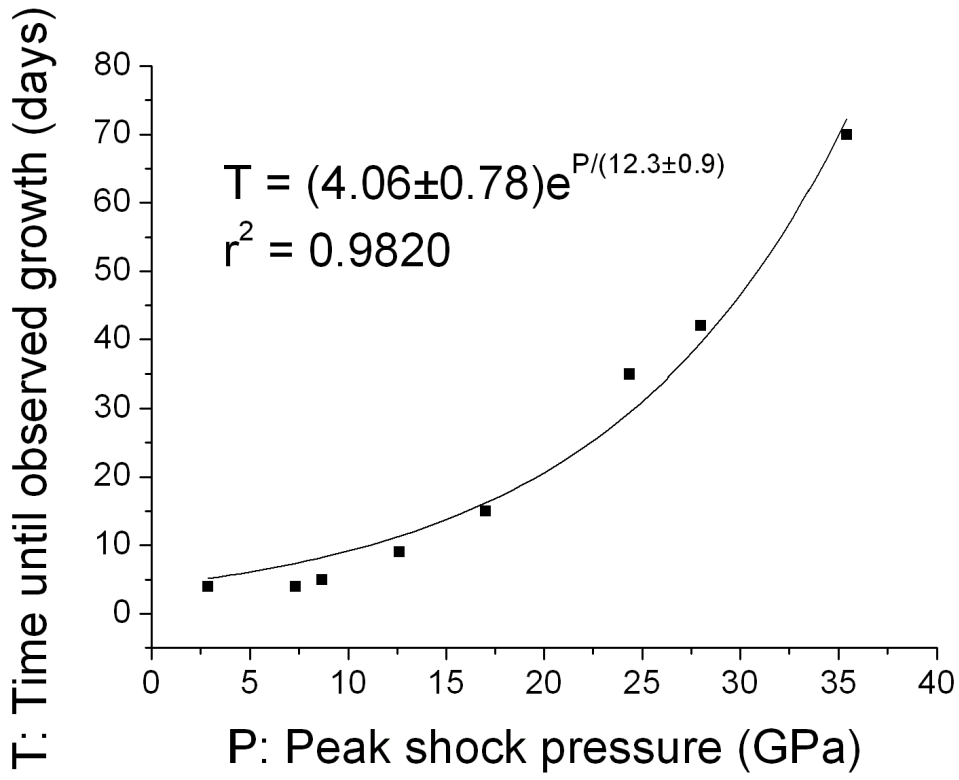

Figure 5.6: Plot of time to on-set of phytoplankton growth versus peak shock pressure after impact induced shock. The fit shows an exponentially increasing delay with increasing shock pressure until appreciable growth occurs.

As stated above, it has been proposed by Burchell (2007) and Burchell et al. (2010) that survival rates versus peak shock pressures fall into two distinct regimes, as shown schematically in Fig. 5.9. It shows there is a relatively slow decrease in survival at low peak pressures, but above some critical (organism dependant) value (typically a few GPa), the decrease becomes exponential. At the very high pressure end of the curve (50 – 100 GPa), there are extra effects to be considered such as associated high peak

shock temperatures, and prolonged heating on release from the shocked states. Impacts at these speeds causes partial melting of rock and metal targets and thus can be assumed to be completely sterilising. Hence all survival curves would tend to converge in this shock pressure regime (Price et al., 2013) and it is likely that phytoplankton are no exception to this, and future quantitative work will aim to establish if this trend for survival is indeed correct for phytoplankton.

Related work by Zimmerman (1971) and Heremans (1982) has shown that for yeast cells, high pressure has detrimental effects on many of the cellular structures, including those required during mitosis (Zimmerman, 1970), and it is thus possible that some changes in cell morphology could result from high pressure impacts and the disruption of the cell replication machinery. Fig. 5.10 presents some images of shocked samples of phytoplankton, and it can be seen that if there is any damage to the DNA in the cells of the phytoplankton, it has not altered the morphology of their external cellular structure. There may be damage, and changes in morphology, internal to the cell, but these are not evident from an external viewpoint. It is therefore concluded that the size and external shape of the surviving cells of *Nannochloropsis oculata* Phytoplankton are the same before and after impact.

Additionally we see no change or damage to the cells due to the temperatures created during hypervelocity impacts. For example, during the impact that causes the highest peak temperature (6.93 km s^{-1}), this temperature peak is experienced 30.00 ns after impact and returns to tolerable temperatures within a further 150 ns. The short time interval this occurs in reduces the amount of energy transfer. Therefore, the peak temperatures reached during the impact event dissipate on short enough timescales as to not cause extensive damage or death to the micro-organisms, rendering them non-sterilising.

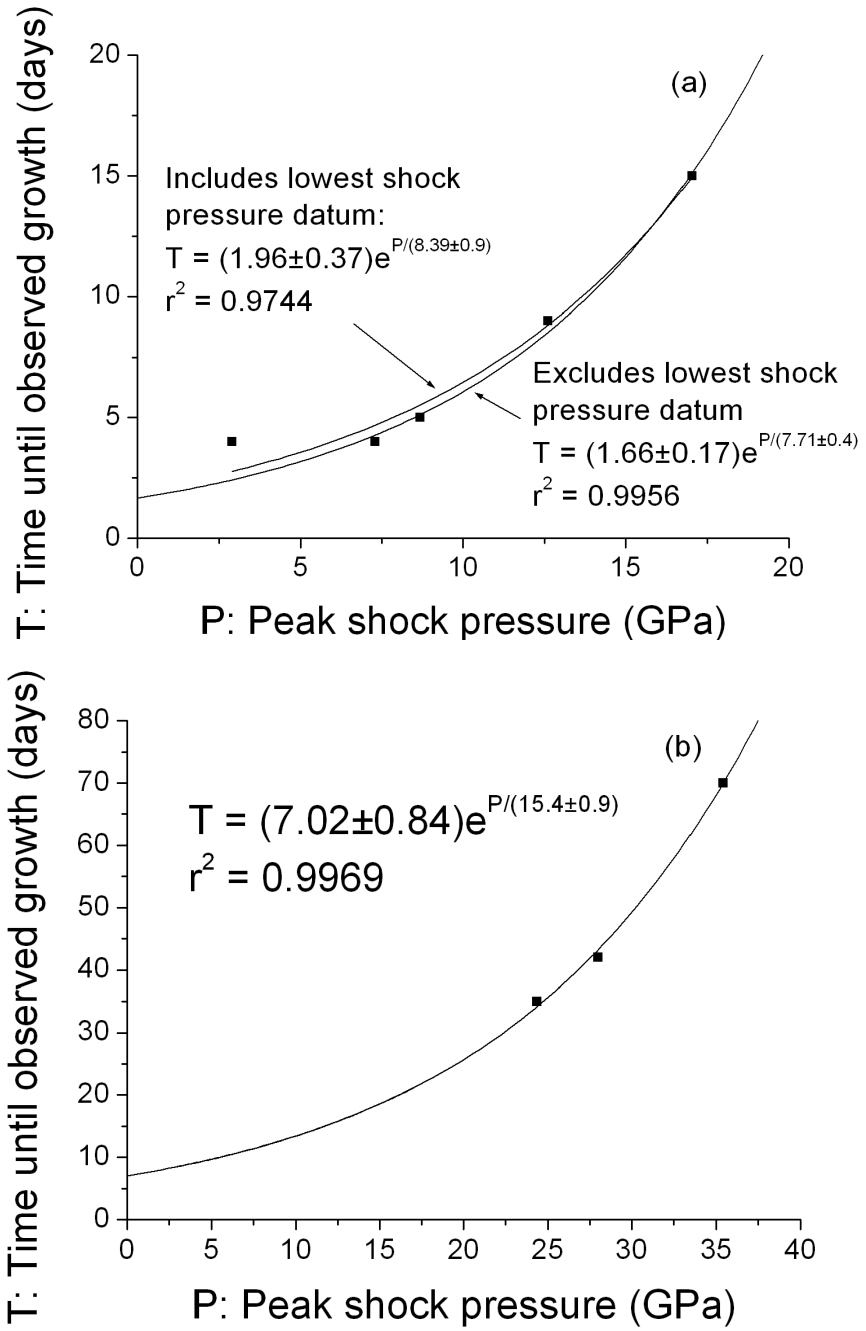

Figure 5.7: Individual plots of the data for the two different sized projectiles used in shot programme #2. **(a)** Larger projectile for lower speed (< 5 km s^{-1}) shots, and **(b)** Smaller projectile for higher speed (> 5 km s^{-1}) shots.

Both plots in Fig. 5.8 show similar trends. However, the difference in the fit parameters, with a slower time until growth at higher impact speeds could potentially be indicative of the critical point between the two regimes of survival proposed by Burchell (2007) and Burchell et al., (2010). In Fig. 5.8(a) the fit is performed twice, excluding the lowest shock pressure datum as a test of sensitivity to low shock pressures.

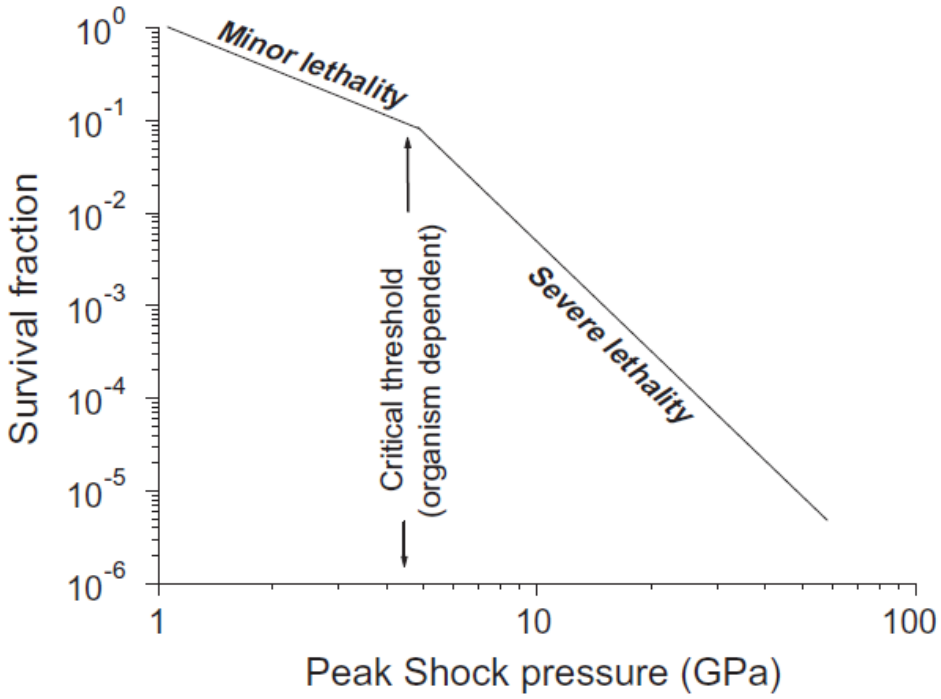

Figure 5.8: Schematic showing the evolution of survival with peak shock pressure (adapted from Fig. 7 in Price et al., 2013)

If the kinetic recovery time of the shocked cells is assumed to be constant (or the difference negligible), then the time until growth is witnessed can be taken as a measure of the survival rate of the cells (see Fig. 5.10). Although no direct survival rates can be measured, the pattern does show the

same trend that Burchell, M. et al. (2010) suggests could be the two regime pattern for most micro-organisms.

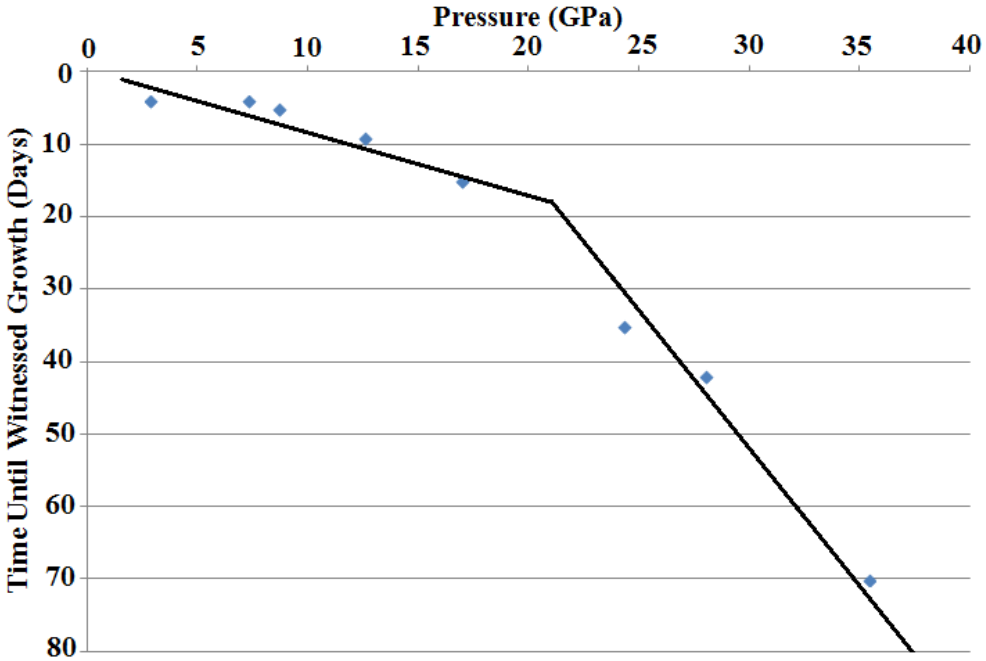

Figure 5.10: Showing time until visible growth is witnessed in recovered shocked phytoplankton cells against the pressure experienced by the cells, when assuming negligible changes to kinetic recovery, the time can be taken as an indicator of survival rate. The trend matches the proposed trend for micro-organisms by Burchell, M. et al. 2010.

Willis et al., (2006) also carried out some studies that are relevant in the high pressure regime. They fired plates at targets that contained liquid suspensions of *Escherichia coli* bacteria, generating shock pressures in the samples of 2 – 3 GPa. When they recovered the targets, they obtained transmission electron microscope (TEM) images of the bacteria. They found evidence of delineation of the cell walls. Various mechanisms were put forward to explain this observation, either instabilities as shocks pass through

materials with different impedances, or possibly rupture due to over-pressure (i.e. if high pressure phases of ice formed in the surrounding water media). The onset of this (increasingly lethal) damage to the cell walls occurred at peak pressures of a few GPa, and this applied to the bulk of the sample. The small degree of lethality observed at low pressures may be due to shock damage to weaker members of the sample, local environmental conditions, etc.

The critical shock threshold most likely depends on the organism itself, as suggested by Burchell (2007). The nature of the surrounding media may also play a role, but experiments to date have used a wide variety of media, such as samples carried in liquid suspensions, samples frozen in different ices, samples on (and within) rock, etc. Even with this wide range of media, the general shape of the survival curves is similar, which suggests whatever role it plays (if any) does not overly change the result. Another suggestion is that some other property of the shock event may be a responsible factor for the lethality observed, such as elevated temperatures in the samples after impact shocking.

Hazell et al. (2010) have shown that, when impacted by a flyer plate, an oil based target solution shows increased emulsification. The bubbles observed in the emulsions in these experiments had diameters ranging between 1 – 20 microns, indicating that objects at this size scale are being influenced by shockwaves propagating through the sample. This is comparable to the size range of *Nannochloropsis oculata* Phytoplankton which range (in the sample used here) in a size distribution between 3 – 12 microns, with an average size of 6.5 microns; this distribution was the same for all samples analysed. Thus it is likely that the cells of the phytoplankton are indeed being influenced in some way, albeit one that is undetectable to the probes used here.

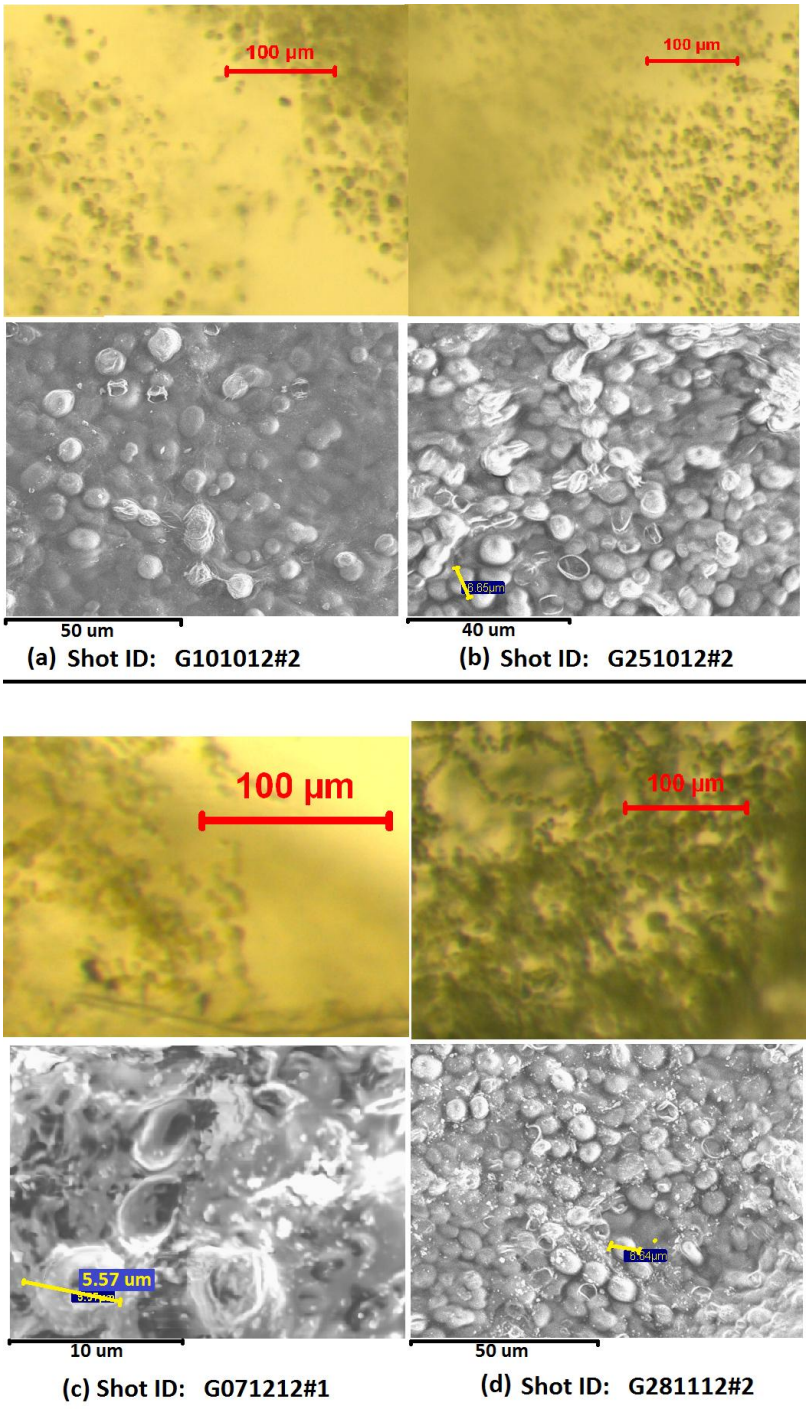

Figure 5.11: Images of shocked samples of phytoplankton from four separate shots. In each case the upper images were taken with an optical microscope and the lower images are SEM images. Comparison of the samples with each other and with the unshocked samples show no obvious signs of change in morphology, or size.

5.9 Contamination

Two standard contamination control checks of unused target water (the contamination control checks for shots G311012#1 and G110113#3) showed, what seemed to be at first, a small growth of phytoplankton. The level of growth witnessed in these two controls was very low, and took 45 and 52 days respectively to be seen. The growth in both cases was confined to a single small region, a small spot on the bottom of the glass bottle for G311012#1, and a small spot on the water's surface for G110113#3. Each spot only grew to a very small size in comparison with the actual fired samples, and therefore even, if the same contamination occurred in the actual shot samples, it could not account for the growth witnessed in these shots. Both of these corresponding samples from the actual shots showed appreciable growth on much faster time scales (9 and 35 days respectively) and showed far more growth in total. They also gave the water a mild green colouration due to the concentration of the organism in the fluid, but the contaminated controls never developed this colouration throughout the whole experiment that was terminated much later (224 days after G311012#1 and 152 days after G110113#3). The illumination for all samples was the same and constant, and all bottles were sealed so the air supply, although limited, was equal for all samples.

One further example of contamination was seen in the low speed ice contamination control check shot G221112#3 (see Fig. 5.12). After 62 days a green 'blob' appeared on the bottom of the glass bottle. However, as this green blob grew it was clearly a distinctly brighter green colour than the phytoplankton samples used in the experiment. It also grew in a different way, preferring to build on itself in a bulbous fashion (as opposed to phytoplankton which cling to the waterline, grow on the surface in sheets, or simply free float in the liquid as individual cells giving the water its green

colouration). After further examination under the SEM it was discovered that it was an unknown contaminant, as the cell morphology was completely different to that of the phytoplankton, and thus could be neglected with regards to phytoplankton contamination (of which there was none in both ice control shots, and their respective unfired contamination control check samples). It is speculated that the contaminant may be some form of bacteria due to the tubular shape of its cells, and the chains these cells are arranged in, or potentially a subspecies of algae that forms in chains.

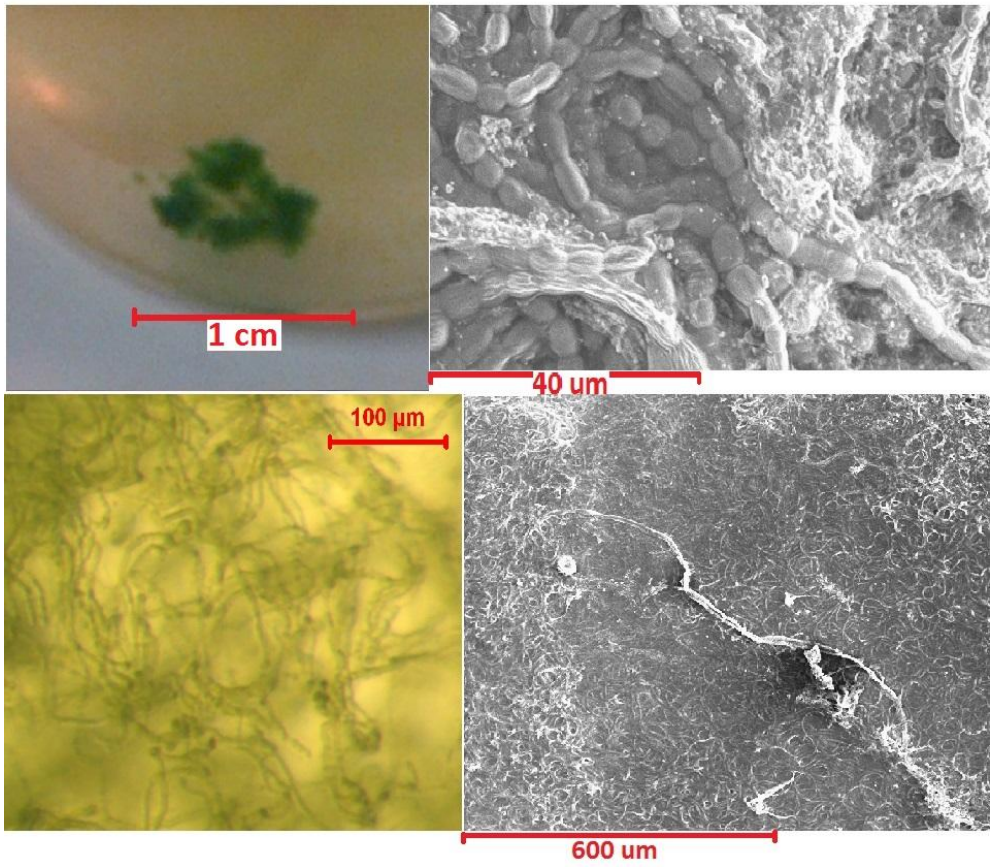

Figure 5.12: Unknown (presumed bacterial) contamination in low speed ice control shot (G221112#3)**. Top left:** photograph of the contamination in the glass bottle. **Bottom left:** optical microscope image of a small sample of the contamination. **Top and bottom right:** SEM images of a small sample of the contamination showing its tubular chain 'bacteria-like' structure.

5.10 Conclusion

This chapter reported on the experimental and computational techniques performed to test the phytoplankton species *Nannochloropsis oculata* for survival during hypervelocity impact events. It was discovered that *Nannochloropsis oculata* can indeed survive hypervelocity impact events up to at least 6.93 km s^{-1} (the highest speed shot performed) into a water target (peak pressure approximately ~ 58.6 GPa) albeit with a sharper decline after 20-25 GPa where the lethality turns from 'minor' to 'severe'. This further expands the knowledge of the types of organisms that can survive this shock regime.

A water target was used to simulate an oceanic impact, as described in Milner et al., (2006), and the projectiles were fired using a two stage light gas gun (Burchell et al. 1999). Water targets were used as this represents an impact onto the majority of the surface of the Earth, and would be the required habitat for the survival and reproduction of migrant phytoplankton cells.

Modelling and simulations of the hypervelocity impact events of the experimental programme showed that the survival regime during hypervelocity impacts for *Nannochloropsis oculata* is approximately ~ 2.84 GPa – 58.6 GPa, (pressures below 2.84 GPa would correspond to velocities lower than 1.25 km s^{-1} which would fall below the threshold of hypervelocity).

The peak temperatures experienced by the cells dissipates quickly enough after initial impact so as not to cause significant damage to the micro-organism, allowing it to survive an otherwise sterilising temperature.

Finally, contamination of one control sample was found to contain an unidentified strain of bacteria, but no phytoplankton contamination was

found in any control samples, providing evidence that all witnessed growth in ‘live’ shot samples was indeed from the individual performed shots, and that the sterilisation techniques between shots were sufficient.

CHAPTER 6
THE SURVIVAL OF THE TARDIGRADE SPECIES HYPSIBIUS DUJARDINI

"When provoked, the itsy-bitsy invertebrates known as tardigrades can suspend their metabolism. In that state, they can survive temperatures of... 73 K (-328 degrees F) for days on end, making them hardy enough to endure being stranded on Neptune. So the next time you need space travellers with the right stuff, you might want to choose yeast and tardigrades, and leave your astronauts, cosmonauts, and taikonauts at home."

Neil DeGrasse Tyson

6.1 Introduction

Following the successful work of the phytoplankton shot programme described in the previous chapter, another shot programme was embarked upon. This new shot programme aimed to test a new species of micro-organism for survival during hypervelocity impact events – the tardigrade species *Hypsibius dujardini*. This chapter will describe in detail information regarding the experimental 'velocity range' shot programme that was performed, as well as describing the results of this programme. The results from the hydrocode modelling and calculations are then detailed. Analysis and discussion and a temperature study of tardigrades frozen in water ice is then presented, before a discussion on the implications these results have for panspermia. Finally, concluding remarks are passed.

6.2 Target Preparation

Several samples of tardigrades were sourced from Sciento (www.sciento.co.uk). These were first examined to ascertain how many viable organisms were in each divided sample (approximately 400 - 500 organisms), then the samples were placed in a plastic target (see Fig. 6.1) and put into a freezer at approx. -25^{o}C.

Figure 6.1: Plastic target (base 51 × 51 mm) filled to 1 cm depth with the tardigrades in frozen water ice with algal food for sustenance upon thawing.

A shot program was undertaken with velocities ranging from 0.372 to 5.49 km s^{-1}, firing a cylindrical nylon projectile (diameter 4.4 mm × length 4.5 mm) at a target (51 × 51 × 10 mm) of ice containing frozen tardigrades.

The target was housed within an aluminium target holder designed to allow a projectile in to impact the target, but minimise the ejecta loss due to impact. This was achieved by having an aluminium box surrounding the target holder with a small hole for the projectile to travel through. The box itself stops any ejecta escaping, allowing it to collect at the bottom of the holder in a tray for collection, see Fig. 6.2. Several different version were used throughout the shot programmes due to damage caused by the high velocity impacts

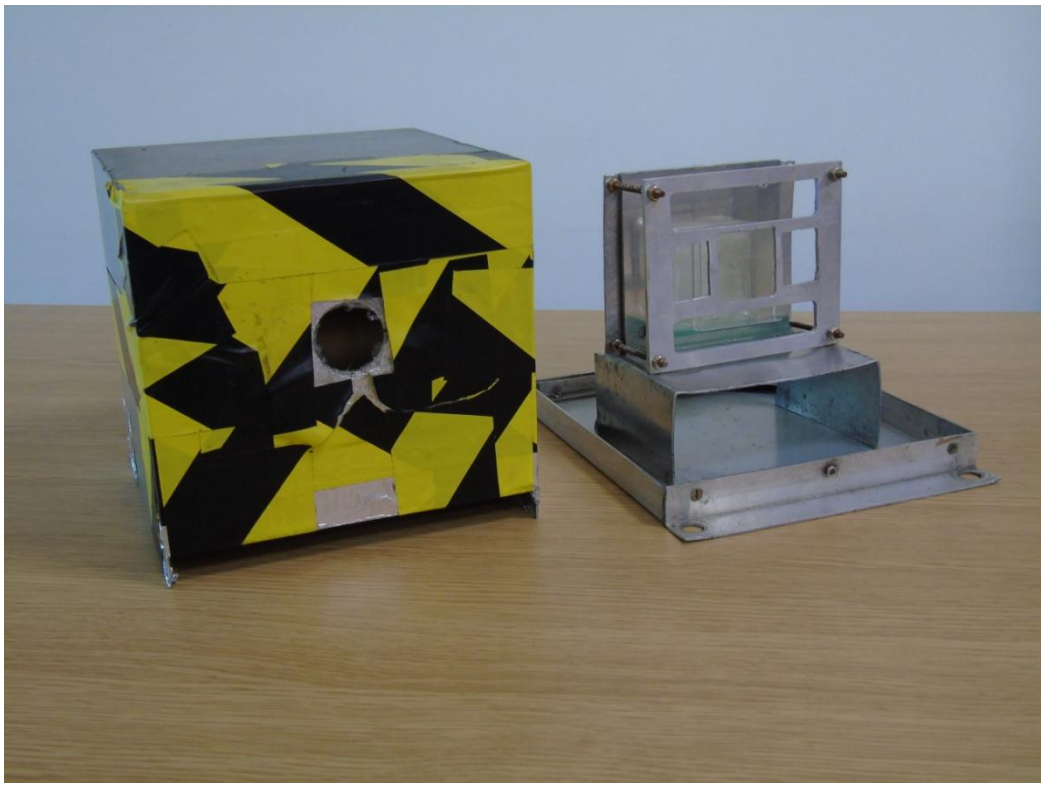

Figure 6.2: Target holder (right) with housing (left) removed (target is placed such that the top face of the ice is within the central square hole in the inner holder). The housing box is 17.5 cm wide, 17.5 cm deep, and 17.0 cm high. This is one of several different holders used due to damage sustained by the high velocity impacts.

6.3 Shot Programme

For each sample impacted, another was also removed from the freezer and thawed, this served as the unshocked control sample. Table 6.1 gives details of the shot programme performed.

This experimental procedure used of the Light Gas Gun (LGG) (described in Chapter 4) to fire a sterile, solid cylindrical, nylon projectile. The target was left in a freezer at -25^{o}C until the LGG was ready for shooting, at which point it was removed and placed directly into the target chamber to minimise melting of the target media. Then the LGG was evacuated to a pressure of 50 mBar - this is as low as it could be taken to avoid significant sublimation of the ice target. Once the LGG's target chamber was at 50 mBar, the room was evacuated of personnel and the LGG was fired. The approximate time interval between loading the projectile and firing the gun was 15 minutes. Several tests of control samples showed that no significant melting occurred in this time interval using this experimental set up.

In order to accurately measure the velocity achieved, the projectile passes through two laser light curtains, (also described in Chapter 4) allowing for an accuracy of calculation of the speed of the shot to be made that is accurate to within $\pm$1%.

After a shot, the target chamber was returned to atmospheric pressure and the target holder immediately removed. The water and ice remaining in the target holder was carefully poured through a sterile glass funnel into a sterile petri dish (diameter 8 cm). A small glass pipette was then used to extract all remaining drops of water and ice from the target holder, and these were also placed in the petri dish.

Table 6.1: *Parameters of the shot programme performed.*

Shot Number	***Shot ID***	***Time Frozen Prior to Shot (days)***	***Impact Velocity (km s^{-1})***
S1	G281113#1	14	0.37
S2	G100414#1	8	0.65
S3	G211113#1	7	1.03
S4	G240414#1	22	1.40
S5	G160414#1	14	1.41
S6	G030414#1	1	1.42
S7	G041213#1	21	1.95
S8	G060214#2	13.5	2.23
S9	G300114#1	6.5	2.80
S10	G131213#1	1	3.23
S11	G280414#1	26	3.45
S12	G120214#2	20	4.29
S13	G280214#1	36	5.18
S14	G200214#3	28	5.49

Both the control and the 'live' shot samples were placed into an 'Exo-Terra' egg incubator (see Fig. 6.3) under a constant light source at a stable temperature of 25^{o}C $\pm$1^{o}C for 24 hours. At this point they were then removed so analysis could begin.

Figure 6.3: 'Exotherma' incubator, used to store the post-shock and control tardigrade samples ready for analysis.

6.4 Post-Shock Analysis

Each target contained between approximately 400 and 500 organisms. These were randomly distributed throughout the whole of the target. Analysis of several samples before freezing showed an almost uniform distribution of organisms across the bottom of the target. Several areas (approximately 1/6th of the sample) were chosen at random within three different samples and the

organisms counted. This yielded similar results each time with only minimal deviation.

Table 6.2: *The distribution of organisms within the samples. Three random samples were chosen, and each had three random small areas of the same size analysed – approximately 1/6th of the sample area (~3x10^3 mm^2).*

Counting Area	***Number of organisms***
Sample 1 Area 1	65
Sample 1 Area 2	71
Sample 1 Area 3	68
Sample 2 Area 1	66
Sample 2 Area 2	68
Sample 2 Area 3	70
Sample 3 Area 1	71
Sample 3 Area 2	68
Sample 3 Area 3	66

Table 6.2 shows the distribution of tardigrades in the sample is fairly even across the target (there were in some instances grouping and voids but only on very small scales, and thus did not affect the overall distribution across larger areas). Each random area thus showed an average of 68 $\pm$ 3 organisms.

Each sample was analysed using an optical microscope at 1000× magnification. For each shot two frozen targets were used (each frozen at the same time): one was fired on (and thus shocked) then left to thaw, the other was simply left to thaw as a control. After 24 hours both samples were analysed under the optical microscope and all organisms were counted and their condition documented.

To determine where an individual tardigrade was living or dead required several factors to be considered. Overt movement was an obvious sign of life; however, tiny involuntary movements *within* the organisms also confirmed life even if the organism was overtly still. Additional to these factors, dead tardigrades showed a particular morphology indicating no muscle tension. The determination of live or dead was challenging in the first instance: however, after many test batches the observer's eye became more attuned to the determination of live or dead.

Approximately 350 total organisms (approximately 70 – 85% of a sample) were counted for each sample (living and dead). The ratio of living-to-dead organisms within a shocked sample gave a measure of the survival rate when compared to the ratio of the corresponding control sample.

The post-shock survival fraction of the shots was derived by first finding the ratio of living-to-total organisms, of both control and shocked samples (eggs and discarded cuticles were not included, only fully hatched whole organisms). It should be noted that even within the control samples a certain fraction of the organisms had died. These ratios were then divided by one another – shocked by control – to determine the post-shock survival fraction of the organisms.

$$S_{ff} = \frac{L_s/T_s}{L_f/T_f} \qquad \text{(Eq. 6.1)}$$

where S_{ff} is the survival fraction for shocked organisms that have previously survived freezing, L_f and T_f are the number of living and of total (living and dead) organisms respectively, in a frozen, then thawed, control sample, L_s and T_s are the number of living and of total (living and dead) organisms respectively in a frozen, then shocked, then thawed, sample. However, this only showed the fraction of survival from those that could survive in the frozen state.

To find the post-shock survival fraction of an initial unfrozen population, the living–to–total ratio of the shocked sample was divided by the living–to–total ratio of an initial unfrozen sample, such as would be found naturally in a wild population. This provides the post-shock survival fraction for an initial population in a normal natural state before the specific shot that was performed.

$$S_{fi} = \frac{L_s/T_s}{L_i/T_i} \qquad \text{(Eq. 6.2)}$$

where S_{fi} is the survival fraction for shocked organisms from an initially natural state, L_i and T_i are the number of living and of total (living and dead) organisms respectively in an initial unfrozen, control sample, L_s and T_s are the number of living and of total (living and dead) organisms respectively in a frozen, then shocked, then thawed, sample.

For the temperature studies, the survival fraction after freezing was found using the same basic methodology. However, the living–to–total ratio of the thawed frozen sample was divided by the living–to–total ratio of the *same* sample before it was frozen rather than a separate control.

6.5 Modelling and Simulation of Results:

As described in Chapter 5, two methods were used to determine an estimate of the pressure conditions experienced by the Phytoplankton *Nannochloropsis oculata* during the hypervelocity impact process, The Late-Stage Effective Energy method and hydrocode modelling using Ansys' AUTODYN. However, as the Late-Stage Effective Energy method can only give estimates of the peak pressures experienced during an impact this is of no use here.

Here the pressure range across the whole target containing the tardigrades is required in order to determine the pressures the target is exposed to during impact. The goal here is to determine the point at which the minimum peak pressure occurs in the target as this is the minimum pressure that the entire target and thus every tardigrade in that target has been subjected to. Therefore any surviving tardigrades will have *at least* survived this pressure if not higher. This can be used to constrain the limits of survival for the tardigrades. These computer simulations were performed to accurately gauge the impact induced shock pressures felt at all points in the target's back edge, where the tardigrades were located.

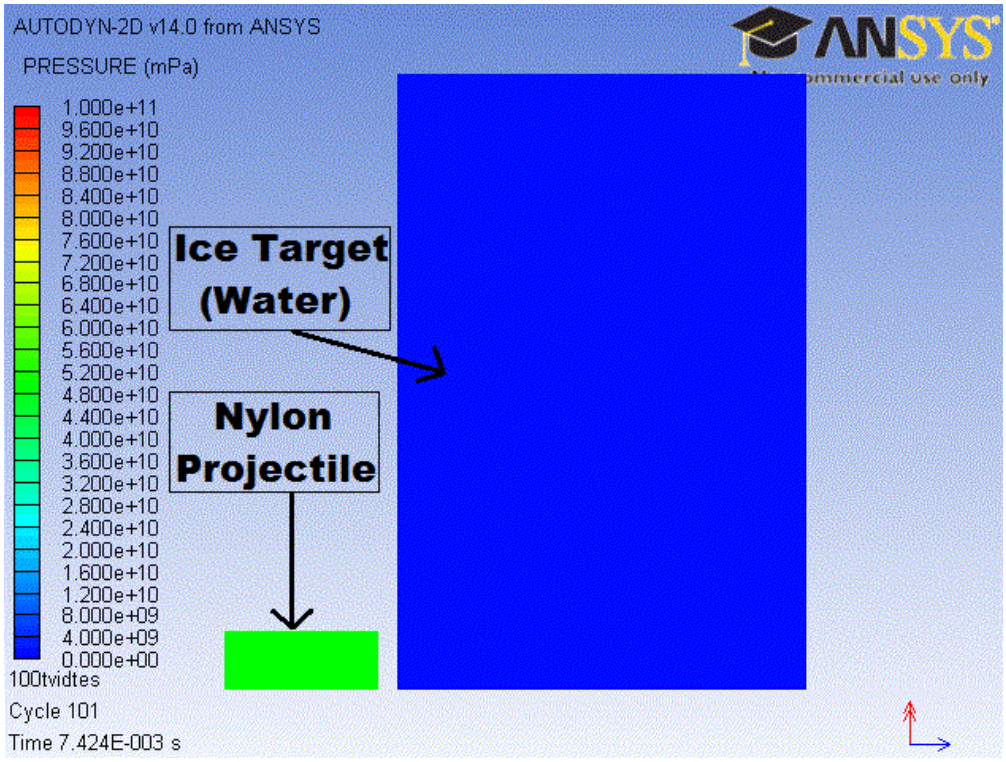

Figure 6.4: Example of Ansys AUTODYN simulation using 2D axial symmetry for a cylindrical nylon projectile impacting an ice target at 5.49 km s^{-1} just before impact.

As described in Chapter 4, Ansys' AUTODYN is a commercially available hydrocode (Hayhurst & Clegg, 1997). Here it was used to model the peak shock pressures experienced within the tardigrade doped water ice targets at various locations across the target. AUTODYN allows for an accurate determination of the shock pressure, as well as allowing estimates of the pressure versus time to be made across the target.

The experiment was modelled using a lagrangian mesh and the target was modelled as a 72 mm long rectangular water target with a thickness of 10 mm, effectively taking a slice through the target diagonally corner to corner. However, due to the axial symmetry of the model, this was modelled as a

half-space giving a target that was a rectangle of water 36 mm × 10 mm, comprising 3600 equally sized cells (see Fig. 6.5).

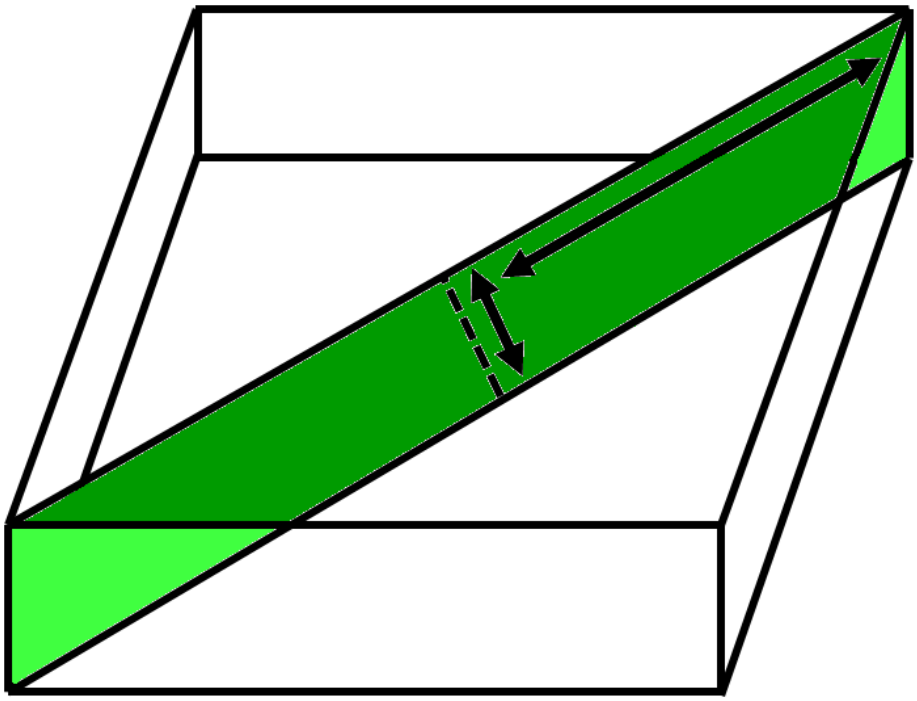

Figure 6.5: Schematic showing the 'slice' used in the hydrocode model. The small arrow is 10 mm and the larger arrow is 36 mm.

The projectile was modelled as a 4.5 mm long nylon cylinder with a diameter of 4.4 mm. Due to the 2-D symmetry, this was modelled as a rectangle 4.5 mm × 2.2 mm comprised of 99 cells (Fig. 6.6). One hundred and sixty software gauges (or 'tracers') were placed inside the cells within the target in order to track the pressure during the impact event. The equation-of-state parameters were taken from the AUTODYN material library and are detailed for nylon in Matuska (1984) and water in Trunin et al. (2001). As with the simulations for the phytoplankton shots in Chapter 5, the target was modelled as pure liquid water to simplify the model and as Price et al. (2012) demonstrated these approximations can be deemed as

valid. The peak pressures in the simulations occur just after the projectile penetrates the water target (Fig. 6.2), and see Tables 6.3 & 6.4 for the results of these simulations. However, the pressures given are those at the far edge of the target (where the tracking gauges were placed) as this is where the tardigrades were located, and the maximum pressures experienced by the organisms is what is of interest here, not the pressures at the impact point.

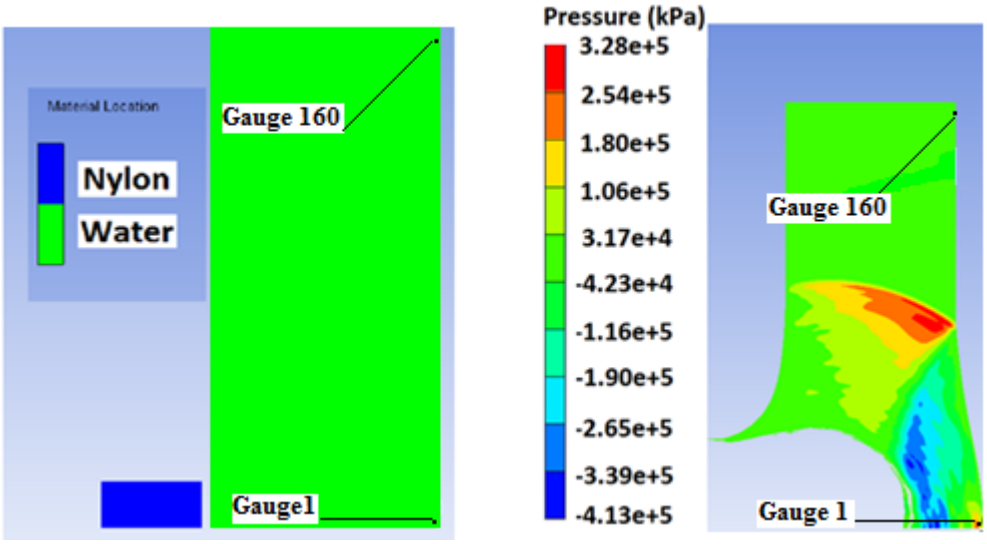

Figure 6.6. AUTODYN simulation showing: **Left.** Set up showing the positions of gauges #1 and #160 for reference. **Right:** Pressure contours during a 3.23 km s^{-1} impact, (snapshot taken 6.13 μs after impact).

6.6 Results and Analysis

To test the viability of the shocked samples, the ice and water collected after impact were left to thaw for 24 hours inside the incubator, and then analysed under an optical microscope. In all of the shocked samples surviving organisms were observed. Most of these surviving organisms were found to be in an active state, moving around and eating algae, just as the living organisms in unshocked samples had shown, some were unmoving but

movement could be seen inside the motionless organism showing it was still alive, just not active, again as seen in unshocked controls.

The original sample of tardigrades showed an approximately ratio of living-to-dead organisms of ~1.0, a living-to-total ratio of ~0.5, i.e. ~50%. After freezing at -25°C (using fourteen samples for varying time intervals) this drops significantly (Table 6.3). However, the survival rate appears to be almost constant regardless of the length of time the sample is frozen, with a mean living-to-dead ratio of 0.31 ± 0.02 (Fig. 6.7).

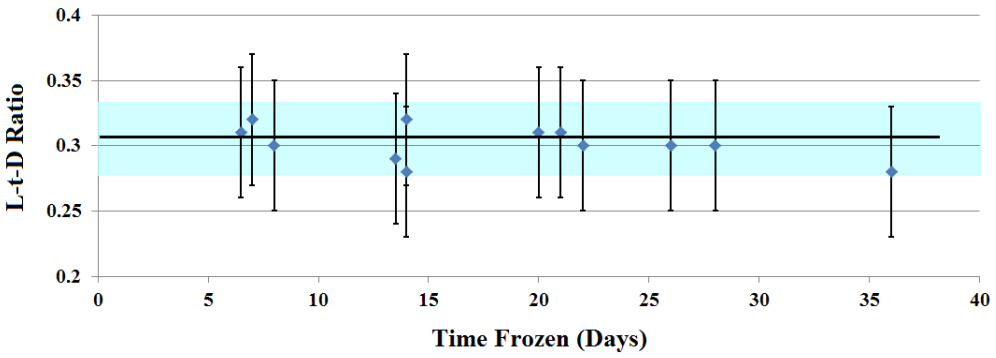

Figure 6.7. Graph showing the living-to-dead ratio against the time frozen (at -25°C) for un-shocked control samples. The mean line is also plotted for reference, with the associated error (shaded area) within which the data should fall regardless of time frozen.

Table 6.3: *Results from the shot programme. 'LtD' denotes Living-to-Dead ratio. *Orig = Original sample, unfrozen, and unshocked.*

Shot No.	***Impact Speed (km s^{-1})***	***Pressure AUTODYN (MPa)***	***Time Frozen (Days)***	***LtD ratio (Shocked Sample)***	***LtD ratio (Control Sample)***
Orig	N/A	N/A	N/A	N/A	1.00
S1	0.37	4.15 – 71.1	14	0.120	0.28
S2	0.65	9.23 – 107	8	0.117	0.30
S3	1.03	24.8 – 166	7	0.115	0.32
S4	1.40	51.3 – 232	22	0.113	0.30
S5	1.41	54.5 – 234	14	0.113	0.32
S6	1.42	56.6 – 238	1	0.113	0.33
S7	1.95	99.9 – 368	21	0.111	0.31
S8	2.23	111 – 440	13.5	0.100	0.29
S9	2.80	172 – 634	6.5	0.091	0.31
S10	3.23	219 – 971	1*	0.076	0.37*
S11	3.45	235 – 1218	26	0.073	0.30
S12	4.29	288 – 1752	20	0.071	0.31
S13	5.18	371 – 2935	36	0.030	0.28
S14	5.49	374 – 3348	28	0.018	0.30

*= Control was only frozen ~12 hours, increasing the LtD ratio, see Fig. 6.11.

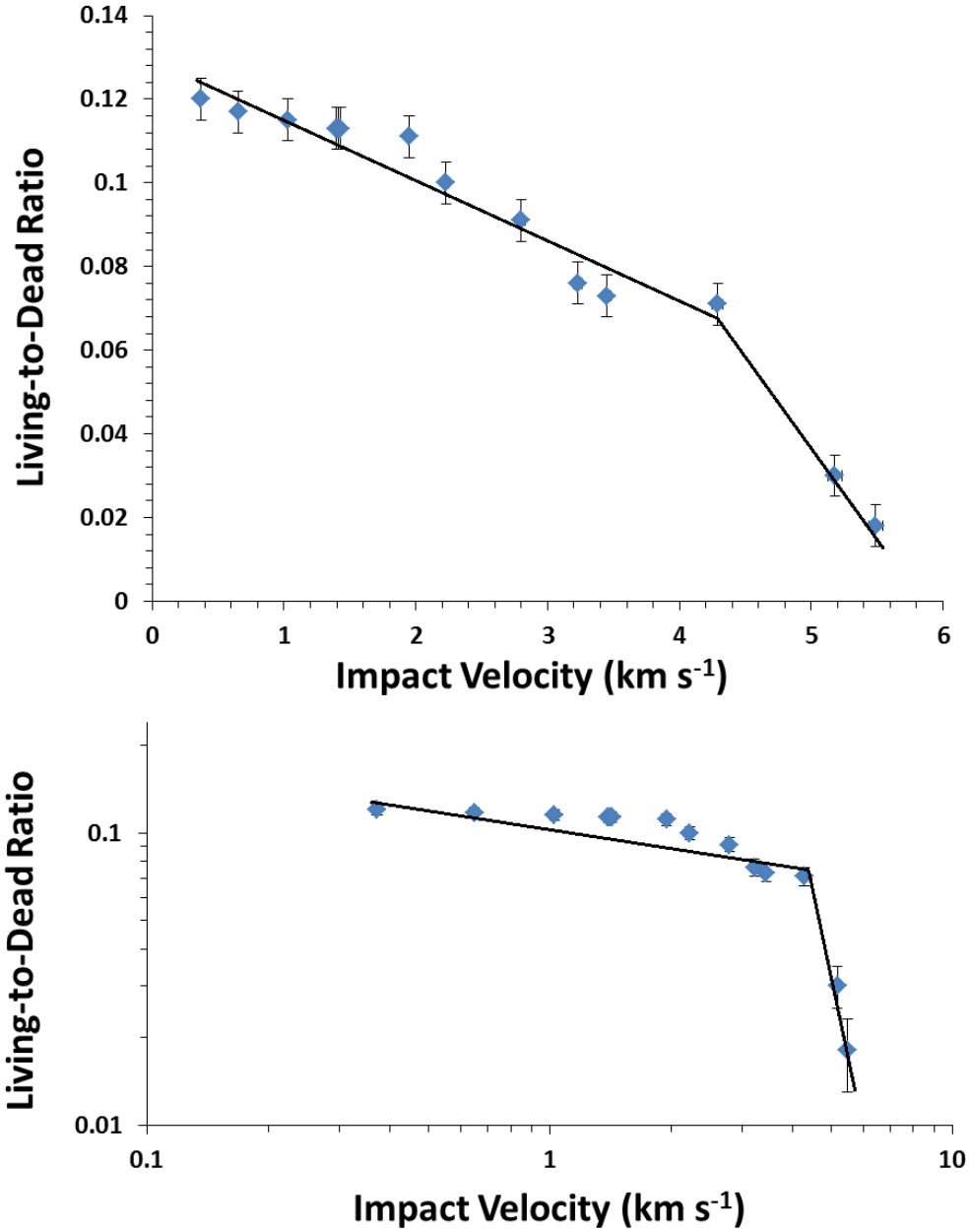

Figure 6.8. Graph showing living-to-dead ratio vs. impact velocity for shocked samples of tardigrades**. Top:** Linear plot**. Bottom**: Same data plotted with logarithmic axes.

The data for the 1 day frozen control is not plotted in Fig. 6.7 as this sample was only frozen for 12 hours and it is possible that some organisms survived between ice crystals before the entire sample could freeze thoroughly.

The fourteen shocked samples show a decreased survival rate with a clear trend; as the impact velocity (and shock pressure) increases, the living-to-dead ratio of the organisms drops significantly (Table 6.3 & Fig. 6.8).

When the living-to-dead ratio is plotted against the minimum and maximum pressure ranges experienced during the impacts (as modelled with AUTODYN), the same overall trend is seen (Fig. 6.9). However, as there were a range of pressures experienced across the target, and no way to determine the exact position of the surviving organisms within the target at the time of impact, only a lower limit (Fig. 6.9's lower valued curve – blue data points) can be taken as conclusive.

Realistically, the true pressure that any one organism survives will be slightly higher, as it is unlikely that all the surviving organisms were clustered in the one spot that experienced the lowest peak pressure. It is thus suggested that the actual pressures survived lie close to – but above – the lower limit curve (blue data points), but well below the higher valued curve (red data points) in Fig. 6.9.

Here it is shown that complete lethality will occur at around ~400 MPa (although realistically this will be slightly higher), this compares well to water pressure experiments performed by Seki K. et al. (1998) that showed the upper limit for survival by tardigrades in perfluorocarbon was approximately ~600 MPa.

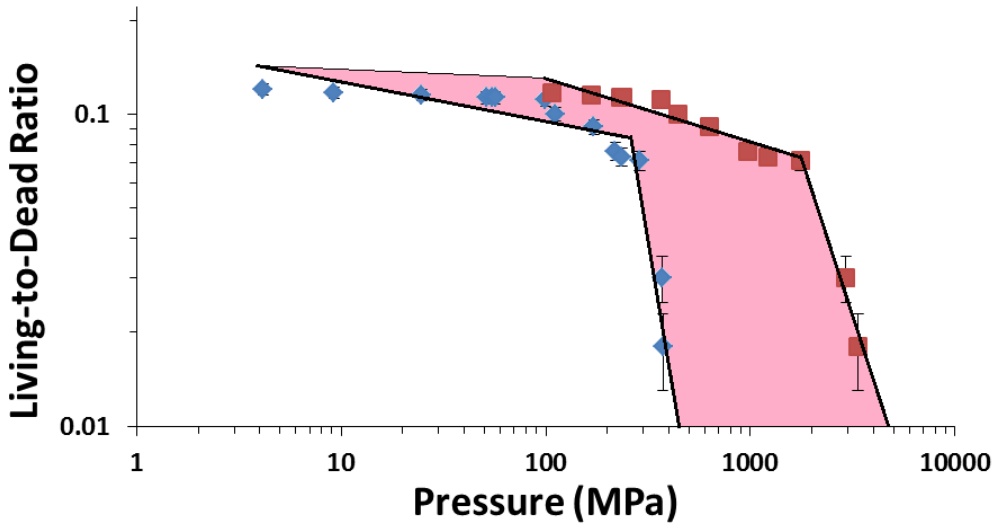

Figure 6.9. Graph showing living-to-dead ratio against the pressure range experienced by the organisms. Each shot (and corresponding living-to-dead ratio) has two data points. Blue data points show the lowest pressures per shot, red data points show the highest pressure per shot. Thus, the true survival curve will lie somewhere within the shaded pink area.

The data shows that there is a higher survival rate for the frozen state to shocked state stage, than from an initially unfrozen 'natural' state to shocked state stage. This is due to some organisms not surviving the freezing stage of the total process. For the purposes of panspermia we would need to consider the survival fraction post-impact from an initial population that was in its natural habitat, i.e. unfrozen, at the time. The survival fraction of such a population will clearly be lower than that for an already frozen (but live) population, due to the death of some organisms during freezing. (see Table 6.4, and Figs. 6.10 and 6.11.)

Using the data from Table 6.4 and applying equations 6.1 and 6.2, the survival fractions for post-shock tardigrades can be calculated (see Table 6.5

and Figs. 6.10 and 6.11). Figures 6.10 and 6.11 show both the survival from shock alone, and survival from freezing and shock.

Table 6.4: *The ratio of Living–to–Total organisms for frozen then shocked then thawed, frozen then thawed, and initial population, for a range of shots.*

Shot No.	***L-t-T Shocked***	***L-t-T Frozen***	***L-t-T Initial***
S1	0.1075	0.2199	0.5
S2	0.1043	0.2296	0.5
S3	0.1030	0.2403	0.5
S4	0.1016	0.2326	0.5
S5	0.1011	0.2400	0.5
S6	0.1015	0.2500	0.5
S7	0.1000	0.2398	0.5
S8	0.0909	0.2270	0.5
S9	0.0833	0.2381	0.5
S10	0.0702	0.2727	0.5
S11	0.0685	0.2333	0.5
S12	0.0666	0.2398	0.5
S13	0.0291	0.2174	0.5
S14	0.0181	0.2313	0.5

Table 6.5. *Resulting survival fractions for tardigrades fired in the shot programme.*

Shot No.	***Pressure Lower Limit (MPa)***	***Survival Fraction From Frozen Population to Shocked Population***	***Survival Fraction From Initial Population to Shocked Population***
S1	4.15	0.489	0.215
S2	9.23	0.455	0.208
S3	24.8	0.429	0.206
S4	51.3	0.437	0.203
S5	54.5	0.421	0.202
S6	56.6	0.406	0.203
S7	99.9	0.417	0.200
S8	111	0.400	0.182
S9	172	0.350	0.166
S10	219	0.257	0.140
S11	235	0.293	0.137
S12	288	0.278	0.133
S13	371	0.134	0.058
S14	374	0.079	0.036

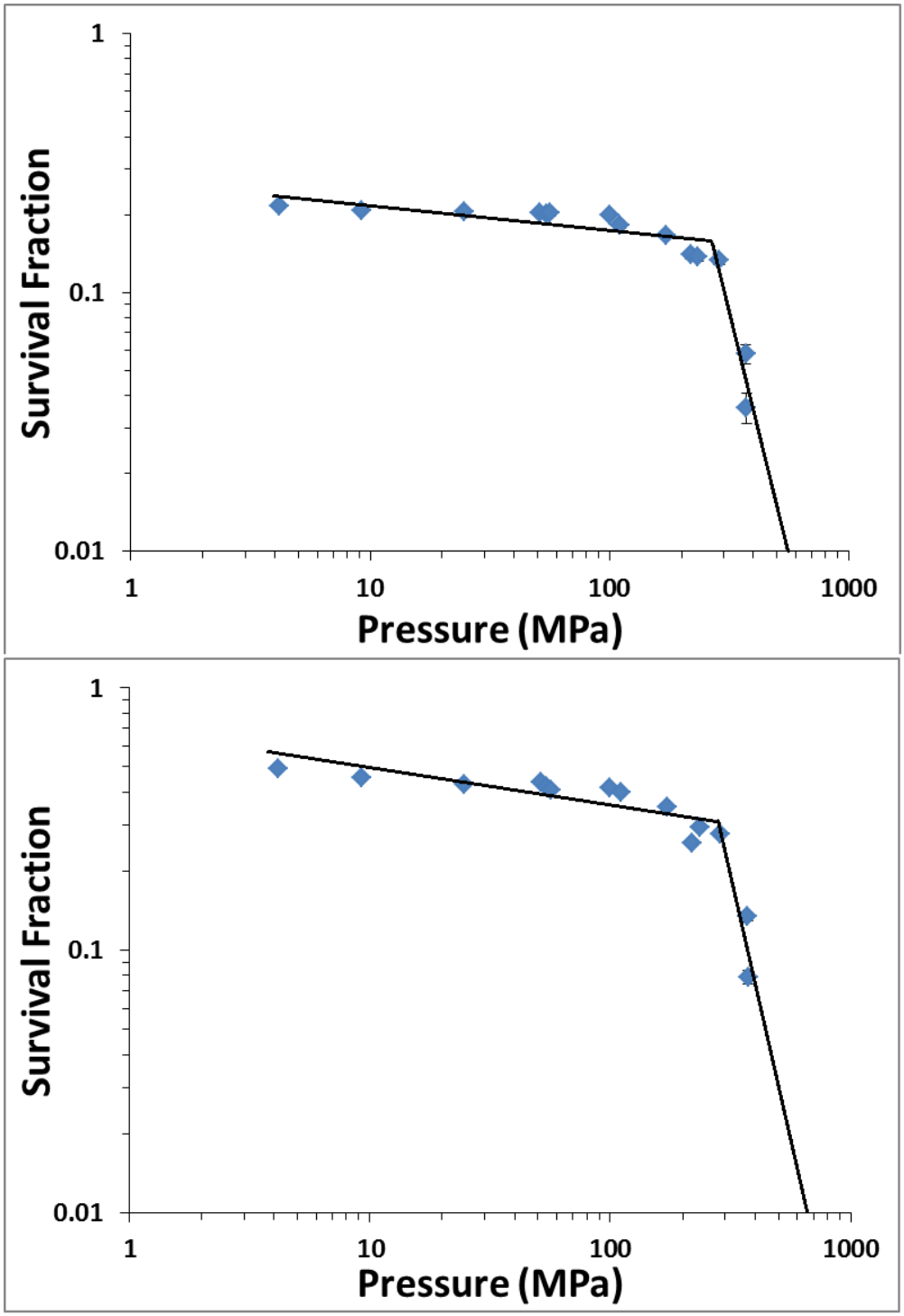

Figure 6.10. Top: Survival fraction of shocked tardigrades from the initial 'natural' population (lower limit). **Bottom:** Survival fraction of shocked tardigrades from the surviving (frozen) population (lower limit).

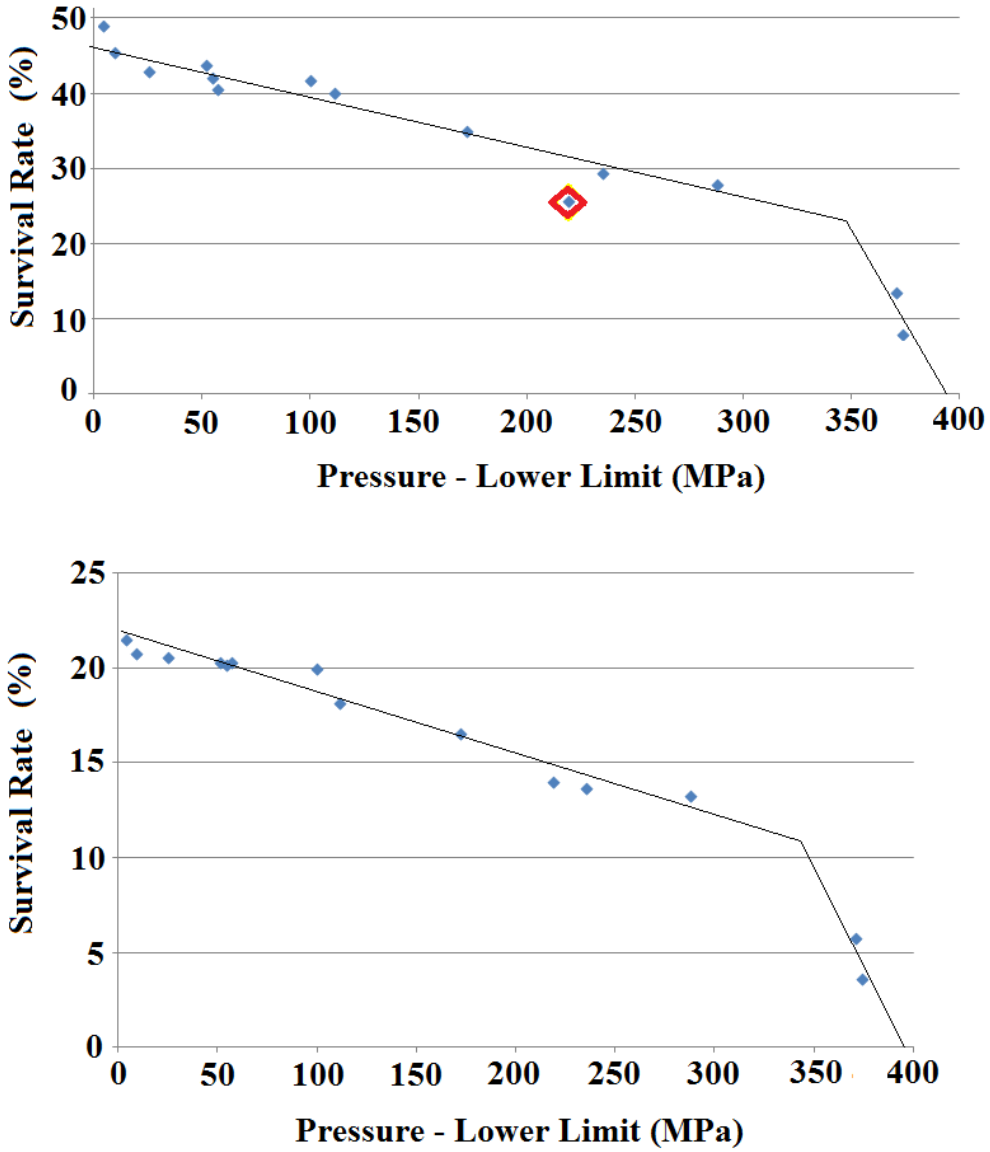

Figure 6.11: Top: Percentage survival rate of shocked tardigrades from the surviving (frozen) population (lower limit). **Bottom:** Percentage survival rate of shocked tardigrades from the initial 'natural' population (lower limit). Note – the highlighted datum appears outside the main trend - as stated above, the control sample for this shot was only frozen for 12 hours and it is likely that some organisms survived between ice crystals before the entire sample could freeze thoroughly, whereas the shocked sample was frozen fully, and thus would have had a lower starting population upon firing, thereby lowering the result from Eqn. 6.1 for this datum.

The results presented here follow the same trend that has been shown for other organisms, such as yeast (Price et al. 2013), and bacteria (Burchell et al. 2004). The description of the trend, as proposed by Burchell (2007) and Burchell et al. (2010), is that survival rates for micro-organisms versus peak shock pressures fall into two distinct regimes; (shown schematically in Chapter 5, Fig. 5.9). It shows there is a relatively slow decrease in survival at low peak pressures, but above some critical (organism dependant) value, the decrease becomes exponential. The small degree of lethality observed at low pressures may be due to shock damage to weaker members of the sample, local environmental conditions, etc. which has the effect of causing an initial shallower curve before the sharper curve, creating the 'knee joint' or critical threshold between the two regimes, (if all members of the sample were absolutely identical, conditions were identical for each member, and shocked identically then the curve would simply be a vertical line at the point of lethality). As described in Chapter 5 all survival curves would tend to converge in the high pressure end of the curve (50 – 100 GPa; Price et al., 2013).

This high pressure convergence is not relevant for tardigrades as they experience complete lethality well before such extremely high pressures are reached. It is reassuring though to see the same trend repeated for this organism in this work, and this lends yet more weight to the idea that this truly is a universal trend for all micro-organisms, even complex multi-cellular ones.

The flyer plate experiments by Hazell et al. (2010) mentioned previously in chapter 5 have indicated that objects with diameters ranging between 1 – 20 microns are being influenced by shockwaves propagating through the sample. This is comparable to the size range of the tardigrades' cells of ~4 microns. The tardigrades in the sample used here have an average length of 170 microns (this size distribution was the same for all samples

analysed), and assuming a roughly cylindrical shape have a radius of around 50 microns, and with an average of 40,000 cells per organism this yields an approximate cell length of 4 microns. Thus it is likely that the cells of the tardigrades are being influenced in some way, albeit one that is undetectable to the probes used here, as all surviving organisms appeared to be healthy and behave in a similar state to how they did before being frozen and impacted.

Zimmerman (1971) and Heremans (1982) work on yeast cells has shown that high pressure has detrimental effects on many of the cellular structures, including those required during mitosis (Zimmerman, 1970), and thus high pressure impacts and the disruption of the cell replication machinery could possibly cause some changes in cell morphology. Fig. 6.12 presents some images of shocked samples of tardigrades, and it can be seen that if there is any damage to the DNA in the cells of the tardigrades, it has not altered their observable behaviour. There may be damage, and changes in morphology internal to the tardigrades' cells, but these are not evident from an external viewpoint. It is therefore concluded that the cells of the surviving organisms are the same before, and after. impact. A shocked population would have to be observed after reproducing offspring to see if there were any evident changes in morphology due to damaged DNA. However, such studies were not performed here.

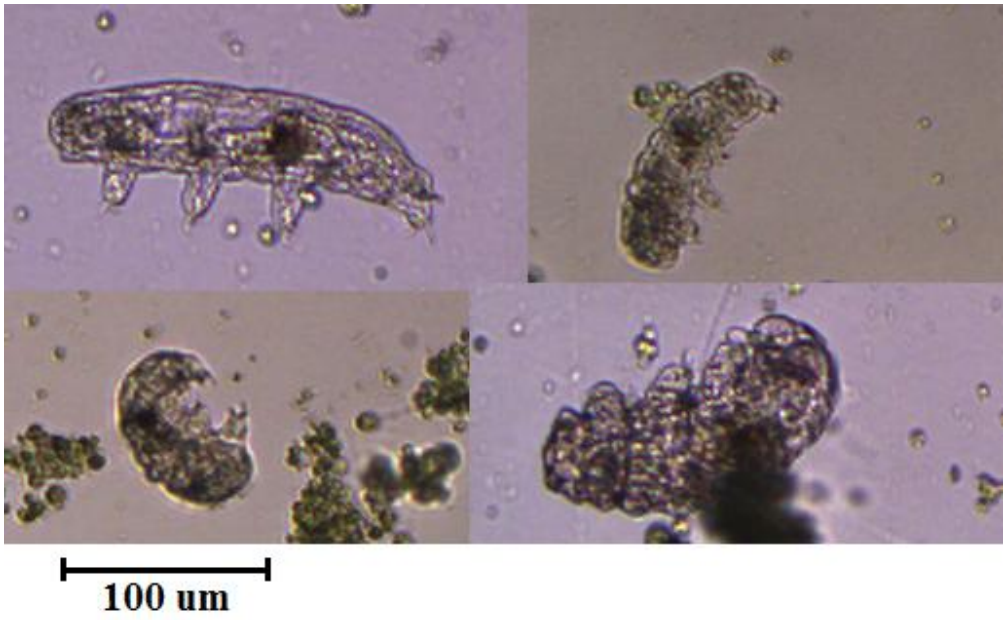

Figure 6.12. Surviving tardigrades. **Top left:** S5 (1.409 km s^{-1}). **Top Right:** S8 (2.23 km s^{-1}). **Bottom Left:** S11 (3.45 km s^{-1}). **Bottom Right:** S13 (5.18 km s^{-1}).

During the experiments there were also two individual examples of eggs that were almost at the point of hatching before impact. These eggs survived and hatched after the impact, showing that eggs in a non-desiccated state can also survive such extreme pressures and still be viable when thawed. This also suggests that the tardigrades can survive extreme shocks without being in their desiccated state. However, survival at higher pressures is not sustainable without being in the desiccated state, future work to determine the cut-off from when survival is only attainable during the desiccated state would provide a useful addition to this work.

6.7 Temperature Testing

As the temperatures in space can vary depending on the local environment (i.e. close to a star can be extremely hot, where as the void

between galaxies can be as low as 3 K), any tardigrades capable of a panspermia style journey must be able to survive the temperatures of space between the home planet and the destination planet. Therefore, during the main programme an additional study was undertaken to measure the survivability of tardigrades as a function of different freezing temperatures. Various different freezing temperatures (-25^{o}C, -80^{o}C, -140^{o}C, and -196^{o}C) were explored during the experiment, (however, none of these samples were fired onto in the main experiment). Each sample in the temperature study was frozen for 48 hours at the desired temperature, and then left to thaw for 24 hours before analysis was performed.

The results show a gradual decrease in survival with lower temperatures. However, surviving organisms were found in all tests performed; see Table 6.6 and Fig. 6.13.

Table 6.6. *Results of the temperature studies performed*.

Temperature (^{o}C)	***Living-to-Dead Ratio***	***Survival Fraction From Initial Population***
-25	0.30	0.46
-80	0.15	0.27
-140	0.12	0.22
-196	0.07	0.13

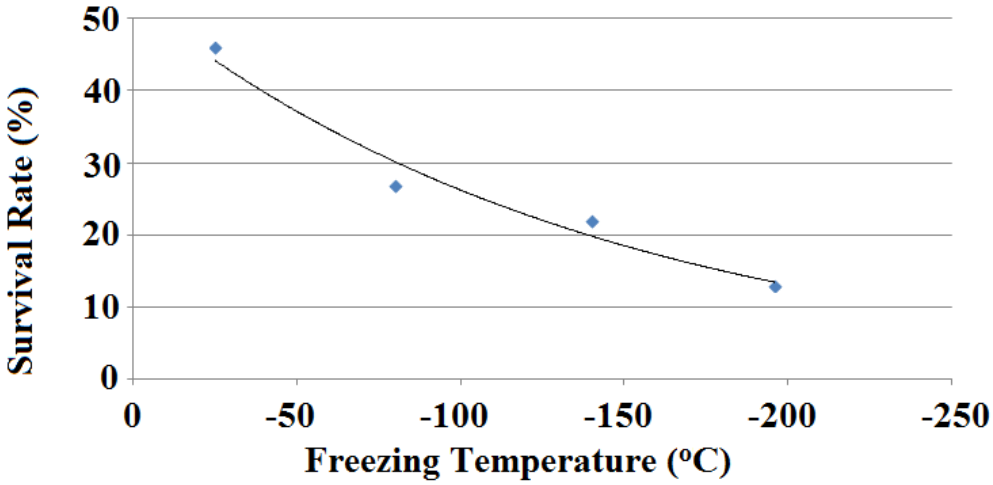

Figure 6.13: Showing the survival rate of tardigrades after the freezing process at different temperatures.

While the percentage of tardigrades that can survive an impact does not depend on temperature, the temperature results presented here show that progressively less organisms survive the freezing process as temperatures drop. This implies that for any impact scenarios (in which tardigrades are frozen during impact), where the only variable parameter is temperature, (i.e. projectile and target, size, shape, velocity, and materials, are identical), and a desired number of survivors is required, then in order to have the same number of surviving organisms at the end of the process, the size of the initial starting population will be subject to change. The size of the initial population will thus be dependent upon the freezing temperature the organisms experience via some constant of proportionality which determines the population size in order to achieve a given survival objective for identical impacts where only the temperature of freezing changes.

Therefore, to estimate the surviving population of an impact scenario, the survival rate of the temperature of the freezing process must first be

applied to an initial population, and then the survival rate of the pressure of the impact must be applied to this, to find the probability of survival for a given starting population.

6.8 Implications for Panspermia

Complementary work with hydrocode modelling (see Chapter 7) has shown that the shock pressures that tardigrades are able to survive would allow the tardigrade to survive impacts into bodies such the Moon, Enceladus, Europa, and other small moons and asteroids within the Solar System, as well as any other extra-solar bodies of similar size and mass (Pasini et al., 2014, 2015). Tardigrades could, under favourable conditions (i.e. via spallation, see below), also be ejected into space, escaping the Earth's gravitational field (the initial requirement for any type of naturally occurring panspermia to happen). The impacts necessary for such ejection from the Earth generate peak pressures much higher than those that a tardigrade can survive. Peak pressures at the site of a giant impact that is capable of lifting material into space from the Earth can be extreme: 10's – 100's of GPa; this is beyond the range of survival for tardigrades. However, studies have shown that even large fragments ejected through spallation that reach space, can experience peak pressures an order of magnitude lower than those at the initial impact site (Fajardo-Cavazos et al. 2009). This would allow tardigrades to be effectively ejected from the Earth and into space where they can then be transferred to other bodies within the Solar System, allowing a successful panspermia style transfer. Also, as tardigrades are often found with copious quantities of their main food source (phytoplankton), any impact event that ejects (through spallation) the tardigrades into space would also likely eject the phytoplankton too, and as previous shown in Chapter 5, this too can survive panspermia style impacts (Pasini et al. 2013a, 2013b),

thus any tardigrades that successfully make it to another planetary body would likely have a surviving food source with them also, allowing for a much greater chance of continued survival in their new habitat.

The range of organisms that survive hypervelocity impacts has now been extended to include the tardigrade species *Hypsibius dujardini*. Other groups (Stoffler et al. 2007, Horneck et al. 2008, Price et al. 2013, Pasini et al. 2013a, 2013b, & Burchell et al. 2001, 2004) have reported that lichens, yeast, phytoplankton, and bacteria can survive shocks that allow for transfer between planetary bodies. This work demonstrates that not only these organisms, but much more complex forms of life could survive the ejection and delivery onto another planetary body, or survive ejection from the Earth on to the Moon (Burchell et al., 2010). There are, of course, other factors that will influence the survival in impacts of rocks and ice onto planetary bodies. One example is the heat pulse generated during an atmospheric entry, this will sterilise the upper few millimetres of a body traversing the atmosphere (de la Torre et al., 2010). Another example is the material into which the projectile impacts: rocks, ices, snows, various liquids, sands, etc.; these various different surfaces will change the shock pressure experienced by any organisms on an impactor, and some will be more beneficial to life than others after impact (e.g. some may retain more impact generated heat, some will be more conducive to life, some will be hostile).

The experimental work presented here used a frozen water ice target containing the life-forms, suggestive of an oceanic/ice-shelf impact on an Earth-like planet. This was an appropriate set up for experimental investigations of the concept of panspermia, as an added feature of this type of event is that such an impact could cause fractures and fissures in the impactor. These can open up in the surviving projectile material, and allow water to infiltrate down into the interior, releasing material trapped, but protected, during the journey through space that could have otherwise remain

entombed in an interior surrounded by a glassy melt exterior caused by atmospheric heating during entry.

It is also possible that icy satellites with sub-surface oceans (e.g. Europa, and Enceladus) may exchange impact ejected material with other icy satellites. In this case so called "icy-satellite" panspermia may occur (see Burchell et al. 2003 for a discussion and demonstration of high speed, impact induced, ejection of viable micro-organism from an icy surface). If transferred, organisms could then penetrate the icy cover on the new body and reach the sub-surface ocean, they may then multiply and flourish.

This is the first time a multi-cellular complex organism has been shown to be able to survive a natural transfer between planetary bodies within the Solar System. It is therefore found that the tardigrade species *Hypsibius dujardini*, a multi-cellular, micro-organism, could survive ejection from, and impact onto, another planetary body with a viable ecosphere, and, assuming a viable food source, could establish itself on that world. It could also serve as a food source for any potential life-forms that already exist there, thus altering the course and shape of evolution for an entire planet and its ecosphere.

6.9 Conclusion

This chapter reported on the experimental and computational techniques performed to test the tardigrade species *Hypsibius dujardini* for survival during hypervelocity impact events. It was discovered that *Hypsibius dujardini* can indeed survive being shocked during hypervelocity impact events up to 5.49 km s^{-1}, surviving in pressures ranging from 374 MPa – 3348 MPa). It is seen that the lethality turns from minor to severe at

approximately 4.29 km s^{-1} in these tests (surviving in pressures ranging from 288 MPa – 1752 MPa).

Modelling and simulations of the hypervelocity impact events of the experimental programme showed that the survival regime during hypervelocity impacts for *Hypsibius dujardini* is up to at least 374 MPa (as a lower limit). As seen in the previous chapter with phytoplankton, the peak temperatures experienced during impact dissipate quickly enough after initial impact so as not to cause significant damage to the micro-organism allowing it to survive an otherwise sterilising temperature.

Finally, temperature testing shows that at increasingly lower temperatures, tardigrades frozen in ice will have a correspondingly lower survival rate upon thawing. This, in turn, affects the overall survival percentage from a natural population during an impact at lower temperatures. However, even when frozen in liquid nitrogen at -196^{o}C there was still significant survival of organisms that could go on to survive further impacts at the velocities and pressures discussed above.

CHAPTER 7
PANSPERMIA SURVIVAL SCENARIOS FOR DIFFERENT EXTREMOPHILE SPECIES

"In the Solar System, Enceladus ought to be one of the highest priorities for the world's space agencies. Enceladus has a source of energy (tidal heating), organic material, and liquid water. That's a textbook-like list of those properties needed for life. Moreover, nature has provided astrobiologists with the ultimate free lunch: jets that spurt Enceladus's organic material into space."

David C. Catling

7.1 Introduction

Having demonstrated the survivability of both the phytoplankton species *Nannochloropsis oculata*, and the tardigrade species *Hypsibius dujardini* in the previous Chapters, a consideration is now made with regard to other species that have been shown to survive hypervelocity impacts. A comparison of various extremophile life-forms against different simulated impact regimes is then considered to understand the limits of panspermia scenarios to which different micro-organisms are tolerant. To do this, hydrocode models are used to simulate different impact scenarios based on the known parameters of survival tolerance for the five chosen micro-organisms.

This chapter begins by looking at the five different species of extremophile that will be considered in the analysis of different panspermia scenarios (see Chapter 8), so that their survival parameters can be used to create hydrocode impact models that can later be compared to the micro-organisms' tolerances. The detailed construction of these models and their reasoning is explained. This is followed by a presentation of the results of these simulations. Finally, concluding remarks are given ahead of the in-depth analysis and discussion of Chapter 8.

7.2 Extremophiles Used for Comparison

Previous experimental studies have demonstrated the survivability of living cells during hypervelocity impact events, testing the panspermia and litho-panspermia hypotheses (Burchell, M. et al. 2004). It has been demonstrated in Chapter 5 that *Nannochloropsis oculata* Phytoplankton (see Fig. 7.1) can survive impacts up to 6.93 km s^{-1} and thus impact induced shock pressures of approximately 40 GPa) (Pasini, D. et al 2013a, Pasini, D. et al. 2013b).

Chapter 6 also demonstrated the survival of the tardigrade species *Hypsibius dujardini* (a complex micro-animal consisting of 40,000 cells, see Fig. 7.2), when subjected to impacts up to 5.49 km s^{-1}, surviving pressures of 374 MPa (and possibly higher; Pasini, D. et al 2014a, Pasini, D. et al. 2014b). It has also been shown by Seki, K. et al. (1998) that tardigrades can survive sustained pressures up to 600 MPa using a water filled pressure capsule.

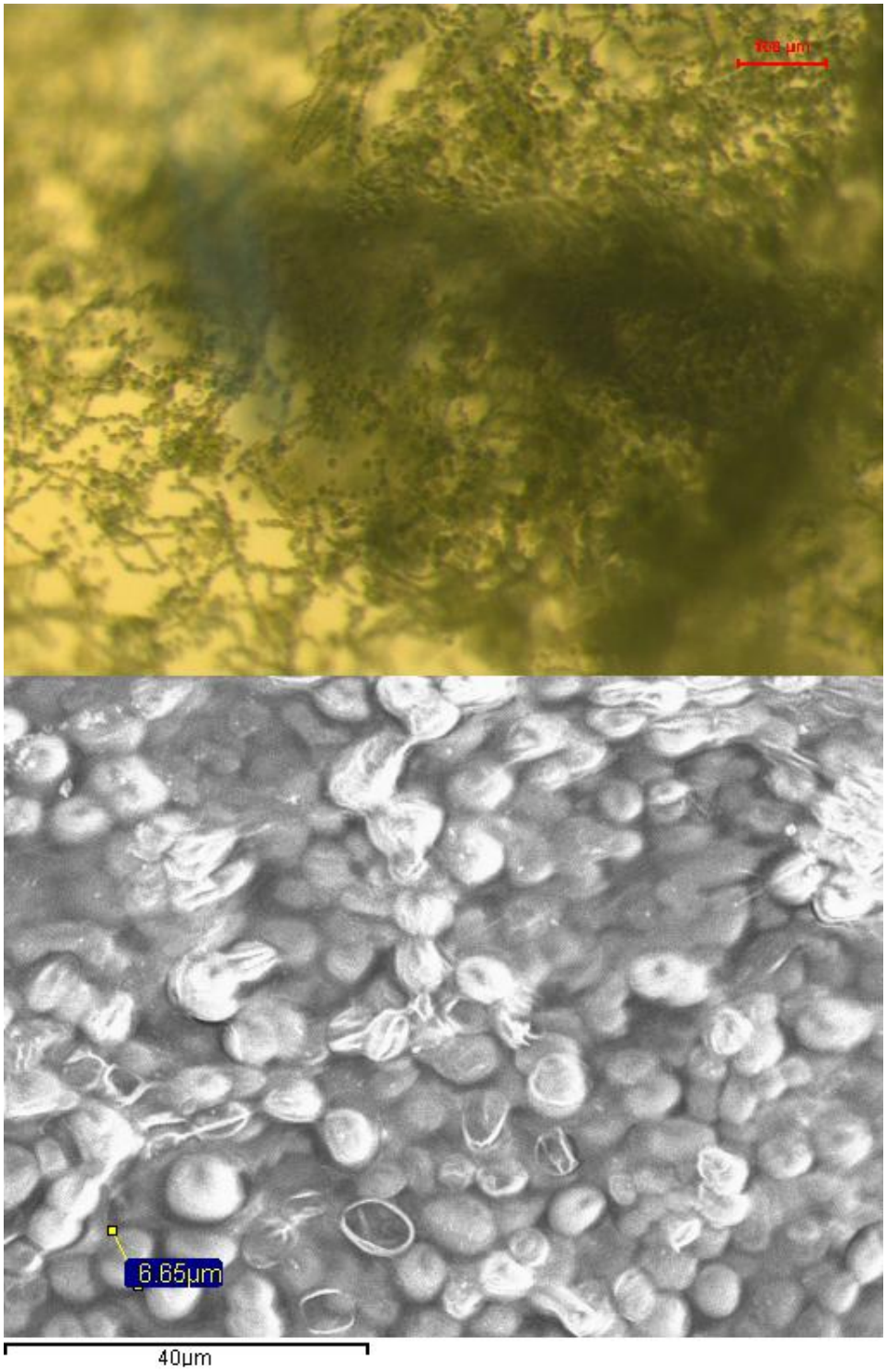

Figure 7.1: Optical (top) and Scanning Electron Microscope (bottom) images of *Nannochloropsis oculata*.

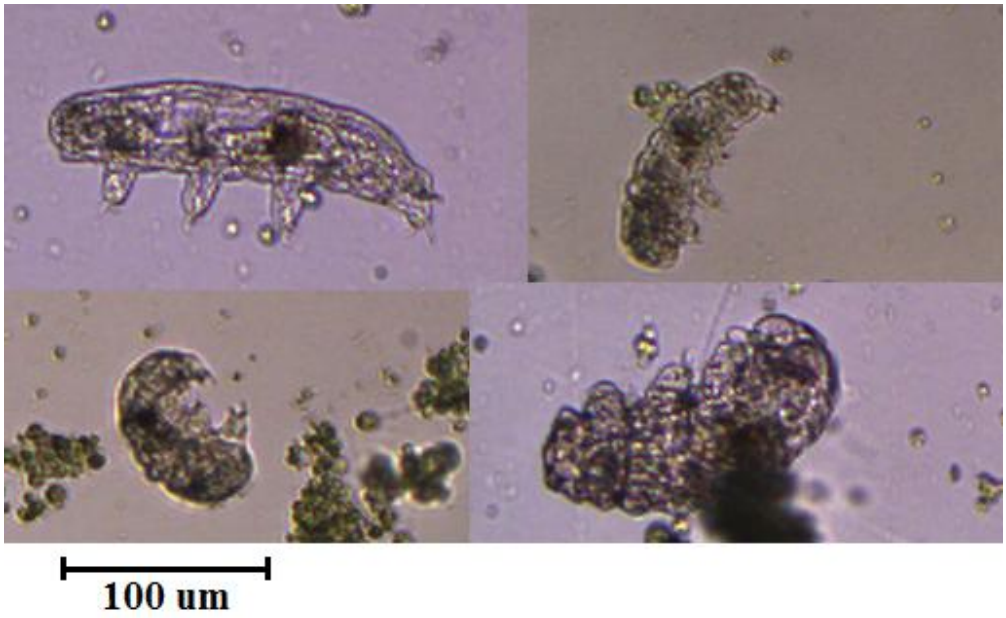

Figure 7.2: Images of the tardigrade species *Hypsibius dujardini* under optical microscope at ×350 magnification.

Additionally bacteria (see Fig. 7.3) have been shown to survive impacts up to 5.4 km s^{-1} (approx. shock pressure ~30 GPa) – albeit with a low probability of survival (Burchell, M. et al. 2004). There has also been experiments to test the survivability of yeast spores (see Fig 7.4) in hypervelocity impacts up to 7.4 km s^{-1} (approx. shock pressure ~30 GPa) (Price, M. et al. 2013).

Other groups have also reported that the lichen *Xanthoria elegans* (see Fig. 7.5) is able to survive shocks in similar pressure ranges (approximate shock pressure ~40 GPa; Horneck, G. et al. 2008).

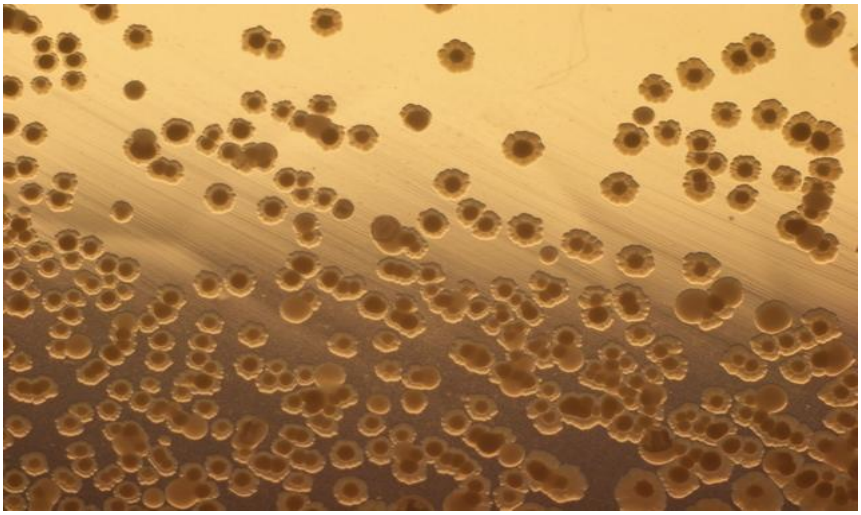

Figure 7.3: Bacteria used in impact studies up to 5.4 km s^{-1} (approximate shock pressure ~30GPa). *(Image courtesy: Burchell M. J. et. al. (2004))*

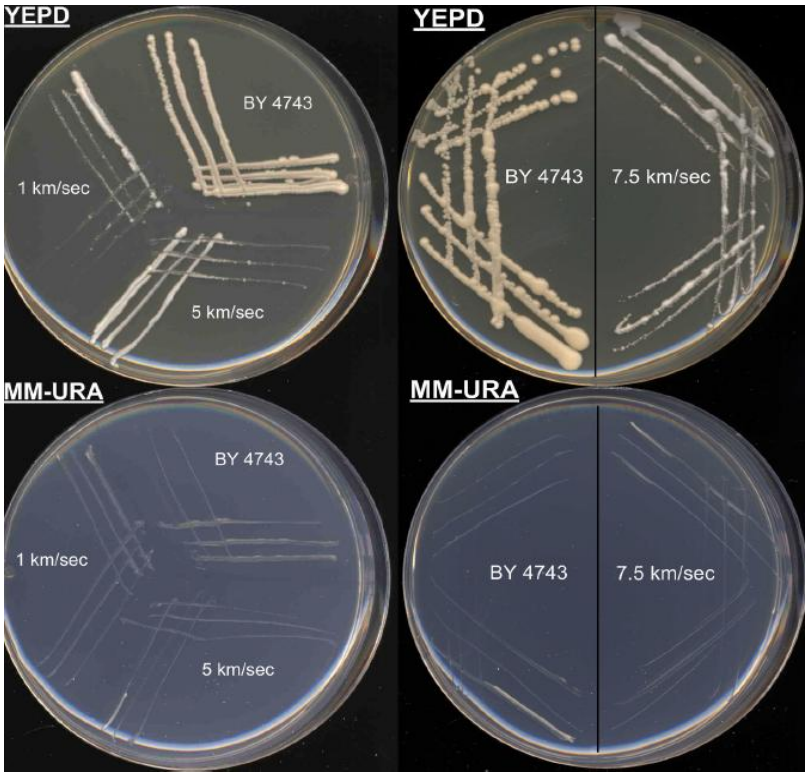

Figure 7.4: Growth of recovered yeast after spores were fired at several different velocities. *(Image courtesy: Price M. C. et. al. (2013))*

Fig 7.5: The lichen species *Xanthoria elegans*. *(Image courtesy: lichen.com)*

These five species of extremophile will be used to compare against impact modelling, to determine what (if any) types of panspermia style impact scenarios they are capable of surviving. Table 7.1 below lists each of the species of micro-organism being considered, along with the maximum impact pressure that they have been shown to withstand and still survive. These can later be directly compared with the results of hydrocode models of hypervelocity impact simulations for a number of different panspermia style impact scenarios (based on the various species' tolerance regime), to constrain the limits of survivability for these micro-organisms under the different conditions of each scenario.

Table 7.1: *Showing the different micro-organisms used for comparison and their associated maximum pressures they have been shown to survive.*

Extremophile Life-form	***Maximum Survival Pressure (GPa)***	***Source***
Tardigrade species *Hypsibius dujardini*	0.6	Seki, K. et al. 1998
Bacteria species *bactillus subtilis*	30	Burchell, M. et al. 2001
Yeast species *Saccharomyces cerevisiae*	30	Price, M. et al. 2013
Phytoplankton species *Nannochloropsis oculata*	40	Pasini, D. et al 2013b
Lichen species *Xanthoria elegans*	45	Horneck, G. et al. 2008

7.3 Hydrocode Impact Models

7.3.1 Shock Pressure Experienced During Impact

Using Ansys' AUTODYN software, a series of simulated impacts were modelled. As the hypothetical impacts being modelled have an axial symmetry in the direction of the impact, this can be used to greatly reduce the computational time need to run the simulations. The models were therefore created using a 2-D lagrangian mesh solver with axial symmetry. The 2-D lagrangian mesh solver effectively flattens the problem, and the axial symmetry allows the number of cells in the problem to be halved. For example, a spherical projectile is flattened to a circle and then halved to create a semi-circle, as the result will be identical for any halved cross-sectional area that cuts through the entire axis of motion.

First a series of test models where created to identify the point on the projectile that experiences the lowest peak pressure during the impact. For a best case scenario it is assumed that organisms are spread across the whole projectile so that survival is constrained only by the lowest peak pressure experienced across the projectile. These simulations consisted of a spherical ice body projectile (modelled as liquid water for simplicity) impacting into either a large ocean, or a large rocky silicate body (see Fig. 7.6).

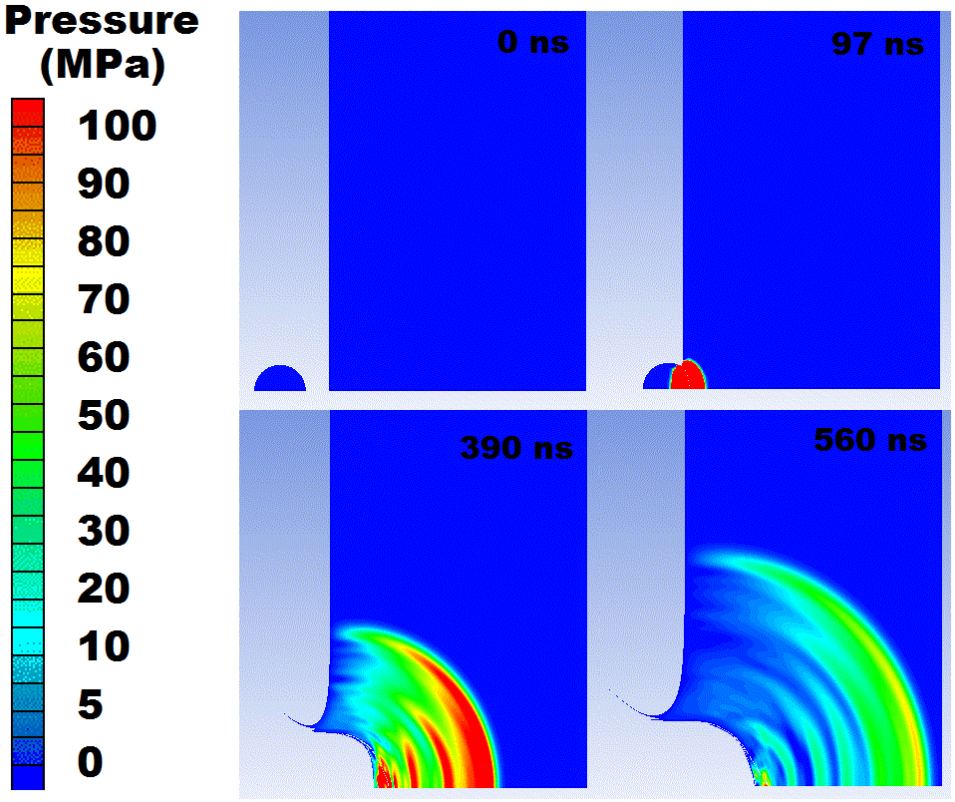

Figure 7.6: Ansys AUTODYN simulation showing pressure contours for a spherical water ice projectile (with a radius of 200 m) impacting into an ocean at 1.5 km s^{-1}. (Image timesteps - 0, 97, 390, & 560 ms into run).

Glass is used to simulate the rocky silicate body, as work to validate a realistic basaltic analogue model has proved to be very difficult and was still ongoing when these models were being created. Silicate glass has many similar properties to basalt, such as material strength and density, two of the main factors considered in the calculations the model uses to simulate hypervelocity impact events.

The target in the simulations will always be much larger than the projectile, as the target must remain intact in a panspermia style impact. If the target body was destroyed, there would be no celestial body left for life to survive and propagate on. Therefore, the shape of the target in these simulations remains the same for all instances, with only, composition of target, velocity of projectile, and size of both target and projectile (relative size between both remains constant), changing between different simulated impact scenarios.

A target 'ocean' was created consisting of approximately 60,000 cells (300 high × 200 wide). This was deemed large enough to be considered "semi-infinite". Then, a projectile was created consisting of approximately 625 cells (a semi circle with a 20 cell radius). Throughout this projectile 37 pressure tracking gauges were placed to record the pressures experienced by any micro-organism within the projectile during the impact event (see Fig. 7.7). Velocity vectors were then added to each cell of the projectile in each model, and then the model was run. This allowed the relation between peak pressure at the 'Optimal Point' of the projectile, and the associated impact velocity of the model to be plotted graphically for analysis.

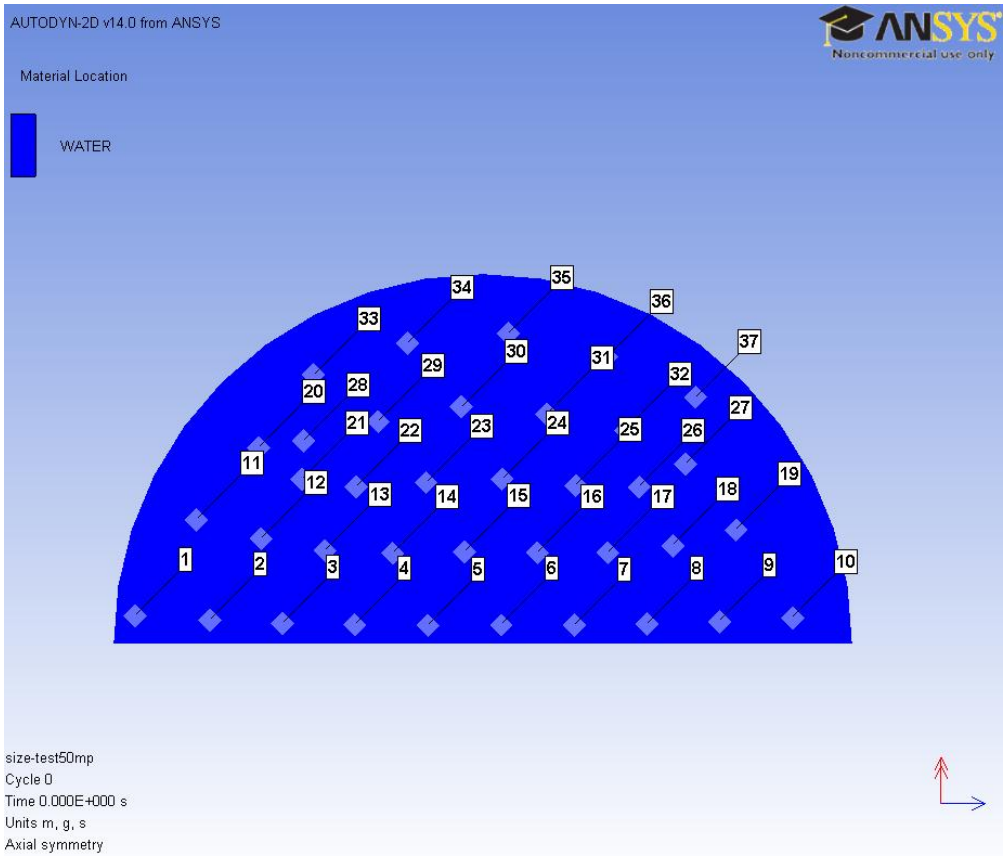

Figure 7.7: Simulated water ice impactor showing position of pressure tracking gauges. The impactor is travelling left to right onto a target on the extreme right (not shown).

7.3.2 Size and Pressure Independence

Once the 'Optimal Point' of lowest peak pressure experienced during the impact event was found, another series of tests were performed to confirm the independence of peak pressure during an impact event to the size of the event.

Models with 23 different sized projectiles were created (with radii ranging from 0.01 m to 10,000 m). These were then simulated impacting into a target ocean to confirm that the peak pressure (at the same relative point in

the projectile – gauge Number. 10 at the very front of the target was arbitrarily chosen) does not depend on the size of the impactor. The 23 different sized projectiles in the models were then each also tested at nine different impact velocities (0.25 – 5.0 km s^{-1}).

7.3.3 Impact Velocities

The optimum situation for survival of any life-form during a panspermia style impact event will be when the impact velocity is as low as possible. The lowest velocity possible for a projectile impacting a larger celestial body (not accounting for other factors such as atmospheric drag) will be the case of a projectile passing near to a target body and being captured by the target body's own gravity well, and entering into a freefall descent. In such a case, the impact velocity will be equal to the body's local escape velocity. This is of course the 'best case scenario', and typical impact speeds on Solar System bodies will vary (see Zahnle, K. et al. 2003). The escape velocities used for all bodies considered here are the 'best case scenario' and thus lowest possible velocities that could be experienced, and were calculated via Eq. 7.1:

$$V_{esc} = \sqrt{\left(\frac{2GM}{R}\right)} \qquad \text{(Eq. 7.1)}$$

where G is the gravitational constant (m^3 kg^{-1} s^{-2}), and M and R are the target body's mass (kg) and radius (m) respectively.

A number of different planetary bodies are considered for panspermia style impacts by the five species chosen for comparison. Table 7.2 gives a list of the bodies considered with their associated escape velocities, and thus best case scenario impact velocities. Also considered are two 'Super-Earth' exoplanets Gliese 581 d and g. Their composition is currently unknown, so

the cases for both an ice planet and a rocky planet are considered; see Chapter 8 Section 8.3.2 for determination of the planetary radii used to calculate the escape velocities for both compositional make ups.

Table 7.2: *Escape velocities for various planetary bodies considered during the hydrocode modelling.*

Target Body for Impact	***Escape Velocity (km s^{-1})***
Enceladus	0.25
Ceres	0.51
Pluto	1.27
Europa	2.02
The Moon	2.38
Titan	2.65
Mercury	4.25
Mars	5.02
Earth	11.2
*Gliese 581d	19.5
†Gliese 581d	22.0
*Gliese 581g	13.9
†Gliese 581g	16.1

* = if a water/ice composition, † = if a rocky composition

7.4 Results of Impact Models

7.4.1 Shock Pressure Experienced During Impact

After 207 test simulations were completed (23 different sized projectiles, each of which was tested at nine different velocities), the 'Optimal Point' of lowest peak pressure experienced during the impact event was found to be gauge Number 1 in every instance (see Fig. 7.8). Thus, it is the peak pressure values at this location on the projectile that represents the 'Best Case' scenario for the survival of life-forms within the impactor. And, as one would expect, this is located at the very rear of the projectile. Therefore, all the peak pressure results for the impact scenarios that follow are from gauge Number 1 located at this 'Optimal Point'.

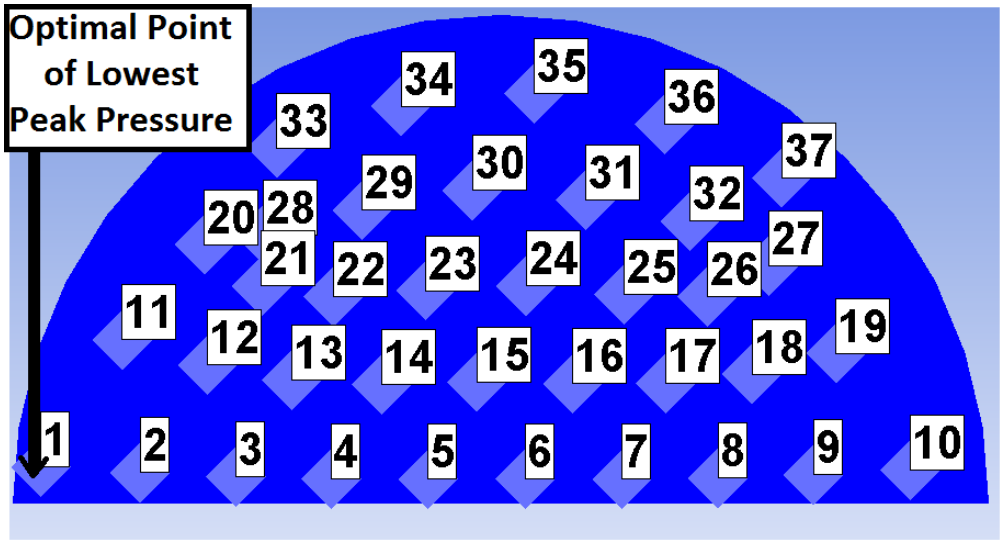

Figure 7.8: Spherical projectile model showing 37 gauges, with the 'Optimal Point' for survival (Gauge Number 1) highlighted, projectile is travelling towards target from left to right.

7.4.2 Size and Pressure Independence

After the test simulations were completed the results showed that the peak pressure (for any one gauge) for each size projectile at the same velocity was the same value. When all 23 sizes of projectile were plotted against the nine different velocities the same independence of size was witnessed (see Table 7.3 and Fig. 7.9).

Table 7.3: *Showing the independence of size to peak pressures experienced during an impact for the same relative point on the projectile (results shown are for gauge Number 10, chosen at random). – four different size scales shown for comparison.*

Impact Velocity (km s^{-1})	***Peak Pressure Experienced During Impact For Spherical Projectiles Of Different Radii (GPa)***				***Time After Contact (ms)***
	At 0.01 m	***At 1 m***	***At 100 m***	***At 10,000 m***	
0.25	0.0674	0.0674	0.0674	0.0674	149
0.50	0.2250	0.2250	0.2250	0.2250	100
1.00	0.9727	0.9727	0.9727	0.9727	67.0
1.50	2.0640	2.0640	2.0640	2.0640	52.0
2.00	3.4550	3.4550	3.4550	3.4550	43.1
2.50	5.1450	5.1450	5.1450	5.1450	37.2
3.00	7.2310	7.2310	7.2310	7.2310	32.1
4.00	12.905	12.905	12.905	12.905	25.8
5.00	21.293	21.293	21.293	21.293	21.6

As the peak pressures experienced during an impact event are shown to be independent of the size of the projectile; the size of the projectile is thus rendered irrelevant during the simulations (this was not unexpected, as the water and glass strength models do not have strain-rate dependence, and will therefore be size independent). Therefore all of the subsequent impact simulations need not consider different sized projectiles, so a 400 m diameter projectile is used.

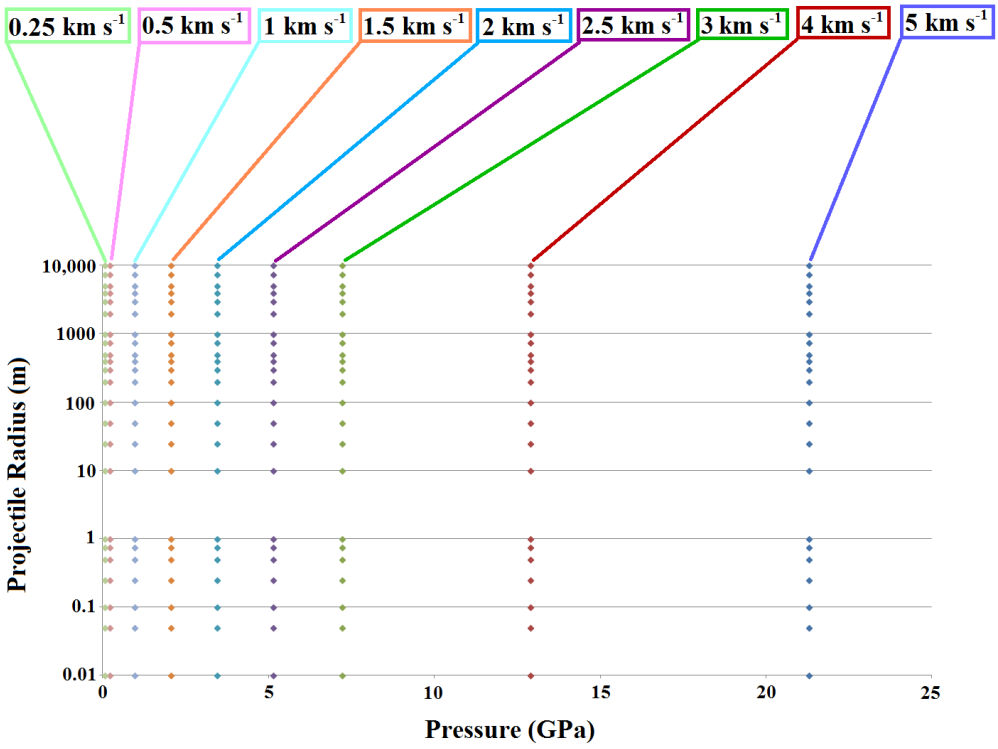

Figure 7.9: Impactor size versus peak shock pressure - for nine different impact velocities, showing that the peak impact pressure is independent of size.

7.4.3 Impacts into Rocky Bodies

A plot of the results for hypervelocity impacts across a range of velocities (0.25 – 15.5 km s^{-1}), for an icy projectile impacting onto the surface of a rocky body yields the graph shown in Fig. 7.10.

The results presented here only determine the peak pressure experienced by a life-form at the 'Optimal Point' in the projectile. However, rocky body impacts will also produce cratering and any life that survives will have to contend with these effects. These will be discussed in Chapter 8, Section 8.5.

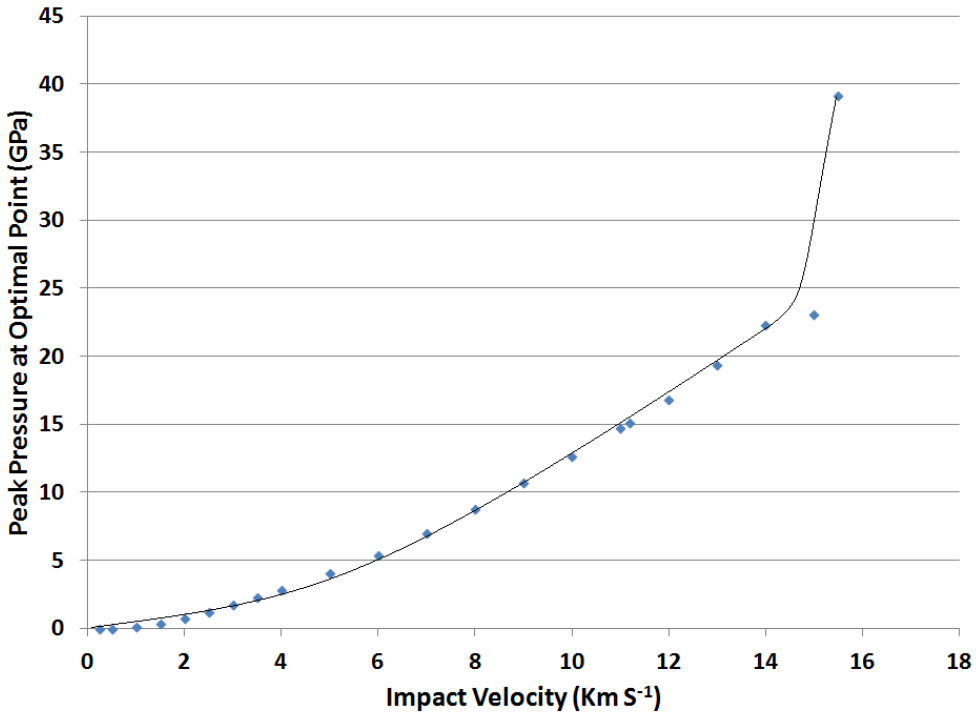

Figure 7.10: Results of simulated impacts of an icy projectile onto the surface of a rocky body, showing the impact velocity against the peak pressure experienced at the 'Optimal Point'.

7.4.4. Impacts into Icy Bodies

A plot of the results for hypervelocity impacts across a range of velocities (0.25 – 20 km s^{-1}), for an icy projectile impacting into an ocean yield the graph shown in Fig. 7.11.

Both Fig. 7.10 and 7.11 show a deviation to an otherwise constant trend in the data at higher velocities (<14 km s^{-1} for rocky impacts, and <18 km s^{-1} for oceanic impacts). There is potentially a numerical error propagating in the data at higher velocities, and this is addressed in Chapter 8, Section 8.4.

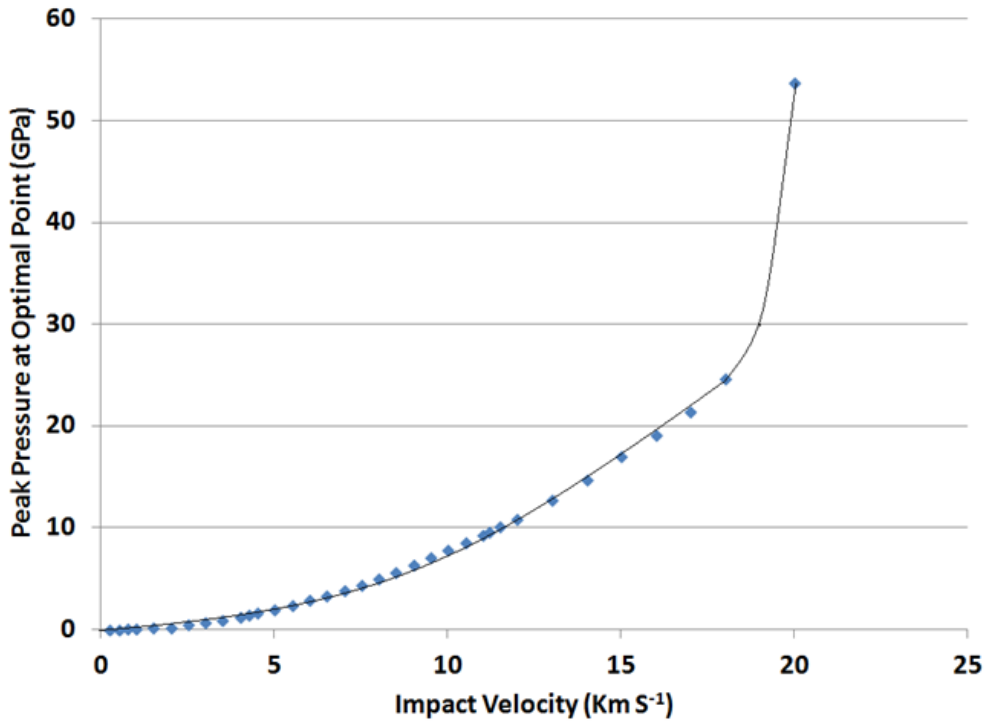

Figure 7.11: Results of simulated impacts of an icy projectile onto the surface of an ocean, showing the impact velocity against the peak pressure experienced at the 'Optimal Point'.

7.5 Conclusion

This chapter described five species of extremophile, and the impact induced pressures that they can survive. In order to compare these species to different impact scenarios, hydrocode models of various impact scenarios were created.

Test models were created to find the optimum point of survival within a spherical impactor, and to test the independence of impact pressure to projectile size. The escape velocities and thus optimum impact velocities for a number of different planetary bodies were calculated, including two extrasolar planets Gliese 581 g and d. The results of the test models were then presented, and the optimum point for survival on a spherical impactor was determined to be at the rear of the impactor (but below the depth of any possible fusion crust formation). Further results showed the independence of impactor size to peak pressure experienced at a given location on the projectile, allowing a significant saving on computational runtime for different simulations.

The results for a range of impact velocities (0.25 – 15.5 km s^{-1}), on to a rocky body target were presented. Finally the results for a range of impact velocities (0.25 – 20 km s^{-1}), onto an oceanic target were presented. The analysis of these results applied in relation to the five species chosen for comparison will be presented in the next chapter, with an in-depth discussion about the implications for a number of difference scenarios relating to the panspermia hypothesis.

CHAPTER 8

ANALYSIS AND DISCUSSION

"I was its king once, a long time ago, when the great gods decided to send the Flood. Five gods decided, and they took an oath to keep the plan secret. Ea also, the cleverest of the gods, had taken the oath, but I heard him whisper the secret to the reed fence around my house. 'Reed fence, reed fence, listen to my words. King of Shuruppak, quickly, quickly tear down your house and build a great ship, leave your possessions, save your life. The ship must be square, so that its length equals its width. Build a roof over it, just as the Great Deep is covered by the earth. Then gather and take aboard the ship examples of every living creature."

Excerpt from 'The Epic of Gilgamesh'

8.1 Introduction

Following on from the two experimental investigations (of phytoplankton and tardigrades), and the selection of three other species of extremophile for consideration in creating hydrocode models of different panspermia style scenarios, a comparison of these five species to the results of these models are presented with detailed in-depth analysis and discussion of the implications. This analysis will be conducted with the different extremophile species. Various simulated impact regimes are presented to show which scenarios are conducive to the panspermia hypothesis – the natural transfer of life (via an icy body) through space to an extraterrestrial environment. Analyses for both local Solar System transfers, as well as interstellar transfers are presented. Potential numerical errors within the hydrocode models are then discussed, and further speculation of the data is considered. Other factors, such as cratering in rocky impacts are discussed, and intriguing life-seeding scenarios are considered. Finally concluding remarks are passed.

8.2 Panspermia: Best Case Scenario

Based on the work so far, the 'Best Case' scenario would thus be:

1) A projectile laden with life that was ejected into space from its parent body via spallation effects, some distance from the main impact site, ensuring a higher probability of survival for any life-forms present.

2) An icy projectile with life-forms evenly distributed throughout (or at least some micro-organisms residing at the 'Optimal Point' within the projectile).

3) A projectile that is large enough that any organisms within are well protected against prolonged exposure to the radiation environment of space.

4) A projectile that is on an optimal transfer path between celestial bodies to minimise as much as possible the time frozen, and the exposure to space.

5) A projectile that is also large enough that if any atmosphere is encountered upon arrival, the following are true: a) thermal heating caused by the atmosphere will not destroy it, b) a fusion crust is able to form, protecting any life-forms within from potentially sterilising high temperatures, c) the velocity is reduced via the drag force felt whilst travelling through the atmosphere.

6) An impact velocity that is equal to the local escape velocity of the body onto which the projectile is impacting (or potentially lower still if any atmosphere is present to cause drag effects).

It is with the assumption that all of these conditions are fulfilled, that the following analysis is presented as the 'Best Case Scenario' for each of the scenarios considered.

8.3 Panspermia Scenarios

Table 8.1 below shows a variety of target bodies and the different species that could survive impact onto them.

Table 8.1: *Maximum pressures, and the associated species survival for various impact environments (or other celestial bodies with equal V_{esc}.).*

Target Body for Impact	***Escape Velocity (km s^{-1})***	***Pressure at Op.P. (Oceanic Impact) AUTODYN (MPa)***	***Species That Could Survive (Oceanic Impact)***	***Pressure at Op.P. (Rocky Impact) AUTODYN (MPa)***	***Species That Could Survive (Rocky Impact)***
Enceladus	0.25	7.53	TBYLP	11.15	TBYLP
Ceres	0.51	17.25	TBYLP	34.20	TBYLP
Pluto	1.27	142.2	TBYLP	312.8	TBYLP
Europa	2.02	342.7	TBYLP	787.7	T*BYLP
The Moon	2.38	459.0	TBYLP	1113	BYLP
Titan	2.65	552.0	TBYLP	1368	BYLP
Mercury	4.25	1428	BYPL	3161	BYLP
Mars	5.02	2001	BYPL	4105	BYLP
Earth	11.2	9632	BYPL	15180	BYLP
*GJ 581d	19.5	23200	BYPL	N/A	N/A
†GJ 581d	22.0	N/A	N/A	63180	None
*GJ 581g	13.9	14560	BYPL	N/A	N/A
†GJ 581g	16.1	N/A	N/A	51041	None

GJ = Gliese, * = if a water/ice composition, † = if a rocky composition. Op.P. = 'Optimal Point', T = Tardigrade, B = Bacteria, Y = Yeast, P = Phytoplankton, L = Lichen, and T* = Possible T survival if population is suitably large enough and/or atmospheric drag effects reduce the projectile's velocity.

A plot of the results for hypervelocity impacts across a range of velocities (0.25 – 15.5 km s^{-1}), for an icy projectile impacting onto the surface of a rocky body in Fig. 8.1, shows that tardigrades cannot survive impact velocities higher than ~2 km s^{-1}, bacteria and yeast can survive impact velocities up to 15.25 km s^{-1}, and phytoplankton and lichen can survive up to and, possibly, just beyond 15.5 km s^{-1}.

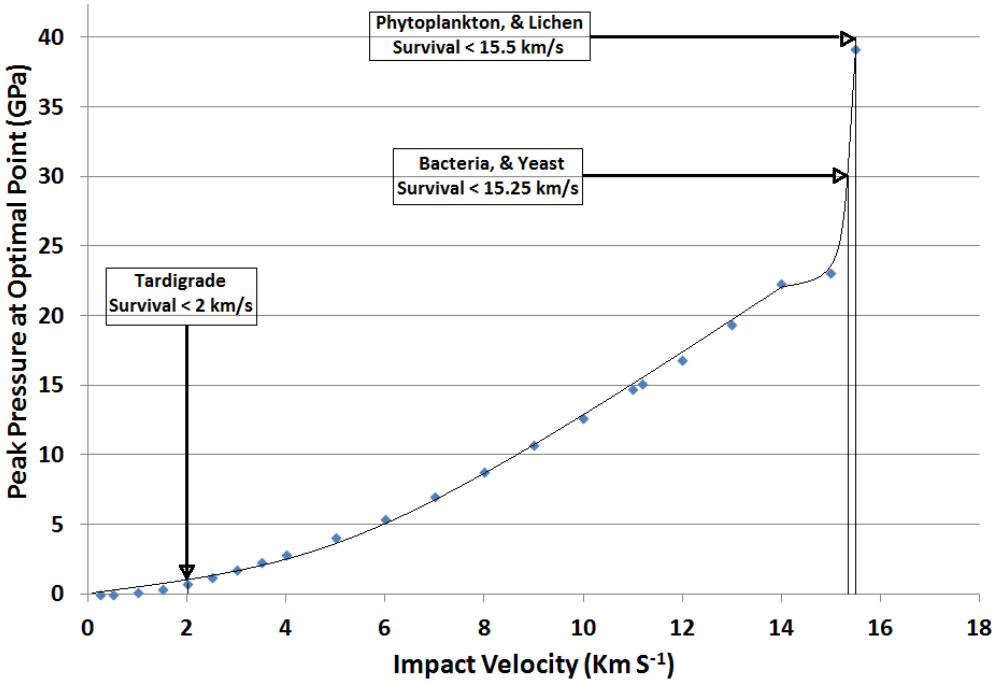

Figure 8.1: Results of simulated impacts of an icy projectile onto the surface of a rocky body, showing the impact velocity against the peak pressure experienced at the 'Optimal Point'. The maximum survival tolerances for this scenario are highlighted, showing that tardigrades cannot survive impact velocities higher than 2 km s^{-1}, Bacteria and yeast can survive impact velocities up to 15.25 km s^{-1}, and Phytoplankton and Lichen can survive up to and possibly just beyond 15.5 km s^{-1}.

A plot of the results for hypervelocity impacts across a range of velocities (0.25 – 20 km s^{-1}), for an icy projectile impacting onto the surface of an ocean shown in Fig. 8.2, shows that tardigrades cannot survive impact

velocities higher than ~3 km s^{-1}, Bacteria and yeast can survive impact velocities up to 19 km s^{-1}, and Phytoplankton and Lichen can survive up to and possibly just beyond 19.5 km s^{-1}.

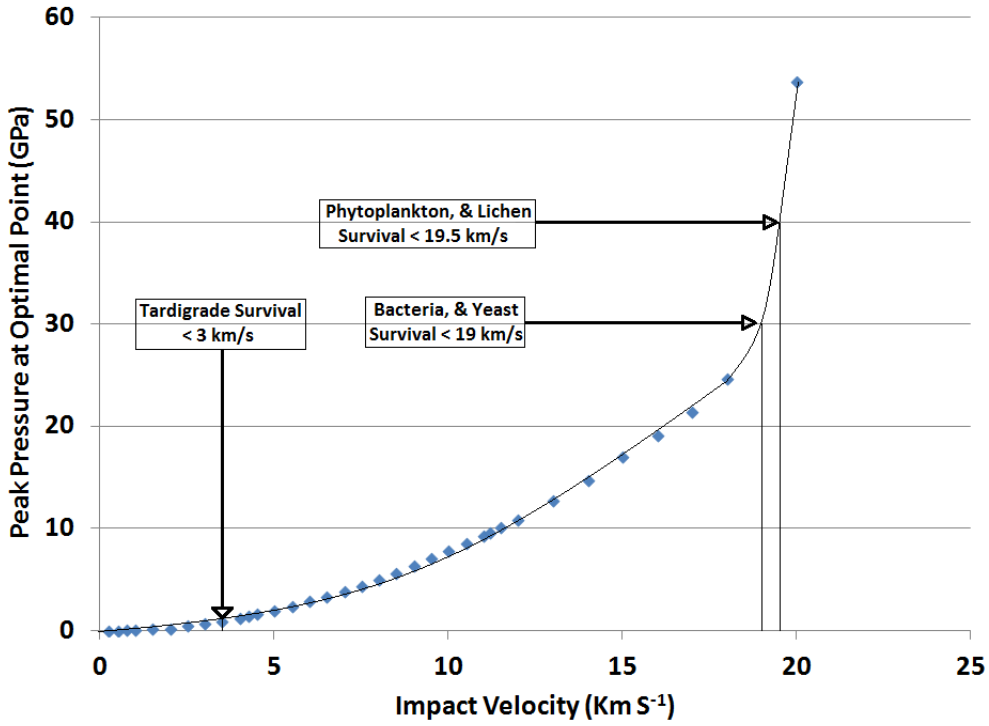

Figure 8.2: Results of simulated impacts of an icy projectile onto the surface of an ocean, showing the impact velocity against the peak pressure experienced at the 'Optimal Point'. The maximum survival tolerances for this scenario are highlighted, showing that tardigrades cannot survive impact velocities higher than 3 km s^{-1}, bacteria and yeast can survive impact velocities up to 19 km s^{-1}, and phytoplankton and lichen can survive up to and possibly just beyond 19.5 km s^{-1}.

8.3.1. Survival within the Solar System

The results presented here indicate that the tardigrade species could only survive oceanic and rocky impacts up to 3, and 2 km s^{-1} respectively (Fig. 8.1 and 8.2). Therefore, survival of panspermia style impacts can occur

on bodies such as Enceladus, Ceres (and all other asteroids within our Solar System), Pluto (and similar-sized, or smaller, Kuiper Belt Objects), Europa, as well as any bodies that are similar to the Moon or Titan and have substantial liquid bodies on their surfaces. However, the other four organisms considered here (bacteria, yeast, phytoplankton, and lichen) show that survival of panspermia style impacts can occur anywhere within the Solar System, with the exception of the four outer Solar System gas planets.

8.3.2 Extrasolar Planetary Impact Events

Two Super-Earth exoplanets, Gliese 581d and Gliese 581g, are included in this analysis. However, doubt has recently been cast on the existence of these two exoplanets. Roberson, P. et al., (2014), suggest that it is actually stellar activity that is seen in the data, and that the data has not been corrected to account for this. However, Guillem, A. et al., (2015) questioned the methods used to challenge the planets' existence, insisting that using a more accurate model, they are confident that the signals seen in the data are indeed real, despite stellar variability. Regardless of whether these two exoplanets exist or not, they can be used in this analysis as analogues for exoplanets of similar size and mass, existing within the habitable zone around their parent star.

If these two exoplanets are homogeneous, and composed primarily of the perovskite phase of $MgSiO_3$ (Earth-like), then the radii of Gliese 581d and Gliese 581g are expected to be 1.8 and 1.5 Earth radii respectively, or 2.3 and 2.0 Earth radii, if water-ice (Wordsworth, R. et al., 2011**,** and Vogt, S. et al., 2010). However, all radii are predicted to be approximately 20% smaller if the planet is differentiated (Wordsworth, R. et al., 2011). The optimal case is considered here, e.g. these, or similar sized planets, are found to be orbiting

within the habitable zone of their parent star, and thus have the potential for liquid water on their surfaces (see Fig. 8.3).

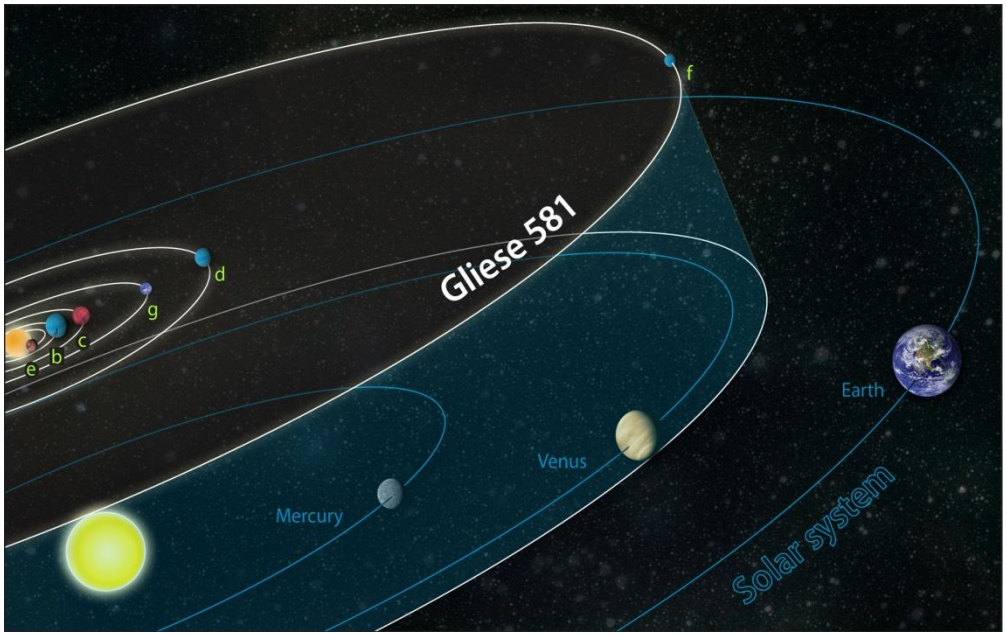

Figure 8.3: The orbits of planets in the Gliese 581 system compared to those of our Solar System. The star Gliese 581 is approximately 0.3 solar masses, and the fourth planet, Gliese 581g, is a planet that orbits within the habitable zone and could potentially sustain life. *Image Courtesy: Zina Deretsky, National Science Foundation*

With the exception of the tardigrade species, survival is still possible by all of the species considered here, during impacts onto Super-Earths beyond our Solar System (of these or similar proportions) composed of water/ice. However, survival appears to be non-viable for these rocky Super-Earths (or those of similar proportions) without some way of reducing the peak shock pressure, such as atmospheric drag forces lowering the impactor's speed significantly to within tolerable levels and/or impacts at very oblique angles.

Extending Table 8.1 to include two additional Super-Earth exoplanet candidates, KoI82.02 and KoI115.02 (see Table 8.2) yields intriguing results.

Table 8.2: *An extension of Table 8.1 including two new Super-Earth candidate exoplanets. KoI 82.02 shows survival of 4 species in both the Europa-like case, and the rocky Earth-like case.*

Target Body for Impact	***Escape Velocity (km s^{-1})***	***Pressure at Op.P. (Oceanic Impact) AUTODYN (MPa)***	***Species That Could Survive (Oceanic Impact)***	***Pressure at Op.P. (Rocky Impact) AUTODYN (MPa)***	***Species That Could Survive (Rocky Impact)***
*GJ 581d	19.5	23220	BYPL	N/A	N/A
†GJ 581d	22.0	N/A	None	63180	None
*GJ 581g	13.9	14557	BYPL	N/A	N/A
†GJ 581g	16.1	~20000¥	BYPL	51041	None
*KoI82.02	13.9	14557	BYPL	N/A	N/A
†KoI82.02	15.4	~18000¥	BYPL	24656	BYPL
*KoI115.02	14.6	16043	BYPL	N/A	N/A
†KoI115.02	16.1	~20000¥	BYPL	51041	None

GJ = Gliese, KoI = Kepler Object of Interest, * = if a water/ice composition, † = if a rocky composition. Op.P. = 'Optimal Point', B = Bacteria, Y = Yeast, P = Phytoplankton, L = Lichen. ¥ = Approximate value based on trend of Fig 8.2 for a scenario such that an ocean exists on the rocky planet.

If these additional two exoplanets are homogeneous, and primarily composed of the perovskite phase of $MgSiO_3$ (Earth-like), then the radii of both KoI82.02 and KoI115.02 are expected to be 1.4 Earth radii, or if

Europa-like, then 1.7 and 1.8 Earth radii respectively (Hadden, S. and Lithwick, Y. 2014). Again, all radii are predicted to be 20% smaller if the planet is differentiated (Wordsworth, R. et al., 2011).

The analysis of these two new exoplanets shows that survival by the same four species is attainable on both of the Europa-like exoplanets (as it was for the water/ice exoplanets Gliese 581 d and g). However, now a rocky Earth-like exoplanet (KoI82.02) shows the survival of the same four species, although a rocky KoI115.02 is still beyond the survival tolerance of all species considered. A difference in size of just 0.1 Earth radius, between Gliese 581g and KoI82.02 changes the escape velocity from 16.1 to 15.4 km s^{-1} bringing the rocky KoI82.02 Super-Earth within the survival window for the various species considered here (with the exception of the tardigrade). There are, however, other factors to account for when debating the possibility of interstellar panspermia.

When considering panspermia between two solar systems, the vast distance between them becomes a larger issue, as the time to cross interstellar space (as opposed to the distance between two planets in the same system) for a body carrying life-forms will be greatly increased. For example, taking a projectile travelling at an impact velocity just within the tolerance of survival for phytoplankton and lichen (if an atmosphere is present on the body they are impacting onto) – 20 km s^{-1} (630.72 million km per year) – from the Earth, it would take 62,790 years to reach even the closest star to our sun, Proxima Centauri, at 4.2 light years distant. When comparing this to the Hohmann transfer orbit times (see Table 3.2 in Chapter 3) for optimum journeys through our Solar System, the vast difference can be seen when considering 62,790 years is just the time to reach Proxima Centuari, and there would likely be similar timescales to the Hohmann transfer orbit times in the most optimistic case (or more, if the orbit is not in the plane of the system) for the projectile, once gravitationally bound to the star system, before it

eventually encounters a planet in that system. However, 62,790 years is far less than the average (non optimal) transfer time between planets within the Solar System, and thus, although similar timescales to the average transfer between planets will still apply at the destination star system, the travel time between these two systems will not add much increase to the total time between ejection from Earth to impact onto a planet in the Proxima Centuari star system. The interstellar journey will of course start to significantly add to the transfer time when the distances between two star systems begin to increase.

If the Gliese 581 star system (approximately 20 light years distant) is considered, then a projectile travelling at 20 km s^{-1} would take approximately 299,000 years to reach that system from the Earth. Going further into the galaxy, the distances become so vast that transfers between star systems begin to enter the regime of 'millions of years'. So, the question becomes, can life-forms survive such timescales?

In 2000, Vreeland, R. et al., announced they had successfully revived from a state of suspended animation, a previously unrecognized spore-forming bacterium (Bacillus species, designated 2-9-3) from a brine inclusion within a 250 million year old salt crystal, from the Permian Salado Formation (breaking the previous record of a bacterial spore most closely related to *Bactillus sphaericus*, that was revived from the abdominal contents of extinct bees, preserved in amber for 25 – 40 million years (Cano, R. and Borucki, M. 1995). Complete gene sequences of the 16S ribosomal DNA show that this organism is part of the lineage of *Bacillus marismortui* and *Virgibacillus pantothenticus* (Vreeland, R. et al., 2000). If this organism is capable of surviving similar pressure extremes as its relative (*Bacillus subtilis*), then interstellar panspermia becomes a possibility. This 250 million year timescale is of the same order of magnitude as for the time it takes the entire Milky Way galaxy to fully rotate around its centre. Using recently determined

values of our sun's position from the Milky Way's galactic centre (8 kpc) and its orbital velocity around that centre (238 km s^{-1}; Honma, M. et al. 2012, 2015), the rotational period of the Milky Way is calculated to be approximately 205 million years (Sofue, Y. 2017). Any such bacteria in a projectile travelling at 20 km s^{-1}, would be able to traverse 16,722.4 light years in that revival window of 250 million years; just over a third of the distance of the Milky Way's radius! (See Fig. 8.4).

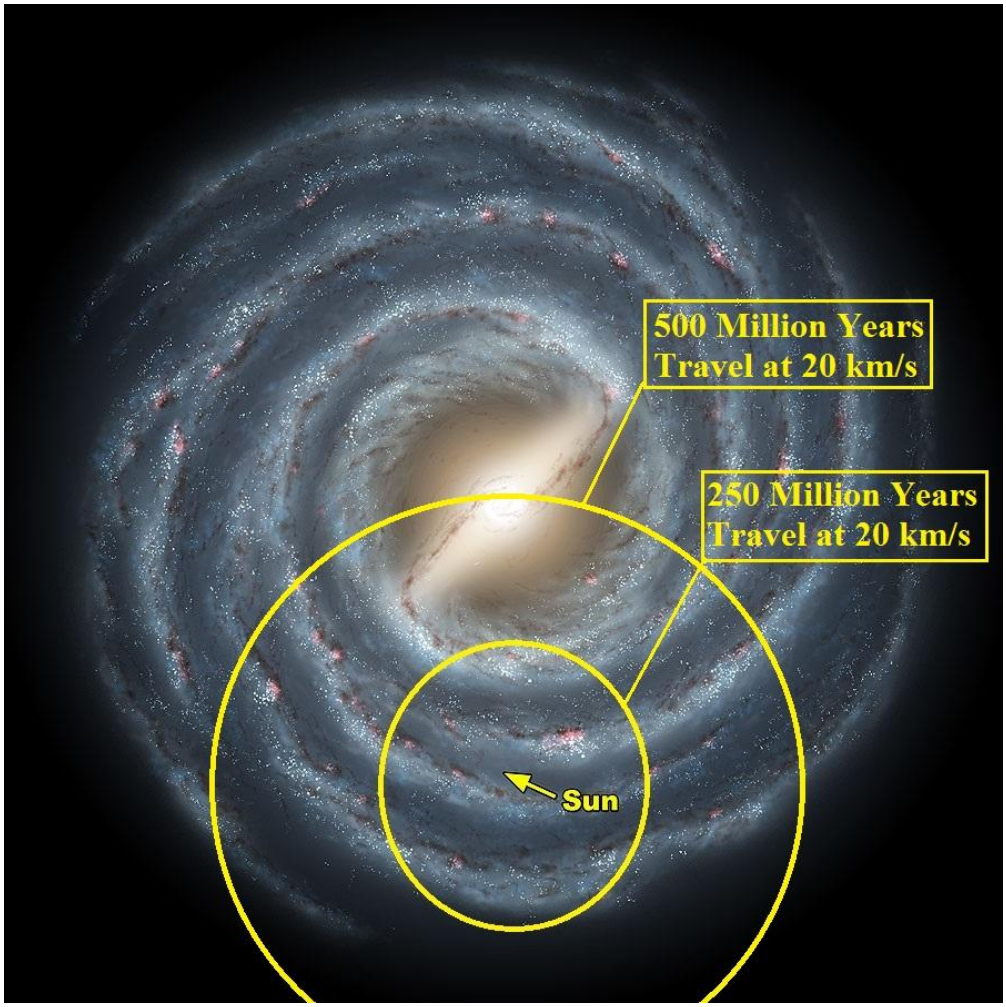

Figure 8.4: Artist's impression of the Milky Way galaxy, the position of our sun is highlighted. Superimposed on this image are the radii showing how far a projectile from our Solar System travelling at 20 km s^{-1} could travel in 250 and 500 million years. *Original image courtesy: Nasa*

Valtonen, M. et al., (2009) has shown that *D. radiodurans*-like bacteria can survive the radiation environment of interstellar space for up to 500 million years if suitably housed within a group of ejecta fragments that have individual minimum radii of 2.67 m. As the bacteria previously discussed were fully revived after 250 million years in suspended animation, there is no reason to assume this suspended animation stage could not have lasted even longer, had they not been found and revived when they were. So, if they are capable of surviving another 250 million years in such a state, this means there would be no reason they could not potentially travel upwards of 33,000 light years within the galaxy and still survive the cosmic radiation, and impact, and be revived to an active state on a far distant planet elsewhere in the galaxy (see Fig. 8.4).

So, what about intergalactic panspermia? Looking at our nearest galactic neighbours (ignoring Canis Major Dwarf galaxy at ~25,000 light years from Earth (Lewis, G. et al., 2004) – closer to us than our own galactic centre, and whose status as a galaxy is still in dispute), the nearest galaxy is a small satellite galaxy; the Sagittarius Dwarf Spheroidal Galaxy, approximately ~81,000 light years from Earth (Karachentsev, I. 2004). The nearest large galaxy to us (indeed the largest in the local group) is the Andromeda Galaxy (M31) located ~2.56 million light years from Earth (McConnachie, A. et al., 2005), and heading towards us on a collision course (which will not occur for over a billion years or so yet). A projectile travelling at 20 km s^{-1} would take approximately 1.21 billion years to reach out nearest galactic neighbour, the Sagittarius Dwarf Spheroidal Galaxy. The same projectile would take approximately 38.3 billion years to reach the Andromeda Galaxy, almost three times the age of the universe itself; indeed, the Andromeda Galaxy will reach us and collide with our own Milky Way Galaxy long before then. So far, no life has ever been found in suspended animation and revived from such a long time ago as this (indeed the universe

is not old enough for the higher of the two timescales!). This does not mean such life does not exist, indeed, it may be that there are extremophiles already discovered and analysed that may be capable of surviving such timescales. For now, with current discoveries, it cannot be said whether such a trip would be survivable, or not, by any life-form. So, while intergalactic panspermia is considered (virtually) impossible, interstellar panspermia may be possible for some extremely hardy micro-organisms.

8.4 AUTODYN: Numerical Error Propagation

Further analysis to the impact simulations (continuing impact velocities up to 38 km s^{-1}) has shown the introduction of a numerical error propagating through the data (see Fig. 8.5). This means the slight deviation seen in the plots in Figs. 7.10, 7.11, 8.1, and 8.2, may be due to this numerical error, and thus not correct. The error appears to be a sinusoidal pattern overlaid onto otherwise valid data. It is possible that this was caused by numerical erosion of heavily distorted cells (which can happen with high speeds). A solution to this may possibly be to run the model at a much higher resolution. However, time constraints meant this was not able to be done at the time.

To explore into the higher velocity regime a small extrapolation of the data before the problem occurs is considered; enough to conjecture further on the limits of survival already considered.

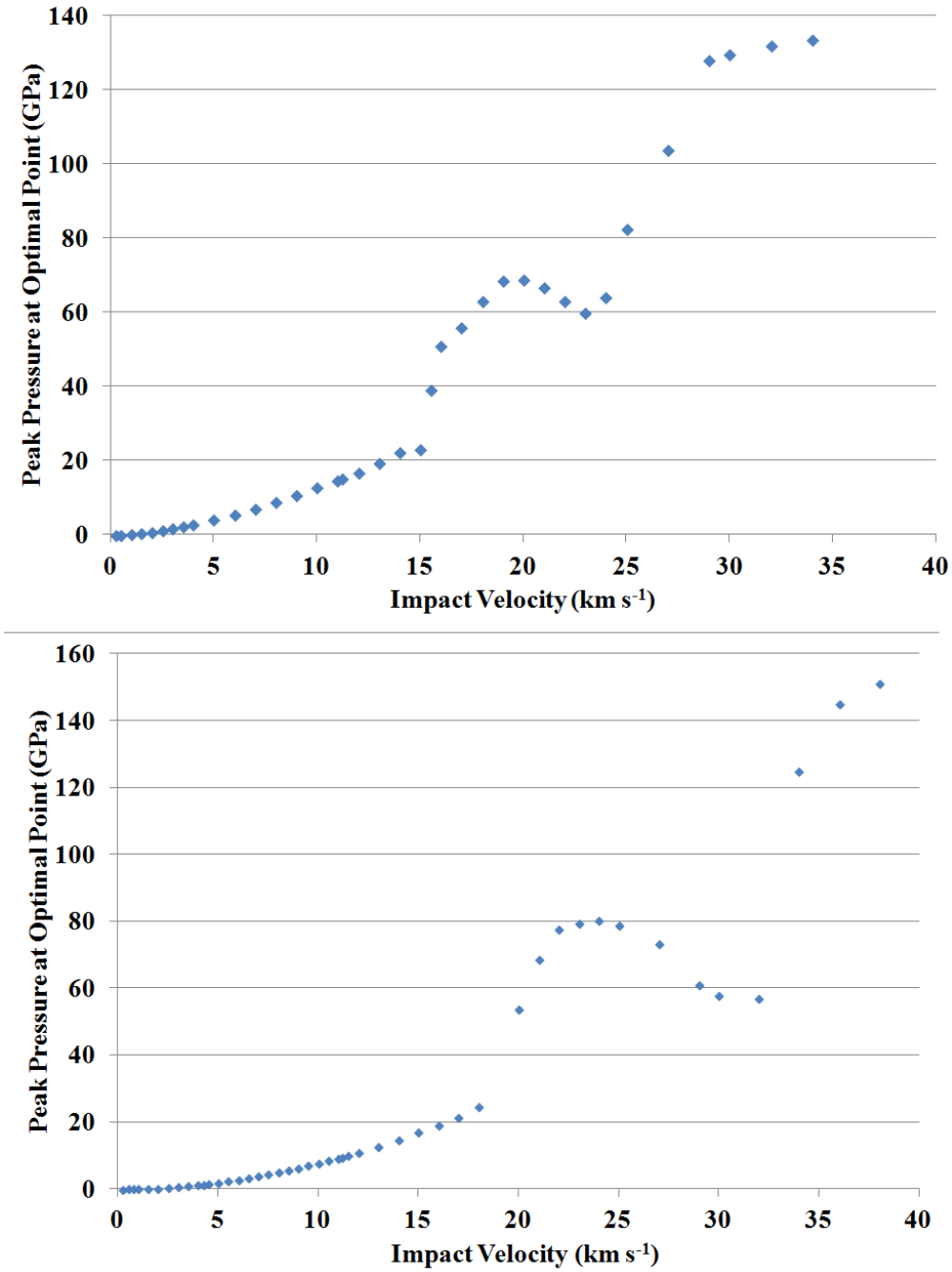

Figure 8.5: Results of simulated impacts of an icy projectile onto the surface of rocky body (Top) and an ocean (Bottom), showing the impact velocity against the peak pressure experienced at the 'Optimal Point'. Notice the introduction of a numerical (sinusoidal-like) error at ~14–15 km s^{-1} (Top) and ~18 km s^{-1} (Bottom) and propagating through the higher velocity data.

Figs. 8.6 and 8.7 show these extrapolated trends and the points at which some species impact velocity survival range has increased.

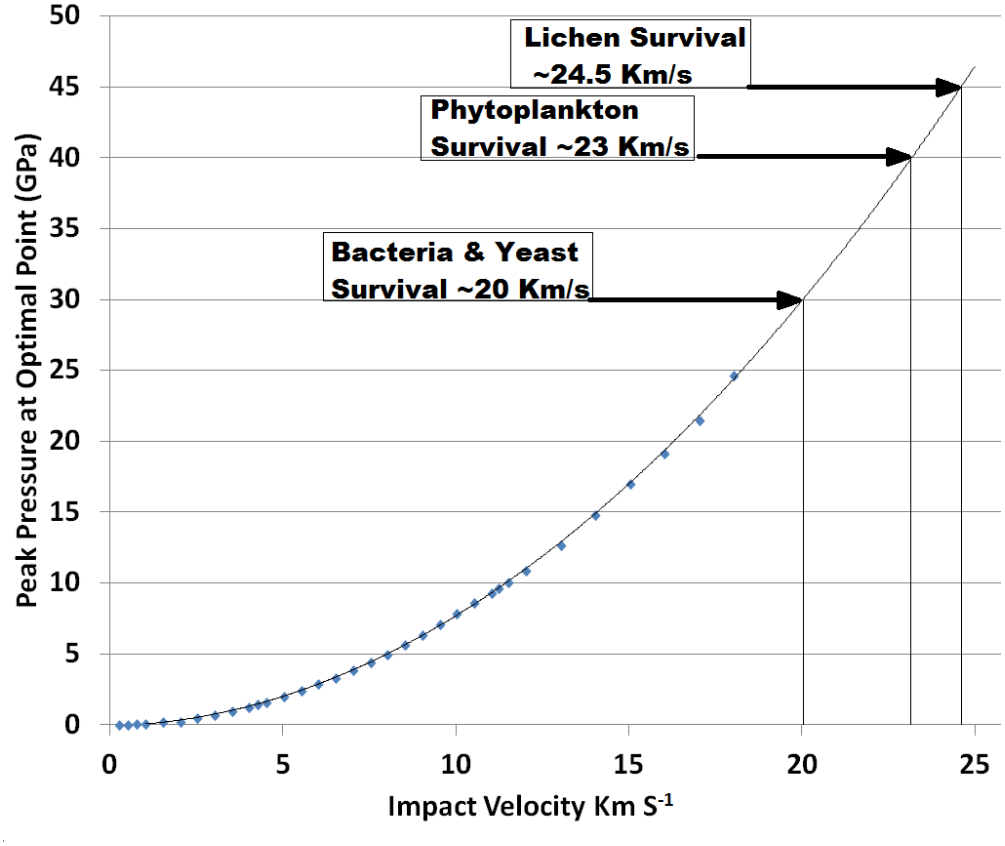

Figure 8.6: Results of simulated impacts of an icy projectile onto the surface of an ocean, showing the impact velocity against the peak pressure experienced at the 'Optimal Point', with new trend showing survival could be achieved at higher impact velocities than previously shown. This new trend suggests bacteria and yeast could survive impacts up to 20 km s^{-1}, phytoplankton could survive impacts up to 23 km s^{-1}, and lichen could survive impacts up to 24.5 km s^{-1}.

With these new trend lines it is suggested that survival could occur at even higher impact velocities than previously suggested. For the case of an icy projectile impacting into an ocean the suggestion is that bacteria and yeast could survive impact velocities up to 20 km s^{-1} (previously 19.5 km s^{-1}), phytoplankton could survive impact velocities up to 23 km s^{-1} (previously

19.5 km s^{-1}), and lichen could potentially survive impact velocities up to 24.5 km s^{-1} (previously 19.5 km s^{-1}). This implies that even larger icy/ocean planets than previously considered could still be within survival ranges for some species.

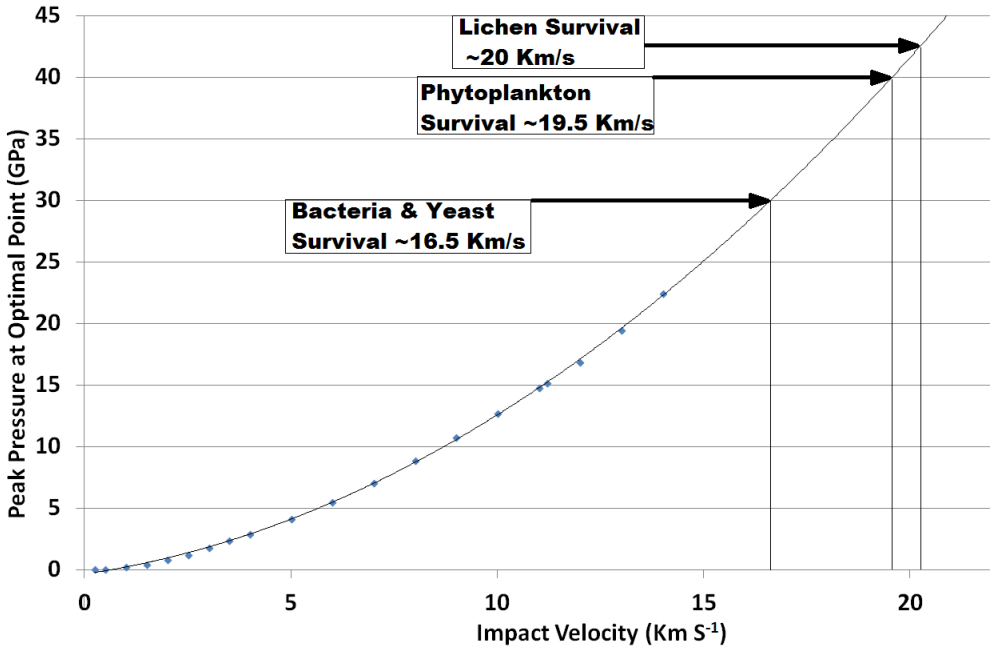

Figure 8.7: Results of simulated impacts of an icy projectile onto the surface of a rocky body, showing the impact velocity against the peak pressure experienced at the 'Optimal Point', with new trend showing survival could be achieved at higher impact velocities than previously shown. This new trend suggests bacteria and yeast could survive impacts up to 16.5 km s^{-1}, phytoplankton could survive impacts up to 17 km s^{-1}, and lichen could survive impacts up to 18 km s^{-1}. This implies that survival may be possible on the previously unattainable rocky planets KoI115.02, and Gliese 581g.

The new trend line for the case of an icy projectile impacting onto a rocky body suggest that bacteria and yeast could survive impact velocities up to 16.5 km s^{-1} (previously 15.25 km s^{-1}), phytoplankton and lichen could

survive impact velocities up to 19.5 km s^{-1}, and 20 km s^{-1} respectively (both previously 15.5 km s^{-1}). This implies that like KoI82.02, the rocky forms of exoplanets KoI115.02, and Gliese 581g could actually be within survival ranges for bacteria, yeast, phytoplankton and lichen, although a rocky Gliese 581d still remains out of reach.

8.5 Impact Cratering at Destination

As discussed in Chapter 3, Section 3.4.1, when hypervelocity impacts occur onto solid bodies (e.g. a rocky or icy planet), craters are formed. This cratering process can affect any life that has managed to survive thus far in its journey to a new world. The vaporisation effects that can accompany larger scale impact events would need to be avoided by any life-form arriving on the impacting projectile. This could occur several ways. The impacting projectile could break up due to drag forces and/or thermal stresses during entry to the target body's atmosphere. The resulting multiple impacts will be on much smaller scales, and thus the time for impact generated temperatures to drop within tolerable levels, will be reduced – for life to survive they would have to reduce fast enough that any transfer of heat energy is not sterilising. The projectile could also impact at an oblique angle such that some of the projectile is thrown as ejecta away from the main impact site, thus impacting with less force elsewhere.

If the impact is large and any companion life-forms do manage to escape the vaporisation at the impact site as ejecta, only those thrown far enough away from the main impact site will stand a chance of survival, as large impacts can produce extremely high temperatures remaining in the crater for long periods of time (Weiss, D. et al., 2016, and Abramov, O. et al., 2016) before they cool enough for life to survive. Any life-forms in ejecta

that falls back into such a crater would then have to contend with these long duration high temperatures.

If the impact is such that the temperature in the crater returns to tolerable levels before any life falls back into the crater, another potential risk they face is that material can bury them, either the ejecta or collapsing structures within the crater. Whist some organisms can survive beneath, or within, rocks, and could thrive, other organisms, like photosynthetic life-forms, would not likely survive such entombment.

If any life does manage to survive the panspermia process and make it to a new world alive, there is still one final obstacle the process could deliver; any impact that initiates changes to the local or global environment such that the newly transported life could not survive, thus dying out almost immediately. Impacts that cause a rupture to magma pockets within thin planetary crusts, or initiate extreme volcanism (Werner, S. et al., 2016), or fill the atmosphere with material such that the heating from the parent star is reduced to non habitable levels; the latter may only be a temporary effect and any life that survived frozen in space may still later recover again if the planet later returned to habitable conditions again.

8.6 A Cosmic Noah's Ark

While considering different panspermia style scenarios, there is another case to consider – the Noah's ark scenario. Suppose a large impacting body, such as an asteroid or comet, hits a planet that houses life, (similar to the impact that created the Chicxulub crater buried beneath the Yucatan peninsula and initiated the Cretaceous–Tertiary 'K–T' extinction event (Alvarez, L. et al., 1980), around 65 million years ago (Swisher, C. et al., 1992)). Suppose this impact causes the onset of an extinction level event

that eventually sterilises the planet of life. The impact itself may, through spallation effects, lift life-forms, with rocks, dust, and water/ice, into space protecting them from the extinction event in progress on their home world. With sufficient time the planet may recover, conditions may once again be conducive to life, but the planet is barren. Material laden with dormant life, drifting in space for hundreds, thousands, or even millions of years, could pass by the parent planet close enough to get caught in its gravity well, and then fall to the planet. Any surviving life-forms would therefore re-seed the planet with life, allowing it to begin growing and evolving once again. Or, the material could impact onto a different planet in the star system; it could even be ejected from the star system altogether, and eventually land on a planet elsewhere in the galaxy, seeding a new planet with life.

8.7 Are We All Martians?

A final question on the panspermia hypothesis relating to our own species; are we all Martians? Once it was an outlandish idea whose answer was a clear 'no', and the door for debate firmly closed. However, the question now seems thrown open for debate once again. The research shown here throughout this thesis obviously cannot answer this question (indeed it may never be answered), but it can place a foot in the doorway leaving it once again open for some serious debate. Panspermia style impacts *can* happen, and some life-forms *can* survive them. So, while this research cannot definitively answer the question of whether panspermia has occurred on our world (or any other), it does show that panspermia *could* happen, and should therefore be seriously considered in any debate about the origins of life on our planet, or indeed any other planet, should we happen upon life elsewhere in the universe in the future; after all, we may just be related!

So, with evidence that early Mars may have been better suited for the genesis of life than the Earth (see Chapter 3, Section 3.2), a host of Martian meteorites are known to have landed on the Earth, as well as, suggestions of micro-fossils in such meteorites, and the Late Heavy Bombardment increasing the probability of an optimal Hohmann style transfer path for material travelling from Mars to Earth, such that multiple optimal impacts could have occurred, right at the time in history when the first evidence for life on Earth is seen, a passing remark is offered.

One line of thought is that, if the conditions for the genesis of life to occur are present (and they were, somewhere – or life would not exist), would it not occur repeatedly? It could be argued that it would be unlikely that it only occurred once, if the conditions were indeed conducive to it forming at all. So, why is it that all life on Earth appears to have originated from a single source? One answer to this, of course, is that life *did not* originate on the Earth. If it originated elsewhere, Mars for example, then it may well have occurred multiple times with many different unrelated basic organisms that had completely unrelated RNA and DNA sequences to one another. A giant impact occurs, launching some of this life into space. Some of this life travels to the Earth, and some of it survives an impact into the planet's surface, and one strain survives, and thrives on the new world. While the conditions are fine for the organism to survive and prosper, they are not right for a genesis of new life to occur, and thus all life on the planet that follows has evolved from this one source, and it is all related, as it shares a common DNA source and has a linked genealogical history. Just as we see on the Earth today.

So, could we really be Martians? Another answer to the singularity of life's origin on Earth is that a Noah's ark style event occurred early in the Earth's history, with just a single species re-seeding the planet. Worth, R. et al. (2013) suggest that this would be a possible mechanism to aid the survival

of early life on Earth during the cataclysmic period of the Late Heavy Bombardment, where it is plausible that the Earth could have been partially or completely sterilised by one or more large impacts. So, for now it seems, the question remains open. However, one thing is certain, and that, is that the panspermia debate is a serious one, and is not going anywhere, anytime soon. So, with that in mind maybe it is time to try to quantify panspermia as a whole, or at least provide a method for that quantification in the form of an equation.

8.8 An Equation for Panspermia

An equation for the probability of life being transferred from one planet to another could be formulated to analyse the probability of life arriving from another world (Eq. 8.1). However, much like the 1961 Drake Equation (Drake, F. 1961.; Drake, F. 1962.; and see Burchell, M. 2006. for a recent review) for the existence of intelligent life in the universe, it will rely on some terms which are currently unknown.

$$P_p = G_l \times L_s \times F_r \times E_f \times T_p \times M_f \times C_p \times S_l \qquad \text{(Eq. 8.1)}$$

where P_p is the number of potentially successful transfers of life (from impacts originating during T_p), G_l is probability for a genesis-of-life event, L_s is percentage of the planet's surface covered with life, F_r is the flux rate of impacts (average number per year during T_p), E_f is the fraction of F_r that could result in material being lifted into space escaping the planet's gravity, T_p is the time period since the genesis-of-life event (or depends on conditions set for analysis), M_f is the average number of fragments of material from each impact, C_p is the probability of entering a planet crossing path, S_l is the survival of life during the transfer (depending on S_e, S_s, S_i, and C_l – see

below), S_e is the survival fraction of life during the impact/spallation lift to space, S_s is the survival fraction of life during extended exposure to space, S_i is the survival fraction of life during the impact seeding event, C_l is the average number of organisms per fragment lifted to space. S_l is determined as:

$$S_l = 1 \; if \; \frac{1}{S_e \times S_s \times S_i} > C_l \qquad \text{(Eq. 8.2)}$$

$$S_l = 0 \; if \; \frac{1}{S_e \times S_s \times S_i} < C_l \qquad \text{(Eq. 8.3)}$$

The first term, G_l, would require an understanding of the conditions needed for life to form, this is something that is still being debated, and no definitive answer has yet been proven. However, to discuss whether life could arrive from a planet (such as Mars for example) it must first be assumed that life had a genesis otherwise there could be no transfer, so for such a case, the condition $G_l = 1$ could be set, if life is assumed to have been present on the parent planet.

The second term, L_s, is related to the probability of life being at an impact site. For a best case scenario it would be assumed that life has spread across the planet and life is found at all points on, or just beneath, the surface (be it ocean surface or rocky surface). Therefore $L_s = 1$ would be assumed. A more conservative approach that assumes only 10% of the surface has life ($L_s = 0.1$) may be more realistic, and if looking at a small time window close to the genesis-of-life, and life has not had time to spread far, this term may be much smaller, as life may be contained within small 'life-friendly' niche environments ($L_s < 0.01$).

The third term, F_r, is the flux rate of impacts over the time period, T_p, being considered. This will change depending on when T_p is, therefore, these two terms are linked and must be considered together.

The fourth term, E_f, is the fraction of F_r capable of lifting material into space, thus $F_r \times E_f$ will give the flux rate of impactors that can eject material into space beyond the parent planet's gravity well.

The fifth term, T_p, is the period of time being considered. Normally this would be from the first point at which life could have formed (but it could start from any time after this depending on what is being analysed). The end point also depends on what is being analysed. If looking at the probability of any transfer at all in the past then $T_p \sim 4.5$ billion years. However, if looking at the origin of life on Earth, then it is until the first evidence of life on Earth 3.8 billion years ago, i.e. $T_p = 4.5 – 3.8$ billion years = 700 million years. F_r must be considered in relation to T_p as this 700 million year period contained the Late Heavy Bombardment that lasted 300 million years, and will have a much higher F_r than the 700 million year period from 700 million years ago until now for example.

The sixth term, M_f, is the average number of individual fragments any single impact that is capable of lifting material to space will produce, as each fragment is a potential meteorite capable of carrying life to another world.

The seventh term, C_p, is the probability of any fragment eventually ending up on a trajectory that crosses the path of a planet such that impact onto that planet occurs.

The eighth term, S_l, is simply a yes or no term to determine if life could survive the process based on how much life is aboard a potential meteorite. This term is somewhat subjective as, in reality, it will depend on

the concentration of life at any given impact point. However, for any potential transfer to be successful the condition for $S_l = 1$ must be fulfilled.

The terms S_e, S_s, and S_i can be determined experimentally for known organisms, and the term C_l can be approximated with impact simulations based on known concentrations of organisms on our own planet. However, these values will only be true for any organism that is being tested, when considering seeding from another world with an unknown life-form these terms cannot be correctly estimated.

One further point to consider here, is that even if a successful transfer of life occurs, this in no way guarantees that the successful life-forms will be successful in living on their new world. If the conditions on the new world do not allow those life-forms to survive, then they will die out despite having survived the panspermia process. This has implications for any fossilised life that may be found in the search for extra-terrestrial life on other planets.

Impacts occur regularly and material is lifted into space from impacts on bodies across the Solar System all the time, and a lot of this material is transferred to other bodies. As this work has shown, there are species capable of surviving the various stages of the journey between bodies. So, it may well be that successful transfers occur with some frequency, but the life-forms that make the trip simply cannot adapt to and survive the conditions of their new environment, which is why we do not see an obvious abundance of life within the Solar System. If any future exploratory missions on other planetary bodies were to discover rocks or cratering that suggests an impact was from material thrown from the Earth at some point in the past, then it may be worth exploring that same area for micro-fossils that could prove that panspermia really does happen.

8.9 The Case for Mars

So, could life on Earth have really been seeded from Mars in the ancient past? The following analysis attempts to determine whether it may have been possible (with the assumption that Mars had a genesis-of-life event, and the Earth did not), and, if so, at what frequency. The analysis that follows here uses some known figures, as well as some assumptions, and is thus merely conjecture, to give an idea of the possibilities.

Assuming in the first instance that life did start on Mars shortly after the Solar System formed, thus setting $G_l = 1$, then, assuming 1% coverage of the surface with life, i.e. $L_s = 1.0 \times 10^{-2}$. The current impact rate on Mars today is 5.23×10^{-14} km^2 s^{-1} for impacts causing craters with effective diameters ≥3.9 m (Daubar, I. et al. 2013). The surface area of Mars is 1.448×10^8 km^2 (Seidelmann, P. et al., 2007), and this gives $F_r = 2.39 \times 10^2$ impacts per year for today. During the 300 million years of the Late Heavy Bombardment this rate was approximately ~250 times today's rate (Fassett, C. I. and Head, J. W. 2011). So, for $T_p = 7.0 \times 10^8$ years (including the Late Heavy Bombardment), $F_r = 2.57 \times 10^4$ per year. Therefore, the number of impacts producing craters with diameters ≥3.9 m, during the 700 million year period 4.5 – 3.8 billion years ago (including the Late Heavy Bombardment), is $F_r \times T_p = 1.80 \times 10^{13}$. Assuming a conservative 1 in 10,000 of these eject material into space beyond Mars' gravity, i.e. $E_f = 1.0 \times 10^{-5}$, then, $F_r \times T_p \times E_f = 1.80 \times 10^8$ impacts capable of lifting material to space.

So, now adding in G_l and L_s the equation becomes $G_l \times L_s \times F_r \times T_p \times E_f = 1.80 \times 10^6$ impacts that could have lifted life into space. The M_f term could be ~ millions, or even billions, but here a hugely conservative 1000 is assumed. So, for $G_l \times L_s \times F_r \times T_p \times E_f \times M_f$ we find that there were 1.80×10^9 rocks with life ejected into space during the period 4.5 – 3.8 billion years

ago, most of which were due to the Late Heavy Bombardment - but how many of these make it to the Earth?

As seen in Chapter 3, Section 5.5, Melosh, H. and Tonks, W. (1993) determined that 20% of all ejecta from Mars will fall to the Earth (usually within 15 million years of the impact that lifted it (Wetherill, G. 1984), therefore, $C_p = 0.2$.

This gives $P_p = 3.6 \times 10^8 \times S_l$. That is 3.6×10^8 Martian meteorite impacts onto the Earth capable of delivering life before or during the Late Heavy Bombardment, and thus before the first documented life on Earth around 3.8 billion years ago.

So, as long as S_l is successfully fulfilled (i.e. the concentration of life at the initial impact site was high enough that the C_l term is sufficiently large for $S_l = 1$), then there could have been 3.6×10^8 instances of life successfully arriving on Earth before 3.8 billion years ago. That is equivalent to one impact every two years, for 700 million years, or one impact every year during the Late Heavy Bombardment, as this is when most impacts would have occurred. Only one of these life-seeding impacts needed to have life that survived the conditions of the early Earth and thrive, for that life to become the diversity of life that is seen today.

This is of course pure conjecture, based on an assumption of a genesis-of-life event on early Mars. However, this does highlight the fact that panspermia needs to be considered in all discussions of life on other worlds, and the origin of life on Earth. The terms of these equations (equations 8.1, 8.2, and 8.3) need to be determined with high accuracy experimentally where possible, and theoretically where not. Like the Drake Equation, this cannot answer the question definitively (only a physical discovery can do that), but it can show us the possibilities for different planetary bodies, and different types of organisms, for different periods of time. These possibilities can help

point future researchers in the right direction of where to look for the best chance of finding any life that may have been transferred if the panspermia hypothesis is correct.

8.10 Conclusion

This chapter described the best case conditions for survival of a panspermia style impact event, and then presented an analysis of hydrocode modelling in relation to five species of extremophile. It was shown that tardigrades can survive impact scenarios onto the surface of small moons and asteroids within the Solar System and possibly beyond it, and that the other four species could all survive impacts on to all bodies in the Solar System, with the exception of the outer gas planets. It was also shown that some icy and rocky Super-Earth exoplanets are with the range of survival for the same four species. Analysis of travel time and protection from the interstellar environment showed that some bacteria could survive interstellar panspermia journeys up to 16,000 light years. Such life could still be protected from the interstellar environment for possibly up to 33,000 light years of travel, so if revival was still attainable after 500 million years, this distance would also be viable. However, natural intergalactic transfers appear to be unfeasible for life with current estimates and evidence for long-term (billions of years) exposure and survival.

Potential numerical errors within the hydrocode models were then discussed, and further speculation of the data was considered, showing perhaps even greater impact velocities are within the survival range of some species. Other factors, such as cratering in rocky impacts and the potential dangers inherent to life in such circumstances were discussed. Intriguing life-seeding scenarios were considered; the case of a cosmic Noah's ark, and the

possibility that life originally began on Mars, and arrived on the Earth via a panspermia style impact during the Late Heavy Bombardment ~4 billion years ago.

Finally, an equation to determine the number of impacts capable of successfully delivering life to another world was considered, and the case for Mars seeding the Earth was conjectured, showing that 3.6×10^8 potential transfers of life could have happened before the first evidence of life on Earth is seen 3.8 billion years ago.

CHAPTER 9
CONCLUSION

"Oh, please, let it all be a dream. A very bad, very twisted dream"

John Crichton, *Farscape*

9.1 Main Conclusions

The aim of the research presented here in this thesis was to investigate the panspermia hypothesis both experimentally, through the use of the Two-Stage Light Gas Gun, and theoretically, through the use of hydrocode models of hypervelocity impact simulations. Two species were fired in the two-stage light gas gun, one flora (phytoplankton species *Nannochloropsis oculata*), and one fauna (tardigrade species *Hypsibius dujardini*). These species were tested under a number of varying impact regimes for survival. After these experiments, hydrocode simulations were carried out to determine what impact scenarios different micro-organisms could potentially survive if the conditions were right. While these experiments and simulations cannot answer the question as to whether or not a panspermia style spreading of micro-organic life has occurred throughout the universe, they can be used to show that, it is at least possible, for some micro-organisms to survive the conditions implicit in such a panspermia style spread of life from one world to another. It is in light of these results that an equation for the number of potentially successful panspermia-style journeys between planets is presented for future use in the quest for life beyond the Earth.

After an introduction to the research, Chapter 2 presented an in-depth discussion about the nature of life, its definition, origins, evolution, and

distribution, on Earth, so that life in the wider universe could be considered. Life, as we know it, is considered to be any entity that has the ability to reproduce, as well as harnessing some form of energy in order to drive chemical reactions. However, as there are often exceptions to the rule, a cautious approach should be applied when considering any definition of what constitutes life. The history of the Earth was examined, before a discussion of the requirements for life as it is currently understood, and where it may have originated. Then, the possible habitats for life in the Solar System and beyond where discussed in relation to extremophile organisms capable of survival in extreme environments.

Chapter 3 presented a detailed discussion of the main panspermia hypothesis. Described as the migration of life throughout the universe, via meteorites, and other interplanetary and cosmic bodies, the three variations of panspermia were presented (radiopanspermia, directed panspermia, and lithopanspermia). The three main phases of the panspermia journey were presented alongside the implicit dangers of these phases, and lithopanspermia was concluded to be the most plausible for any such natural migration of life between planetary bodies. Evidence for the survival of some species of micro-organisms against the dangers implicit for the journey was presented, and it was concluded that these dangers are not necessarily sterilising. Finally the possible routes through the Solar System, and the timescales involved, were presented to complete the discussion of the panspermia process.

Chapter 4 began by looking at the equipment that was used to carry out the experimental hypervelocity shot programmes for this research. A detailed description of the light gas gun used in these programmes was given, before looking at the rationale behind the choice of the two species that were used in these experiments. These species and, the methods to culture them, were then described. The phytoplankton was chosen as it is a eukaryotic photosynthesizing autotroph and a primary producer of oxygen. To survive, it

only needs basic mineral nutrients and light for photosynthesis to occur. It is also capable of sustaining other life, as it is the base of a food chain, and could serve this same function on another world. The tardigrades were chosen as they are extremely hardy organisms, and unlike other species used in hypervelocity impact tests to date, these are complex multi-cellular micro-animals, and phytoplankton can serve as a food source for them. Then, the materials used for the projectiles and the targets in these experiments (and their holders) were looked at. The materials were chosen such that the phytoplankton shots would simulate the organism impacting into a liquid ocean, and the tardigrade shots would simulate an impact (capable of ejecting material from a planet) into a frozen water source containing tardigrades, such as an ice-shelf, or polar cap. The equations for the pressure conditions experienced during impacts were then described, before a brief overview and description of the hydrocodes used for creating models of hypervelocity impact scenarios.

Chapter 5 presented the details of the experiments to test the survival of the phytoplankton species *Nannochloropsis oculata*. Initially a small programme was conducted to test the viability of the species to such experimentation. A very small amount of phytoplankton was fired at 1.26 km s^{-1} into a water target, and the contents of the target holder was placed into a sealed bottle to see if any phytoplankton had survived and could be cultured. After 20 days the first noticeable growth was witnessed, showing that the larger programme was viable. The larger programme involved firing increased volumes of phytoplankton at a range of velocities (1.25 – 6.93 km s^{-1}). A total of eight live shots were fired, and two control shots to check for contamination were also carried out. In all the live shots, phytoplankton was shown to survive, albeit at much slower recovery times in the higher velocity shots. The Late-Stage Effective Energy calculations showed the peak shock pressures survived by the phytoplankton cells ranged from 3.00 – 38.0 GPa

(using the Trunin parameters), and 2.89 – 35.4 GPa (using the Melosh parameters). The AUTODYN results showed good agreement with these at lower velocities, but diverged towards higher velocities giving peak pressures in the range of 2.84 – 58.6 GPa. These results showed that phytoplankton can survive the type of impacts needed to deliver life to another world up to pressures of ~40 GPa. These results also showed the same common two-regime survival trend seen for micro-organisms during extreme shocks, as described by Burchell, M. et al. (2007). Additionally, no changes in morphology or growth were detected post-shock once normal growth had resumed, and the peak temperatures generated during impacts were on small enough timescales as to be non-sterilising to the organisms.

Chapter 6 presented the details of the experiments to test the survival of the tardigrade species *Hypsibius dujardini*. The shot programme involved firing nylon projectiles at a range of velocities (0.37 – 5.49 km s^{-1}), into a target of tardigrades frozen in ice. A total of 14 shots were fired, and in all shots tardigrades were shown to survive, albeit with a much higher lethality in the higher velocity shots. The AUTODYN simulation results for the range of pressures felt across the target yielded a lower limit for survival across the shots of 4.15 – 374 MPa. However, as this is a lower limit it is likely that the true value is somewhat higher than this. These results, combined with the results from Seki, K. (1998), showed that tardigrades can survive the type of impacts needed to deliver life to small bodies such as Enceladus, the Moon, Europa, asteroids or Kuiper belt objects, and extrasolar bodies of similar size and mass, up to pressures of ~600 MPa. These results also showed the same common two-regime survival trend seen for micro-organisms during extreme shocks as described by Burchell, M. et al. (2007). Additionally, no changes in morphology or behaviour were detected post-shock, and the peak temperatures generated during impacts were on small enough timescales as to be non-sterilising to the tardigrades. It was also shown that the survival rate

due to freezing decreases as the freezing temperature drops. However, the survival rate remained almost constant at a fixed temperature regardless of the length of time frozen.

Chapter 7 reported the set-up, and results, of multiple AUTODYN simulations for different panspermia-style impact events, on both oceanic and rocky body surfaces. The optimum point for survival on a spherical impactor was shown to be at the rear of the object, but below the depth of any fusion crust created due to atmospheric heating. The results for peak impact pressures against impact velocities were then presented ready for analysis in Chapter 8 with different micro-organisms.

The analysis and discussion presented in Chapter 8 would suggest that the natural transfer of life throughout the Solar System via impacts is possible for a variety of simple species of extremophiles. Some extrasolar planets (i.e. Super-Earths) beyond our Solar System are also within the survival tolerances of these species, for both oceanic and rocky body situations. It is also shown that oceanic impacts will allow higher survival rates for life-forms, than impacts onto rocky bodies of similar size and mass. However, atmospheric drag effects that would be encountered on bodies that have substantial atmospheres could potentially lower an impactor's velocity, and thus increase the probability of survival for any life-forms aboard the impactor. Even the humble tardigrade (a complex life-form) could survive impacts onto small moons and asteroids within our Solar System, or indeed perhaps beyond. The timescale for successful interplanetary transfers (travelling at velocities within the survival range of several species) is shown to be survivable up to a distance of at least 16,000 lights years. However, natural intergalactic transfers appear to be unfeasible for life with current estimates and evidence for long-term (billions of years) exposure and survival. Finally, an equation for the number of potentially successful panspermia-style journeys that can occur between planets was presented as a

tool for future research into the search for life beyond the Earth, and the verification of the panspermia hypothesis.

9.2 Future Work

The modelling work presented here could be further enhanced by using much higher resolution hydrocode models to simulate the higher velocities where numerical errors begin to appear. This higher resolution could abate the numerical erosion issues that are believed to be responsible for the computational errors seen. However, this is very time consuming, and considering the number of simulations required, a large supercomputing cluster would be needed for a full programme of results to be obtained. Further to this, simulations using varying impact vectors, ranging from normal to very oblique angles for each velocity, would allow for a number of differing (and arguably more realistic) impact scenarios to be considered. Additionally, models that incorporate basic (and with time, more complex) atmospheres, would also allow a more realistic approximation of real-life impact scenarios.

The experimental programmes could also be further complemented, with a thorough examination of the effects of different freezing temperatures for both types of organisms considered here. As well as this, tests for the effects due to prolonged exposure to an analogue space vacuum and radiation environment would also determine the true survival abilities of these organisms when considering the full panspermia journey from impact ejection, to transfer, to impact arrival on another world.

9.3 Implications for Panspermia

The results obtained during the course of this research and presented in this thesis have implications for both the origin of life on Earth and the panspermia hypothesis. These results when combined with previous research demonstrate that a number of species may be capable of surviving the entire process of a panspermia-style journey between different planets, or indeed a 'Noah's ark' type event on the same planet.

This research demonstrates that several species are capable of surviving the impact pressures generated in an impact into an ocean on the Earth's surface, and thus could survive the impact needed to seed life onto the Earth. This allows for the possibility that life did not originate on the Earth, but had a genesis elsewhere, and was transported here at some point before the end of the Late Heavy Bombardment around 3.8 billion years ago. Using equation 8.1 with extremely conservative estimates, it was shown that there could have been at least 3.6×10^8 life bearing impacts onto the early Earth before 3.8 billion years ago from Mars alone, each one potentially able to seed life on the Earth, if Mars was capable of a genesis-of-life event in the distant past, rather than the Earth. The potential for panspermia as the origin for life on Earth is further enhanced by the results that show bacteria capable of surviving 250 million years of suspended animation, could travel up to 16,000 light years across the galaxy at a velocity conducive to survival upon impact at the Earth, within clusters of rocks capable of protecting against the interstellar medium for up to 500 million years. This does not mean that life did originate via panspermia, only that the possibility that it could have done, must be considered in all origin of life on Earth discussions and research, until conclusively proven otherwise.

The very fact that Earth is bombarded with tens of thousands of meteorites every year, combined with these results, implies that if life has

formed elsewhere in the Solar System, the Earth may well have been seeded with life at some (or many) points in the past. It follows then that the search for extra-terrestrial life could be conducted right here on Earth. If any life-forms showing no genetic connection to life as we know it were to be discovered, it would not necessarily point to a second genesis event on the Earth, but could be indicative of an extra-terrestrial life-form delivered via panspermia in the past. This also suggests that meteorites upon collection on Earth should be handled with care such that no unnecessary terrestrial contamination occurs, before the meteorite can be analysed for any potential extra-terrestrial life, or fossils it may contain.

9.4 Final Summary

In conclusion, this thesis has presented research that has shown that the phytoplankton species *Nannochloropsis oculata* can survive impact events where pressures are of the order ~40 GPa, corresponding to oceanic impacts into predominantly water/ice planets at ~19.5 km s^{-1}, and predominantly rocky body planets at ~15.5 km s^{-1}. The tardigrade species *Hypsibius dujardini* can survive impact induced pressures up to ~600 MPa, corresponding to oceanic impacts into water/ice planets at ~3.0 km s^{-1}, and predominantly rocky body planets at ~2.0 km s^{-1}. These results show that if material ejected from the Earth contained either of these species then the resulting impacts into other bodies could seed life, in multiple places in the Solar System, and even beyond. However, it must be stated here, that this research does not suggest that panspermia *has* ever happened, only that it is possible, and *could* have happened.

AUTHOR'S PUBLICATION LIST

Conference Papers

2013, Survival of Nannochloropsis Phytoplankton in Hypervelocity Impact Events up to Velocities of 4 km/s. *44th Lunar and Planetary Science Conference.* LPI Contribution No. **1719**, p.1497.

2013, Spacecraft Shielding: An Experimental Comparison Between Open Cell Aluminium Foam Core Sandwich Panel Structures and Whipple Shielding. *European Planetary Science Congress 2013, EPSC Abstracts*. **8**, EPSC2013-397.

2013, Survival of Nannochloropsis Phytoplankton in Hypervelocity Impact Events up to Velocities of 6.07 km/s. *European Planetary Science Congress 2013, EPSC Abstracts*. **8**, EPSC2013-396.

2014, Survival of the Tardigrade *Hypsibius Dujardini* During Hypervelocity Impact Events up to 3.23 km s^{-1}. *45th Lunar and Planetary Science Conference.* LPI Contribution No. **1777**, p.1789.

2014, Survival of the Tardigrade *Hypsibius Dujardini* during Hypervelocity Impact Events up to 5.49 km s^{-1}. *European Planetary Science Congress 2014, EPSC Abstracts*. **9**, EPSC2014-67.

2014, Panspermia Survival Scenarios for Organisms that Survive Typical Hypervelocity Solar System Impact Events. *European Planetary Science Congress 2014, EPSC Abstracts*. **9**, EPSC2014-68.

2015, Panspermia Survival Scenarios for Organisms that Survive Typical Hypervelocity Solar System Impact Events. *46th Lunar and Planetary Science Conference.* LPI Contribution No. **1832**, p.2725.

Interviews

April 2013 Interview

EoS Transactions American geophysical Union. Volume **94,** Issue 15.

September 2013 Podcast

https://www.thenakedscientists.com/articles/interviews/could-life-have-come-mars

https://www.thenakedscientists.com/podcasts/naked-astronomy/exploring-solar-system

September 2013 Press Release

European Planetary Science Congress 2013, University College London, 08 – 13 September 2013, London, United Kingdom.

June 2014 Interview

Discover Magazine. June 2014 Issue.

October 2014 Interview

Science Uncovered Magazine. Issue 11.

References

Abramov, O. Mojzsis, S. J (2016). The thermal effects of bombardments on Noachian Mars. *Earth and Planetary Science Letters,* **442,** 108-120.

Alroy, J. (2008). Dynamics of origination and extinction in the marine fossil record. *Proceedings of the National Academy of Sciences of the United States of America.* **105**, 11536–11542.

Alvarez, L. Alvarez, W. Asaro, F. Michel, H. (1980). Extraterrestrial cause for the Cretaceous-Tertiary extinction. *Science,* **208,** 1095-1108

Anderson, C. (1987). An overview of the theory of hydrocodes. *International Journal of Impact engineering,* **5,** 33-59.

Anglada-Escudé, G. Amado, P. J. Barnes, J. Berdinas, Z. M. et. al. (2016). A terrestrial planet candidate in a temperate orbit around Proxima Centauri. *Nature.* **536,** 437–440.

Aristotle. (c.350 BC). De Anima: 'On the soul'. (see Shiffman, M. 2011. for modern translation).

Arrhenius, S. (1903). Die Verbreitung des Lebens im Weltenraum. *Die Umschau* 7: 481-485.

Arrhenius, S. (1908). Worlds in the making. *Harper, London.*

Barnes, R. D. (1982). *Invertebrate Zoology*. Philadelphia, PA: Holt-Saunders International. pp. 877–880

Barsukov, V. L. Volkov, V. P. Khodakovsky, I. L. (1980). The mineral composition of Venus surface rocks – a preliminary prediction. *11th LPSC TX March17-21, 1980, proceedings*. **1**, pp. 765-773.

Behrenfeld, M. J. Randerson, J. T. McClain, C. R. Feldman, G. C. Los, S. Tucker, C. Falkowski, P. G. Field, C. B. Frouin, R. Esaias, W. Kolber, D. and Pollack, N. (2001). Biospheric primary production during an ENSO transition, *Science*, **291**, 2594–2597.

Beltran-Pardo, E. Jonsson, K. I. Harms-Ringdahl, M. Haghdoost, S. Wojcik, A. (2015). Tolerance to Gamma Radiation in the Tardigrade *Hypsibius dujardini* from Embryo to Adult Correlate Inversely with Cellular Proliferation. *PLoS ONE* **10.**

Benner. S. A. (2014). Paradoxes in the Origin of Life. *Origins of Life and Evolution of Biospheres.* **44,** 339-343.

Benner, S. A. Hyo-Joong, K. (2015) The case for a Martian origin for Earth life ", *Proc. SPIE 9606, Instruments, Methods, and Missions for Astrobiology XVII*, 96060C.

Beraldi-Campesi, H. (2013). Early life on land and the first terrestrial ecosystems. *Ecological Processes.* **2,** 1–17.

Bertolani, R. Guidetti, R. Jonsson, K. Altiero, T. Boschini, D. Rebecchi, L. (2004). Experiences with dormancy in tardigrades. *J. Limnol.,* **63**, 16-25.

Beuchat, L. R. (1981). Efficacy of agar media for enumerating two Saccharomyces species in sucrose syrups. *Mycopathologia.* **76**, 13–17.

Blackburn, T. J. Olsen, P. E. Bowring, S. A. McLean, N. M. Kent, D. V. Puffer, J. McHone, G. Rasbury, T. Et-Touhami, M. (2013). Zircon U-

Pb geochronology links the end-triassic extinction with the central atlantic magmatic province. *Science.* **340**, 941–945.

Blundell, S. Blundell, K. (2006). Concepts in thermal physics. *Oxford University Press.*

Bouvier, A. Wadhwa, M. (2010). The age of the solar system redefined by the oldest Pb-Pb age of a meteoritic inclusion. *Nature Geoscience.* **3**, 637–641.

Brandt, A. MeeBen, J. Janicke, R. U. Raguse, M. Ott, S. (2017). Simulated Space Radiation: Impact of Four Different Types of High-Dose Ionizing Radiation on the Lichen Xanthoria elegans. *Astrobiology,* **17,** 136-144.

Bray, V. J. (2009). Impact crater formation on the icy Galilean satallites. *PhD Thesis,* Imperial College London.

Burchell, M. J. Cole, M. J. McDonnell, J. A. M. Zarnecki, J. C. (1999). Hypervelocity impact studies using the 2 MV Van de Graaff accelerator and two-stage light gas gun of the University of Kent at Canterbury. *Meas. Sci. Technol*. **10**, 41–50.

Burchell, M. J. Mann, J. Bunch, A. W. Brandão, P. F. B. (2001). Survivability of bacteria in hypervelocity impact. *Icarus* **154**, 545–547.

Burchell, M. J. Galloway, J. A. Bunch, A. W. Brandão, P. F. B. (2003). Survivability of bacteria ejected from icy surfaces after hypervelocity impact. *Origin Life Evol. Biosphere* **33**, 53–74.

Burchell, M. J. (2004). Panspermia today. *Int. J. Astrobiol*. **3**, 73–80.

Burchell, M. J. Mann, J. R. Bunch, A. W. (2004). Survival of bacteria and spores under extreme shock pressures. *Mon. Not. R. Astron. Soc*. **352 (4)**, 1273–1278.

Burchell, M. J. (2006). W(h)ither the drake equation? *International Journal of Astrobiology*, **5**, 243-250.

Burchell, M. J. (2007). Survival of microbial life under shock compression: Implications for panspermia. In: *Proceedings of SPIE Symposium 6694*, identifier 669416. doi: http://dx.doi.org/10.1117/12.732369.

Burchell, M. J. Parnell, J. Bowden, S. A. Crawford, I. A. (2010). Hypervelocity impact experiments in the laboratory relating to lunar astrobiology. *Earth Moon Planet*. **107 (1)**, 55–66.

Burt, D. M. Knauth, L. P. Wohletz, K. H. (2008). The late heavy bombardment: possible influence on Mars. *Workshop on the Early Solar System Impact Bombardment, held November 19-20, 2008 in Houston, Texas.* LPI Contribution No. **1439**, 23-24

Buseck, P. R. Dunin-Borkowski, R. E. Devouard, B. Frankel, R. B. McCarthy, M. R. Midgley, P. A. Posfai, M. Weyland, M. (2001). Magnetite morphology and life on Mars. *Proceedings of the National Academy of Sciences (USA),* **98,** 13490-13495.

Caleb, S. Nathaniel, V. James, C. H. Masashi, A. Nathanael, A. Arsev, A. Ana, B. Barge, L. M. et al. (2015). A strategy for Origins of Life research. *Astrobiology.* **15,** 1031-1042.

Campbell, I. Czamanske, G. Fedorenko, V. Hill, R. Stepanov, V. (1992). Synchronism of the Siberian Traps and the Permian-Triassic Boundary. *Science.* **258**, 1760–1763.

Cano, R. J. Borucki, M. K. (1995). Revival and identification of bacterial spores in 25- to 40-million-year-old Dominican amber. *Science,* **268,** 1060-1064.

Canup, R. Asphaug, E. (2001). Origin of the Moon in a giant impact near the end of the Earth's formation. *Nature*. **412**, 708–712.

Chyba. C. F. Thomas, P. J. Brookshaw, L. Sagan, C. (1990). Cometary delivery of organic molecules to the early Earth. *Science.* **249,** 366-373.

Chyba, C. F. (2000). Energy for microbial life on Europa. *Nature.* **403,** 381-382.

Chyba, C. F. Phillips, C. B. (2002). Europa as an abode of life. *Origins of Life and Evolution of the Biosphere.* **32,** 47-68.

Clark, B. C. Baker, A. L. Cheng, A. F. Clemett, S. J. McKay, D. McSween, H. Y. Pieters, C. M. Thomas, P. Zolensky, M. (1999). Survival of Life on Asteroids, Comets and Other Small Bodies. *Origin of Life and Evolution of the Biosphere,* **29**, 521-545.

Clark, W. (1908). Mythology of the Blackfoot Indians. *Bison Books,* **ISBN-10:** 0803260237.

Cockell, C. S. Barlow, N. G. (2002). Impact evacuation and the search for subsurface life on Mars. *Icarus,* **155,** 340-349.

Cockell, C. S. Stokes, M. D. (2004). Widespread colonization by polar hypoliths. *Nature.* **431,** 414.

Courtillot, V. (1990). A volcanic eruption. *Scientific American.* **263,** 85-92.

Crenson, Matt (2006-08-06). *"After 10 years, few believe life on Mars"*. Associated Press on USA Today.

Crick, F. H. C. Orgel, L. E. (1973). Directed panspermia. *Icarus,* **19,** 341-346.

Crida, A. (2009). Solar System formation. *Reviews in Modern Astronomy.* **21**, 3008.

Cronin, J. R. Cooper, G. W. Pizzarello, S. (1995). Characteristics and formation of amino acids and hydroxy acids of the Murchison meteorite. *Advances in Space Research.* **15,** 91-97.

Crowe, M. J. (1986). The extraterrestrial life debate 1750-1900. *Cambridge University Press.*

Crozier, W.D. Hume, W. (1957). High-velocity, light gas gun. *Journal of Applied Physics*, **28**, 892-894.

Dauber, I. J. McEwen, A. S. Brrne, S. Kennedy, M. R. Ivanov, B. (2013). The current Martian cratering rate. *Icarus,* **225,** 506-516.

Davies, R. E. (1988). Panspermia: Unlikely, unsupported, but just possible. *Acta Astronautica,* **17,** 129-135.

De la Torre, R. Sancho, L. G. Horneck, G. de los Ríos, A. Wierzchos, J. Olsson, K. Cockell, C. Rettberg, P. Berger, T. de Vera, J-P. Ott, S. Frías, J. M. Melendi, P. G. Lucas, M. M. Reina, M. Pintado, A. and Demets, R. (2010). Survival of lichens and bacteria exposed to outer space conditions – Results of the Lithopanspermia experiments. Icarus **208**, 735–748.

Desch, S. (2007). Mass distribution and planet formation in the Solar Nebula. *The Astrophysical Journal.* **671**, 878–893.

De Vera, J. (2012). Lichens as survivors in space and on Mars. *Fungal Ecology*. **5**, 472-479.

Drake, F. (1961). Project Ozma. *Phys. Today,* **14,** 40-46.

Drake, F. (1962). Intelligent life in space. *Macmillan, New York.*

Eugster, O. Herzog, G. F. Marti, K. Caffee, M. W. (2006). Irradiation Records, Cosmic-Ray Exposure Ages, and Transfer Times of Meteorites. *Meteroritics and the Early Solar System II, LPI*, 829-851

Evans, J. E. Maunder, E. W. (1903). Experiments as to the actuality of the "Canals" observed on Mars. *Monthly Notices of the Royal Astronomical Society,* **63**, 488–499.

Fajardo-Cavazos, P. Langenhorst, F. Melosh, H. J. Nicholson, W. L. (2009). Bacterial spores in granite survive hypervelocity launch by spallation: Implications for Lithopanspermia. *Astrobiology* **9**, 647–657.

Fassett, C. I. Head, J. W. (2011). Sequence and timing of conditions on early Mars. *Icarus*, **211,** 1204–1214.

Field, C. B. Behrenfeld, M. J. Randerson, J. T. and Falkowski, P. G., (1998). Primary production of the biosphere: Integrating terrestrial and oceanic components, *Science*, **281**, 237–240.

Franceschi, T. (1948). Anabiosi nei tardigradi. Bollettino dei Musei e degli *Istituti Biologici dell Università di Genova*, **22**, 47–49.

Frank, E. A. and Mojzsis, S. J. (2010). Cumulative ocean volume estimates of the Solar System. *American Geophysical Union, Fall Meeting 2010*, #P33B-1572.

French, B. M. (1998). Traces of catastrophe: a handbook of shock-metamorphic effects in terrestrial meteorite impact structures. *LPI Contribution No. 954,* Lunar and Planetary Science Institute, Houston.

Frosler, J. Panitz, C. Wingender, J. Flemming, H. C. Rettberg, P. (2017). Survival of Deinococcus geothermalis in Biofilms under Desiccation and Simulated Space and Martian Conditions. *Astrobiology,* **17,** 431-447.

Garcia-Ruiz, J. (1999). Morphological behavior of inorganic precipitation systems. *Proc. SPIE 3755, Instruments, Methods, and Missions for Astrobiology II*, doi: 10.1117/12.375088.

Ghosal, S. Rogers, M. Wray, A. (2001). The Effects of Turbulence on Phytoplankto. *Aerospace Technology Enterprise*. NTRS.

Ghosal S. (2002). *NASA/TM-2001-210935,* 88.

Gibson, E. K. McKay, D. S. Thomas-Keprta, K. L. Wentworth, S. J. Westall, F. Steele, A. Romanek, C. S. Bell, M. S. Toporski, J. (2001). Life on Mars: Evaluation of the evidence within Martian meteorites ALH84001, Nakhla, and Shergotty. *Precambrian Research,* **106,** 15-34.

Gillet, P. H. Barrat, J. A. Heulin, T. Achouak, W. Lesourd, M. Guyot, F. Benzerarak, K. (2000). Bacteria in the Tatahouine meteorite: nanometric-scale life in rocks. *Earth and Planetary Science Letters,* **175,** 161-167.

Gilli, G. Lebonnis, S. Gonzalez-Galindo, F. Lopes-Valverde, M. A. Stolzenbach, A. Lefevre, F. Chaufray, J. Y. Lott, F. (2017). Thermal structure of the upper atmosphere of Venus simulated by ground-to-thermosphere GCM. *Icarus.* **281,** 55-72.

Gladman, B. (1997). Destination: Earth. Martian meteorite delivery. *Icarus,* **130,** 288-246.

Gomes, R. Levison, H. F. Tsiganis, K. Morbidelli, A. (2005). Origin of the cataclysmic Late Heavy Bombardment period of the terrestrial planets. *Nature*. **435**, 466–469.

Groombridge, B. Jenkins, M. D. (2000). Global biodiversity: Earth's living resources in the 21st century. *World Conservation Monitoring Centre, World Conservation Press, Cambridge.*

Guidetti, R. Ingemar Jonsson, K. (2002). Long-term anhydrobiotic survival in semi-terrestrial micrometazoans. *Journal of Zoology*, **257,** 181-187.

Guillard, R. and Ryther, J. (1962). Studies on marine phytoplankton diatoms. *Can. J. Microbiol.* **8**, 229-239

Guillem, A. Mikko, T. (2015). Comment on "Stellar activity masquerading as planets in the habitable zone of the M dwarf Gliese 581". *Science*, **347**, pp. 1080

Hadden, S. Lithwick, Y. (2014). Densities and eccentricities of 139 Kepler plants transit time variations. *The Astrophysical Journal*, **787,** 80

Hanley, J. Thompson, G. L. Roe, H. G. Grundy, W. Tegler, S.C. Lindberg, G. E. Trilling, D. E. (2016). Methane, ethane, and nitrogen liquid stability on Titan. *American Astronomical Society, DPS meeting* #**48**, id502.03.

Hansen, K. (2005). Orbital shuffle for early solar system. *Geotimes, 07/06/2005.*

Hargitai, H. I. Gulick, V. C. Gline, N. H. (2017). Discontinuous drainage systems formed by highland precipitation and ground-water outflow in the Navua Valles and southwest Hadriacus Mons regions, Mars. *Icarus.* **294,** 172-200.

Hart. M. H. (1978). The evolution of the atmosphere of the Earth. *Icarus.* **33,** 23-39.

Hayhurst, C. J. Clegg, R.A. (1997). Cylindrically symmetric SPH simulations of hypervelocity impacts on thin plates. *Int. J. Impact Eng*. **20 (1–5)**, 337–348.

Hazell, P. J. Beveridge, C. Goves, K. Appleby-Thomas, G. J. (2010). The shock compression of microorganism-loaded broths and emulsions: Experiments and simulations. *Int. J. Impact Eng*. **37**, 433–440.

Heremans, K.A.H. (1982). High pressure effects upon proteins and other biomolecules. *Annu. Rev. Biophys. Bioeng*. **11**, 1–21.

Hocking, A. D. Pitt, J. I. (1981). Trichosporonoides nigrescens sp. nov., a new xerophilic yeast-like fungus. *Antonie Van Leeuwenhoek.* **47,** 411–421.

Holm, N. G. Anderson, E. M. (1995). Abiotic synthesis of organic compounds under the conditions of submarine hydrothermal systems: a perspective. *Planetary and Space Science.* **43,** 153-159.

Honma, M. Nagayama, T. Ando, K. Bushimata, T. et al. (2012). Fundemental parameters of the Milky Way galaxy based on VLBI astrometry. *Publications of the Astronomical Society of Japan,* **64**, 136 pp. 13.

Honma, M. Nagayama, T. Sakai, N. (2015). Determining dynamical parameters of the Milky Way Galaxy based on high-accuracy radio astrometry. *Publications of the Astronomical Society of Japan,* **67,** 70.

Horikoshi, K. (1999): Alkaliphiles: some applications of their products for biotechnology. *Microbiology and Molecular Biology Reviews*. **63,** 735-50.

Horneck, G. Bucker, H. Reitz, G. (1994). Long-term survival of bacterial spores in space. *Advances in Space Research* **14**: 41-45.

Horneck, G. (1995). Exobiology: the study of the origin, evolution, and distribution of life within the context of cosmic evolution: a review. *Planetary and Space Science.* **43,** 189-217.

Horneck, G. Rettberg, P. Reitz, G. Wehner, J. Eschweiler, U. Strauch, K. Panitz, C. Starke, V. Baumstark-Khan, C. (2001a). Protection of bacterial spores in space, a contribution to the discussion on Panspermia. *Origins of Life and Evolution of Biospheres* **31**: 527-547.

Horneck, G. Stoffler, D. Eschweiler, U. Hornemann, U. (2001b). Bacterial spores survive simulated meteorite impact. *Icarus* **149**, 285–290.

Horneck, G. Stoffler, D. Ott, S. Hornemann, U, Cockell, C. S. Moeller, R. Meyer, C. De Vera, J-P. Fritz, J. Schade, S. Artemieva, N. A. (2008). Microbial rock inhabitants survive hypervelocity impacts on Mars-like host planets: First phase of Lithopanspermia experimentally tested. *Astrobiology* **8**, 17–44.

Hoyle, F. and Wickramasinghe, C. (1980). The origin of life. *University College Cardiff Press.*

Huggett, R. J. (1995). Geoecology: an evolutionary approach. *Routledge, Chapman & Hall.*

Jackson, F. Moore, P. (1962). Life in the universe. *Routledge and Kegan Paul Ltd.*

Jacobsen, T. (1949). Mesopotamia: the good life, before philosophy; the intellectual adventure of ancient man. *Penguin Books, Baltimore, Maryland*.

Jackosky, B. (1998). The search for life on other planets. *Cambridge University Press.*

JeongAhn, Y. Malhotra, R. (2015). The current impact flux on Mars and its seasonal variation. *Icarus,* **262,** 140-153.

Jerling, A. Burchell, M. J. Tepfer, D. (2008). Survival of seeds in hypervelocity impacts. *Int. J. Astrobiol*. **7**, 217–222.

Johnson, W, and Anderson, C. (1987). History and application of hydrocodes in hypervelocity impact. *International Journal of Impact Engineering*, **5,** 423-439.

Jonsson, K (2007). Tardigrades as a potential model in space research. *Astrobiology* **7**, 757-766.

Karachentsev, I. D. (2004). arXiv:astro-ph/0410065v1 4 Oct 2004

Kawaguchi, Y. Yokobori, S. Hashimoto, H. Yano, H. Tabata, M. Kawai, H. amagishi, A. (2016). Investigation of the Interplanetary Transfer of Microbes in the Tanpopo Mission at the Exposed Facility of the International Space Station. *Astrobiology,* **16,** 363-376.

Kinchin, I. M. (1994). The Biology of Tardigrades, *Ashgate Publishing.*

Kissel, J. Krueger, F. R. (1995). Mass-spectrometric in-situ studies of cometary organics for P/Halley and options for the future. *Advances in Space Research.* **15,** 59-63.

Koonin, E. V., Senkevich, T. G., & Dolja, V. V. (2006). The ancient Virus World and evolution of cells. *Biology Direct*, **1,** 29.

Koonin, E. V. Starokadomskyy, P. (2016). Are viruses alive? The replicator paradigm sheds decisive light on an old but misguided question. *Studies*

in History and Philosophy of Biological and Biomedical Science. **59**, 125-134.

Leighs, J.A. Hazell, P.J. Appleby-Thomas, G.J. (2012). The effect of shock loading on the survival of plant seeds. *Icarus* **220**, 23–28.

Lewis, G. F. Ibata, R. A. Irwin, M. J. Martin, N. F. Bellazzini, M. Conn, B. (2004). The Canis Major Dwarf Galaxy. *Publications of the Astronomical Society of Australia,* **21,** 371-374.

Lin, D. N. C. (2008). The Genesis of Planets. *Scientific American.* **298**, 50–59.

Lo, M. W. Ross, S. D. (1997). Surfing the Solar System: Invariant Manifolds and the Dynamics of the Solar System. *Technical Report. IOM. JPL*. pp. 2–4. 312/97.

Madigan, M. T. Martino, J. M. (2006). Brock biology of microorganisms (11th ed.). *Pearson.*

Maloof, A. C. Porter, S. M. Moore, J. L. Dudas, F. O. Bowring, S. A. Higgins, J. A. Fike, D. A. Eddy, M. P. (2010). The earliest Cambrian record of animals and ocean geochemical change. *Geological Society of America Bulletin.* **122**, 1731–1774.

Margulis, L. Sagan, D. (1986). Origins of sex. Three billion years of genetic recombination. *New Haven: Yale University Press*.

Marietta, D. (1998). Introduction to ancient philosophy. *M. E. Sharpe.*

Martins, Z. Price, M. C. Goldman, N. Sephton, M. A. Burchell, M. J. (2013). Shock-synthesis of amino acids from impacting cometary and icy planet surface analogues. *Nature Geoscience.* **6,** 1045-1049.

Mastrapa, R. M. E. Glazberg, H. Head, J. N. Melosh, H. J. Nicholson, W. L. (2001). Survival of Bacteria Exposed to Extreme Acceleration: Implications for Panspermia. *Earth and Planetary Science Letters* **189**, 1-8.

Matuska, D. A. (1984). HULL Users' Manual. *Air Force Armament Laboratory Document*, AFATL-TR-84-59.

May, R.M., M. Maria & J. Guimard. (1964). Actions différentielles des rayons x et ultraviolets sur le tardigrade Macrobiotus areolatus, à l´état actif et desséché. *Bull. Biol. France Belgique*, **98**: 349-367.

McConnachie, A. W. Irwin, M. J. Ferguson, A. M. N. Ibata, R. A. Lewis, G. F. Tanvir, N. (2005). Distances and metallicites for 17 Local Group galaxies. *Monthly Notices of the Royal Astronomical Society*, **356,** 979-997.

McElwain, J. C. Punyasena, S. W. (2007). Mass extinction events and the plant fossil record. *Trends in Ecology & Evolution.* **22,** 548–557.

McKay, D.S. Gibson, E. K. Thomas-Keprta, K. L. Vali, H. Romanek, C. S. et al. (1996). Search for past life on Mars: possible relic biogenic activity in Martian meteorite ALH84001. *Science*, **273,** 924-930.

McQueen, R, G. Marsh, S. P. Taylor, J. W. Fritz, J. N. (1970). The equation of state of solids from shock wave studies. High Velocity Impact, Ed. R. Kinslow, *Academic Press*.

Melosh, H. J. (1988). The rocky road to panspermia. *Nature* **332**, 687–688.

Melosh, H. J. Impact Cratering: A Geological Process. Oxford Univ. Press 1989. ISBN: 9780195042849.

Melosh, H. J. Tonks, W. B. (1993). Swapping rocks: ejection and exchange of surface material among the terrestrial planets. *Meteoritics*, **28,** 398.

Melott, A. L. Lieberman, B. S. Laird, C. M. Martin, L. D. (2004). Did a gamma-ray burst initiate the late Ordovician mass extinction. *International Journal of Astrobiology*. **3,** 55-61.

Mendel, R. R. Bittner, F. (2006). Cell biology of molybdenum. *Biochimica et Biophysica Acta (BBA) - Molecular Cell Research*, **1763,** 621-635.

Meyer, C. Fritz, J. Misgaiski, M. Stoffler, D. Artemieva, N. A. Hornemann, U. Moeller, R. De Vera, J-P. Cockell, C. S. Horneck, G. Ott, S. Rabbow, E. (2011). Shock experiments in support of the Lithopanspermia theory: The influence of host rock composition, temperature, and shock pressure on the survival rate of endolithic and epilithic microorganisms. *Meteorit. Planet. Sci.* **46**, 701–718.

Meyer, M. Vasavada, A. (2015). Mars Scince Laboratory's rover, Curiosity: ongoing investigations into the habitability of Mars. *American Astronoical Society, DPS meeting* #**47**, id401.01

Mileikowsky, C. Cucinotta, F. A. Wilson, J. W. Gladman, B. Horneck, G. Lindegren, L. Melosh, J. Rickman, H. Valtonen, M. Zheng, J. Q. (2000). Risks threatening viable transfer of microbes between bodies in our Solar System. *Planet. Space Sci*. **48**, 1107–1115.

Miller, S. L. (1953). A production of amino acids under possible primitive Earth conditions. *Science.* **117,** 528-529.

Milner, D.J. Burchell, M.J. Creighton, A. Parnell, J. (2006). Oceanic hypervelocity impact events: A viable mechanism for successful panspermia? *Int. J. Astrobiol*. **5**, 261–267.

Mittlefehldt, D. W. (1994). ALH84001, a cumulate orthopyroxenite member of the Martian meteorite clan. *Meteoritics*, **29,** 214-221.

Mizutani H., Takagi Y., Kawakami S. (1990). New scaling laws on impact fragmentation. *Icarus* **87**, 307 – 326.

Moeller, R. Stackebrandt, E. Reitz, G. Berger, T. Rettberg, P. Doherty, A. J. Horneck, G. Nicholson, W. L. (2007). Role of DNA repair by non-homologous end joining (NHEJ) in Bacillus subtilis spore resistance to extreme dryness, mono- and polychromatic UV and ionizing radiation. *Journal of Bacteriology* **189**: 3306-3311.

Moeller, R. Setlow, P. Horneck, G. Berger, T. Reitz, G. Rettberg, P. Doherty, A. J. Oka-yasu, R. Nicholson, W. L. (2008a). Roles of the major, small, acid-soluble spore proteins and spore-specific and universal DNA repair mechanisms in resistance of Bacillus subtilis spores to ionizing radiation from X rays and highenergy charged-particle bombardment. *Journal of Bacteriology* **190**: 1134-1140.

Moeller, R. Horneck, G. Rabbow, E. Reitz, G. Meyer, C. Hornemann, U. Stoffler, D. (2008b). Role of DNA protection and repair in resistance of Bacillus subtilis spores to ultrahigh shock pressures simulating hypervelocity impacts. *Applied and Environmental Microbiology* **74**: 6682-6689.

Moeller, M. Douki, T. Rettberg, P. Reitz, R. Cadet, J. Nicholson, W. L. Horneck, G. (2010). Genomic bipyrimidine nucleotide frequency and microbial reactions to germicidal UV radiation. *Archives of Microbiology* **192**: 521-529.

Montmerle, T. Augereau, J-C. Chaussidon, M. (2006). Solar System formation and early evolution: the first 100 million years. *Earth, Moon, and Planets, Spinger*. **98,** 39–95.

Moritoh, S. Kawai, N. Nakamura, K.G. Kondo, .K. (2001). Optimization of a compact two-stage light-gas gun aiming at a velocity of 9 km/s. *Review of Scientific Instruments*, **72**, 4270-4272.

Morozova, D. Mohlmann, D. Wagner, D. (2007). Survival of methanogenic archea from Siberian permafrost under simulated Martian thermal conditions. *Origins of Life and Evolution of Biospheres* **37**: 189-200.

Neufeld, J. Clarke, A. Morris, G. J. Fonseca, F. Murray, B. J. Acton, E. Price, H. C. (2013). A low temperature limit for life on Earth. *PLoS ONE.* **8**, e66207

Nickell, J. McGaha, J. (2012). The Roswellian Syndrome: how some UFO myths develop. *Skeptical Inquirer. Committee for Skeptical Inquiry,* **36.**

Nimmo, F. Pappalardo, R. T. (2016). Ocean worlds in the outer Solar System. *Journal of Geophysical Research: Planets.* **121,** 1378–1399.

Nutman, A. P. Mojzsis, S. J. Friend, C. R. L. (1997). Recognition of >3850 Ma water-lain sediments in west Greenland and their significance for the early Archaean Earth. *Geochimica et Cosmochimica Acta.* **61,** 2475-2484.

Ohtomo, Y. Kakegawa, T. Ishida, A. et al. (2014). Evidence for biogenic graphite in early Archaean Isua metasedimentary rocks. Nature Geoscience. **7**, 25–28.

Ollivier, B. Caumette, P. Garcia, J. L. Mah, R. (1994). Anaerobic bacteria from hypersaline environments. *Microbiological Reviews*. **58**, 27–38.

Oro, J. (1961). Comets and the formation of biochemical compounds on the primitive Earth. *Nature.* **190,** 389-390.

Parnell, J. Bowden, S. Lindgren, P. Burchell, M. Milner, D. Price, M. Baldwin, E. Crawford, I. (2010). The Preservation of Fossil Biomarkers during Meteorite Impact Event: Experimental Evidence from Biomarker-rich Projectiles and Target Rocks. *Meteoritics and Planeary Science.* **45,** 1340-1358.

Parry, R. (2010). Democritus. *Stanford Encyclopedia of Philosophy.*

Pasini, D. L. S. Price, M. C. Burchell, M. J. Cole, M. J. (2013a). Survival of Nannochloropsis Phytoplankton in Hypervelocity Impact Events up to Velocities of 6.07 km/s. *European Planetary Science Congress 2013, EPSC Abstracts*. **8**, EPSC2013-396.

Pasini, D. L. S. Price, M. C. Burchell, M. J. Cole, M. J. (2013b). Survival of Nannochloropsis Phytoplankton in Hypervelocity Impact Events up to Velocities of 4 km/s. *44th Lunar and Planetary Science Conference.* LPI Contribution No. **1719**, p.1497.

Pasini, D. (2014). Panspermia Survival Scenarios for Organisms that Survive Typical Hypervelocity Solar System Impact Events. *European Planetary Science Congress 2014, EPSC Abstracts*. **9**, EPSC2014-68.

Pasini, J. L. S. Price, M. C. (2015). Panspermia Survival Scenarios for Organisms that Survive Typical Hypervelocity Solar System Impact Events. *46th Lunar and Planetary Science Conference.* LPI Contribution No. **1832**, p.2725.

Petigura, E. A. Howard, A. W. Marcy, G. W. (2013). Prevalence of Earth-size planets orbiting Sun-like stars. *Proceedings of the National*

Academy of Sciences of the United States of America. **110,** 19273–19278.

Pierazzo, E. and Collins, G. (2004). A brief introduction to hydrocode modelling of impact cratering. In Dypvik, H. Burchell, M. J. Claeys, P. editors, *Cratering in marine environments.* Springer. ISBN 978-3-662-06423-8.

Price, M.C. Kearsley, A.T. Burchell, M.J. (2012). Validation of the Preston–Tonks– Wallace strength model at strain rates of ~10^{13} s^{-1} for Al-1100, Tantalum and Copper using hypervelocity impact crater morphologies. *Int. J. Impact Eng*. http://dx.doi.org/10.1016/j.ijimpeng.2012.09.001.

Price, M. C. Solscheid, C. Burchell, M. J. Josse, L. Adamek, N. Cole, M. J. (2013). Survival of yeast spores in hypervelocity impact events up to velocities of 7.4 km s^{-1}. *Icarus.* **222**. 263–272.

Quaiser, A. Ochsenreiter, T. Lanz, C. Schuster, S. C. Treusch, A. H. Eck, J. Schleper, C. (2003). Acidobacteria form a coherent but highly diverse group within the bacterial domain: evidence from environmental genomics. *Molecular Microbiology.* **50**, 563–575.

Rainey, F. A. Ray, K. Ferreira, M. Gatz, B. Z. Nobre, M. F. Bagaley, D. Rash, B. A. Park, M. J. Earl, A. M. Shank, N. C. Small, A. M. Henk, M. C. Battista, J. R. Kampfer, P. da Costa, M. S. (2005). Extensive diversity of ionizing-radiation-resistant bacteria recovered from Sonoran Desert soil and description of nine new species of the genus Deinococcus obtained from a single soil sample. *Applied and Environmental Microbiology* **71**: 5225-5235.

Ramos, J. L. (2003). Lessons from the genome of a lithoautotroph: making biomass from almost nothing. *J Bacteriol.* **185**, 2690–1.

Rampelotto, P. H. (2010). Resistance of microorganisms to extreme environmental conditions and its contribution to astrobiology. *Sustainability.* **2**, 1602–1623.

Randall, L. (2015). Dark Matter and the Dinosaurs. *New York: Ecco/HarperCollins Publishers*.

Rebecchi, L. Altiero, T. Guidetti, R. Ceari, M. Bertolani, R. Negroni, M. Rizzo, A. M. (2009). Tardigrade Resistance to Space Effects: First Results of Experiments on the LIFE-TARSE Mission on FOTON-M3. *Astrobiology,* **9,** 581-591.

Rebecchi, L. Altiero, T. Cesari, M. Marchioro, T. Giovannini, I. Rizzo, A. M. Ganga, P. L. Vikich, M. Donati, A. Zolesi, V. Bertolani, R. Guidetti, R. (2011). TARDIKISS: tardigrades in the mission STS-134, the last of the shuttle Endeavour. *Abstract of V National meeting of ISSBB: Spazio, la Nuova Frontiera per l'Umanita, Padova*, 17.

Ricci, J. Quidelleur, X. Pavlov, V. Orlov, S. Shatsillo, A. Courtillot, V. (2013). New 40Ar/39Ar and K-Ar ages of the Viluy traps (Eastern Siberia): Further evidence for a relationship with the Frasnian-Famennian mass extinction. *Palaeogeography, Palaeoclimatology, Palaeoecology,* **386,** 531-540.

Rice, M. H. McQueen, R. G. Walsh. (1958). Compression of solids by strong shock waves. Solid State Physics, Vol. 6, Ed. Seitz and Turnball, *Academic Press.*

Riesenman, P. J. Nicholson, W. L. (2000). Role of spore coat layers in Bacillus subtilis: spore resistance to hydrogen peroxide, artificial UV-C, UV-B and solar UV radiation. *Applied and Environmental Microbiology* **66**: 620-626.

Rizzo, A. M. Altiero, T. Corsetto, P. A. Montorfano, G. Guidetti, R. Rebecchi, L. (2015). Space flight effects on antioxidant molecules in dry tardigrades: The TARDIKISS experiment. *Biomedical Research International* 167642:1

Roberts, J. H. Nimmo, F. (2008). Tidal heating and the long-term stability of a subsurface ocean on Enceladus. *Icarus.* **194,** 675-689.

Robertson, P. Mahadevan, S. Endl, M. Roy, A. (2014). Stellar activity masquerading as planets in the habitable zone of the M dwarf Gliese 581. *Science.* **345**: 440–444.

Romaniuk, K. Dziewit, L. Decewicz, P. Mielnicki, S. Radlinska, M. Drewniak, L. (2017). Molecular characterization of the pSinB plasmid of the arsenite oxidizing, metallotolerant Sinorhizobium sp. M14 – insight into the heavy metal resistome of sinorhizobial extrachromosomal replicons. *FEMS Microbiology Ecology.* **93**, 215.

Roten, C. H. Gallusser, A. Borruat, G. D. Udry, S. D. Karamata, D. (1998). Impact resisitence of bacteria entrapped in small meteorites. *Bulletin de la Societe Vaudoise des Sciences Naturelles*, **86,** 1-17.

Ruesch, O. Platz, T. Schenk, P. McFadden, L. A. Castillo-Rogez, J. C. Qucik, L. C. et al. Cyrovolcanism on Ceres. *Science,* **353,** 6303, id.aaf4286.

Schöttler, U. (1979). On the anaerobic metabolism of three species of Nereis (Annelida). *Marine Ecology Progress Series.* **1**, 249–254.

Sears, D. W. (1975). Temperature gradients in meteorites produced by heating during atmospheric passage. Modern *Geology*, **5,** 155-164.

Sears, D. W. and Kral, T. A. (1998). Martian "microfossils" in Lunar meteorites?, *Meteoritics and Planetary Science*, **33,** 791-794.

Secker, J. Wesson, P. S. Lepock, J. R. (1996). Astrophysical and biological constraints on radiopanspermia. *Journal of the Royal Astronomical Society of Canada,* **90,** 184-192.

Seidelmann, P. K. Archinal, B. A. A'Hearn, M. F. Conrad, A. Consolmagno, G. J. Hestroffer, D. Hilton, J. L. Krasinsky, G. A. Neumann, G. Oberst, J. Stooke, P. Tedesco, E. F. Tholen, D. J. Thomas, P. C. Williams, I. P. (2007). Report of the IAU/IAG working group on cartographic coordinates and rotational elements: 2006. *Celestial Mechanics and Dynamical Astronomy.* **98**, 155–180.

Seki, K. Toyoshima, M. (1998). Preserving tardigrades under pressure. *Nature.* **395**, 853-854.

Sephton, M. Gilmore, I. (2000). Macromolecular organic materials in carbonaceous chondrites: a review of their sources and their role in the origin of life on the early Earth. In: Gilmour, I. Koeberl, C. (eds.) Impacts and the early Earth, *Springer.* 27-49.

Sghaier, H. Ghedira, K. Benkahla, A. Barkallah, I. (2008). Basal DNA repair machinery is subject to positive selection in ionizing-radiation-resistant bacteria. *BMC Genomics* **9,** 297.

Sharma, A. Scott, J. H. Cody, G. D. Fogel, M. L. Hazen, R. M. Hemley, R. J. Huntress, W. T. (2002). Microbial activity at gigapascal pressures. *Science.* **295**, 514–1516.

Shiffman, M. (2011). De Anima: On the Soul, *Newburyport, MA: Focus Publishing/R. Pullins Co*.

Shrine, N. R. G. Burchell, M. J. Grey, I. D. S. 2002. Velocity Scaling of Impact Craters in Water Ice over the Range 1 to 7.3 km s-1. *Icarus* **155**, 475-485.

Sioli, H. (1975). Tropical rivers as expressions of their terrestrial environments. In Golley, F. B. Medina, E. Tropical ecological systems/trends in terrestrial and aquatic research. *New York: Springer.* 275–288.

Sitchen, Z. (1976). The 12th Planet, *Stein and Day,* ISBN 0-8128-1939-X

Sofue, Y. (2017). Rotation and mass in the Milky Way and spiral galaxies. *Publications of the Astronomical Society of Japan,* **69,** 1-35.

Sorokhtin, O. G. Chilingarian, G. V. Sorokhtin, N. O. (2011). Evolution of Earth and its climate birth, life and death of Earth. *Amsterdam: Elsevier Science Ltd*

Stephenson, W. B. (1961). Theoretical light-gas gun performance. *Arnold Engineering Development Centre, Air force systems command,* AEDC-TR-61-1.

Stephenson, J. D. Hallis, L. J. Nagashima, K. Freeland, S. J. (2013). Boron enrichment in Martian clay. *PLoS ONE* **8,** e64624.

Stetter, K. (2006). History of discovery of the first hyperthermophiles. *Extremophiles.* **10,** 357–362.

Stöffler, D. Horneck, G. Ott, S. Hornemann, U. Cockell, C. S. Moeller, R. Meyer, C. De Vera, J-P. Fritz, J. Artemieva, N. A. (2007). Experimental evidence for the potential impact ejection of viable micro-organisms from Mars and Mars-like planets. *Icarus* **186**, 585–588.

Sullivan III, W. T. Baross, J. (2007). Planets and life: The emerging science of astrobiology. *Cambridge University Press.*

Swisher, C. C. Granjales-Nishimura, J. M. Montanari, A. et al., (1992). Coeval Ar-40/Ar-39 ages of 65.0 million years ago from Chicxulub crater melt rock and Cretaceous-Tertiary boundary tektites. *Science,* **257,** 954-958.

Temple, R. (1998). The Sirius Mystery. *St. Martins Press*.

Thagard, P. (2012). The cognitive science of science: explanation, discovery, and conceptual change. *MIT Press*, 204–205

Trimble, V. (1997). Origin of the biological elements. *Origins of Life and Evolution of the Biosphere.* **27,** 3-21.

Trunin, R. F. Gudarenko, L. F. Zhernokletov, M. V. Simakov, G. V. (2001). Experimental Data on Shock Compressibility and Adiabatic Expansion of Condensed Substances. *RFNC, Sarov* (in Russian). Data taken from Rusbank database. <http://teos.ficp.ac.ru/rusbank> (accessed April 2012).

Tsiganis, K. Gomes, R. Morbidelli, A. F. Levison, H. (2005). Origin of the orbital architecture of the giant planets of the Solar System. *Nature.* **435**, 459–461.

Valtonen, M. Nurmi, P. Zheng, J. Q. Cucinotta, F. A. et al. (2009). Natural transfer of viable microbes in space from planets in extra-solar systems to a planet in our solar system and vice verse. *The Astrophysical Journal,* **690,** 210-215.

Vaz, J. E. (1972). Ucere meteorite: determination of differential atmospheric heating using its natural thermoluminescence. *Meteoritics,* **7,** 77-86.

Vogt, S. S. Butler, R. P. Rivera, E. J. Haghighipour, N. Henry, G. W. Willianson, M. H. (2010). The Lick-Carnegie Exoplanet Survey: A 3.1

M planet in the habitable zone of the nearby M3V star Gliese 581. *The Astrophysical Journal*, **723**, 954-965.

Vogt, S. S. Wittenmyer, R. A. Butler, R. P. O'Toole, S. Henry, G. W. et al. (2010). A Super-Earth and Two Neptunes Orbiting the Nearby Sun-like Star 61 Virginis. *The Astrophysical Journal.* **708,** 1366-1375.

von Frese, R. Potts, L. Wells, S. Leftwich, T. Kim, H. (2009). GRACE gravity evidence for an impact basin in Wilkes Land, Antarctica. *Geochemistry, Geophysics, Geosystems.* **10.**

Vreeland, R. H. Rosenzweig, W. D. Powers, D. W. (2000). Isolation of a 250 million-year-old halotolerant bacterium from a primary salt crystal. *Nature*, **407,** 897-900.

Vukich, M. Ganga, P. L. Cavalieri, D. Rivero, D. Pollastri, S. Mugnai, S. et al. (2012). BIOKIS: a model payload for multisciplinary experiments in microgravity. *Microgravity Science and Technology*, **24(6),** 397–409.

Wagner, D. Morozova, D. (2008). Life on Mars? Methane-forming microorganisms from Siberian permafrost soils as study objects. Research Highlights 2008. *Alfred Wegener Institute for Polar and Marine Research in the Helmholtz-Gemeinschaft Deutscher Forschungszentren*, pp. 38-41.

Weatherill, G. W. (1984). Orbital evolution of impact ejecta from Mars. *Meteoritics*, **19,** 1-13.

Weiss, B. P. Kirschvink, J. L. Baudenbacker, F. J. Vali, H. Peters, N. T. MacDonald, F. A. Wikswo, J. P. (2000). A low temperature transfer of ALH84001 from Mars to Earth. *Science*, **290,** 791-795.

Weiss, D. K. Head, J. W. (2016). Impact ejecta-induced melting of surface ice deposits on Mars. *Icarus,* **280,** 205-233

Weiss, M. C. Sousa, F. L. Mrnjavic, N. Neukirchen, S. Roettger, M. Nelson-Sathi, S. Martin, W. F. (2016). The physiology and habitat of the last universal common ancestor. *Nature Microbiology,* **1,** 16116.

Werner, S. C. Zhu, M. H. Rolf, T. Wunnemann, K. (2016). Moon: basin-forming impacts in scale, time, and as thermal and mass input. *EGU General Assembly 2016.* 11517

Whitman, W. B. Coleman, D. C. Wiebe, W. J. (1998). Prokaryotes: the unseen majority. *Proceedings of the National Academy of Sciences of the United States of America.* **95**, 6578–6583.

Wierzchos, J. Camara, B. De Los Rios, A. Davila, A. F. Sanchaz-Almazo, M. Artieda, O. Wierzchos, K. Gomez-Silva, B. McKay, C. Ascaso, C. (2011). Microbial colonization of Ca-sulfate crusts in the hyperarid core of the Atacama Desert: Implications for the search for life on Mars. *Geobiology.* **9**, 44–60.

Wiker, B. D. (2002). Alien ideas: Christianity and the search for Extraterrestrial life. *Crisis Magazine,* 4th November 2002.

Willis, M. J. Ahrens, T. J. Bertani, L. Nash, C. Z. (2006). Bugbuster – Survivability of living bacteria upon shock compression. *Earth Planet. Sci. Lett.* **247**, 185–196.

Wilson, L. Keil, K. (1997). The fate of pyroclasts produced in explosive eruptions on the asteroid 4 Vesta. *Meteoritics and Planetary Science*, **32,** 813-823.

Wordsworth R. Forget, F. Selsis, F. Millour, E. Charnay, B. Madeleine, J. (2011). Gliese 581D is the first discovered terrestrial-mass exoplanet in the habitable zone. *The Astrophysical Journal Letters* **733**, L48.

Worth, R. J. Sigurdsson, S. House, C. H. (2013). Seeding life on the Moons of the Outer Planets via Lithopanspermia. *Astrobiology,* **13,** 1155-1165.

Wright, I. P. Yates, P. D. Pillinger, C. T. (2000). Effects of atmospheric heating on infalling meteorites and micrometeorites: relevance to conditions on the early Earth. In Gilmore, and C Koeberl (eds). Impacts and the early Earth. *Springer,* 51-72.

Xue, Y. Nicholson, W. L. (1996). The two major spore DNA repair pathways, nucleotide excision repair and spore photoproduct lyase, are sufficient for the resistance of Bacillus subtilis spores to artificial UV-C and UV-B but not to solar radiation. *Applied and Environmental Microbiology* **62**: 2221-2227.

Yi, S. Demarque, P. Kim, Y-C. Lee, Y-W. Ree, C. H. Lejeune, T. Barnes, S. (2001). Toward better age estimates for stellar populations: the Y^2 isochrones for solar mixture. *Astrophysical Journal Supplement.* **136,** 417-437.

Zahnle, K. Schenk, P. Levison, H. and Dones, L. (2003). Craterinh rates in the outer Solar System. *Icarus.* **163**, 263-289.

Zaparty, M. Siebers, B. (2011). Physiology, metabolism, and enzymology of extremophiles. In Horikoshi, K. Antranikian, G. Bull, A. T. Robb, F. T. Stetter, K. O. Extremophiles handbook. *Tokyo: Springer.* 602–633.

Zhao, Guochun; Cawood, Peter A.; Wilde, Simon A.; Sun, M. (2002). Review of global 2.1–1.8 Ga orogens: implications for a pre-Rodinia supercontinent. *Earth-Science Reviews.* **59**, 125–162.

Zhao, Guochun; Sun, M.; Wilde, Simon A.; Li, S. Z. (2004). A Paleo-Mesoproterozoic supercontinent: assembly, growth and breakup. *Earth-Science Reviews.* **67**, 91–123.

Zimmerman, A. M. (1970). High Pressure Effects on Cellular Processes. *Academic Press,* New York.

Zimmerman, A. M. (1971). High pressure studies in cell biology. *Int. Rev. Cytol*. **30**, 1–47.

Website Addresses

https://www.aerospaceweb.org/question/astronomy/life/alh84001.jpg

http://www.annesastronomynews.com/wp-content/uploads/2012/02/Enceladus.jpg

https://www.astronomy.com/~/media/7ABF9221D31E4D1E9FC7DF626D242957.jpg

https://www.bbvaopenmind.com/wp-content/uploads/2016/11/2_Agua-Marte.jpg

https://www.beforeitsnews.com/contributor/upload/481712/images/Gilgamesh_Enkidu2.jpg

https://www.dsx.weather.com//util/image/w/c9t-lrhvyaah2n6.jpg?v=at&w=1280&h=720&api=7db9fe61-7414-47b5-9871-e17d87b8b6a0

https://www.farm9.staticflickr.com/8683/16620078658_7f9fea4f36.jpg

https://www.graphicnet.co.uk/wp/wp-content/uploads/2013/03/Herzsprung-Russel-Chart.jpg

https://www.hosho.ees.hokudai.ac.jp/~tsuyu/top/dct/map/gondwana.png

https://www.keckobservatory.org/images/made/images/gallery/solar_system/Slides-8_800_600.jpg

https://www.lichen.com/bigphotos/Xeleganslg.jpeg
https://www.meteorcrater.com
https://www.planetaryprotection.nasa.gov/overview
https://www.nsf.gov/news/news_images.jsp?cntn_id=117765
https://www.nssdc.gsfc.nasa.gov/imgcat/hires/a16_m_0692.gif
https://www.p5cdn4static.sharpschool.com
https://www.pages.uoregon.edu/jimbrau/BrauImNew/Chap19/FG19_08.jpg
https://www.reefphyto.co.uk.
https://www.sciento.co.uk
https://www.spenvis.oma.be/help/background/metdeb/metdeb.html
https://www.teos.ficp.ac.ru/rusbank
https://www.themagazine.ca
https://www.universetoday.com/wp-content/uploads/2008/09/sunmilkyway.jpg
https://www.universetoday.com/wp-content/uploads/2012/02/wow_signal.jpg
https://www.en.wikipedia.org/wiki/Last_universal_common_ancestor#/media/File:Phylogenetic_tree.svg
https://www.xearththeory.com/wp-content/uploads/pangaea-3.jpg

Appendix I – Phytoplankton Cell Size

Table AI.1: *Average cell size for phytoplankton samples, smallest and largest measured are also given to show distribution range.*

Sample	***Average cell diameter (µm)***	***Minimum size measured (µm)***	***Maximum size measured (µm)***
Unshocked #1	6.50	4.29	10.0
Unshocked #2	6.59	4.37	7.01
G220312#1	6.61	5.25	9.07
G041012#1	6.31	4.16	8.56
G101012#2	7.50	4.02	9.19
G251012#1	6.65	3.85	9.16
G311012#1	6.64	4.49	9.39
G281112#2	6.91	4.82	9.91
G071212#1	5.80	4.59	8.00
G110113#3	5.90	4.00	7.46
G060213#1	4.69	4.44	6.54